

RAINFALL - RUNOFF MODELLING USING DIGITAL ELEVATION MODEL AND REMOTE SENSING DATA

A THESIS

*submitted in fulfilment of the
requirements for the award of the degree*

of

DOCTOR OF PHILOSOPHY

in

CIVIL ENGINEERING



By

ANJANI KUMAR NIGAM



**DEPARTMENT OF CIVIL ENGINEERING
UNIVERSITY OF ROORKEE
ROORKEE-247 667 (INDIA)**

JULY, 1997


CANDIDATE'S DECLARATION


I hereby certify that the work which is being presented in the thesis entitled "RAINFALL - RUNOFF MODELLING USING DIGITAL ELEVATION MODEL AND REMOTE SENSING DATA" in fulfilment of the requirement for the award of the degree of Doctor of Philosophy and submitted in the Department of CIVIL ENGINEERING of the University is an authentic record of my own work carried out during a period from January 1993 to July 1997 under the supervision of Dr. P. K. GARG and Dr. S. K. GHOSH.

The matter presented in this thesis has not been submitted by me for the award of any other degree of this or any other University.


(ANJANI KUMAR NIGAM)


This is to certify that the above statement made by the candidate is correct to the best of our knowledge.

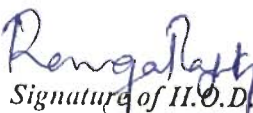

(S. K. GHOSH)
Assistant Professor
Department of Civil Engineering
University of Roorkee, Roorkee


(P. K. GARG)
Assistant Professor
Department of Civil Engineering
University of Roorkee, Roorkee

Date : 16.7.97

The Ph.D. Viva-Voce examination of Sri Anjani Kumar Nigam, Research Scholar, has been held on15.9.98.....


Signature of Supervisor(s) 15/9/98


Signature of H.O.D.


Signature of External Examiner 15/9/98

ABSTRACT

Water is an important natural resource for life, agriculture, forestry, navigation, irrigation, power generation etc. Over the years, its demand is rising due to rapid growth in population, industry and urban areas. Therefore, it is necessary to know the availability of water in an area for its proper management and utilization. The modern technique of remote sensing, integrated with a Digital Elevation Model (DEM), can be used for the estimation of runoff from a catchment, accurately and efficiently. The present research work, thus, focusses on the estimation of runoff, and various hydrologic processes using Watershed Module of Strathclyde River Basin Model (SRBM).

The main objectives of the research work are (i) to identify and assess those hydrologic parameters which can be derived from satellite data and DEM, for runoff generation (ii) integration of remote sensing, DEM, and hydrometeorological data into a hydrologic model in order to compute daily runoff, and (iii) to study the sensitivity of input parameters of the model in relation to runoff and identify the important parameters.

The study area covers a part of Giri river catchment upto Yashwant Nagar, lying between latitudes $30^{\circ} 45'N$ to $31^{\circ} 30'N$ and longitudes $77^{\circ} 00'E$ to $77^{\circ} 45'E$, ranging in elevation from 900m to 3300m above m.s.l. Topographical maps no. 53E and 53F, IRS LISS I digital data of year 1989 and available meteorological data such as rainfall, evaporation and runoff of the catchment are the various data products used to carry out this study.

The SRBM model used here is based on Stanford Watershed Model with modifications to watershed segmentation on the basis of elevation range. The primary input data required by the model are hourly or daily precipitation, daily evaporation and daily runoff data. The entire work has been divided into three components i.e. (i) Development of DEM and its application, (ii) Analysis of remote sensing data and (iii) Runoff simulation using SRBM model

Contours from topographic maps at 200m interval have been digitized to generate a DEM at 500m grid size, using interpolation module of ILWIS

(Integrated Land and Water Information System). The depressions in the DEM have been filled by the lowest elevation present at the rim of the pit. The depressionless DEM is then used for catchment segmentation and computation of slope, flow direction, flow accumulation and overland flow length data.

Flow directions have been computed using flow line approach where flow direction of the previous cell identifies the next cell to be processed. Channel network has been obtained using criteria of minimum contributing area to form a channel. An area equal to 0.75 km². has been found as the threshold value to get a channel network, which is comparable to the channel network shown on topographic maps. This channel network is used to compute flow path slope and overland flow length for each segment as well as for the entire catchment, as required by the model.

The land use information has been extracted from IRS LISS I data using image processing module of ILWIS system, implying Unsupervised clustering technique. Four classes are spectrally separated out, viz. thick forest, thin forest, cultivation and grass land. The overall classification accuracy has been achieved 89%. Interception and Potential Evapotranspiration from Lower Zone parameters have been obtained from landuse data, using area weighted technique for each segment as well as for the entire catchment.

The study has been carried out for two different situations. In first situation, the catchment has been divided into three segments according to their elevation range, i.e., segment 1 is above 2300m, segment 2 is between 1600m to 2300m and segment 3 is below 1600m. In another situation the entire catchment has been considered homogeneous, as one segment.

The values of uniformly distributed rainfall for each segment have been computed using Thiessen Polygon Method. Thus, raingauge adjustment factor in the SRBM model may now be considered as redundant. The parameters of SRBM model have been calibrated for runoff volume for year 1989 using measured runoff values. The calibrated values have been used to compute runoff for years 1991 and 1992 and compared with the measured values to validate the model. The measured and simulated daily flow volume at outlet have been

found to have correlation coefficient varying between 0.991 to 0.999, variance of residual between 4 to 42, and explained variance between 92% to 99%.

Sensitivity analysis of the model parameters has been carried out segmentwise on 1989 data, by changing the value of parameters upto $\pm 30\%$. It is found that the runoff is more sensitive for lower zone soil moisture and ground water recession parameters as compared to infiltration and interflow indices.

It is concluded that the model can be effectively utilized to estimate runoff by integrating it with DEM and remote sensing data. Further, it is found that the segmentation of the catchment improves the computed runoff values when compared with entire catchment as a single homogeneous unit. The proposed model is found to be very sensitive for lower zone soil moisture, hence the value of this parameter requires to be estimated with great care. As the results are found to be promising, the model can be applied to ungauged catchments, with similar environmental and land conditions.

ACKNOWLEDGEMENT

I would like to take this opportunity to express my most sincere appreciation and profound gratitude to **Dr. P.K. Garg** and **Dr. S.K. Ghosh**, the supervisors of my research work, for their constant inspiration, constructive criticism and invaluable guidance in carrying out this work. Their affectionate involvement at all stages is gratefully acknowledged.

The author is also grateful to **Dr. V.K. Jain**, Director, H.B.T.I., **Dr. S.N. Tripathi**, **Dr. C.V.S.K. Rao** and faculty of the Department of Civil Engineering of H.B.T.I., Kanpur, for permitting and cooperating with me to take the research work under Q.I.P. scheme.

The financial assistance provided for the present research work under the Quality Improvement Programme of Ministry of Human Resources and Development, Govt. of India, is gratefully acknowledged. I am also thankful to **Dr. S.C. Handa**, Q.I.P. Coordinator, University of Roorkee, Roorkee for his constant encouragement.

I am thankful to Tehsildar, Shimla; **Dr. K. Singh**, Asstt. Professor in **Dr. Y.S. Parmar** University of Horticulture and Forestry, Solan; **Mr. M.P. Singh**, J.E., Yashwant Nagar and various other Government offices in Himachal Pradesh for their help in the work during field data collection.

My sincere thanks and gratitudes are also due to the faculty member of Civil Engg. Department **Dr. R.S. Tiwari**, **Prof. K.P.Sharma** and **Dr. Bhawani Singh**, **Dr. S.M. Seth**, Director NIH, and all my friends and colleagues. **Shri C.P. Kumar**, **S.K. Singh**, **S.K. Verma**, **S.K. Jain**, **Snehmani**, **Khalid Lotfy** and **Dr. (Mrs.) Nirupama**, for their cooperation and constant encouragement during the progress of this work.

Last but not the least, I ought to express my sentimental gratitude to my parents for their kind blessings. The patience, understanding and unfailing support of my wife **Anita** and sweet smile of my daughter **Akansha** have been a source of continuous encouragement, inspiration and relaxation all through.

(ANJANI KUMAR NIGAM)

TABLE OF CONTENTS

	<i>Page No.</i>
CANDIDATE'S DECLARATION	(i)
ABSTRACT	(ii)
ACKNOWLEDGEMENT	(v)
TABLE OF CONTENTS	(vi)
LIST OF TABLES	(x)
LIST OF FIGURES	(xii)
LIST OF PLATES	(xv)
CHAPTER 1 INTRODUCTION	
1.1 Introduction	1
1.2 Data Requirement for Rainfall-Runoff Modelling	3
1.3 Use of Remote Sensing and DEM in Rainfall-Runoff Modelling	4
1.4 Objectives of the Study	5
1.5 Organisation of Thesis	6
CHAPTER 2 A REVIEW OF VARIOUS RUNOFF MODELS	
2.1 Introduction	7
2.2 Classification of Runoff Models	12
2.2.1 Non-Optimizing Models	12
2.2.1.1 Deterministic Models	12
2.3 Some Important Hydrological Models	15
2.3.1 Soil Conservation Service Model (SCS)	16
2.3.2 Stanford Watershed Model (SWM IV)	16
2.3.3 Strathclyde River Basin Model (SRBM)	17
2.4 Remote Sensing Based Runoff Models	19
2.4.1 Continuous Streamflow Model	19
2.4.2 The SLURP Model	21
2.4.3 The SHE Model	21

2.4.4 Neumann and Schultz Model	24
2.5 Selection of a Hydrological Runoff Model	24

CHAPTER 3 ROLE OF REMOTE SENSING AND DEM IN RUNOFF MODELLING

3.1 Introduction	28
3.2 Spectral Response Curve of Water	28
3.3 Role of Remote Sensing in Runoff Modelling	28
3.3.1 Precipitation	33
3.3.2 Snow Cover Mapping	35
3.3.3 Evapotranspiration Modelling	37
3.3.4 Soil Moisture Mapping	38
3.3.5 Landuse Mapping	40
3.3.6 Catchment Characteristics	43
3.4 Role of DEM in Runoff Modelling	44
3.4.1 Slope and Aspect from DEM	47
3.4.2 Channel Network and Catchment Characteristics from DEM	50

CHAPTER 4 METHODOLOGY ADOPTED FOR RAINFALL RUNOFF MODELLING

4.1 Introduction	56
4.2 Modelling Strategy	56
4.3 Details of Watershed Module of SRBM Model	58
4.4 Development of DEM and Parameter Extraction	62
4.4.1 Generation of DEM	62
4.4.2 Pre-Processing of DEM	64
4.4.3 Catchment Delineation	68
4.4.4 Segmentation of Catchment	71
4.4.5 Computation of Flow Direction	71
4.4.5.1 Flow Line Approach	75

4.4.6	Determination of Flow Accumulation Values and Channel Network	77
4.4.7	Computation of Overland Flow Path and Slope	83
4.5	Processing of Remotely Sensed Data	91
4.5.1	Geometric Registration of Remote Sensing Data	91
4.5.2	Classification of Remote Sensing Data for Landuse	92
4.6	Runoff Simulation using Watershed Module of SRBM Model	93
4.7	Sensitivity Analysis	95

CHAPTER 5 STUDY AREA AND DATA USED

5.1	The Upper Yamuna Catchment	97
5.2	The River Giri Catchment	97
5.2.1	River Network	100
5.2.2	Topography	100
5.2.3	Climate	100
5.2.4	Geology	101
5.2.5	Soils	101
5.2.6	Vegetation	101
5.3	Data Availability	101
5.3.1	Topographical and Other Maps	105
5.3.2	Hydrometeorological Data	105
5.3.2.1	Rainfall Data	106
5.3.2.2	Evaporation Data	106
5.3.2.3	Discharge Data	106
5.3.3	Satellite Data	106

CHAPTER 6 ANALYSIS OF DATA

6.1	Introduction	108
6.2	Development of DEM of Giri Catchment	108
6.3	Analysis of DEM	108

6.3.1	Segmentation of Catchment	109
6.3.2	Computation of Flow Direction and Flow Accumulation Values	109
6.3.3	Extraction of Channel Network	115
6.3.4	Computation of Model Parameters from DEM	115
6.4	Analysis of Remote Sensing Data	119
6.4.1	Geometric Registration of IRS Data	119
6.4.2	Image Statistics of IRS Data	120
6.4.3	Determination of Landuse Information	126
6.4.4	Computation of Model Parameters from Remote Sensing Data	133
6.5	Analysis of Rainfall Data	136

CHAPTER 7 MODEL CALIBRATION, VALIDATION AND SENSITIVITY ANALYSIS

7.1	Introduction	137
7.2	Simulation of Runoff from SRBM Model	137
7.3	Sensitivity Analysis	151
7.3.1	Sensitivity of Lower Zone Soil Moisture (LZSN)	159
7.3.2	Sensitivity of Infiltration Parameter (CB)	159
7.3.3	Sensitivity of Interflow Index (CC)	159
7.3.4	Sensitivity of Interflow Recession Parameter (IRC)	159
7.3.5	Sensitivity of Grounwater Recession Parameter (KK24)	160

CHAPTER 8 CONCLUSIONS AND RECOMMENDATIONS

8.1	Summary	161
8.2	Conclusions	162
8.3	Recommendations and Future Scope	163

APPENDIX A1		165
-------------	--	-----

APPENDIX A2		169
-------------	--	-----

REFERENCES		174
------------	--	-----

LIST OF TABLES

		<i>Page No.</i>
Table 3.1	Hydrologic and Water Management Observational Requirements	32
Table 4.1	List of Watershed Module Parameters and Probable Data Source	61
Table 4.2	Summary of the Methods of DEM Data Collection	63
Table 5.1	Details of Hydrometeorological Data used in the Study	105
Table 5.2	Details of Satellite Data Used	106
Table 6.1	Location of Cells with Undefined Flow Direction	112
Table 6.2	Overland Flow Length for Different Sets of Drainage Networks	118
Table 6.3	Catchment Characteristics Computed by DEM.	118
Table 6.4	Statistics of Registration Points	120
Table 6.5	Univariate Statistics of IRS LISS I, 1989 Data	120
Table 6.6	Variance-Covariance Matrix of IRS LISS I, 1989 Data	121
Table 6.7	Correlation Matrix of IRS LISS I, 1989 Data	121
Table 6.8	Landuse Classes within the Catchment for 1989	126
Table 6.9	Contingency Table Depicting Classification Accuracy	128
Table 6.10	Comparison of Landuse Information for Years 1977, 1980 and 1989	133
Table 6.11	Typical Values of Maximum Interception Rates (EPXM) and Lower Zone Evaporation Parameter (K3)	134
Table 6.12	Values of Parameters EPXM and K3 for the Model.	134
Table 6.13	Segmentwise Area Coverage of Thiessen Polygons	136
Table 7.1	Assumed Values of Some Model Parameters	139
Table 7.2	Typical Values for Gradient (GR), Standard Deviation (SD) and Cut-off point (CP)	140
Table 7.3	Calibrated Values of the Parameters Adapted for the Study Catchment Segmentwise	141

Table 7.4	Summary of Simulated Runoff for Catchment Considering Segmentation	141
Table 7.5	Calibrated Values of the Model Parameters for Catchment Considering as a Single Unit	146
Table 7.6	Summary of Simulated Runoff for Catchment Considering as a Single Unit	146
Table 7.7	Sensitivity Analysis of Calibration Parameters	152

LIST OF FIGURES

		<i>Page No.</i>
Fig. 1.1	The World's Water Distribution	2
Fig. 2.1	Concept of Mathematical Model	8
Fig. 2.2	The Process Involved in Global Hydrologic Cycle	9
Fig. 2.3	Representation of Input, System and Output for a watershed Model	10
Fig. 2.4	A System Representation of watershed Runoff	11
Fig. 2.5	Classification of Hydrological Models	13
Fig. 2.6	Flow Chart of the Stanford Watershed Model IV	18
Fig. 2.7	A Remote Sensing Based Continuous Streamflow Model	20
Fig. 2.8	Flow Chart of the Vertical Water Balance (SLURP Model) Applied to Each Land Class Within Each Group Response Unit	22
Fig. 2.9	Structure of the European Hydrologic System (SHE)	23
Fig. 2.10	Structure of Hydrologic Model using Source Area Concept	25
Fig. 3.1	Reflectance values of Water and Other Features	29
Fig. 3.2	A Passive Microwave Emission Model from Land Surfaces	39
Fig. 3.3	Use of DEM to Extract Hydrologic Parameters	46
Fig. 3.4	A 3 x 3 Elevation Matrix for Computation of Slope and Aspect	48
Fig. 3.5	Illustration of Procedure for Drainage Network Recovery	52
Fig. 4.1	Flow Chart of Methodology Used	57
Fig. 4.2	Flow Chart of Watershed Module of SRBM	59
Fig. 4.3	Identification and Removal of Single Cell Depression	66
Fig. 4.4	Identification and Removal of Multi Cell Depression	67
Fig. 4.5	Flow Chart to get Depressionless DEM	69
Fig. 4.6	Illustration of Catchment Delineation from DEM	70
Fig. 4.7	Flow Chart to Compute Area Elevation Curve from DEM Data	72
Fig. 4.8	Flow Direction Data Codes for Central Cell '9'	74

Fig. 4.9	Flow Direction Computations using Flow Line Approach in a 10 x 10 Sample Elevation Data	76
Fig. 4.10	Illustration of Method to Resolve Conflicting Flow Direction	78
Fig. 4.11	Flow Chart to get Flow Direction	79
Fig. 4.12	Flow Chart of Subroutine FLODR	80
Fig. 4.13	Flow Chart of Subroutine FLOW2	82
Fig. 4.14	Flow Chart to get Flow Accumulation and Channel Matrix	84
Fig. 4.15	Slope Computation for Central Cell P_0 with Relation to its Four Neighbours P_1, P_2, P_3 and P_4	87
Fig. 4.16	Flow Chart of Ritter's Algorithm for Computing Slope	88
Fig. 4.17	Flow Chart to Obtain Segmentwise Information of Overland Flow Path, Average Channel Slope and Landuse Area	89
Fig. 4.18	Flow Chart for Computation of Segmentwise Rainfall using Thiessen Polygon	94
Fig. 5.1	The Upper Yamuna Catchment	98
Fig. 5.2	Giri Catchment upto Yashwant Nagar Gauging Site	99
Fig. 5.3	Geological Map of River Giri Catchment	102
Fig. 5.4	Soil Map of River Giri Catchment	103
Fig. 5.5	Landuse Map Prepared from IRS Imageries of Nov. 88 & March 89 and SOI Maps	104
Fig. 6.1	Area Elevation Curve of Giri Catchment	109
Fig. 6.2	Flow Direction Map using Conventional Method	113
Fig. 6.3	Flow Direction map using Flow Line Approach	114
Fig. 6.4	Channel Network for Various Threshold Contributing Area	116
Fig. 6.5	Histogram of IRS LISP I Bands 1, 2, 3 and 4	123
Fig. 6.6	Landuse Prepared from LANDSAT MSS FCC of March 1977	131
Fig. 6.7	Landuse Prepared from LANDSAT MSS Band 5 Imagery of October 1980	132
Fig. 7.1	Calibration of Watershed Module of SRBM Considering all the Three Segments for Year 1989.	142

Fig. 7.2	Validation of Watershed Module of SRBM Considering all the Three Segments for Year 1991.	143
Fig. 7.3	Validation of Watershed Module of SRBM Considering all the Three Segments for Year 1992.	144
Fig. 7.4	Calibration of Watershed Module of SRBM Considering Entire Catchment as a Single Unit for Year 1989.	148
Fig. 7.5	Validation of Watershed Module of SRBM Considering Entire Catchment as a Single Unit for Year 1991.	149
Fig. 7.6	Validation of Watershed Module of SRBM Considering Entire Catchment as a Single Unit for Year 1992	150
Fig. 7.7	Sensitivity of Nominal Lower Zone Soil Moisture Parameter (LZSN)	153
Fig. 7.8	Sensitivity of Infiltration Parameter (CB)	154
Fig. 7.9	Sensitivity of Interflow Parameter (CC)	155
Fig. 7.10	Sensitivity of Interflow Recession Parameter (IRC)	156
Fig. 7.11	Sensitivity of Groundwater Recession Parameter (KK24)	157
Fig. 7.12	Sensitivity of Various Parameter	158

LIST OF PLATES

		<i>Page No.</i>
Plate 6.1	Elevation Segment Map of Giri Catchment	111
Plate 6.2	(a) Linearly Stretched Image of Band 1	124
	(b) Linearly Stretched Image of Band 2	124
	(c) Linearly Stretched Image of Band 3	125
	(d) Linearly Stretched Image of Band 4	125
Plate 6.3	False Colour Composite of Giri Catchment	127
Plate 6.4	Segmentwise Landuse Map of Giri Catchment	127
Plate 6.5	Runoff Gauging Site at Yashwant Nagar	129
Plate 6.6	Thick Forest in Giri Catchment	129
Plate 6.7	Thin Forest in Giri Catchment	130
Plate 6.8	Cultivated and Grassland in Giri Catchment	130
Plate 6.9	Thiessen Polygon Map of Giri Catchment	135

CHAPTER 1

INTRODUCTION

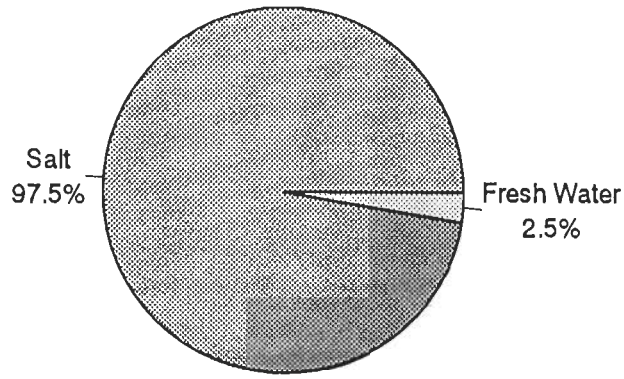
1.1 INTRODUCTION

Water is a vital resource to mankind and its everyday activities. Its demand is continuously increasing, due to rapid growth in population, urbanisation and industrialisation. Water is the essence of life; but when scarce, or excess, or contaminated, it can be the cause of disease or even death.

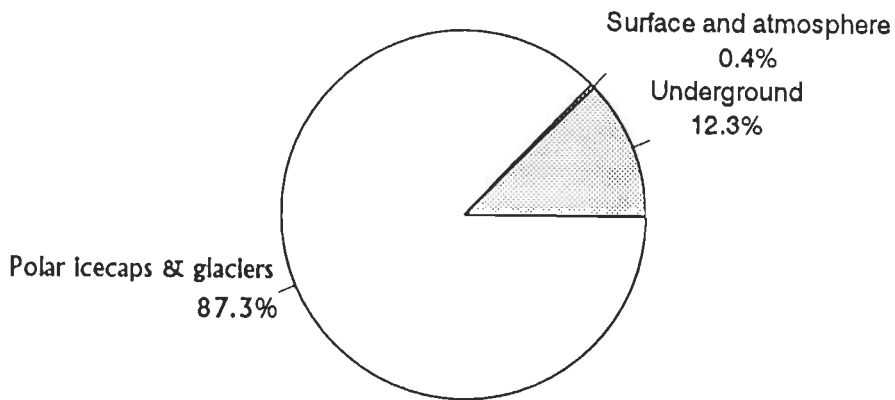
The world's water distribution is shown in Fig. 1.1, in which about 97% of water on earth is contained in the oceans as saline water, and about 3% as fresh water available in ice caps, groundwater, lakes, rivers, soil moisture and in the atmosphere as water vapour. In lakes, rivers and streams, the available water is about 0.4% of fresh water (Singh, 1994). Thus, only a small fraction of the total water is available to human beings and other organisms for consumption. It is believed that the water resources on the earth are sufficient to meet the growing needs for an indefinite time, provided an appropriate scientific approach of using water and reshaping the hydrologic cycle and water balance is adopted. To plan the optimum utilisation of water, it is therefore essential to first estimate the availability of water, and then use the scientific approach for its management and utilisation.

India is one of the few countries in the world which has abundant water resources, but requires an efficient management programme for its judicious use (Ramamoorthi et al., 1991). The average precipitation over the country is estimated to be 1190 mm spread over a geographical area of approximately 3.05×10^6 km². Average annual water resources in various river catchments of the country is estimated to be around 548 mm, which is about 46% of precipitation (Subramanya, 1987).

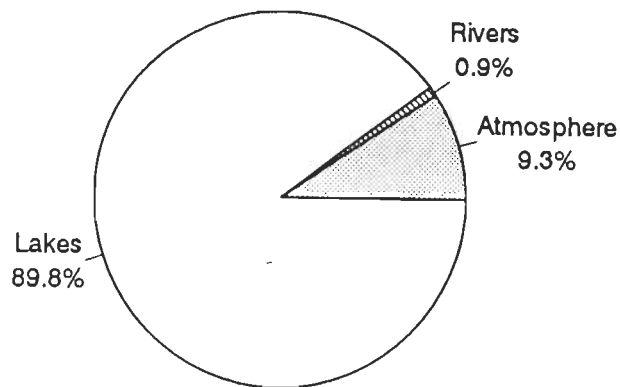
The planning and management of water are dependent on information relating to spatial and temporal distribution of hydrologic parameters. Conventionally, the



World's total water: $1.32 \times 10^9 \text{ km}^3$



Fresh water: $3.25 \times 10^7 \text{ km}^3$



Surface and atmospheric water : $1.36 \times 10^5 \text{ km}^3$

Fig. 1.1 : The World's Water Distribution
(Source : Morris, 1968)

information for hydrologic parameters can be extracted from an extensive data base which may require long time to collect data pertaining to the various themes such as runoff, slope, land use, soil types etc. In order to acquire information for these themes over a period of time and space, a suitable approach has to be developed which may require the use of mathematical based hydrological model. With the advent of high speed computers, mathematical modelling has now proved to be an effective tool for the analysis of hydrological processes.

Runoff from a catchment is an important parameter in hydrologic modelling. Its accurate and timely prediction is required for the estimation of streamflow, flood forecasting and warning, navigation, reservoir sedimentation, water quality assessment and monitoring, hydropower generation and other water resources applications. Runoff is also needed to take decision regarding utilisation, conservation and management of water and also for the design of any hydraulic structures.

1.2 DATA REQUIREMENT FOR RAINFALL-RUNOFF MODELLING

Runoff depends on a number of parameters such as rainfall, infiltration, interception, evaporation, recession, landuse, topography, soil etc. (Subramanya, 1987). There are various methods available to estimate runoff. One of the methods for estimation is to use rainfall-runoff models. In conventional approach, site observations are taken regularly at fixed interval of time. Sometimes, due to adverse conditions or inaccessibility of the catchment, it may not be possible to take any observations. Under such circumstances, rainfall-runoff modelling may provide estimates of runoff.

Most of the input data required by runoff models can be obtained from maps, field, engineering handbooks, tables and equations. These data are related to catchment characteristics, channel characteristics with meteorological and streamflow data (Viessman et al., 1977). Catchment characteristics relates to area and shape of catchment, overland flow length, slope, soil type, landuse etc., while channel characteristics relate to channel length and its cross section, drainage pattern, drainage

density, channel slope, Manning's coefficient etc. Meteorological and streamflow data comprises of rainfall, evaporation, radiation, wind speed, temperature, humidity, streamflow data, flood frequency data, rating curves such as stage discharge, velocity discharge etc.

Runoff models require most of the above data as input in one form or the other to estimate the runoff values. The accuracy of runoff assessment, however, depends on the accuracy with which these data have been collected. It is therefore important that the input data is collected precisely using latest available techniques.

Initial studies carried by Salomonson (1975), Jackson and Ragan(1977 a & b) and Peck et al. (1981, b) indicate that remote sensing can provide useful information for hydrologic modelling.

1.3 USE OF REMOTE SENSING AND DEM IN RAINFALL-RUNOFF MODELLING

Remote sensing is currently being used as an important source of data and information for hydrologic modelling and other water resources management problems (Chakroborti, 1992). Remote sensing provides some of the input parameters as required by the hydrologic models to assess runoff. Presently, there are two broad approaches wherein remote sensing has been providing input data for the computation of runoff. The first one is based on producing input data for empirical flood peaks, annual runoff or low flow equations (Engman and Gurney, 1991,a). These relationships may be empirical in nature, based on various geomorphic characteristics of the catchment and can be determined using near real time remote sensing data. The examples of such models are developed by Killpack and McCoy (1981) and Chidley and Drayton (1986). The relationships were established between runoff, area of catchment and stream frequency which were derived from remote sensing data. In the second approach, runoff models which are based on cloud cover or landuse information can be modified so that these informations are obtained from the analysis of aerial photographs and multispectral satellite data. The studies by Salomonson et al. (1975), Groves et al. (1983), Strubing and Schultz (1983), and Kite (1991) are the examples of such type of runoff models.

Runoff prediction models also require topographic parameters such as slope, aspect, flow direction, drainage network, sub-catchment etc., as an input which can be automatically extracted using a Digital Elevation Model (DEM). DEM is a numerical representation of the elevation values, which represents the land surface as a matrix of elevation. It can also be used for the computation of number and length of channels, drainage density, drainage frequency etc. The advantage of using a DEM is to compute the quantitative spatial information about the topographic parameters which can directly be used as input into hydrologic models (Hogg. et al., 1993).

Kemp (1992) stressed that the hydrological models include two distinct geographic models. Since, water originates as a distributed input to a river catchment, thus runoff modelling is an important component. Further, water quickly concentrates in channel network which may require network analysis model. Digital terrain data is an important input to both types of model. Due to this reason, efficient methods for collecting DEM data for hydrological modelling are required to be developed. Engman and Gurney (1991, b) and DeVantier et al. (1993) focussed on the potential of remote sensing to obtain many hydrologically significant parameters, including land cover, vegetation properties, moisture indices, snow cover and imperviousness. Peck (1981, b) demonstrated the usefulness of remote sensing data in hydrological models. These studies, therefore, suggest the integrated use of remote sensing and DEM data for a hydrological modelling.

1.4 OBJECTIVES OF THE STUDY

The main objectives of this study is to compute the runoff from a catchment using input parameters from topographic map, DEM, field and satellite data. For effective management and utilisation of water resources of a catchment, daily runoff values at desired location is required to be known. Practically, it is not possible to install runoff measuring devices at large number of locations along the channel, for measuring the discharge. Even for gauged catchments, manytimes either the instruments may not function properly or observations are not recorded daily due to adverse weather and

inaccessible terrain conditions. To overcome such problems, it is desirable to adopt rainfall-runoff modelling techniques where most of the hydrologic data may be obtained through remote sensing and DEM to assess the runoff in a catchment.

The increasing rate of developmental activities and utilization of water uses including domestic and industrial purposes, have focussed the attention on quantification of available water. Increasingly sophisticated hydrological models are in demand to address the severe problems arising from the adverse impact of man's activities on the hydrological cycle, and hence on water resource development and management. In the present study, an attempt has been made to estimate runoff from an Indian catchment using modern techniques of remote sensing and digital elevation model. The main objectives of the present research work can be outlined as follows :

- i. To identify and assess the hydrologic parameters which can be derived from satellite data and DEM for runoff modelling.
- ii. To integrate remote sensing data, DEM and hydro- meteorological data in a hydrologic model for the computation of daily runoff.
- iii. To compute runoff, verify the results and study the sensitivity of input model parameters in relation to runoff and identify important parameters.

1.5 ORGANISATION OF THESIS

For detailing and clarity of presentation, the research work has been presented in seven chapters. A brief review of various hydrologic models and their selection criteria has been given in chapter-2. Available studies on various catchments, using remotely sensed data and DEM, have been summarized in chapter-3. The description of model used in this study and the methodology for determination of various input parameters for the model have been discussed in chapter-4. The details of study area and available data have been presented in chapter-5. The model parameters extracted from analysis of remote sensing data and DEM have been discussed in chapter-6. Chapter-7 describes the calibration of model, comparison of runoff with observed values and sensitivity of model parameters. Chapter-8 deals with the discussion of results, conclusions and future scope of the work.

CHAPTER - 2

A REVIEW OF VARIOUS RUNOFF MODELS

2.1 INTRODUCTION

In water resources planning & management, the use of hydrologic simulation models has become a common approach. The development and application of such models have tremendously increased during last few decades. The mathematical functions can be designed to simulate the natural hydrological processes as closely as possible within the present constraints of data availability and user requirements. The concept of mathematical modelling is to minimize the error difference between recorded and simulated output (Fig. 2.1).

A mathematical model may be defined as a numerical system inter-relating in a given time reference a sample of input, cause or stimulus of matter, energy or information and a sample of output, effect or response of information, energy or matter (Fleming, 1975). In simple terms, a hydrological model is a simplified description of the hydrological cycle (Fig. 2.2). The hydrologic cycle is an endless recirculation of water from water vapour to precipitation, infiltration, interflow, streamflow, lakes and oceans and returning to water vapour through evaporation and transpiration.

Runoff modelling requires the interaction of an input (e.g. rainfall) with a system (e.g. catchment) and produces an output (e.g. outflow hydrograph) (Fig. 2.3). An ideal runoff model must represent all necessary hydrological processes such as infiltration, deep percolation, ground water runoff, quick and delayed subsurface runoff, interception, evapotranspiration etc., (Fig. 2.4). Such models may produce accurate results, however, they may require a large quantity of input data.

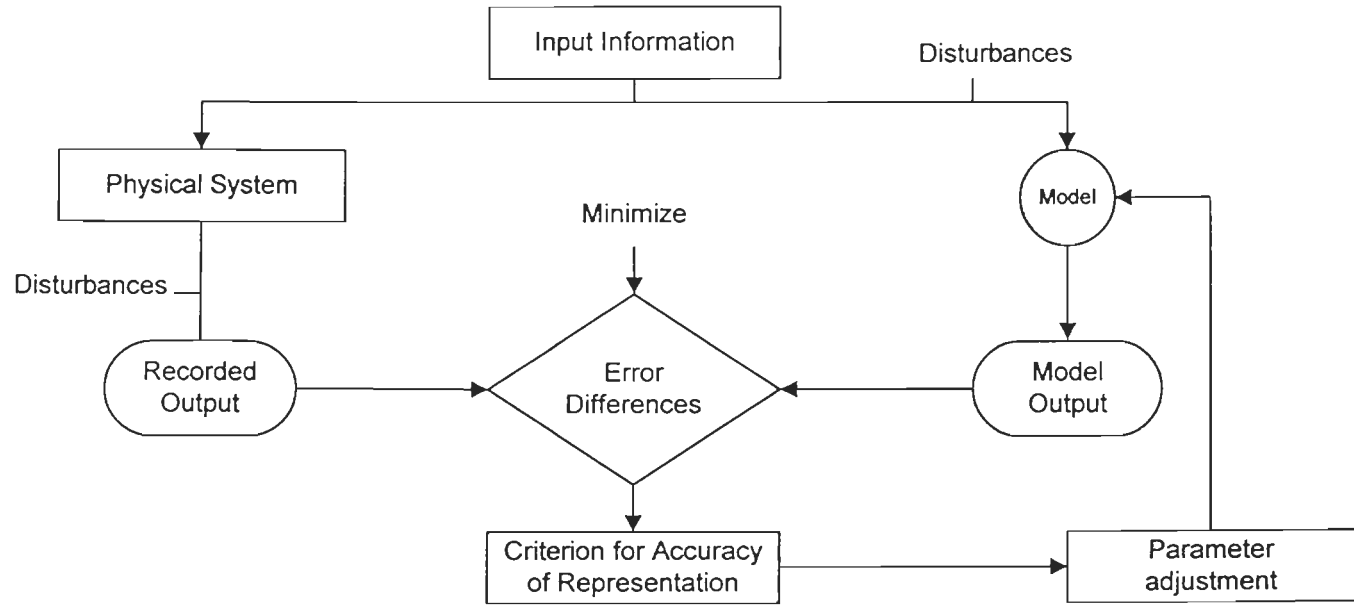


Fig. 2.1 Concept of Mathematical Model
(Source : Fleming, 1975)

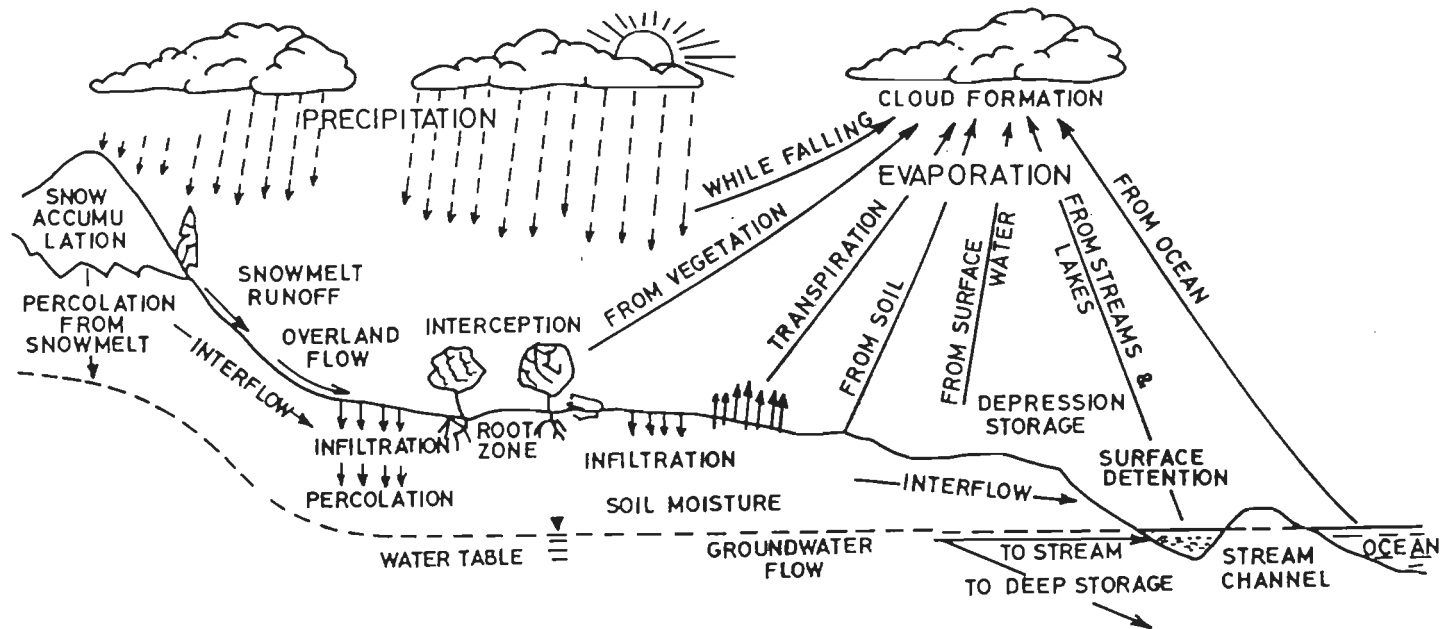


FIG. 2-2: THE PROCESSES INVOLVED IN GLOBAL HYDROLOGIC CYCLE
(SOURCE ENGMAN AND GURNEY, 1991)

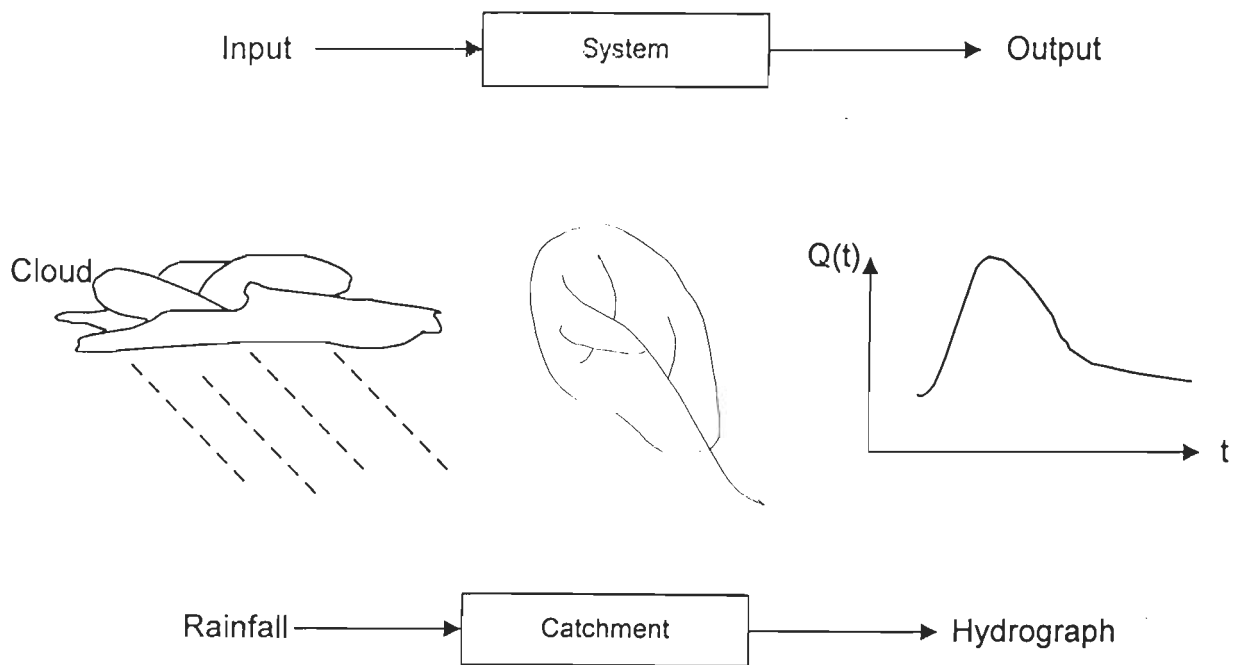


Fig. 2.3 : Representation of Input, System and Output for a Watershed Model
 (Source : Danish Hydraulic Institute, Lecture Notes, 1989)

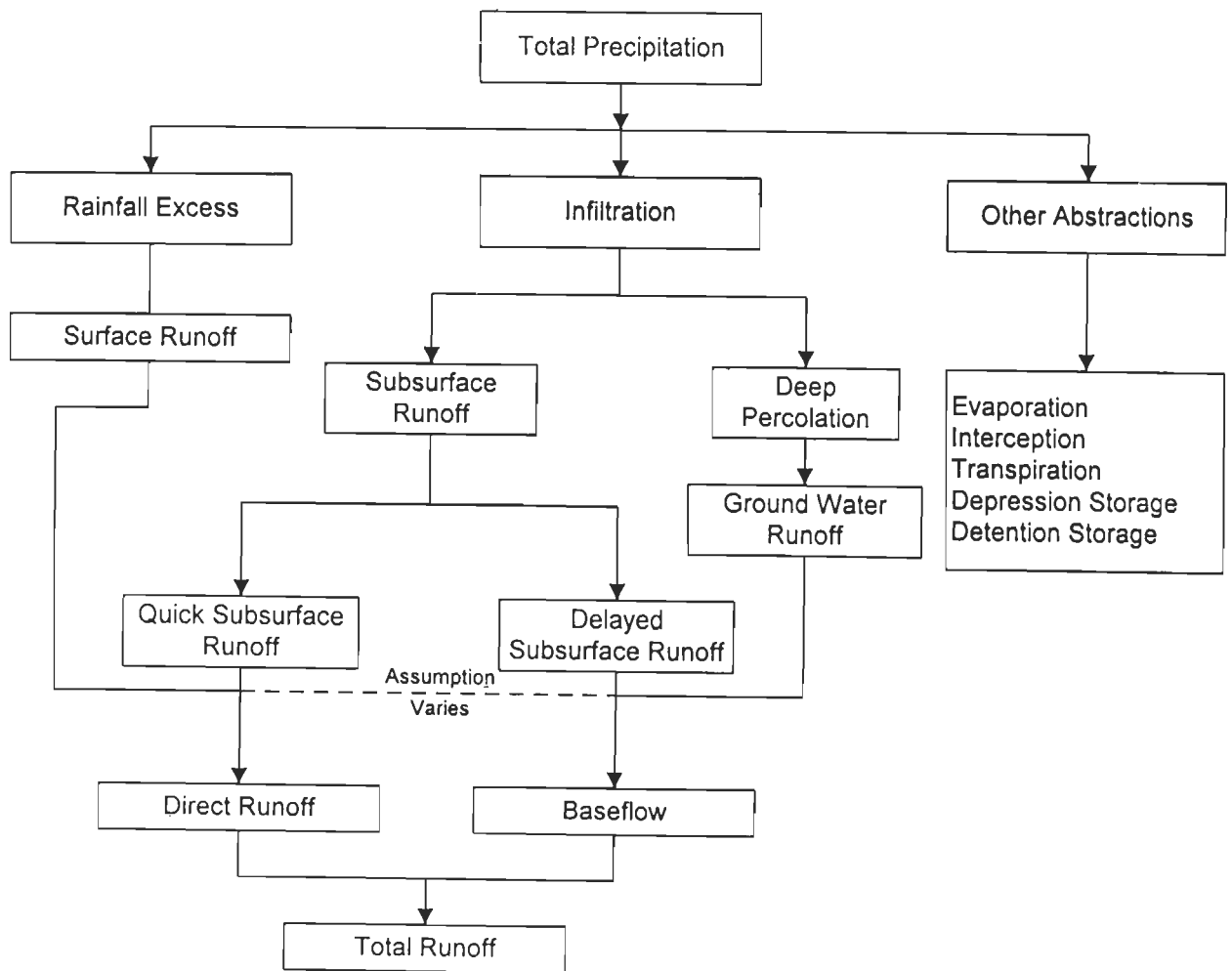


Fig. 2.4 : A System Representation of Watershed Runoff
(Source : Chow, 1964)

2.2 CLASSIFICATION OF RUNOFF MODELS

There are several types of hydrological models available in the literature. A general classification is derived mainly from Fleming (1975) and Woolhiser (1973), as presented in Fig.2.5. As shown in the figure, there are two major categories of hydrological models i.e. the models which (i) require optimization and (ii) do not require optimization. First category models use statistical and decision theory or mathematical programming for optimization, while the second category covers deterministic and statistical models. Deterministic models are subdivided as empirical, lumped and distributed models and statistical models are subdivided as regression and correlation model, probabilistic model and stochastic models. A brief description of deterministic models is given later. A related but less general classification is also presented by Clarke (1973), which indicates that many of the hydrologic models can be divided into deterministic or stochastic models. These two groups can be further divided into conceptual and empirical models. Further subdivision is also possible between spatially lumped or spatially distributed, linear or non-linear and discrete or continuous models.

2.2.1 NON-OPTIMIZING MODELS

Non-optimizing models are generally associated with the assessment of hydrological data, and are used to quantify the physical hydrologic processes. They are divided according to two fundamentally different approaches i.e. the deterministic approach and the statistical approach. Despite a difference in approach, both the approaches have a strong interplay because the processes involved in hydrologic cycle are partly casual and partly random (Fleming, 1975). Hence, some deterministic models contain random functions to relate the processes, while some statistical models contain casual or deterministic functions as part of their structure. The interplay between the two approaches includes the use of results obtained from one approach into another approach.

2.2.1.1 Deterministic Models

These models attempt to consider the various hydrological processes (e.g. interception, infiltration, evaporation etc.) individually, which are combined

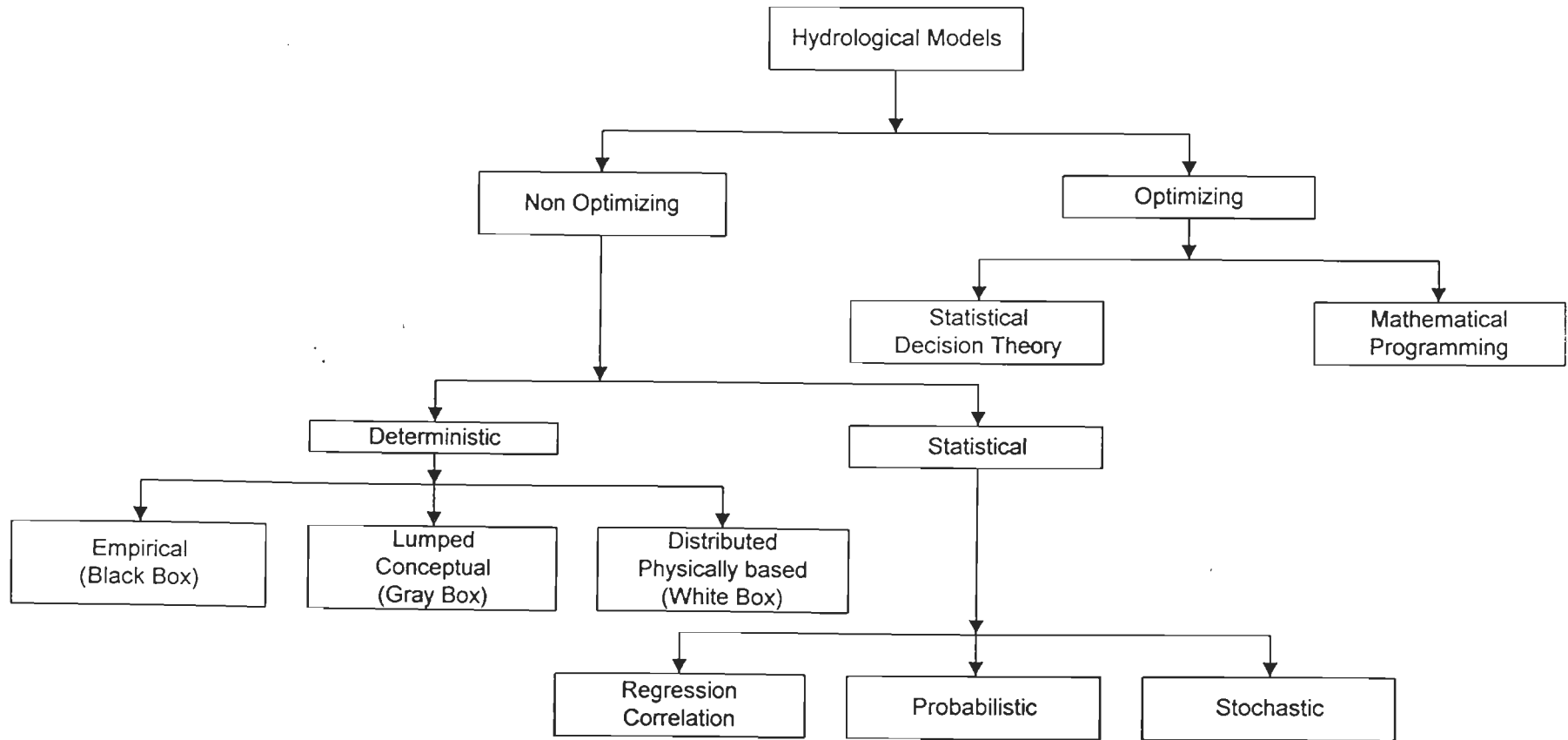


Fig. 2.5 : Classification of Hydrological Models
(Source : Danish Hydraulic Institute, Lecture Notes, 1989)

conceptually to represent the time variant interaction of processes constituting the hydrologic cycle (Fleming, 1975). Deterministic models can be classified into two groups; (i) according to description of the catchment area as spatially lumped or distributed, and (ii) according to description of hydrologic processes as empirical, conceptual or physically based. In practice, most conceptual models are lumped, whereas most physically based models are distributed (Danish Hydraulic Institute, Lecture Notes, 1989).

Development over recent decades has been in the form of a natural progression from black box models to gray box models (lumped conceptual), and onward to increasingly sophisticated physically based distributed models (white box) (Kumar, 1991). In addition, the sophisticated models are in more demand to address the severe problems arising from the adverse impacts of man's activities on the hydrological cycle, and hence on water resources development and management. Some of the deterministic models are described below :

(a) Empirical models (Black Box)

These models do not have physical basis of the processes relating the input to output (Fleming, 1975). In such models, the relationship between input and output is established through calibration using hydrometeorological data. These models may be more successful within the range of calibration. However, in extrapolating beyond the range of calibration, the physical link is lost and the prediction of results depends upon the mathematical techniques alone. Such extrapolation normally is not very precise, and therefore it is not recommended (Anderson and Burt, 1985). The best known black box models in hydrology are the unit hydrograph model and the models applying the principles of unit hydrograph (Sherman, 1932). Presently, black box concepts are more often used to form components of a larger model.

(b) Lumped conceptual models (Gray Box)

These models attempt to represent the time and space variant interaction between all processes that affect the catchment response, and add physical relevance to the parameters

used in the mathematical functions representing the interaction. In lumped models, the catchment is regarded as one unit, and inputs, variables and parameters represent the average values for the entire catchment. These parameters are generally estimated using statistical techniques.

One of the first lumped conceptual models was the Stanford Watershed Model (Linsley and Crawford, 1960). Tank model (Sugawara, 1961), NAM model (Nielsen and Hansen, 1973), USDAHL-74 model (Holtan et al., 1975) and Water balance model of Eagleson (1978) are the examples of lumped conceptual models. Blackie and Eeles (1985), Fleming (1975), Viessman et al. (1977) and Singh (1989). have described several lumped conceptual models and their application to hydrological forecasting.

(c) Distributed, physically based models (White Box)

These models are based on understanding of the physics of the hydrological processes which control catchment response and use physically based equations to describe these processes. Physically based models are spatially distributed as they simulate the spatial variation in hydrological conditions within a catchment as well as simple outflows and bulk storage volumes. Such models require huge data and computational time, and are costly to develop and operate, but are more accurate if parameterised properly.

Systeme Hydrologique European (SHE) model (Abbott et al., 1986 a & b), HYDROTEL model (Fortin et al., 1986), WATFLOOD model (Kouwen, 1988) and Institute of Hydrology Distributed model (Morris, 1980) are some of the examples of physically distributed models. A detailed description of physically based distributed models has been presented by Beven (1985).

2.3 SOME IMPORTANT HYDROLOGICAL MODELS

Presently number of deterministic hydrologic models are available such as SSARR, SWM IV, OPSET, STORM etc. Initially these models were not developed to use remote sensing data. Peck et al. (1981, b) recommended to modify existing models or to

develop new models for using remote sensing data. Some important hydrological models such as Soil Conservation Service Model, Stanford Watershed Model and Strathclyde River Basin Model are described below;

2.3.1 SOIL CONSERVATION SERVICE MODEL (SCS)

This model was originally developed for predicting the runoff volumes from agricultural fields and small watersheds. US Department of Agriculture developed Curve Number as a part of hydrologic modelling procedure in this model (U.S. Department of Agriculture, 1972). The major input parameters are defined in terms of land cover, soil type and moisture condition of the catchment.

In initial stages, most of the work focusing on adapting remote sensing to hydrological modelling was with Soil Conservation Service (SCS) runoff curve number model (Ragan and Jackson, 1975; Jackson and Ragan, 1977 a & b; Bondelid et al., 1980; Ragan and Jackson, 1980; Slack and Welch, 1980; and Jackson and Bondelid, 1984). They evaluated the potentials of remote sensing data in the estimation of runoff curve number, through land cover analysis. The conclusion that can be drawn from these studies, are that LANDSAT data provides a better identification, analysis and mapping compared with aerial photographs, and that it is extremely cost effective. The cost of using LANDSAT data was only 2350.00 dollars as compared to 14000.00 dollars for conventional methods. The magnitude of the cost effectiveness was a function of watershed size and the conventional approach being used. Also areas smaller than 1km². can be mapped and analysed when using satellite data.

2.3.2 STANFORD WATERSHED MODEL (SWM IV)

This model, designed by Crawford and Linsley in 1966, is most widely accepted model for the simulation of land phase of the hydrologic cycle. It has been applied to many watersheds throughout the world, and many modified versions of it are now available (Fleming and Black, 1974; Llamas et al. 1980). Originally it was not developed to use with remote sensing data, but Peck et al. (1981, b) suggested the usefulness of remote sensing data with reference to this model. In the model (Fig. 2.6), incoming

rainfall is distributed among interception, infiltration, interflow, baseflow and channel flow. The infiltration and upper zone storage eventually percolate to lower zone storage and to active & inactive groundwater storage.

Hourly and daily precipitation, daily temperature, radiation, wind speed, monthly or daily evaporation and catchment parameters constitute the inputs to the model, and hourly or daily streamflow at the downstream of catchment is the output. Time interval for the calculation of runoff is 15 minutes. The model is lumped with 34 input parameters; most of them being physically based and only four of these pertaining to infiltration, soil moisture zones and interflow are obtained by using an optimization scheme. If snowmelt estimation is not required, the model parameters reduce to 25 only.

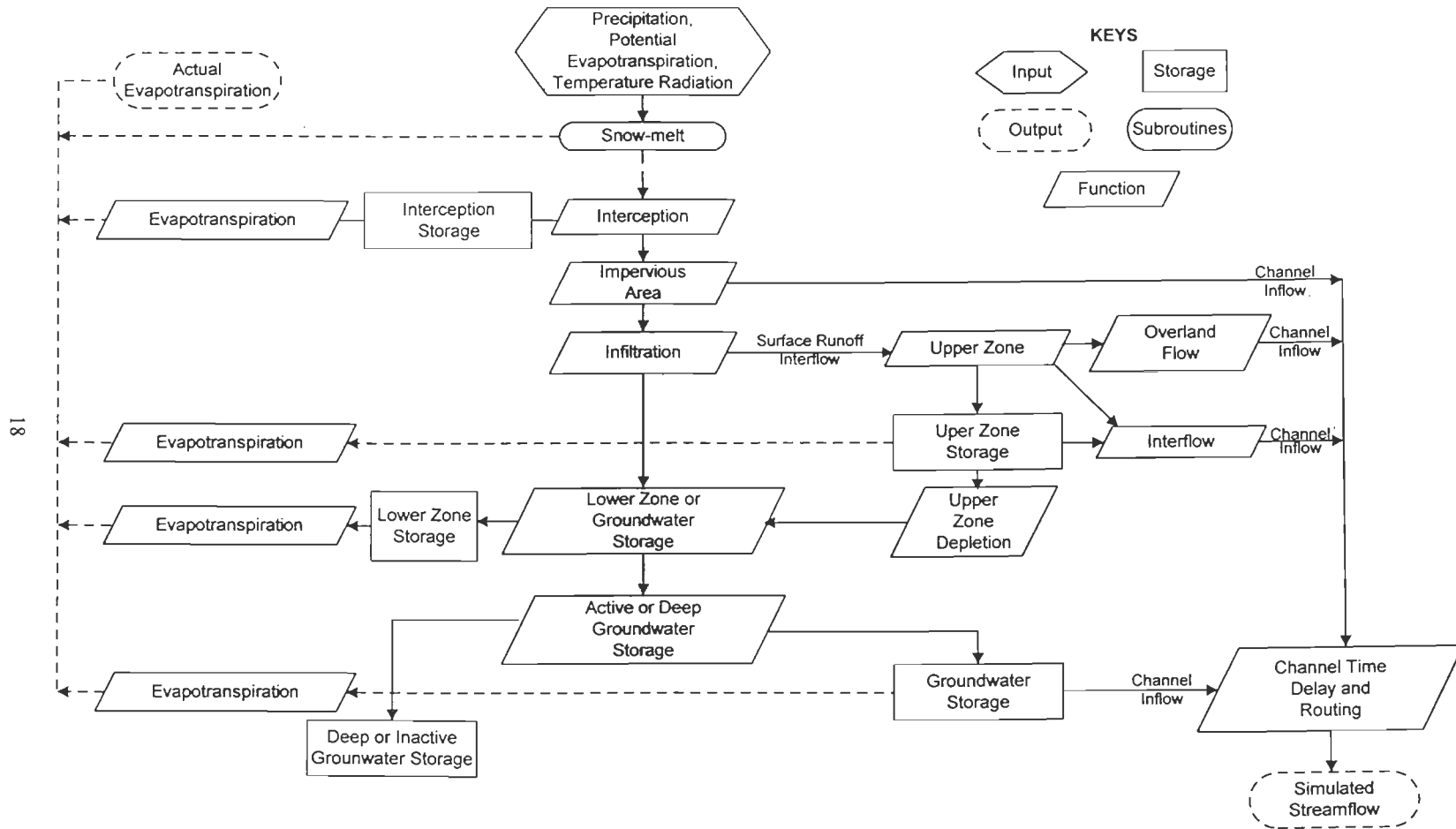
Salmonson (1975) suggested that six parameters i.e. impervious area, water bodies, forested area, overland flow roughness coefficient, density of vegetation and overland flow length could be determined using remote sensing. Three of them are related with areal extent of surface features such as impervious area, water bodies and extent of forest area, two parameters require density of vegetation and one parameter requires length over which overland flow occurs.

2.3.3 STRATHCLYDE RIVER BASIN MODEL (SRBM)

The SRBM is a deterministic conceptual lumped model, developed by Fleming and Mckenzie in 1983. The model attempts to simulate the water and sediment balance of a catchment, and comprises of three separate modules;

- (i) Watershed module
- (ii) Sediment module and
- (iii) Routing module

The watershed module processes precipitation and meteorological data to produce overland flow, throughfall and total flow. The sediment module uses the information derived from Watershed model with some additional data to produce land and channel



81

Fig. 2.6 : Flow Chart of the Stanford Watershed Model IV
 (Source : Crawford and Linsley, 1966)

erosion. Finally, the routing module uses total flow from watershed model and other information to route the flow of water through the channel network. In this model, impervious area, canopy interception and evapotranspiration could be obtained using remote sensing data. Further details of the model is given in article 4.3 of chapter 4.

2.4 REMOTE SENSING BASED RUNOFF MODELS

The effective use of remote sensing data in hydrologic modelling was started in late 70s with SCS and other models. Peck et al. (1981, b) considered the use of remotely sensed data in either calibration, periodic updates or regular input mode and recommends the development of a new series of models conceived and structured to accept the type of data available from satellite sensors. The pioneering attempt was reported in 1983 (Groves and Ragan, 1983).

A number of models using remote sensing data are available such as models developed by, Fortin et al. (1986), Connors et al. (1986), Johnson (1989), Neumann and Schultz (1989), Kouwen et al. (1993). A few remote sensing based models have been described below;

2.4.1 CONTINUOUS STREAMFLOW MODEL

This model, developed by Groves and Ragan (1983), is a physically based streamflow model specifically structured to incorporate information obtained from space platforms (Fig. 2.7). The linkage and concepts are similar to those as of the Stanford Watershed Model IV, but with individual components restructured to interface better with remotely sensed data. The principal changes from the Stanford model are a new concept for infiltration process and a continuous moisture accounting submodel. For infiltration process, soil type and initial surface condition could be determined using remote sensing data and for surface moisture accounting daily data of surface temperature, radiation and cloud cover and periodic surface soil moisture are obtained through remote sensing data.

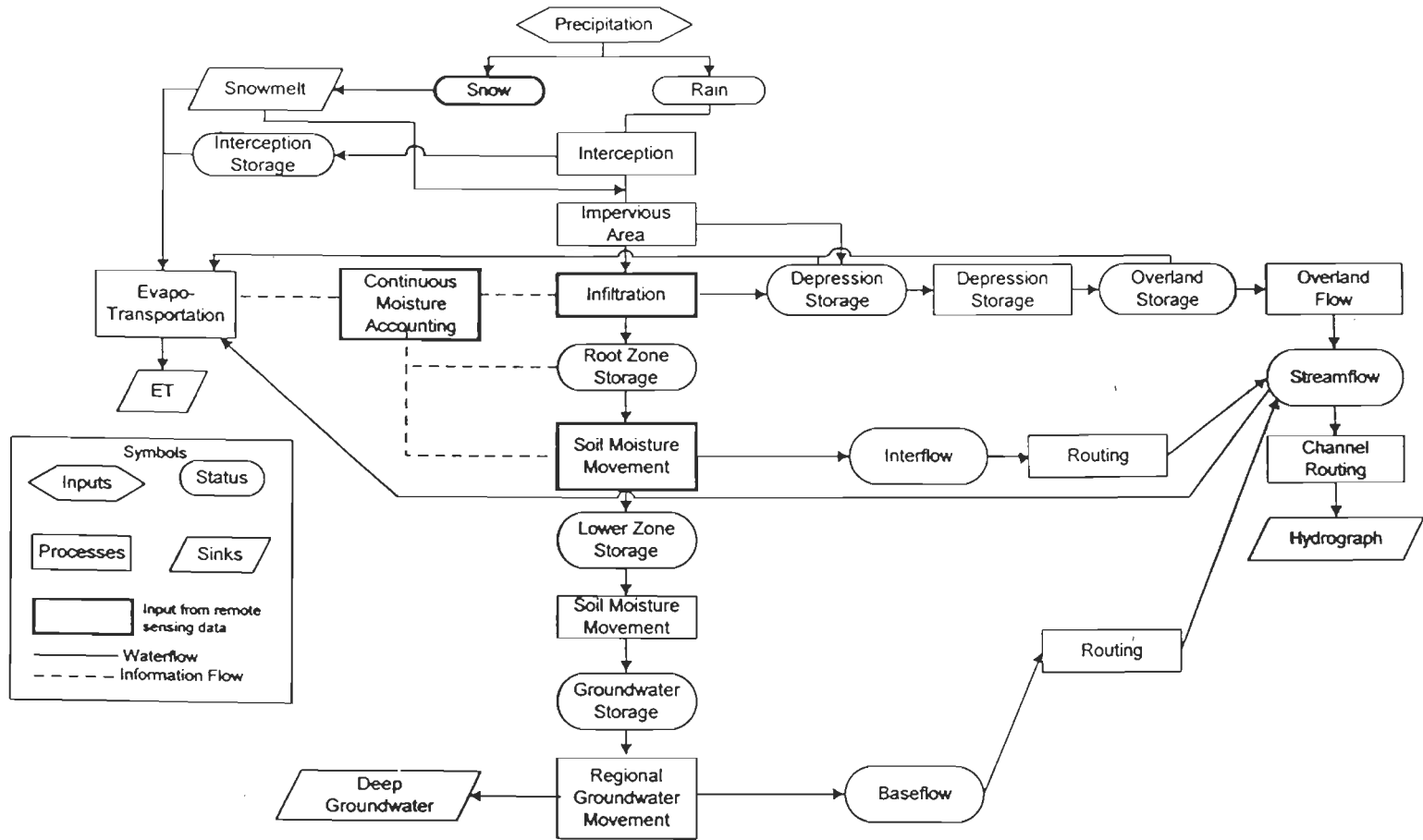


Fig. 2.7 : A Remote Sensing Based Continuous Streamflow Model
(Source : Groves and Ragan, 1983)

Both remote sensing and ground based input data are incorporated into the model through a grid cell Geographic Information System (GIS), which provides a data management tool to handle the various spatial data. Remote sensing data combined with digital elevation data in GIS offers the opportunity for automatic delineation of zones in which there are major differences in the relative importance of individual hydrologic processes.

2.4.2 THE SLURP MODEL

The SLURP is a distributed conceptual watershed model developed by Kite (1978), as shown in Fig. 2.8. The storage of water in the catchment is represented by three tanks; snow-pack, combined surface storage and top soil storage, and deep groundwater storage. These tanks have specified values of initial contents, with maximum depth of surface and groundwater storage. The model divides a catchment watershed into Group Response Units (GRUs), according to areas of different land covers. Updated land cover information is obtained from the analysis of remote sensing data, and are used in SLURP as an indicator of climatic zone, vegetation type, soil characteristics and physiography.

For each land cover type, the model carries out a vertical water balance at each time interval using land cover roughness, infiltration rate and hydraulic conductivity. The resulting rapid and slow runoff are routed within the GRU using physiographic data in a GIS. The routed runoff from each land cover are combined into a streamflow from the GRU, and transported to the next GRU.

2.4.3 THE SHE MODEL

The SHE (Systeme Hydrologique European) is developed jointly by the Danish Hydraulic Institute, the British Institute of Hydrology and SOGREAH (France) (Abbott et al. 1986, a). The structure of the model and physical processes considered in the SHE are schematized in Fig. 2.9. This model employs a physically-based distributed modelling approach in order to provide realistic representation of the hydrological processes viz. interception, evapotranspiration, overland and channel flows, subsurface

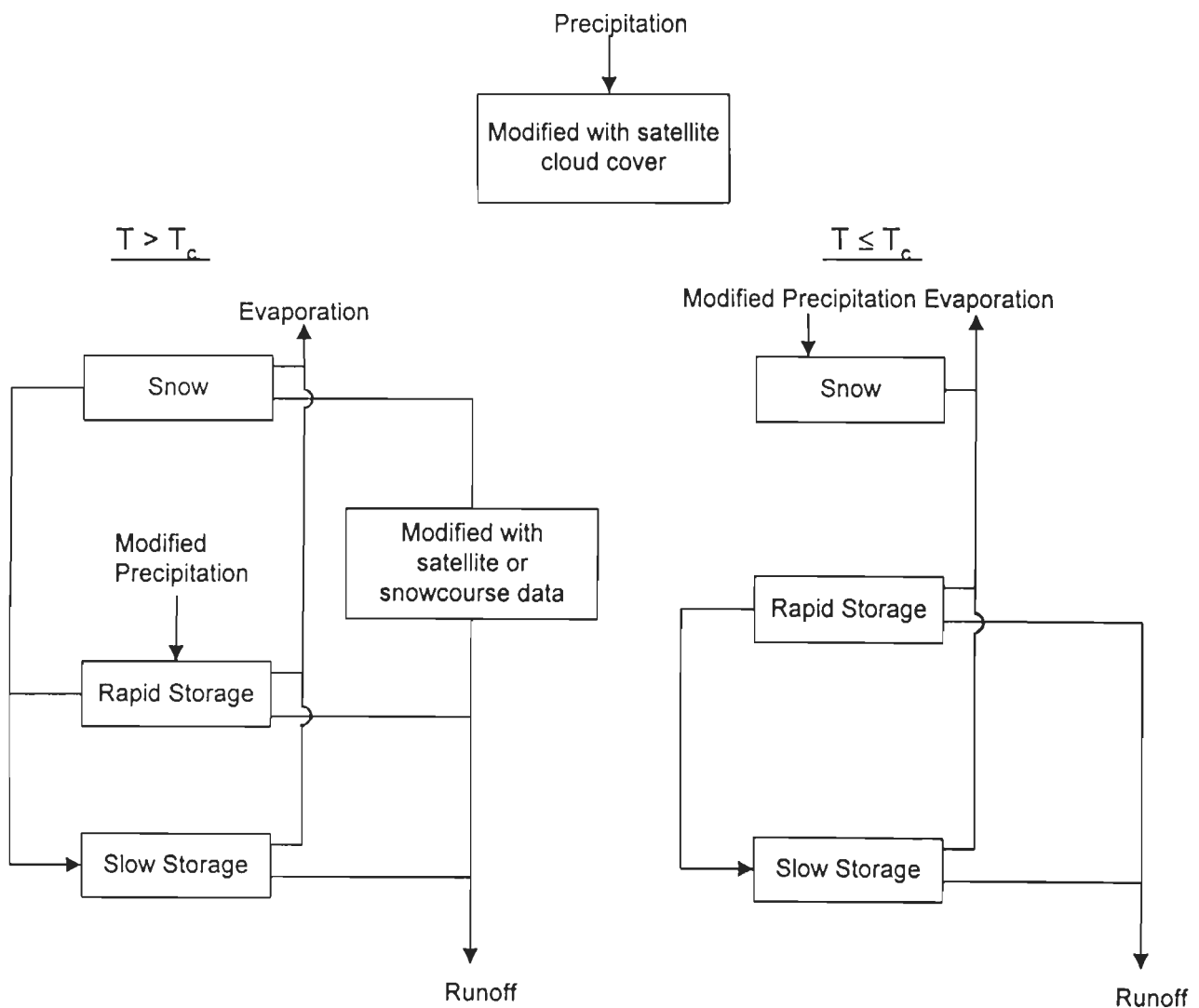


Fig. 2.8 : Flow Chart of the Vertical Water Balance (SLURP Model) Applied to Each Land Class within Each Group Response Unit
 (Source : Kite, 1991)

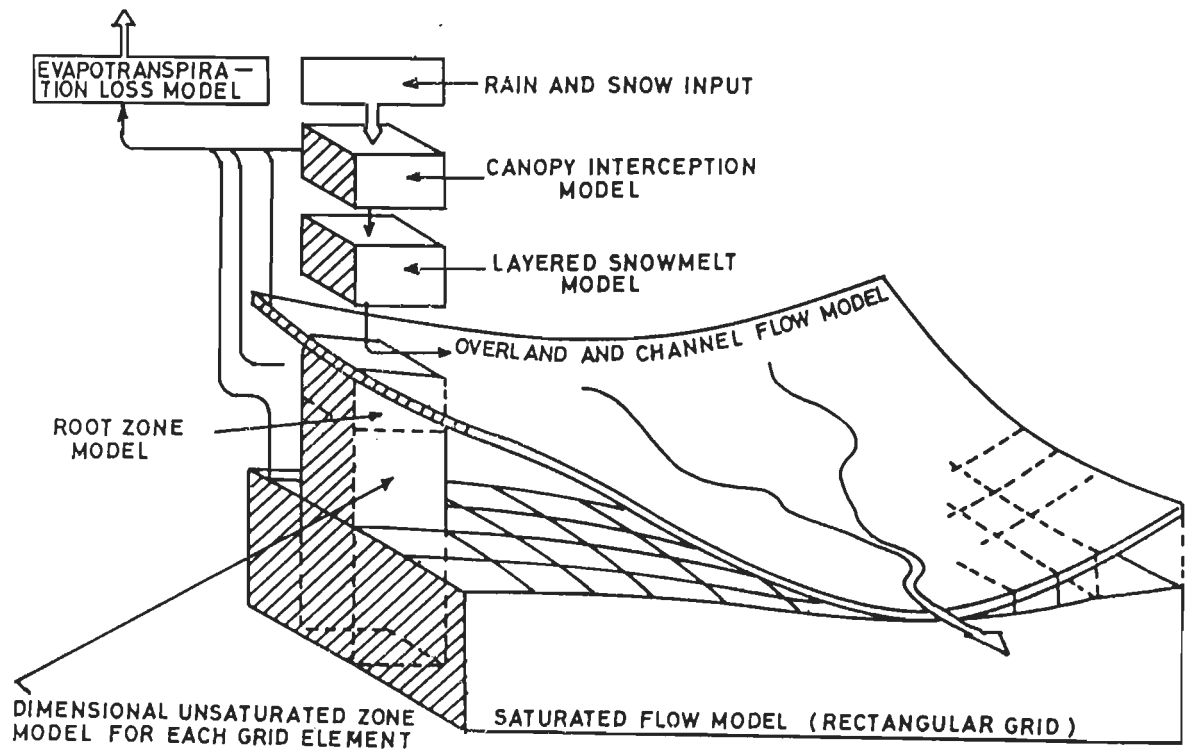


FIG. 2-9: STRUCTURE OF THE EUROPEAN HYDROLOGIC SYSTEM (SHE)
 (SOURCE : ABBOTT et al. 1986, a)

flows in the soil root, unsaturated and saturated zones, snowmelt etc. as well as their complex interaction in time and space.

The model subdivides the catchment into square grids, taking into consideration soil types and landuse distribution. It is capable of predicting the effects of landuse changes, runoff from ungauged watersheds and also for providing the hydrological basis for water quality and soil erosion modelling. Remote sensing techniques are able to provide, on cost effective basis, large amount of spatially and temporally distributed data, for this model.

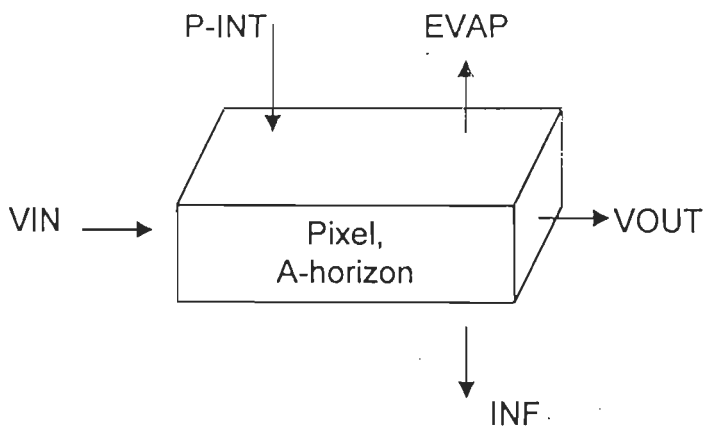
2.4.4 NEUMANN AND SCHULTZ MODEL

Neumann and Schultz (1989) presented a hydrological distributed rainfall-runoff model, which uses remote sensing data and GIS for the estimation of runoff (Fig. 2.10). The model is based on the concept of source areas contributing to surface runoff which are saturated zones, mainly located adjacent to the channels. The computation of location and size of source area is based on a procedure developed by O'Loughlin (1986). Infiltration is computed on the basis of Green and Ampt approach.

For each pixel of the catchment, A and B horizons are assumed. If 'A' horizon is saturated, water flows over, i.e. it now belongs to the source area. Water in the channel originates only from the source areas and is related to the catchment outlet.

2.5 SELECTION OF A HYDROLOGICAL RUNOFF MODEL

Presently, a large number of hydrological models exist. However, many of these models function fundamentally, in the same way with minor variations in presentation (Danish Hydraulic Institute, Lecture Notes, 1989). For some hydrological problems, the selection of a model is more or less dependent on the purpose, e.g. for flood frequency analysis a probabilistic model is suitable or stochastic time series models for the generation of long synthetic streamflow series. Empirical models are mainly of interest as single event models or as sub-component of more complicated models.



- P-INT = Precipitation minus Interception
- VIN = Flow from pixel above
- VOUT = Flow to pixel below
- INF = Infiltration in B-horizon
- EVAP = Evapotranspiration
- z = Depth of Infiltrated wetting front
- K = Conductivity of B-horizon
- S_{av} = Capillary suction at wetting front

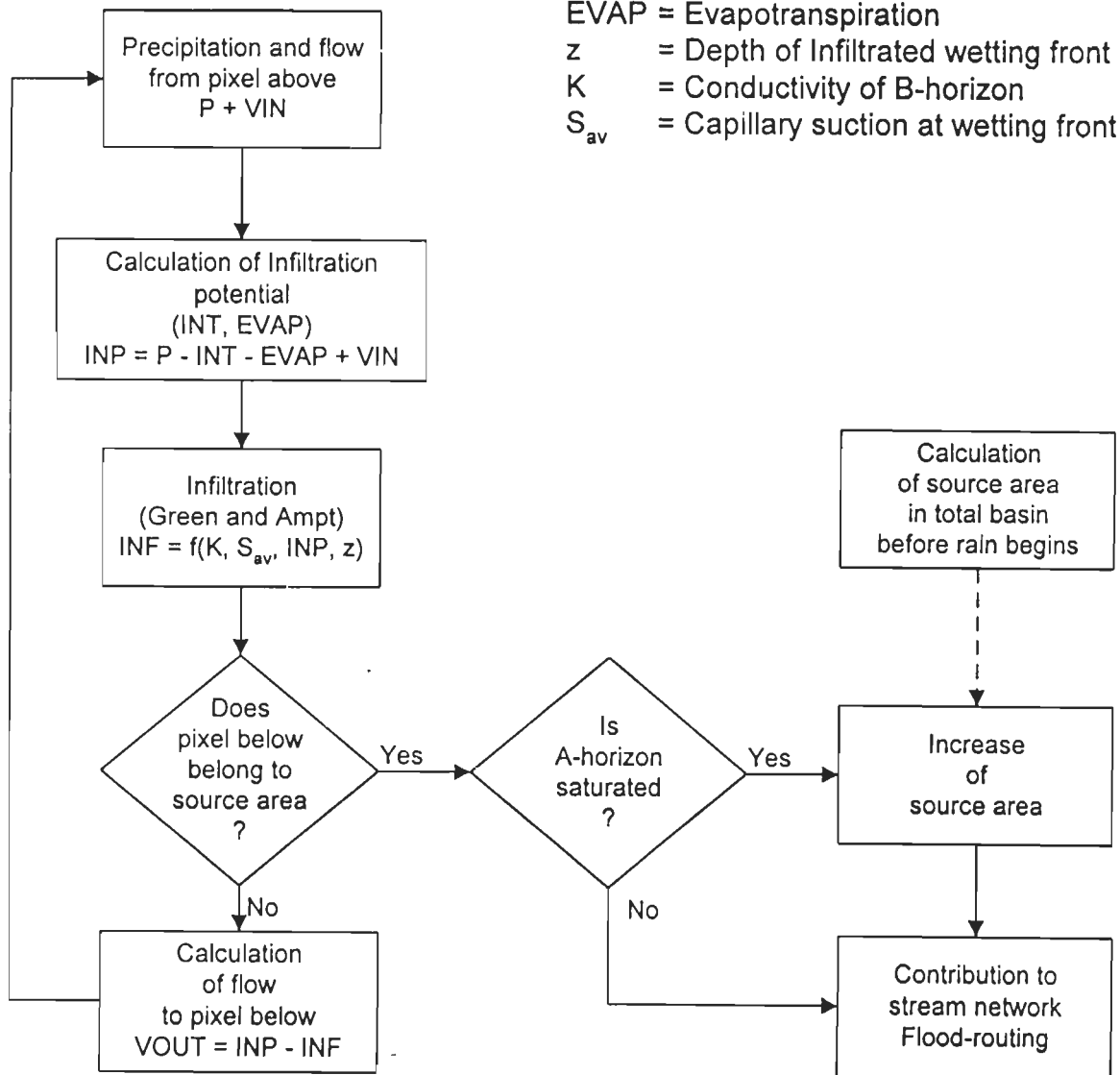


Fig. 2.10 : Structure of Hydrological Model using Source Area Concept
(Source : Neumann and Schultz, 1989)

For simulation of rainfall-runoff process, lumped conceptual models are well suited when sufficiently long hydrological time series exist for model calibration (Danish Hydraulic Institute, Lecture Notes, 1989). The typical field of applications for lumped models may be; (i) extension of short streamflow records based on long rainfall records, and (ii) real time rainfall-runoff simulation for flood forecasting. Lumped conceptual models can be used when a better model is not readily available for applications, such as runoff prediction from an ungauged catchment, general water balance studies, availability of ground water resources, irrigation etc.

Physically-based distributed models can, in principle, be applied to almost any kind of hydrological problems; the solution of which is obtained using cheaper and less sophisticated empirical, lumped conceptual or statistical models. However, for more complicated problems and applying spatial pattern of hydrological conditions within a catchment, physically based distributed models are well suited (Beven, 1985).

Beven (1985) identified four major areas which offer the greatest potential for the application of distributed models;

- i. forecasting the effects of land use change,
- ii. forecasting the effects of spatially variable inputs and outputs,
- iii. forecasting the movement of pollutants and sediments, and
- iv. forecasting the hydrological response of ungauged catchments where no data are available for calibration of a lumped model.

The choice of a model for a particular application is never a simple one. It is generally based on non-hydrological criteria such as the time, manpower and money available to support the investigations, availability of input data, desired accuracy of results and available facilities and resources. Selecting a model requires balancing the degree to which the model represents the hydrological system against the general difficulty in obtaining the desired results (Overtone and Meadows, 1976).

In this study, it is proposed to use Watershed module of Strathclyde River Basin Model (SRBM) as there is potential to incorporate input from remote sensing and DEM. Once the SRBM is selected, the next task is to collect the information about the input parameters precisely and efficiently. It is, therefore, essential that latest available techniques for data collection are used to extract information about input parameters.

Next chapter describes the use of remote sensing and DEM for the extraction of hydrological parameters, required for various runoff models.

CHAPTER 3

ROLE OF REMOTE SENSING AND DEM IN RUNOFF MODELLING

3.1 INTRODUCTION

Since, water is an important natural resource for human life, agriculture, forestry, navigation, irrigation, power etc., its assessment needs to be done using modern techniques of remote sensing. Many scientists e.g. Ragan and Jackson (1980), Johnson (1989), Cruise and Miller (1993) and Quinn and Beven (1993) have used hydrologic models which integrate remote sensing data and Digital Elevation Model (DEM) for rainfall-runoff modelling. Literature on rainfall-runoff modelling is voluminous and ever growing. This chapter demonstrates the utility of remote sensing data and DEM in runoff modelling, based on selected studies in the literature.

3.2 SPECTRAL RESPONSE CURVE OF WATER

Water is a unique feature to be delineated from remote sensing data. In general, the characteristic spectral reflectance curve for water shows reduction in reflectance values with increasing wavelength, so that in the near infrared wavelength the reflectance of deep and clear water is virtually zero, as shown in Fig. 3.1 (Mather, 1987). However, the spectral reflectance of water may be affected by the presence of organic and inorganic material and by the depth of waterbody itself. Due to unique characteristic in near infrared wavelength, water features are easily distinguishable on LANDSAT MSS band 4, TM band 4, SPOT band 3 and IRS band 4 images.

3.3 ROLE OF REMOTE SENSING IN RUNOFF MODELLING

Remote Sensing data offer synoptic and repetitive coverage of the catchment to determine and monitor the catchment characteristics, which otherwise is a time consuming and tedious task by conventional approach. Anderson (1979) discussed the use of remote

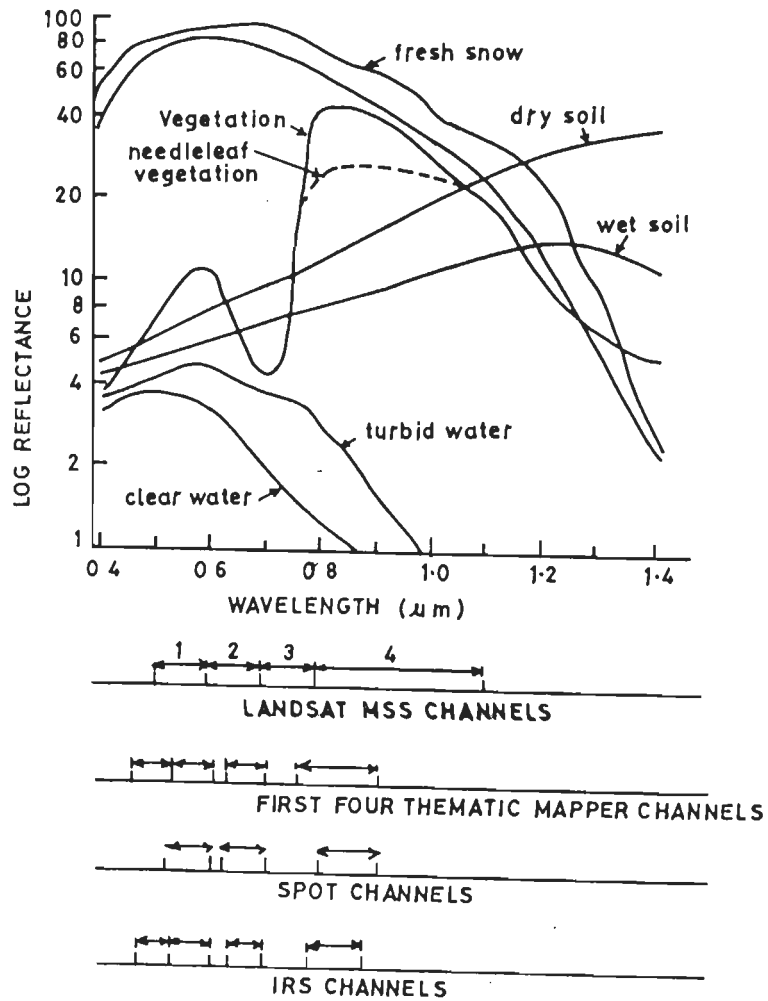


FIG.3-1: REFLECTANCE VALUES OF WATER AND OTHER FEATURES (SOURCE : HARDY, 1981)

sensing versus conventional methods in hydrology under three broad categories. In the first category, it is suggested that the conventional methods of data collection can be replaced by remote sensing data collection methods. The second category of research concentrates on combining both conventional and satellite data into hydrological modelling, while the third category initiates the efforts on problem solving unique to satellite capabilities. It was concluded that the satellite and conventional data tend to be complementary and may be considered for use in hydrologic studies.

Cragwall (1979) supported the use of satellite data as an input to hydrological model. As many of the hydrologic processes such as, overland runoff, erosion, groundwater recharge, including land cover, soil type, precipitation, are affected by various surface factors. He mentioned that a concerted effort is needed such that input from satellite can be incorporated in order to estimate these processes.

Ragan and Jackson (1980) recognised the potential of using LANDSAT data to derive land cover information in a cost effective and less tedious manner. They compared the conventional approach to a simplified procedure using the percentage of area covered by each hydrologic soil group, and found that the results from both the approaches are in agreement. They also tested the effect of changing the land cover classification scheme due to coarser set of categories with LANDSAT, and found that the coarser classification did not have a significant effect on runoff.

Peck et al. (1981, a) reviewed seven hydrological models for evaluating the use of remote sensing data. Study of the input and process parameters for the models revealed that in their present form, these models are not suitable for use with remote sensing data. Subsequently, Peck et.al. (1981, b) reviewed these models for their usefulness to extract soil moisture, land cover, impervious area, areal extent of snowcover, areal extent of frozen ground and water equivalent of snow cover from remote sensing data. Results indicated that the remote sensing data have only limited use in the hydrologic models in their present form but with minor modifications to the models, their usefulness could be enhanced. With reference to SWM IV, it is suggested that remote sensing data can be related to nominal lower zone storage, infiltration index and interflow index parameters.

Link (1983) discussed the capabilities of existing and emerging hydrologic models in relation to the data acquisition capabilities of remote sensing techniques. In a number of hydrologic models, the watershed physical descriptors such as landuse, land cover, channels, valley cross section and drainage network can be obtained through the analysis of remote sensing data. The hydrologic process parameters such as interception, infiltration, streamflow etc., can not be sensed directly from remote sensing data but the status of the other variables such as surface temperature, soil moisture, area of water bodies etc. can provide valuable feed back on the state of individual process. It was summarized that through enhanced inputs, periodic update of model and comprehensive calibration procedures, remote sensing technology can prove an asset in upgrading the model performance. Current and future capabilities of remote sensing for rainfall, snow cover, cloud cover, landuse, valley cross section, drainage network soil moisture, surface water and evapotranspiration which impact hydrologic modelling, have also been presented in this study.

Barrett and Herschy (1986) have summarised the observational requirement for hydrological application and water management, without taking any account of the sources or methods by which these data might be obtained. The requirements in terms of the feasibility of meeting these needs with existing or firmly anticipated remote sensing data have been presented in Table 3.1. This table reveals that many observational requirements are not fulfilled and that new satellite and sensor systems alongwith the algorithms are required to be developed for applications in hydrology and water management.

Johnson (1989) developed a digital map based hydrologic model known as MAPHYD. This model has been applied to Lena Gulch urban catchment in west of Denver, Colorado. The various information such as soil, landuse, elevation, groundwater, precipitation etc. are input in the form of digital data base. This model performs calculations for various hydrologic processes, and the peak discharge and its timing are compared with results of unit hydrograph procedure. Insignificant difference were found between two.

Ghosh (1991) has effectively used Watershed Module of Strathclyde River Basin Model, which derives remote sensing input coupled with DEM to determine evapotranspiration on a

Table 3.1 : Hydrological and Water Management Observational Requirements
(Source : Barrett and Herschy, 1986)

Parameters	Resolution			Frequency			Accuracy		
	Max	Min	Opt	Max	Min	Opt	Max	Min	Opt
A. Precipitation	100m	10km	1km	5min	1M	1h	10%	30%	20%
B. Snow Depth	30m	10km	1km	12h	1M	24h	2cm	10cm	5cm
C. Ice Cover	10m	1km	25m	12h*	7d	24h*	1%	20%	10%
D. Glaciers -Dimensions	10m	500m	25m	1y	10y	2y	1%*	5%	2%
E. Surface water areal extent	10m	100m	30m	12h*	7d	24h	1%	5%	3%
F. Groundwater - aquifer maps	50m	1km	100m	1y	5y	3y	5m	30m	10m
G. Evaporation	100m*	10km	1km	12h	10d	1d	10%*	30%	20%
H. Water quality - turbidity	30m*	300m	100m*	3h*	24h	6h*	10%*	50%	20%
I. Drainage -drainage area	10m	100m	20m*	3y	10y	5y	0.1%	1%	0.5%

Legend

FREQUENCY : h = hour ; d = day ; M = month ; y = year.

FEASIBILITY = Requirement can be generally met by existing satellite(s)

* = Requirement should be generally met by near future satellite(s)

Note : where a value is neither with box or asterix the observational requirement cannot generally be met either by existing or firmly expected future satellites, given the present state of the art.

daily basis for River Oykel in North Scotland, U.K. The results obtained have been encouraging for the use of remote sensing and DEM in hydrologic modelling.

DeVantier and Feldman (1993) reviewed the past efforts and current trends in using digital terrain model and GIS for hydrological studies, with the use of raster, triangular network and vector data storage methods and their computational and hydrologic aspects. It is suggested that the hydrologically significant parameters such as land cover, vegetation properties, thermal and moisture indices, snow cover and imperviousness, can be obtained through the analysis of remote sensing data. Lumped parameter, physically based and hybrid approaches to hydrologic models with respect to geographic data inputs have also been discussed, with greater emphasis to GIS application.

Rango (1985), Engman and Gurney (1991, a), and Chakraborti (1992) have pointed out the impact of remote sensing in hydrology. They all stressed that the remote sensing data can provide quick information which is not available through other means. Although many experiments may be needed to tie these observations together with conventional observations to validate them.

It is evident that runoff is one of the important hydrologic variables which is frequently used by hydrologists and water resource planners. Although, runoff can not be directly measured by remote sensing techniques, however the required input data can be derived from remote sensing for the estimation of model parameters and coefficients. Remote sensing data have been frequently used to provide information on precipitation, snow, evapotranspiration, soil moisture, land cover and catchment characteristics. A brief description on the use of remote sensing data to extract these parameters is given below:

3.3.1 PRECIPITATION

Precipitation, which is a major input to all hydrologic models, occur either in liquid form as rainfall or in solid form as snow. Conventionally, it is measured as point data using rain gauges, though satellites may provide useful information on the spatial distribution of rain producing clouds (Barrett and Martin, 1981). The remote sensing data currently

being used for quantitative estimates of rainfall, include visible and infrared images, microwave radiometry, spaceborne RADAR and ground based RADAR data. The detailed description of these techniques are given by Barrett and Martin (1981) and Engman and Gurney (1991, a).

Follansbee (1973) carried out a study in Mekong river catchment using a simple cloud indexing method which employs a fixed weighting system for different categories of clouds, identified from NOAA satellite. The resulting estimates of mean areal rainfall served as input for forecasting the river discharge and floods.

Amorocho (1975) calibrated the satellite estimates with the streamflow records for a catchment in Colombia. The model reproduced the major flood events quite well, although there was a tendency for it to smooth and subdue the smaller flood peaks.

Klatt and Schultz (1983) described a method for flood forecast which requires observed rainfall and runoff data as well as precipitation forecast. For this purpose, rainfall is measured by RADAR in a part of river Danube in Germany. On the basis of the rainfall observed up to the time of forecast, expected rainfall for the immediate future is forecasted by a probabilistic model. Both the rainfall measured by RADAR and precipitation forecast are input to rainfall-runoff model, which are used for the computation of real time forecasts. The flood hydrograph resulting from linearly decreasing rainfall intensity in probabilistic model is found to be more accurate than the constant intensity rainfall. Strubing and Schultz (1983) estimated the monthly runoff of river Baise in Southern France using NOAA satellite imagery. The mean daily temperature, weighted cloud cover index is calculated as input to the linear black box model.

METEOSAT data has been used as indicator of rainfall input to a runoff model (Rott, 1986). A cloud index was developed from thermal data and applied over two basins in Europe. This concept demonstrated that it was possible to predict runoff for 1 to 3 days ahead, starting from the measured flow.

Infra-red data from polar orbiting satellites and geo-stationary satellites can be used to generate long term runoff records in basins with sparse data, using a cloud cover index (Schultz, 1986). These indices can be developed from cloud top temperature and then transformed into runoff using a linear transformation function. For short term flood forecasts, he suggested the development of rainfall input from near-real time satellite data, and combining them with a ground based RADAR data. The flood flows can then be simulated using a runoff model capable of using this input.

3.3.2 SNOW COVER MAPPING

Snow, a renewable water resource, represents one of the most complicated parameters to be measured. The crystal size, temperature, liquid water content, density and thickness of snow vary within a short distance and rapidly over time. Since, field measurements of snow are hazardous and not very practical, remote sensing can offer time and cost effective means in inventorying and monitoring of snow cover area. Snowmelt runoff forecast requires several information related to snow pack properties such as snow cover area, snow depth, snow water equivalent and snow condition. Remote sensing promises to be an effective potential tool for monitoring many of the snow pack properties (Chakraborti 1992, Engman, 1993).

Rango (1980) used LANDSAT and NOAA satellite data in empirical seasonal snow melt runoff estimation and short term modelling approaches. Over a three years period, error in seasonal streamflow estimates for three basins in California were found to be reduced from 15% to 10% by using satellite data. For modelling studies in River Boise basin, satellite data produced a decrease in forecast error, for various short term periods, ranging from -2% to 9.6%.

Bagchi (1981) computed snowmelt runoff in Beas basin using LANDSAT images. A method was developed for the estimation of snowline altitude in the basin from the altitudes of a neighbouring basin obtained from the imagery. The streamflow generated with and without the help of LANDSAT images have been compared with the observed discharge and found to be satisfactory.

Dhanju (1983) studied the variations in snow covered areas of the Himalayas using weekly charts prepared by NESDIS of the National Oceanic and Atmospheric Administration, USA. TIROS-N and GOES images were used to prepare these charts to determine three categories of snow cover, employing a dot grid method. The height and fluctuation of snow line were observed by comparing area above known contour heights. Estimates of snowmelt were made by integrating the area under heavy snow cover graph for each season.

Eckhardt and Leaf (1986) used Sub Alpine Water Balance Model to forecast residual streamflow available in Windy Gap basin. The model can be updated through the adjustment of simulated water equivalent based on GOES satellite transmission of real time snow pillow data. During the runoff season, additional control can be achieved using direct estimates of areal snow cover from LANDSAT or other remote sensing systems.

Rango (1988) developed a method for forecasting the snowmelt runoff using Snowmelt Runoff Model (SRM). In a real time simulation, snow cover data up to the start of the forecast period can be generated, provided an estimate of depletion of snow cover during entire forecast period is made. Snow cover information were computed by using an average snow cover depletion curve, and no updating with actual snow cover data were used. In another test area, SRM was used with automatic updating of snow cover data.

The SLURP model developed by Kite (1991) simulates basin snowmelt runoff on a daily basis using inputs from LANDSAT and NOAA data. Other data used in the model included daily precipitation, daily maximum and minimum temperatures, daily hours of sunshine, elevation, aspect and slope, snow depth and water equivalent. The model has been calibrated for the Kootenay Basin in Canada without satellite data, and applied afterwards with snow cover and cloud cover estimated from satellite images. It is found that the model performance is best when satellite based snow cover data are used.

3.3.3 EVAPOTRANSPIRATION MODELLING

Evapotranspiration (ET) is the loss of water from the land and water surfaces of a catchment due to combined processes of evaporation and transpiration (Fleming, 1975). The process of evapotranspiration is of major importance in the simulation of runoff. The potential ET can be defined as the maximum rate at which water leaves the land surface in a given time assuming an unlimited supply of available moisture (Fleming, 1975). It varies both in time and space.

Remote sensing can not measure evaporation directly. However, there has been little progress made in the direct remote sensing of the atmospheric parameters which affects ET, such as near surface air temperature, near surface water vapour gradients and near surface winds (Engman and Gurney, 1991, a). Estimation of ET has been carried out using infrared satellite data (Soer, 1980; Jupp and Kalma, 1989). Very little work has been reported where satellite data in visible region have been used as input for the estimation of ET (Kotoda, 1986; Uchida and Hoshi, 1988). A procedure for estimating the regional ET for different crops has been reported by Caselles and Delegido (1987). They used satellite measured global radiation and maximum air temperature for this purpose.

Uchida and Hoshi (1988) developed a system to estimate actual ET utilizing LANDSAT derived landuse data, elevation and ground observed meteorological data of catchments in Japan. Landuse categories were used to assign albedo and soil heat flux constant empirically. The accuracy of estimation of ET was found to be fairly good for summer months.

Ghosh and Fleming (1993) estimated ET for a Scottish basin using LANDSAT-5 TM data and MORECS system (Meteorological Office Rainfall and Evaporation Calculation System). It was found that the landuse information derived through satellite data to estimate potential ET gives better results, and subsequently improves the discharge simulation. This approach requires elevation, slope, aspect, hydrologic landuse, temperature and solar radiation information, as input for the computation of potential ET.

Thus, various parameters such as solar radiation, land use, surface temperature and soil moisture can be assessed from remotely sensed data and ground data to compute the evapotranspiration.

3.3.4 SOIL MOISTURE MAPPING

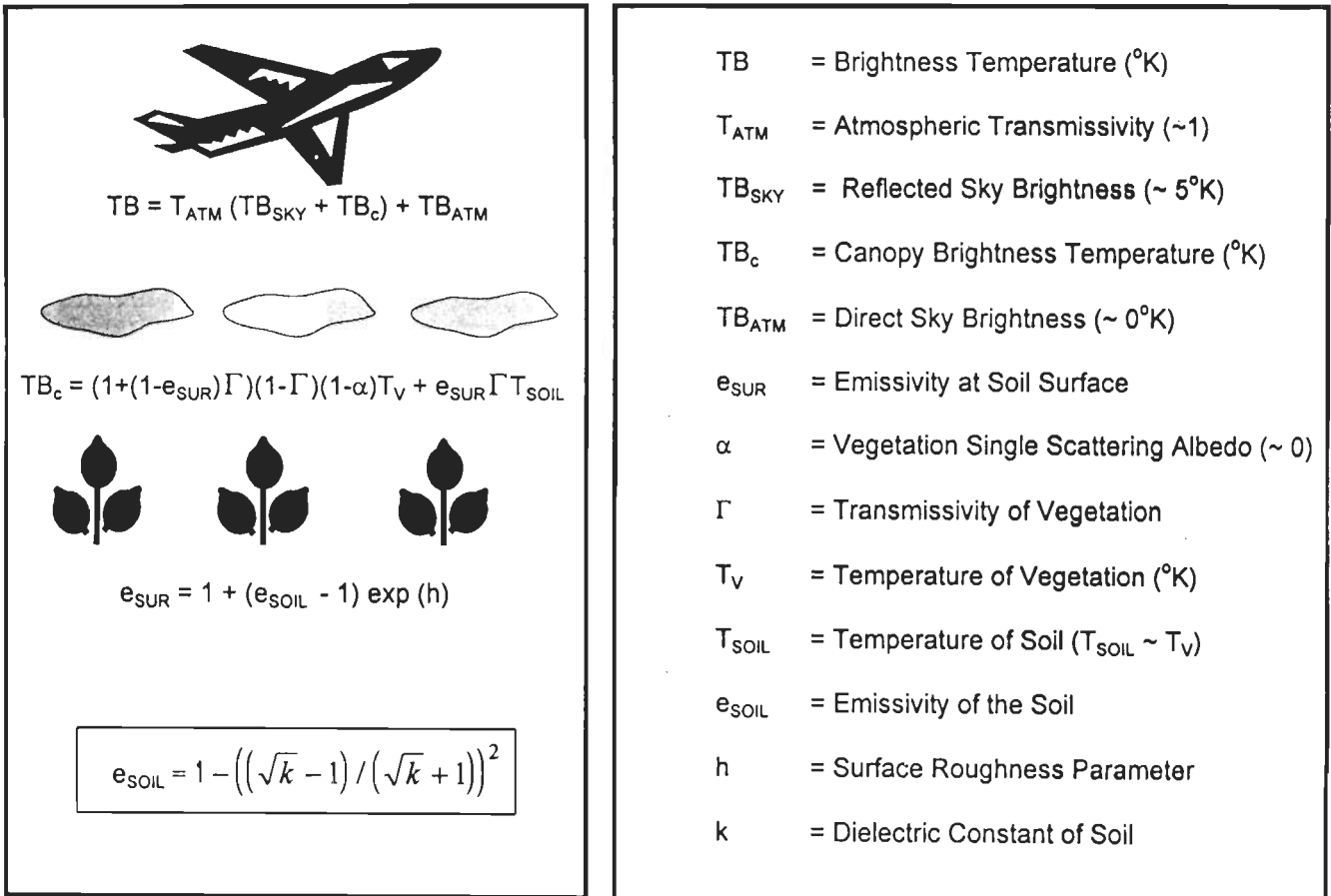
Soil moisture is one of the few observable hydrological variables that has an important role in water and energy budgets. In a catchment, it is highly variable due to inhomogeneity of soil properties, topography, land cover and the non-uniformity of rainfall (Engman and Gurney, 1991, a). At present, there is no practical approach to measure and monitor the soil moisture at the desired frequency. Remotely sensed data in microwave region offers the potential for quantitative measurements of soil moisture (Jackson, 1993). Fellows and Ragan (1986) and Das et al. (1992) used LANDSAT data for categorising the hydrologic soils to compute the runoff from SCS model.

Groves et. al. (1983) described a physically based stream flow model which incorporates information from remote sensing and ground data using grid cell approach in GIS. The linkage and operating concepts are very similar to Stanford Watershed Model IV with the inclusion of some modified components for simulating infiltration and soil moisture redistribution processes. The validation and testing of this model was limited only to runoff volume on the basis of a single event. For continuous simulation, a basic framework was suggested.

Groves and Ragan (1983) used Smith Parlange model for simulating the infiltration, which requires soil hydraulic parameter (depends on soil texture group) as input to the model, derived from remote sensing data. For continuous accounting of the moisture, the model needs daily satellite sensing of meteorological data such as surface temperature, solar radiation and cloud cover.

Jackson (1993) described an optimum system for soil moisture estimation and a microwave simulation model (Fig. 3.2). This model computes brightness temperature through the emissivity or reflectivity of the soil. The calibrated brightness temperature is

**PASSIVE MICROWAVE RADIOMETER MEASUREMENT OF SOIL
MOISTURE AT NADIR**



$k = f(\text{Volumetric Soil Moisture (\%)})$

Fig. 3.2 : A Passive Microwave Emission Model from Land Surfaces
(Source : Jackson, 1993)

used to categorise the ground element in respective cover condition, and dielectric constant is computed for the surface layer. Finally, the soil moisture is estimated using dielectric mixing model relationships and soil texture properties which are available on a global basis.

The possibility of using soil moisture as input data allows hydrologists to redesign models so that the soil zone, sub surface flow to ground water, interflow or baseflow can be conceptualized in a more physically realistic manner. The modelling of surface runoff could be accomplished with an infiltration approach that is spatially distributed requiring remotely measured soil moisture signature.

3.3.5 LANDUSE MAPPING

Landuse is one of the major and important parameters in runoff modelling, which is obtained from remotely sensed data. There are two general approaches where remote sensing has currently been used as input data for computing runoff (Engman and Gurney, 1991, a). In the first approach, runoff models that are based on landuse component have been modified to use multispectral satellite data to delineate landuse. In second approach, the runoff is computed by using relationships which are used in various geographic description of the catchment.

Allord and Scarpace (1979) estimated low flow and flood frequency in two Southwestern Wisconsin basins, which have been significantly improved by delineating the land cover from LANDSAT imagery. With the use of LANDSAT derived land cover, the standard error of estimates were lowered by 9% in each basin. In this study, relationship for low flow and flood flow were also developed. It has been found that the standard error (SE) of estimates for 2 years recurrence interval was 35% when using LANDSAT image, as compared to SE of 44% for conventional landuse data. The SE for 10 years recurrence interval relation was reduced from 52 % to 41% when LANDSAT data were used. Similarly, results of flood frequency analysis were improved using LANDSAT images. Low flow relations were improved from 17 to 20% and flood frequency relations from 45 to 50%, when LANDSAT images were used.

LANDSAT derived landuse has been used as an input to HEC hydrological model (U.S.Army Corps, 1981), for six basins spread over the U.S.A. (Rango et al., 1983). The results of the study had some very important conclusions as listed below;

(i) LANDSAT data reveals a 64 percent landuse classification as compared to conventional approaches, using a grid based data management system. On the other hand, aggregation of grid cells, on a watershed basis, produces a LANDSAT classification of about 95 percent.

(ii) Runoff simulation, using conventional and LANDSAT landuse data inputs, showed a very insignificant difference.

(iii) For basins larger than 25 km², LANDSAT approach is more cost effective compared with conventional methods. It amounts to approximately one quarter of the costs involved for conventional data.

For calculating flood hydrographs for Dreisam watershed in West Germany (Mauser, 1984) used SCS TR-20 Model (U.S.D.A., 1965). The satellite digital data was classified using a Maximum Likelihood for landuse classification. In order to provide compatibility between different types of ancillary data, such as soil, slope and aspect information to satellite derived landuse a GIS was also linked. The grid size was 64m by 104m. He was able to produce the flood frequency history of the basin, and extended his approach to simulate the landuse changes caused by a hypothetical deforestation triggered by air pollution, on a runoff hydrograph.

LANDSAT MSS images have been used to estimate basinwide runoff index for changing landuse within the Econlockhatchee basin (Still and Shih, 1985). It was found that an unsupervised classification technique using LANDSAT MSS band 5 and 7 could identify 22 classes of landuse. Excellent agreement between LANDSAT derived landuse maps when compared with USGS landuse maps was found for barrenland, urban, forestland and agriculture. Even though the basin had experienced vast changes in landuse,

the change in basinwide runoff index was negligible, suggesting no change in runoff for the entire basin.

France and Hedges (1989) used LANDSAT MSS & TM and SPOT data for landuse classification in North Wales and Italy. Both, digital and manual methods were compared from a hydrological standpoint, and the results showed improvement in the identification of small water bodies, as spatial resolution of satellite data increases. Overall, the results were found to be satisfactory for the TM imagery.

Das et al.(1992) computed the runoff curve numbers for Tilaiya catchment, India, using SCS model. Soil map was modified through visual interpretation of MSS FCC, utilizing physiography cum pattern recognition technique. Land cover map has been prepared using MSS images, which is further classified using vegetation index value. To validate the use of vegetation index in the model, the computations have been carried out both with and without vegetation index. Higher runoff values were found with the use of vegetation index which implies that actual surface condition has lower intercepting capacity than the one assumed on the basis of land cover class only.

Cruise and Miller (1993) demonstrated the use of remotely sensed digital data which can be integrated with a mathematical model to form an effective tool for the evaluation of watershed management practices. Images of airborne radiance data provided ground cover information, and were used in conjunction with topographic and soil data to provide input to runoff and sediment yield simulations. GLEAMS (Ground Water Loading Effects of Agricultural Management System) model has been used to evaluate the relative contributions of agricultural and forested land practices to runoff and sediment yields from Rasario basin. They suggested that the integration of DEM with remotely sensed images can be used to determine the optimum simulation strategies and required data input for future modelling efforts.

Kouwen et al. (1993) introduced a method to use distributed hydrologic model that eliminates the need for small computational areas, while maintaining the requirement of computing runoff for homogeneous watershed. The model was formulated to use remotely

sensed data, rainfall and initial soil moisture from weather RADAR, land cover and snow cover extent from LANDSAT or SPOT data. The method employs grouping of hydrologic response units having similar response characteristics on the basis of land cover maps. Model parameters are unique to individual land cover class which reduce the need for their calibration, and allow for the transfer of input parameters in time and space. The model has been calibrated for Grand River catchment using LANDSAT derived land cover data and RADAR rainfall data. It was verified on Saugeen and Humber river catchments of Southern Ontario, Canada, and applied to other watersheds. It was found that the error in average peak flow is between 19% to 41%. In some cases, the error was due to a poor distribution of rain gauges in the watershed, while in other case the error was due to inaccurate classification of satellite data into various land cover classes.

3.3.6 CATCHMENT CHARACTERISTICS

In hydrological modelling, information regarding the catchment characteristics are essentially required as input data. Catchment area, length of channels, perimeter and length of catchment are the basic catchment characteristics, which can be easily obtained through remote sensing data. To assess behaviour of catchment, various other characteristics can also be derived such as bifurcation ratio, overland flow length, stream frequency, drainage density, form factor, circularity ratio and elongation ratio (Eash, 1994).

Remote Sensing data can be used to obtain almost any information that is typically obtained from maps (Engman and Gurney, 1991, b). Killpack and McCoy (1981) used LANDSAT imagery to extract the drainage basin variables namely, basin area, total length of stream network, length of main channel and basin perimeter, to develop an empirical regional hydrological model for the prediction of streamflow. They concluded that since all four parameters are highly correlated, therefore, any of them could be used to compute the streamflow. Subsequently, an empirical relationship between streamflow and basin area was evaluated for 20 basins of the Wasatch Mountains which yielded a correlation coefficient of 0.92.

Chidley and Drayton (1986) compared the basin area and stream frequency with U.K. Flood Studies Report, summer and winter LANDSAT images at 1:250000 scale. Estimation of catchment area was generally found to be of the same order as that from maps, except summer LANDSAT image that provided a low level of details, excluding majority of low order streams. Length of main river from winter image was found to be 68% correct and that from the summer image 61%. A regression model which used LANDSAT derived parameters i.e. catchment area and stream frequency, was used to estimate mean annual flood with a correlation coefficient of 0.82.

Seethapathi et al. (1989) carried out several studies to extract the geomorphological characteristics for Indian basins. LANDSAT imagery was found to be a useful analytical tool for the evaluation of basin characteristics for Sabarmati basin. Chakraborti (1992) also emphasized that the remote sensing techniques are useful in evaluating the basin characteristics at spatial and temporal scale.

Nigam et al. (1995) attempted to identify and assess the basin characteristics of various sub basins in a part of Giri river basin using toposheets and visual interpretation of IRS-LISS II FCC. It was observed that the basin characteristics can be computed accurately from LISS II imagery which are particularly useful for those areas where either the toposheets are outdated, or not at all available.

With the above cited literature, it is clear that a majority of information can be obtained through satellite data, useful for hydrological investigations. Remotely sensed data are currently being used by many hydrologists, and a general consensus is that these data are extremely valuable. Information regarding catchment geometry are also computed through the use of DEM.

3.4 ROLE OF DEM IN RUNOFF MODELLING

The large quantity of elevation data required for runoff studies can easily be handled through a computer using a DEM. DEM is an array of values that represent topographic elevations in square or rectangular grid format. The DEM can be generated from ground

survey, digitizing methods and photogrammetric methods using stereo air photos and satellite data (Petrie, 1990). The DEM are generated typically in two forms i.e. (i) grid based DEM and (ii) Triangulated Irregular Network, TIN (Hogg et al., 1993).

Researches over the past decade have demonstrated the feasibility of extracting topographic information of hydrological interest, directly from DEM. Automated techniques are available for extracting the slope, drainage area, drainage divides, channel networks etc. These techniques are faster and provide more precise measurements than traditional manual techniques. As such, they have the potential to greatly assist in the parameterization of hydrologic runoff models, especially for larger catchments where the manual determination of channel network and catchment characteristics is a tedious, time consuming, error prone and often a subjective process. Automated techniques also have the advantage of generating digital data that can be readily imported and analysed in other systems.

In general, the hydrological models require physical characteristics, meteorological data and hydrological data of the catchment, as input in order to simulate runoff. Amongst these, the physical characteristics are related with topographic features which can be defined in terms of elevation. It is a spatial variable and has correlation with other variables such as hydrology, soil type, vegetation of the area (Briggs, 1981). Many quantitative hydrologic parameters such as contributing area, channel network, slope etc. may be interpreted from DEM, which has great potential in hydrologic models as shown in Fig. 3.3.

The need to understand the relationship between precipitation over a river catchment and resulting runoff is a fundamental problem in geomorphology and hydrology. Surface water runoff is a function of many inter-related factors that include climate, soil, landuse and physiography of catchment (Hogg et al., 1993). An effective method of quantifying drainage basin characteristics makes it possible to relate many of these factors to surface water runoff. Recently, physically-based hydrologic models that use topographic features extracted from DEMs have found increased applicability for the runoff prediction (Moore et al., 1991; and Quinn et al., 1991).

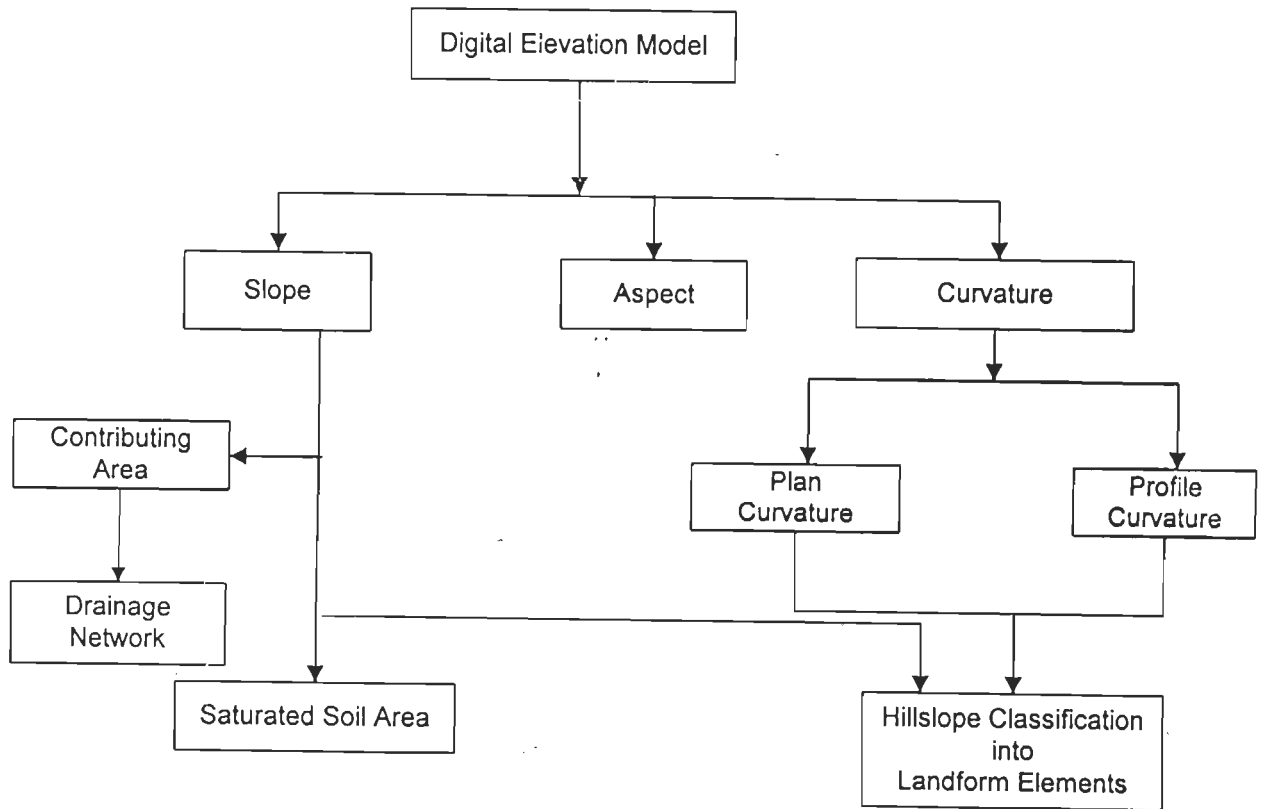


Fig. 3.3 : Use of DEM to Extract Hydrological Parameters
 (Source : Garg, 1991)

Quinn and Beven (1993) proposed a physically-based hydrological model, called TOPMODEL, which represents the effect of catchment heterogeneity, particularly with reference to topography on dynamics of hydrological response. It consists of two functions; (i) the probability density function that describes likely saturation potential, and (ii) the depth transmissivity relationship across the soil profile to a storage runoff relationship. These two functions may be combined to get a soil topographic distribution function.

In most of the modelling approach, water is allowed to flow only in one direction i.e. the steepest downward slope. Quinn et al. (1991) have, however, suggested two different distribution functions i.e. one directional distribution and the multi-directional distribution. It is observed that multi-directional flow gives a more realistic pattern, except in valley bottoms, where the algorithm could be improved by overlaying the actual drainage system. Holmgren (1994) also defined a similar distribution function for proportioning the runoff towards downward slopes in multi-directions. Runoff proportions in multiple directions are further converged by introducing the flow distribution function.

A number of parameters related to physical description of the catchment which can be obtained from DEM, include delineation of catchment boundaries, channel network, slope and aspect of catchment, land cover, surface and subsurface geology (Hogg et al., 1993).

3.4.1 SLOPE AND ASPECT FROM DEM

Slope and aspect which are standard derivatives of the terrain are required almost in every hydrologic study. Slope is defined by a plane tangent to the surface, as modelled by the DEM at a point (Burrough,1986). It has two components, viz., gradient, which is the maximum rate of change in altitude, and aspect which is the compass direction of this maximum rate of change in altitude (Skidmore, 1989).

Slope affects the runoff, sedimentation rate and many other hydrologic processes. Sharpnack and Akin (1969) developed an algorithm for computing the slope and aspect from

a 3x3 elevation matrix using a regression coefficient. As shown in Fig. 3.4, the relationships for regression coefficients slope and aspect are as follows;

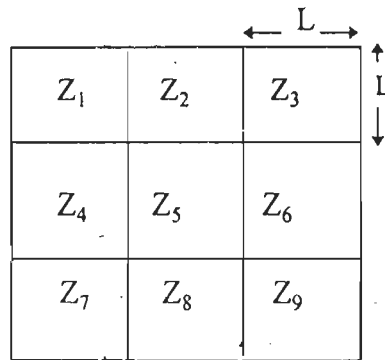


Fig. 3.4 A 3x3 Elevation Matrix for Computation of Slope and Aspect

$$\text{Slope} = (B_1^2 + B_2^2)^{1/2} \quad (3.1)$$

$$\text{Aspect} = \arctan (B_2 / B_1) \quad (3.2)$$

where

$$B = \begin{bmatrix} B_1 \\ B_2 \end{bmatrix} = \begin{bmatrix} (Z_1 + Z_2 + Z_3 - Z_7 - Z_8 - Z_9) / 6L \\ (Z_3 + Z_6 + Z_9 - Z_1 - Z_4 - Z_7) / 6L \end{bmatrix}$$

Z_1, Z_2, \dots, Z_9 = elevation values

L = grid size

Papo and Gelbman (1984) proposed a two dimensional Fourier Transformation algorithm to define the slope as first derivative and curvature as the second derivative at any point within the DEM. This algorithm provides an insight into the inherent characteristics of the topography by examining the spectral density matrix to produce more accurate results.

A vector based algorithm is proposed by Ritter (1987) to determine the slope and aspect using a four neighbour connectivity from its normal vector. In this algorithm, only four neighbours of a 3x3 matrix are taken into account. The normal vector is an arrow with its tail in the center of the pixel pointing at right angle to the pixels plane. The amount and direction of tilt of the vector is related to the slope and aspect of the pixel respectively.

The assumptions made in the algorithm are that the pixels are square rather than rectangular and that they are aligned in the north-south direction. This algorithm is a good compromise between accuracy and computational complexity as it takes only four pixels.

Zevenbergen and Thorne (1987) represented the surface by following equation;

$$Z = A x^2 y^2 + B x^2 y + C x y^2 + D x^2 + E y^2 + F xy + G x + H y + I \quad (3.3)$$

where

$$A = [(Z_1+Z_3+Z_7+Z_9)/4 - (Z_2+Z_4+Z_6+Z_8)/2+Z_5]/L^4$$

$$B = [(Z_1+Z_3-Z_7-Z_9)/4-(Z_2-Z_8)/2]/L^3$$

$$C = [(-Z_1+Z_3-Z_7+Z_9)/4+(Z_4-Z_6)/2]/L^3$$

$$D = [(Z_4+Z_6)/2-Z_5]/L^2$$

$$E = [(Z_2+Z_8)/2-Z_5]/L^2$$

$$F = (-Z_1+Z_3+Z_7-Z_9)/4L^2$$

$$G = (-Z_4+Z_6)/2L$$

$$H = (Z_2-Z_8)/2L$$

$$I = Z_5$$

$$\text{Slope} = (G^2 + H^2)^{1/2} \quad (3.4)$$

$$\text{Aspect} = \arctan (H/G) \quad (3.5)$$

Where Z is the elevation and x,y are the coordinates of the cell with origin as central cell. The nine coefficients, A,B,C,... I, can be determined from the nine elevations of the 3x3 matrix (Fig.3.4) by Lagrange Polynomials. After having determined the coefficients, the slope, aspect and curvature can be computed. The upslope drainage area and maximum drainage distance are also determined for every point within the altitude matrix.

Skidmore (1989) compared six algorithms to ascertain the effectiveness to compute the aspect and gradient from a gridded DEM, based on a 3x3 moving window. The first method defines gradient as the gradient of maximum drop, while the second method considers gradient as the gradient of steepest drop or steepest rise. The third method tested was a second order finite difference method, while the fourth one was a third order finite difference method. The fifth and sixth methods computed gradient as the derivatives of

linear and quadratic surface respectively. The general regression model and the third order finite difference method were found to be the most accurate.

3.4.2 CHANNEL NETWORK AND CATCHMENT CHARACTERISTICS FROM DEM

Methods of extracting characteristics of catchments and channel network from DEM have been studied extensively over the past three decades (Moore et al. 1991). Determination of stream network in a catchment is an important characteristics, which is related to water flow, erosion and sediment deposition (Hogg et al., 1993). Numerous quantitative measurements of catchment characteristics such as bifurcation ratio, drainage density, drainage frequency, shape factor etc., which are dependent on area and perimeter of catchment, length of channels, distance of farthest point etc., and can be obtained from DEM.

Peucker and Douglas (1975) developed a method to detect the surface specific points and lines e.g. pits, peaks, ridge lines, ravine lines and break lines from DEM. This algorithm extracts the global information (i.e. catchment information) through local operation (i.e. using a 3x3 window) only. The discreteness of array in all three dimensions poses problems in recognizing intrinsically continuous features. The main drawback of this algorithm is that the detection of feature is strictly local and have no continuity. Many pits appear as isolated dots, while channels may be broken. Therefore, to check the discontinuity, preprocessing is performed before applying any procedure.

Mark (1983) described two algorithms for the detection of drainage network from a depressionless DEM. One of these detects points of local upward concavity which is similar to Peucker's method, while the other simulates runoff process to predict channel locations. The second approach accumulates the drainage area to successively lower pixels, delineating the major drainage lines. The former algorithm is fast but has poor relationship to hydrologic processes, while the second one is physically sound but takes more computation time.

248192



O' Callaghan and Mark (1984) presented a more sound method (Fig. 3.5) of extracting drainage network from gridded elevation data. The elevation matrix is smoothed using a 3x3 window to reduce the number of pits. After smoothing, drainage direction matrix (DDIRN), drainage feature matrix (DLABL), drainage basin matrix (DBASN), drainage accumulation matrix (DAREA) and drainage link matrix (DLINK) are computed which ultimately gives channel network.

Band (1986) described an approach to automatically extract the channel and divide network from DEM. Peucker's (1975) approach was used to flag ridge and channel lines which are discontinuous and thick. These segments are thinned to one pixel wide lines using an iterative parallel processor. After thinning process, segments were connected by draining downstream node to successively lower pixels until another stream segment is encountered. Once again, thinning process is applied to achieve channel network. Useful input information to hydrological data is provided by registering the remote sensing imagery and soil information with DEM.

Jenson (1985) described a process in which drainage cells are identified by examining the symmetric and asymmetric cross sections in a 3x3 window. Identified channel cells are grouped starting from lowest elevation. Channels are labelled and at the end drainage basins are linked. It is assumed that all points having elevation equal or higher will be a part of catchment. As an extension to this, Jenson and Trautwein (1987) developed a method to identify depressions which are hydrologically significant. Removal of unwanted depressions simplifies the automatic finding of watershed boundaries. This procedure is slower, being iterative.

Further improvement to the above approach was carried out by Jenson and Domingue (1988) in order to extract topographic structure and delineate catchment and overland flow path from DEM. They presented a detailed description of conditioning procedures which generate three types of data sets; (i) depressionless DEM, (ii) flow direction data, and (iii) flow accumulation data. These data sets are further processed in order to delineate drainage networks, overland paths, catchment and subcatchment delineation. Jenson (1991) applied the above approach to two data sets of different resolution at five minute arc cell

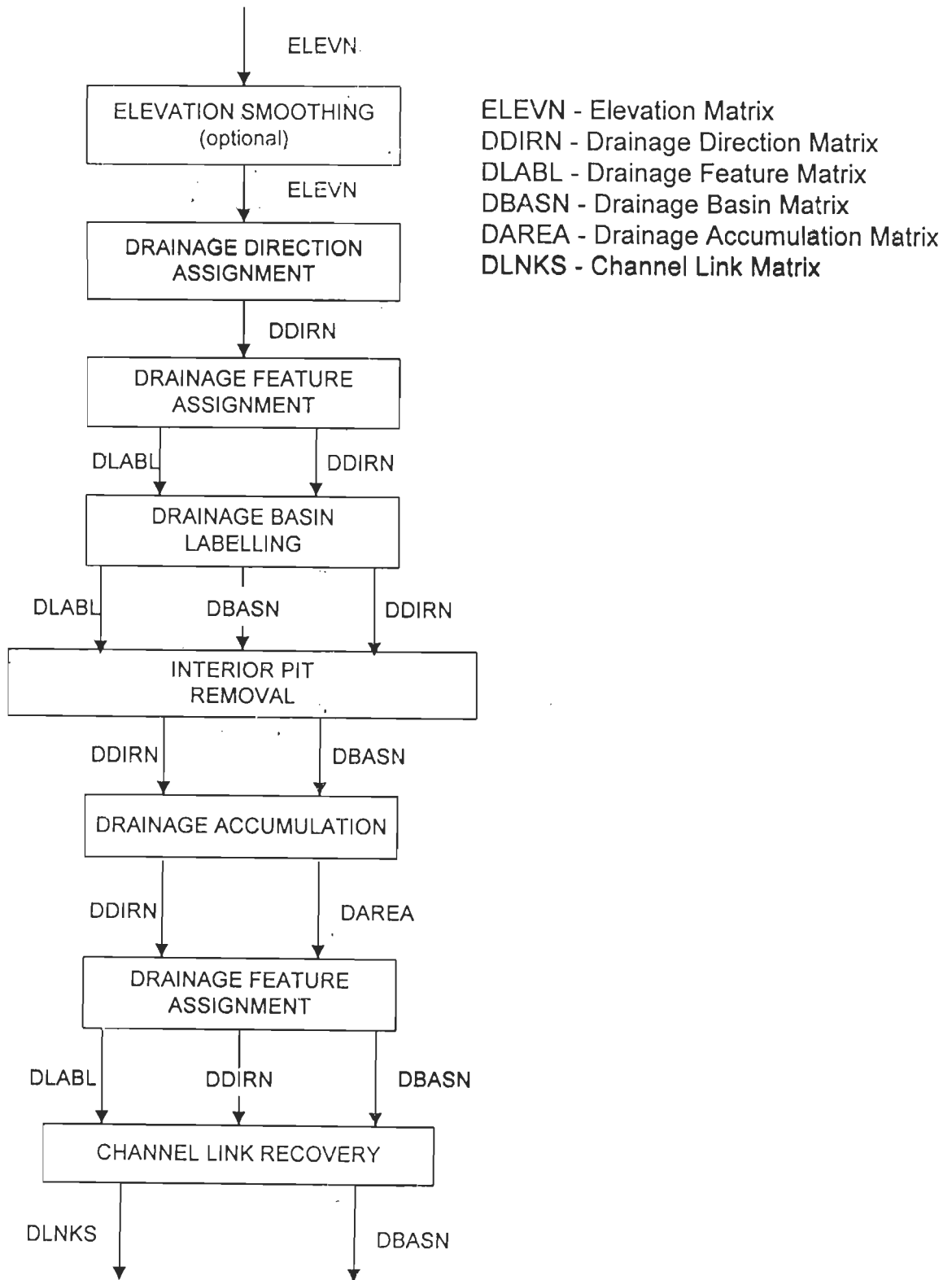


Fig. 3.5 : Illustration of Procedure for Drainage Network Recovery
 (Source : O'Callaghan and Mark, 1984)

size and other at 30 second arc resolution. It is found that increase in cell size produced lower slope value which is a function of both horizontal and vertical resolution of the DEM.

Smith and Brilly (1992) described an automated method of numbering grid cell elements of a DEM which was subsequently used to dictate the order of computations within a distributed parameter model for overland flow computations. Similar to Jenson and Domingue (1988), they have computed flow directions on the basis of steepest downward slope.

Martz and Garbrecht (1993) developed a computer program called DEDNM (Digital Elevation Drainage Network Model) to delineate drainage network and subwatershed parameters, directly from DEM. In a depressionless DEM, relief was imposed on all flat areas for obtaining flow direction in a flat area. The areas where more than one direction have equal downward slope, the flow direction has been arbitrarily assigned in the direction of maximum slope encountered first. All cells with a drainage area greater than a user specified channel maintenance constant have been classified as part of the drainage network. Garbrecht and Martz (1993) applied the above approach on Bill Creak catchment, and computed channel length, slope, drainage density, bifurcation ratio etc., from DEM and topographic maps. It was found that on an average the values of these parameters are within 5% of those derived from topographical maps.

A common method of channel network extraction is based on minimum contributing area, i.e. an area required to drain from a point to form a channel, which is termed as threshold area. Helminger et al. (1993) studied the effect of threshold area selection on morphometric properties such as drainage density, length of drainage path, external and internal links, and scaling properties based on Horton's law. The DEM for three catchments, having a grid cell size of 30m, have been selected for examination. The results indicated that morphometric properties vary considerably with the threshold area value. However, they have suggested that a variation in threshold area value does affect the channel network extraction and hence should be used with caution in hydrological analysis. Furthermore, no relationship could be established between threshold area value and

channel network extraction. Use of any arbitrary value has been suggested for threshold area, depending upon the correspondence to existing channel network.

Eash (1994) developed a system known as Basin Characteristic System (BCS), to create digital maps representing drainage divide, drainage network, elevation contour and basin length, and to assign attributes to these features. It computes 24 morphometric characteristics of catchment, and quantifies two climatic characteristics i.e. mean annual precipitation and 24 hour precipitation for two years. Insignificant differences were observed when BCS measurements compared to topographic map measurements.

Agyei et al. (1995) carried similar analysis to Helmlinger et al. (1993) using smaller threshold area increments and a wider range of geomorphological parameters. The study focuses its attention on the variation of map scale to geomorphological parameters such as drainage density, bifurcation ratio, area ratio, length ratio, link length and main stream length. At a fixed map scale, the mean absolute percentage error in the geomorphological parameters caused by a decrease in vertical resolution was within 0-5% range for medium size catchments, and 0-10% range for the small catchments. It has been suggested that the vertical resolution of the DEM be considered satisfactory if the ratio of the average drop per pixel and vertical resolution is greater than unity. This ratio criteria may be used to define the minimum pixel area for reliable channel network.

Thus, it is observed that various catchment characteristics which can be obtained directly from a DEM, include drainage area, channel length, drainage density etc. These characteristics could be easily and effectively used in rainfall- runoff modelling.

It is concluded from above studies that large number of parameters are required for distributed hydrologic model to consider spatial variation of land parameters. It is not practicable to measure these data directly in field particularly for a large catchment. Because of scale on which variations exist in the real world, all distributed models approximate spatial variability of parameters in a way that could be referred to as lumping. Whereas a lumped parameter model attempts to condense all influences of spatial nonuniformities into

mathematically equivalent point coefficient value which require less number of parameters to define all hydrologic processes. In this study, it is therefore proposed to examine the utility of satellite and DEM derived input parameters into SRBM, a lumped hydrologic model.

The next chapter outlines an approach used for rainfall-runoff modelling where input data are extracted from various sources such as field, published literature, topographic map, DEM and remote sensing products.

CHAPTER 4

METHODOLOGY ADOPTED FOR RAINFALL - RUNOFF MODELLING

4.1 INTRODUCTION

The main object of this study is to generate runoff values for a catchment using a hydrological model requiring inputs as hydrometeorological and physical characteristics of catchment derived from remote sensing and other sources. This chapter describes in detail the structure of Watershed Module of Strathclyde River Basin Model (SRBM) as well as various input and calibration parameters used in this study. The methodology used for the computation of flow direction, flow accumulation values and catchment characteristics from DEM, and assessment of landuse information from remotely sensed data has also been described. Finally a sensitivity analysis of various parameters has been carried in order to study the effect of these on the runoff simulation.

4.2 MODELLING STRATEGY

The various steps, followed in the present study are presented in Fig. 4.1. Broadly, three types of data have been used to calibrate model parameters for simulation. Topographical maps have been used to develop a Digital Elevation Model (DEM) and to compute catchment characteristics, remotely sensed data to collect landuse information, and field data for meteorological information. The modelling approach consists of three components ;

- (i) Development of DEM and extraction of catchment parameters
- (ii) Analysis of remote sensing data and
- (iii) Integration of field data, DEM and remote sensing data in model to assess runoff

For all the above components, various programs in FORTRAN 77 have been developed and used in the study.

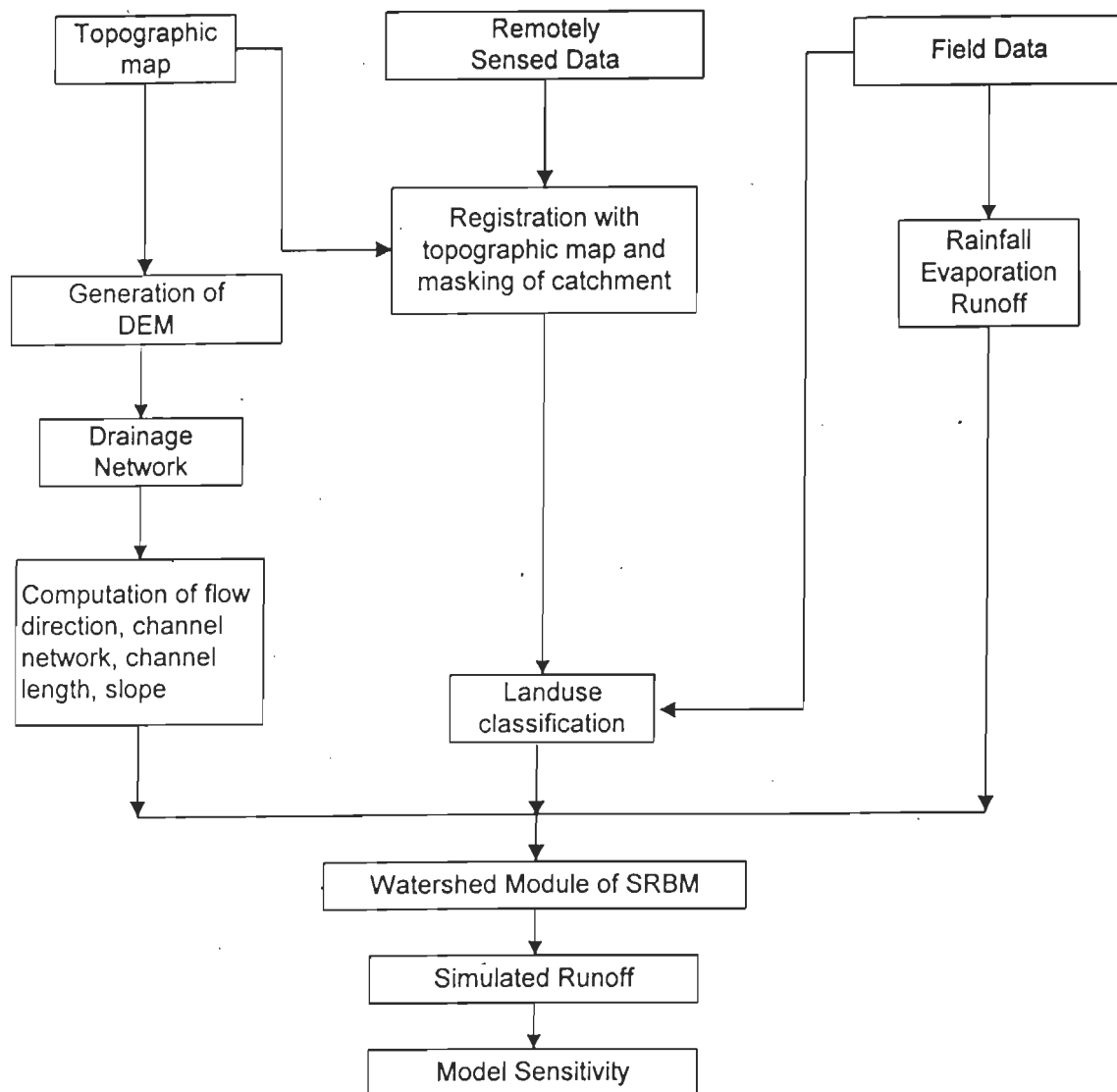


Fig. 4.1 Flow Chart of Methodology Used

The Watershed Module of Strathclyde River Basin Model is selected for this study. This model has been used for catchments spread over Australia, Britain, Europe and Nigeria (Black, 1973; Walker, 1979; McKenzie, 1983; Hynes, 1985; Oke, 1991 and Ghosh, 1991). It is capable of simulating the snowmelt, rainfall distribution ranging from hour to year time basis from daily data. It can generate runoff at a time frame of 15 minutes. Furthermore the physical characteristics of the catchment may be split into two categories (i) channel characteristics and (ii) landuse characteristics. Conventionally both the characteristics are derived from topographical maps, while in this study the methodology has been developed to use DEM and remote sensing data. The Strathclyde River Basin Model is briefly described in the next section.

4.3 DETAILS OF WATERSHED MODULE OF SRBM MODEL

The Strathclyde River Basin Model (Fleming and Mckenzie, 1983), as explained in section 2.3.3, consists of three main modules;

- (i) The Watershed Module to simulate land surface response,
- (ii) The Sediment Erosion Module to simulate erosion, transport and deposition of sediments,
- (iii) The Water and Sediment Routing Module to estimate the yield at the outlet of catchment

Since, the main objective of this study is runoff simulation, only the Watershed Module has been used, as shown by flow chart in Fig. 4.2. The model has been used worldwide with success attributed to its high degree of sophistication and versatility. The practical advantages of the SRBM includes:

- (i) Forecasting of floods and droughts both long term and real time (Dickson, 1984).
- (ii) Study of river channel design vis-a-vis flood (Fleming and Hynes, 1985)
- (iii) Planning landuse types to assess the effect of landuse and their changes to water and sediment response (Fleming and Hynes, 1985; Fleming and Dowling, 1987).

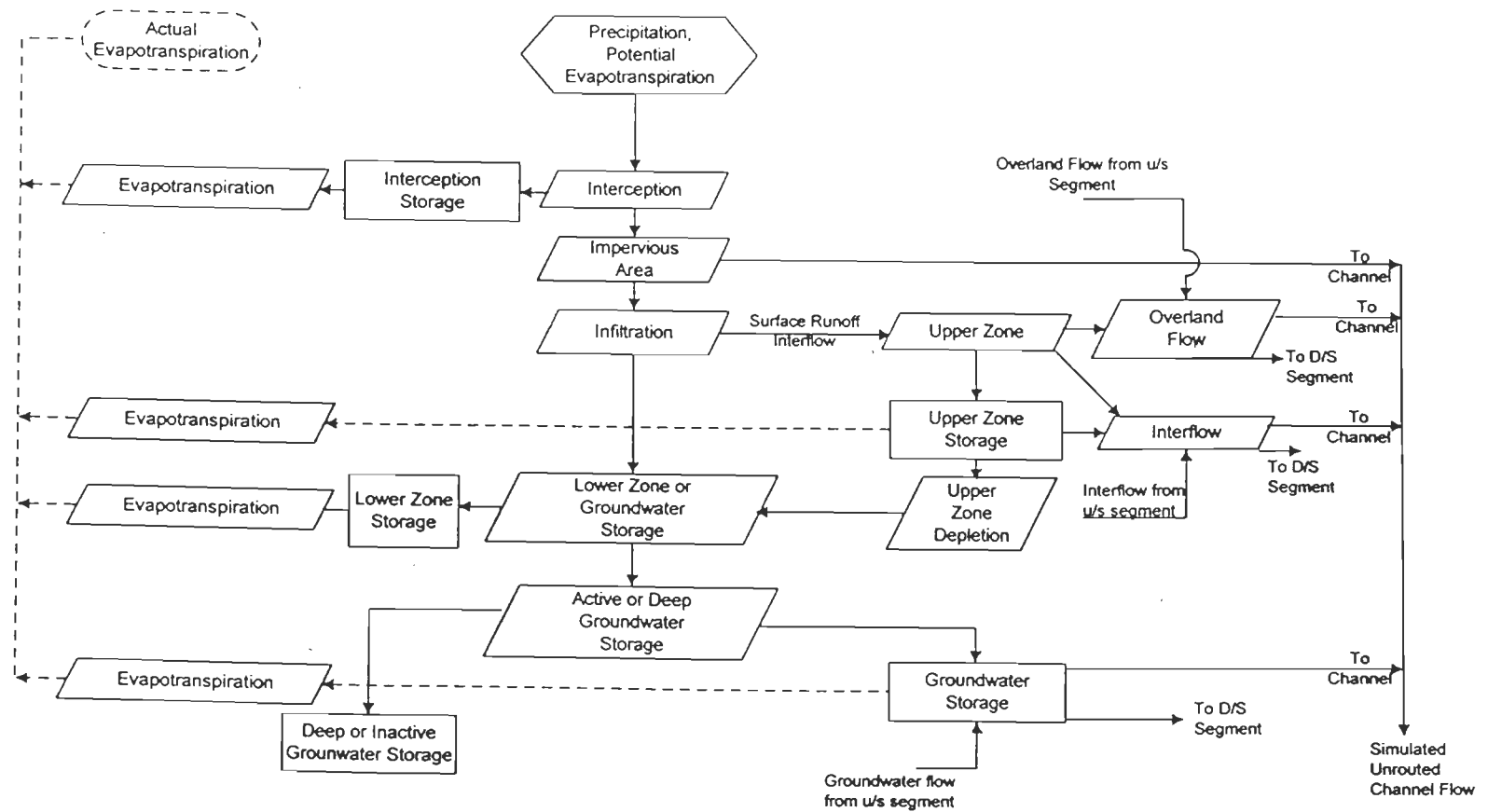


Fig. 4.2 Flow Chart of the Watershed Module of SRBM
(Source : Fleming and McKenzie, 1983)

- (iv) Assessment of water yield for reservoir design (Oke, 1991).
- (v) Study of reservoir sedimentation and related economics (Oke, 1991).
- (vi) Study the impact of changing landuse on evapotranspiration values and generation of runoff using remote sensing inputs (Ghosh, 1991).

This module is primarily based on Stanford Watershed Model IV (SWM IV). The Watershed Module has the flexibility to process the daily rainfall data into hourly values. The results of this module, if required, can directly be used by other two modules i.e. Sediment Erosion Module and Water and Sediment Routing Module. One of the major advantages in the SRBM is the representation of segments in terms of elevation. The model performs the simulation by dividing it into a maximum of three segments, on the basis of elevation as upland, midland and lowland segments.

The model requires precipitation, evaporation and catchment characteristics as inputs to produce the total runoff. The various processes represented by the model are interception, evapotranspiration, infiltration, interflow, ground water flow etc. These processes are described by 32 assigned and calibration parameters, as listed in Table 4.1. A detailed description of these parameters is given in Appendix A-1.

In the main program of the model, subroutine named 'DHOURLI' converts daily precipitation data into hourly values. For the conversion of the same, three parameters namely gradient (GR), standard deviation (SD), and cut-off point (CP) have been defined (refer to Table 4.1) and is dependent on the characteristics of hourly rainfall pattern (appendix A-1).

The model parameters such as proportion of impervious area (IMPV), canopy interception (EPXM) and ET from lower zone (K3) are associated with landuse, while overland flow path (L), slope of flow path (SS) and ratio of segment area to total catchment area (RIVER) are associated with DEM. The nominal upper zone soil moisture (UZSN), nominal lower zone soil moisture (LZSN), infiltration parameter (CB) and interflow index (CC) are the main calibration parameters of the model. Interflow recession (IRC),

Table 4.1 List of Watershed Module Parameters and Probable Data Source

(Source: Fleming and Mckenzie, 1983)

<i>S.N.</i>	<i>Parameter</i>	<i>Description</i>	<i>Source</i>
1	POWER	Exponent in the infiltration function	Assigned
2	POINT	Run indicator of with or without snow case	-do-
3	UZSNWF	Weight Factor for AEPI	-do-
4	PEADJ	ET adjustment factor for catchment	-do-
5	GAGEPE	Adjustment factor for pot. ET for segments	-do-
6	K1	Proportion of segment to gauge precipitation	-do-
7	IMPV	Proportion of impervious area to segment area	Remote Sensing
8	EPXM	Canopy interception	-do-
9	UZSN	Nominal upper zone storage	Calibration
10	LZSN	Nominal lower zone storage	-do-
11	CB	Infiltration rate into the lower zone	-do-
12	CC	Ratio of interflow detention and surface detention	-do-
13	K3	Evapotranspiration from lower zone	Remote Sensing
14	K24L	Fraction of groundwater lost to inactive groundwater	Calibration
15	K24EL	Evapotranspiration from groundwater	-do-
16	L	Average flow path length	DEM
17	SS	Average flow path slope	-do-
18	NN	Manning's coefficient for overland flow	Assigned
19	IRC	Daily interflow recession	Calibration
20	KK24	Daily groundwater recession	-do-
21	KV	Variable recession rate of groundwater	-do-
22	RIVER	Ratio of segment area contributing directly to channel to total catchment area	DEM
23	UZSI	Upper zone initial storage	Assigned
24	SGWI	Initial groundwater storage	-do-
25	GWSI	Initial groundwater slope storage	-do-
26	RESI	Initial surface detention storage	-do-
27	SRGXI	Initial interflow detention storage	-do-
28	SCEPI	Initial interception storage	-do-
29	AEPI	Antecedent potential evapotranspiration storage	-do-
30	GR	Gradient used to calculate the number and duration of rain events from daily total	-do-
31	SD	Standard deviation relating to gradients	-do-
32	CP	Cut-off points for the gradients	-do-

groundwater recession (KK24), variable groundwater recession (KV) subsurface flow (K24L) and evaporation from groundwater (K24EL) are the other calibration parameters. Fraction of groundwater loss to deep inactive groundwater (K24L) and evaporation from groundwater storage parameter (K24EL) are usually assigned zero values. Similarly variable groundwater recession parameter (KV) is also set at zero and increased, if necessary, to improve groundwater recession. The initial storage parameters are usually estimated after a few trial runs.

The parameters which are associated with DEM can be extracted by using DEM of the area. Development of DEM and extraction of model parameters is described in next section.

4.4 DEVELOPMENT OF DEM AND PARAMETER EXTRACTION

DEM is one of the important data bases required for hydrologic modelling. Integration of DEM with remote sensing and other data to the proposed watershed model is one of the major objectives of this study. The methodology of DEM generation and its pre-processing to get a depressionless DEM is explained below. The depressionless DEM has been used to extract various catchment parameters, such as delineation of catchment, segmentation of catchment on the basis of elevation, determination of flow direction and flow accumulation, extraction of channel network and hence the channel length and slope values. Most of these parameters have been extracted from depressionless DEM using a 3X3 elevation window.

4.4.1 GENERATION OF DEM

For the generation of a DEM, the very first question arises as to which technique should be considered for the collection of elevation data. Generally, three methods are available to acquire the elevation data (Petrie, 1990) ;

- (i) Ground survey methods
- (ii) Photogrammetric methods and
- (iii) Digitizing methods

A brief summary of these three methods, as applied to terrain modelling, in terms of the elevation accuracy required and the extent of area which has to be modelled, is presented in Table 4.2. It is evident from this Table that the topographic maps are most suited in this study to generate DEM. Therefore, the contours, spot levels, bench marks and triangulation stations have been digitized. This digitized data have been further subjected to interpolation at a grid size of 500m using interpolation module of ILWIS (Integrated Land and Water Information System) package. The gridded DEM, thus generated, has been used for the extraction of catchment characteristics.

Table 4.2 Summary of the methods of DEM data collection

(Source: Petrie, 1990)

<i>Source of DEM data</i>	<i>Method used</i>	<i>DEM accuracy</i>	<i>Areal coverage</i>
Ground survey	Total or semi total station	Very high	Limited to specific sites
Photogrammetric measurement	Stereoplotting machines	(i) High from spot heights (ii) Low from contours	Large area projects especially in rough terrain
Carto-graphic (existing topographic maps)	(i) manual digitizing (ii) semi automatic digitizing (iii) fully automatic raster scanning	Low - derived from contours on medium and small scale topo maps	Nationwide at small scale

4.4.2 PRE-PROCESSING OF DEM

Almost every DEM contains depressions, which may occur mainly due to two reasons; either they are actually present in the area, or they are introduced by the algorithm used for the interpolation of elevation data. Generally, it is observed that these depressions may be present either as a single cell or multi cells. In both the cases, the depressions cause hindrance to flow routing, as the algorithm is unable to decide the next direction of flow to advance the water from depression. It is therefore extremely important to remove these depressions from a DEM, before it is used for the extraction of catchment characteristics.

There are several methods available to remove the depressions from DEM. O'Callaghan and Mark (1984) suggested that the depressions can be removed by raising the elevation of depression cell by a weighted sum of a point and its eight neighbours in a 3x3 window. Another method is to raise the total depression area by assigning the lowest value along its boundary (Jenson and Domingue, 1988).

In the proposed work, the removal of depressions have been undertaken, based on Jenson and Domingue's approach (1988), wherein all the cells in depressions are raised to the lowest elevation along the rim of depression. First of all single cell depressions are removed and then the multi cell depressions are removed. The steps followed in each case are given below, using a 3x3 window:

Identification and removal of Single Cell Depression:

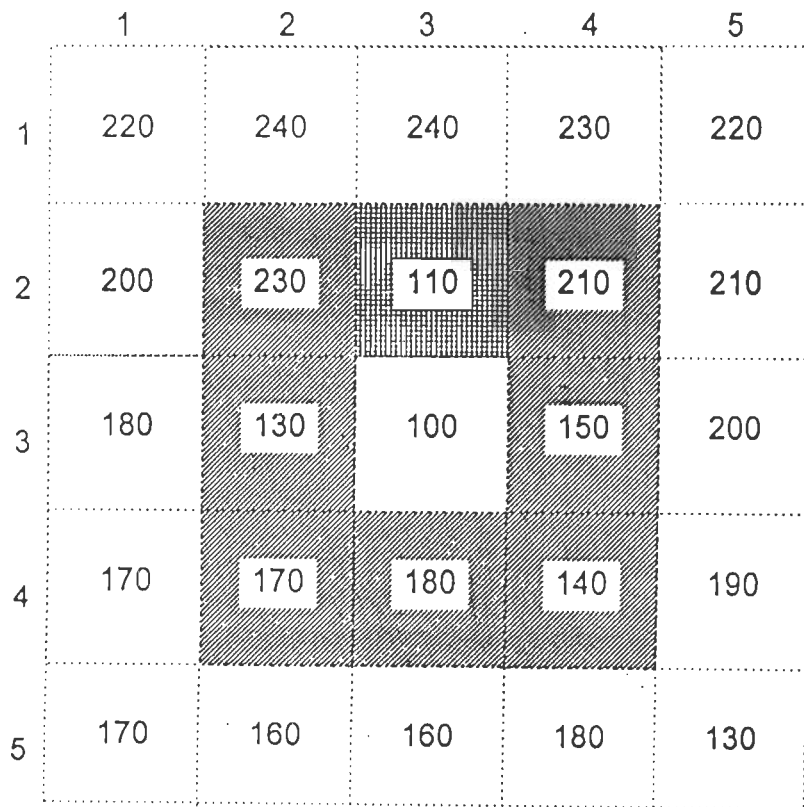
1. The elevation of the central cell in a 3x3 window is compared with the elevation of neighbouring cells. If all the neighbourhood cells of the central cell have elevation greater than the elevation of the central cell, then the central cell is identified as a pit or depression.
2. The identified single cell depression is removed by assigning lowest elevation value of its neighbourhood cells.
3. The above steps are repeated to remove all single cell depressions present within the DEM.

An example is presented in Fig. 4.3 where a single cell depression at cell (3,3) of value 100m (Fig.4.3 (a)) is raised to 110m by examining the neighbour cells so as to remove the depression (Fig. 4.3 (b)). After removing single cell depression, check is required for multicell depressions. The steps for identifying multi cells depression and its removal has been given below;

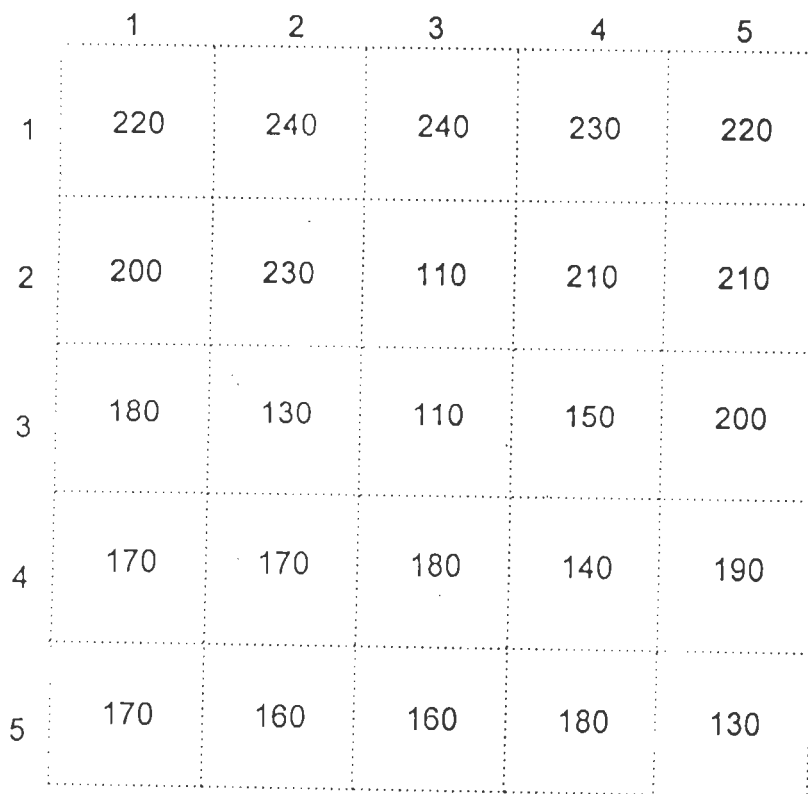
Identification and Removal of Multi Cells Depressions:

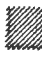
1. First of all, those cells within the neighbourhood have equal elevations are located and marked out.
2. Subsequently, all the cells surrounding this group of equal elevation cells, are also marked out. The surrounding cells are called as rim cells while the equal elevation cells are called as multi cell depression.
3. Identify the cell having lowest elevation amongst the rim cells.
4. Determine if an outlet exist i.e. the lowest elevation of the rim cells is equal to or less than the elevation of multi cell depression. If yes, proceed to next multi cell depression within the data set, or else go to next step.
5. Raise the elevation of multi cells depression to the lowest elevation of the rim cell and also include this cell into the multi cell depression.
6. Go to step 2 and continue till an outlet is identified at step 4.


Fig. 4.4 illustrates the identification and removal of multi cell depression. After removal of single cell depression, cells (2,3) and (3,3) have the same elevation value. These cells are found to be in depression when compared to the elevation values of cells on the rim of depression as shown by hatched cells in Fig. 4.4 (a). Now the elevation of these cells are raised to 130m (Fig. 4.4(b)) i.e. the lowest elevation on the rim of depression cells. Now the depression has been enlarged by one more cell i.e. cell (3,2) has been added to the multi



(a) Original DEM Data

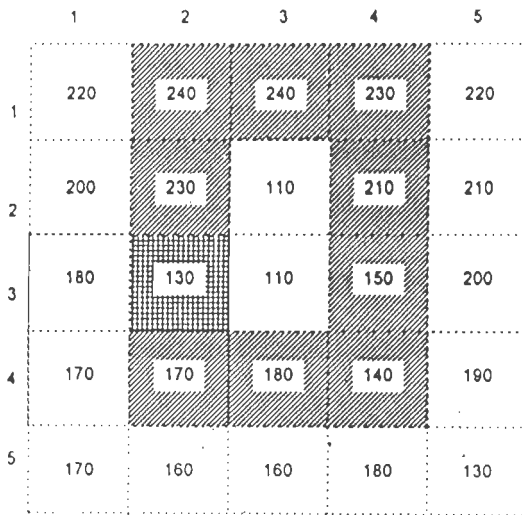


 Cells along rim of depression

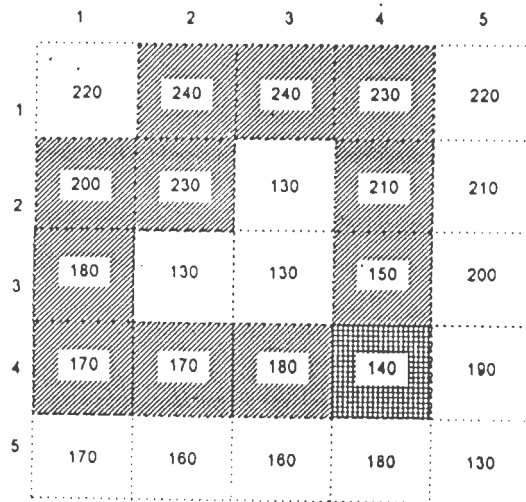
 Lowest elevation cell on rim

(b) Modified DEM after Single Cell Depression Removal

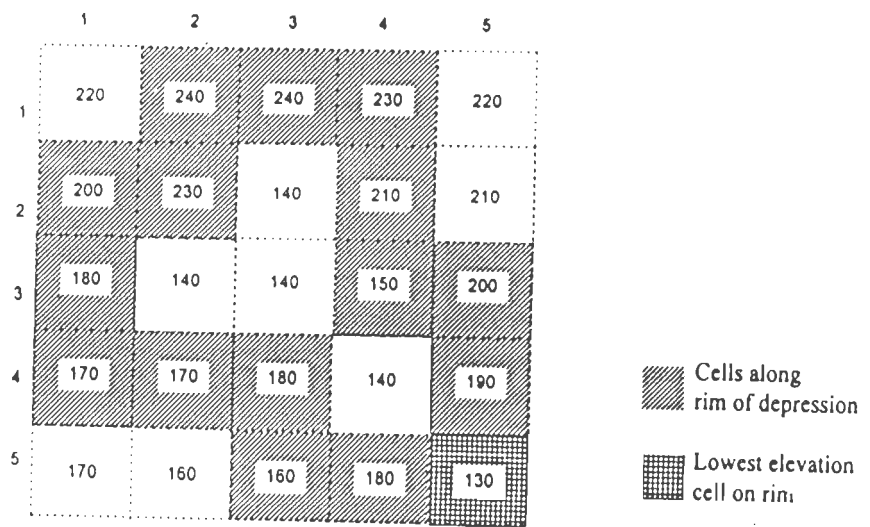
Fig. 4.3 : Identification and Removal of Single Cell Depression



(a) Elevation Values after Removal of Single Cell Depression



(b) Growing of Multi Cell Depression



(c) DEM After Removal of Multi Cell Depression

Fig. 4.4 : Identification and Removal of Multi Cell Depression

cell depression. A new rim is therefore created around cells (2,3),(3,2) and (3,3) as shown in Fig. 4.4 (b). The lowest elevation on this rim is 140m of cell (4,4) and therefore the elevation of all the depression cells (i.e. cell (2,3), (3,2) and (3,3)) are replaced by 140m. Cell (4,4) is now added in the previous depression thereby enlarging the rim size. On examining this rim, cell (5,5) has the lowest elevation value as 130m and this cell now provides an outlet (Fig. 4.4 (c)) the multi cells depression.

A computer program in FORTRAN 77 has been developed to obtain a depressionless DEM. The flow chart of the program has been presented in Fig. 4.5. The depressionless DEM, thus obtained, is used for further processing.

4.4.3 CATCHMENT DELINEATION

The term catchment or watershed or river basin may be defined as the area drained by the river system (Fleming, 1975). Several methods are available for the delineation of catchment and drainage network from a depressionless DEM, as described by O'callaghan and Mark, (1984); Band, (1985); Jenson, (1985); Jenson and Trautwein, (1987); and Jenson and Domingue, (1988).

The catchment delineation may be carried out effectively using the seed growth method (Jenson, 1988). In this method, the elevation and location of lowest point of the catchment (called the seed point), which is generally the gauging station of the stream, is known. All other points having elevation equal or greater than the seed point constitute the catchment.

In Fig. 4.6 (a) the central cell with elevation value 270m is assumed to be the seed point. All points having elevations equal or greater to the elevation of seed point are marked as 1 (Fig. 4.6 (b)). All these points, now flagged off in the catchment elevation matrix, act as seed points and are stored in a column matrix, known as LIFO stack (last in first out). The top most point in LIFO stack is now taken for examination using similar logic. This process is continued till no points are left in LIFO stack. All points having elevations less than the seed point are marked as '0'. In this fashion, the entire catchment boundary is delineated

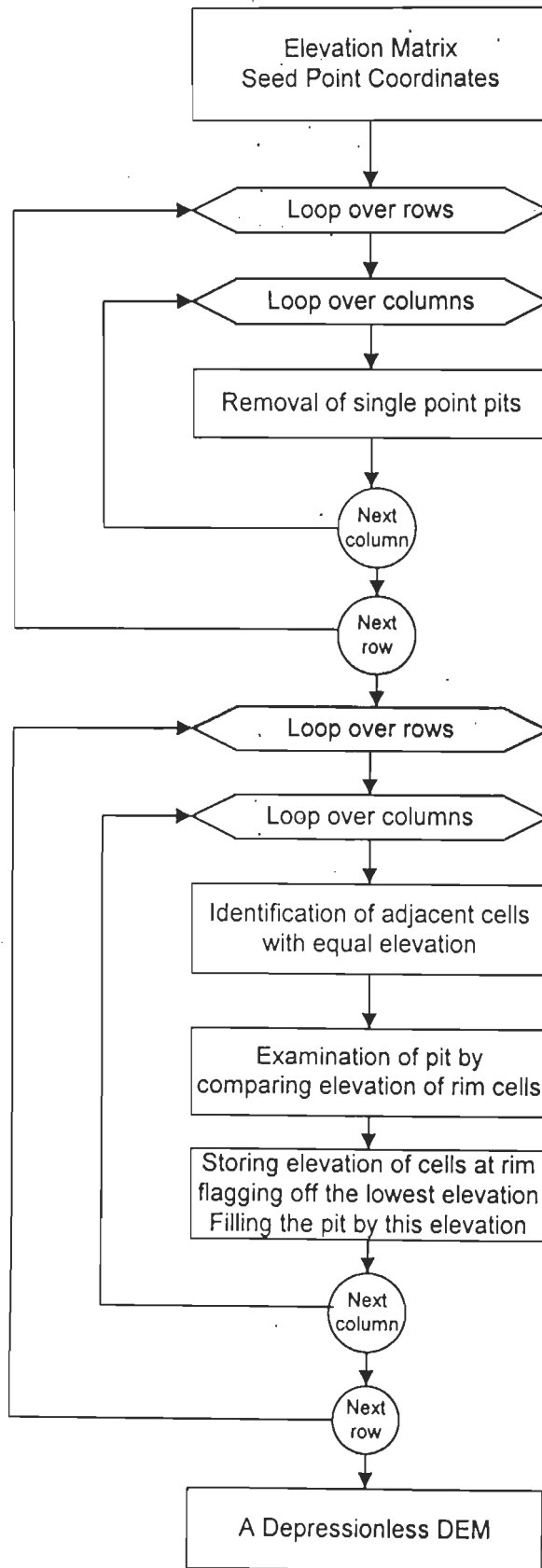


Fig. 4.5 Flow Chart to get Depressionless DEM

280	320	330
280	270	240
270	230	220

(a) Sample Elevation Data

1	1	1
1	X	0
1	0	0

(b) Identification of Catchment Cells

Fig. 4.6 : Illustration of Catchment Delineation from DEM

In this study, the delineation of catchment is not carried out from DEM as it was transferred from topographical maps.

4.4.4 SEGMENTATION OF CATCHMENT

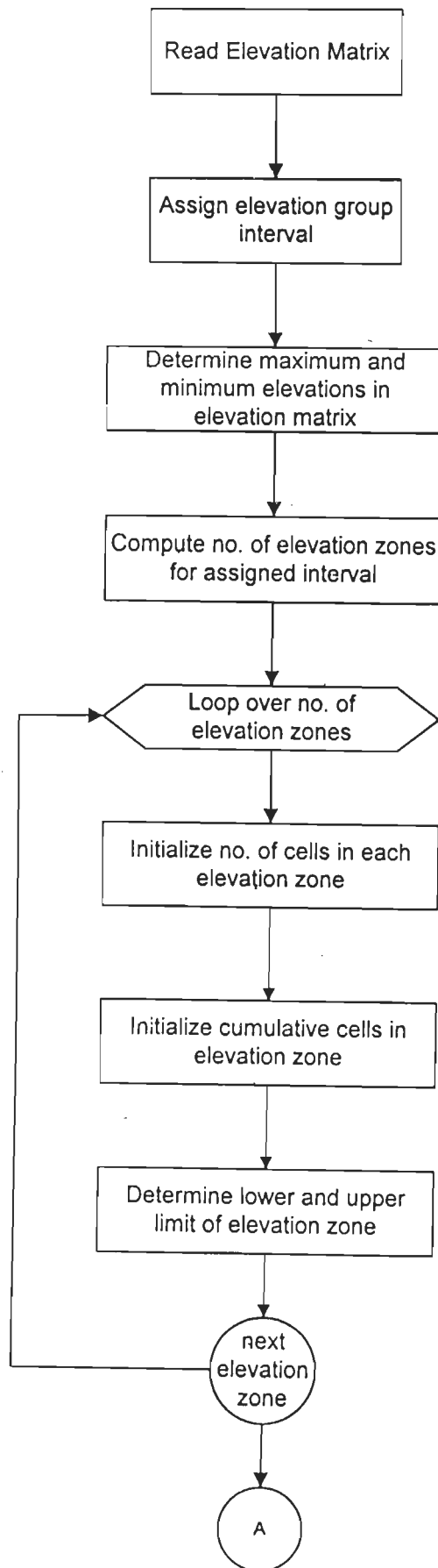
In this model, the catchment is required to be divided into three segments according to relief in the area. The area-elevation curve is plotted and divided into three segments. In the present study, a computer program in FORTRAN 77 has been written to compute the percent area of catchment above a particular elevation. A flow chart of program has been presented in Fig. 4.7. A segment matrix may be prepared after deciding limiting elevation values for segments.

The information regarding channel length, slope, area and landuse of the catchment have been computed for each segment. A parameter RIVER (in SRBM model), the ratio of segment area contributing directly to channel to total catchment area is also extracted for each segment.

4.4.5 COMPUTATION OF FLOW DIRECTION

The flow direction for a cell is the direction in which water flows out of the cell. The flow directions can be encoded to correspond the direction of one of the eight cells that surround the central cell (9) as shown in Fig. 4.8. For example, if the water flows towards east from the central cell, the flow direction of this cell is denoted by 2. If grids are oriented in N-S direction the flow direction codes from 1 to 8 represent NE, E, SE, S, SW, W, NW, N directions respectively.

In this study, the flow directions have been computed on the basis of steepest downward slope from the central cell. A different approach named as Flow Line Approach has been proposed. The details of this approach is given in the following section.



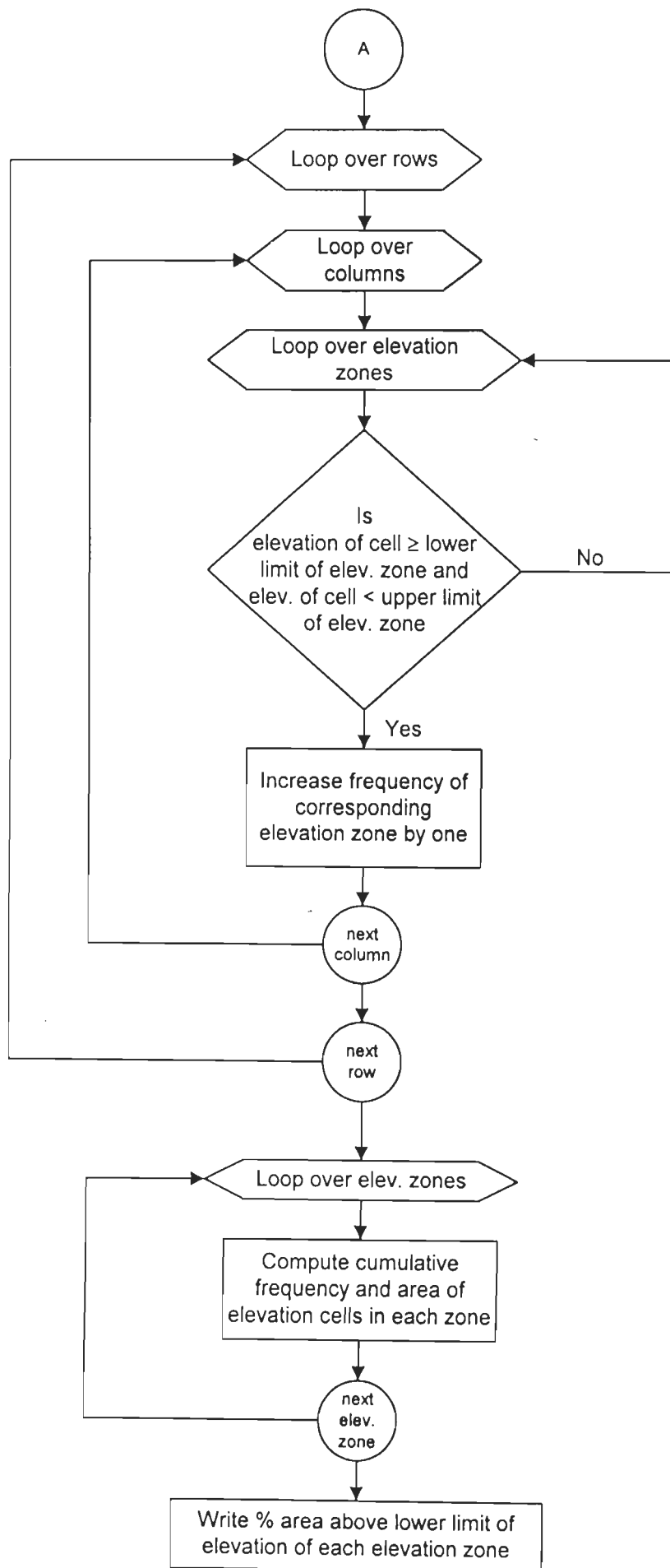


Fig. 4.7 Flow Chart to Compute Area Elevation Curve from DEM Data

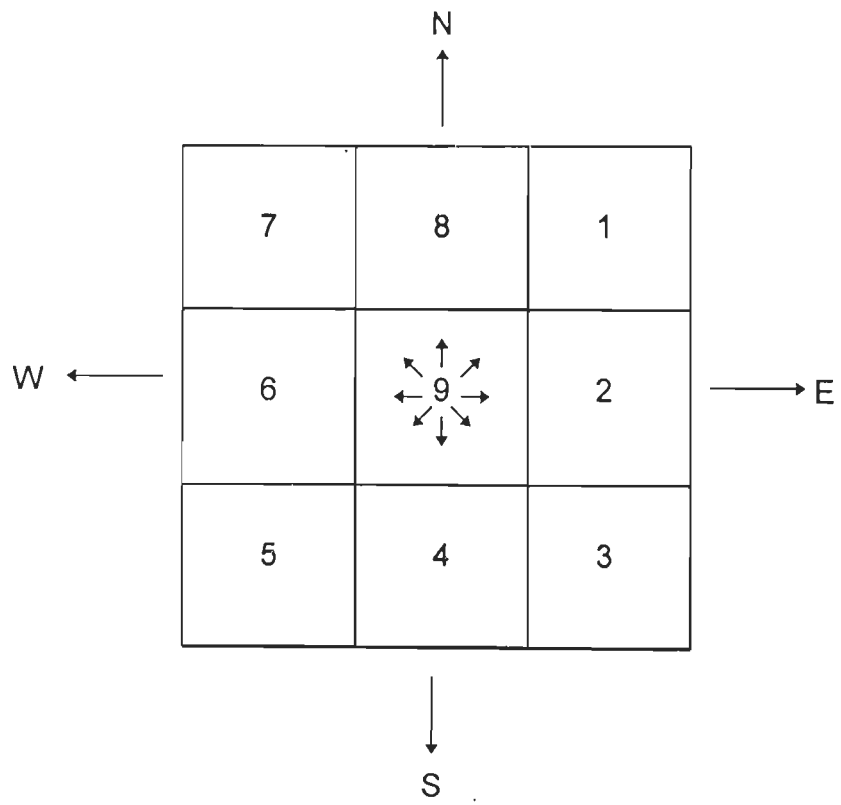


Fig 4.8 : Flow Direction Data Codes for Central Cell '9'

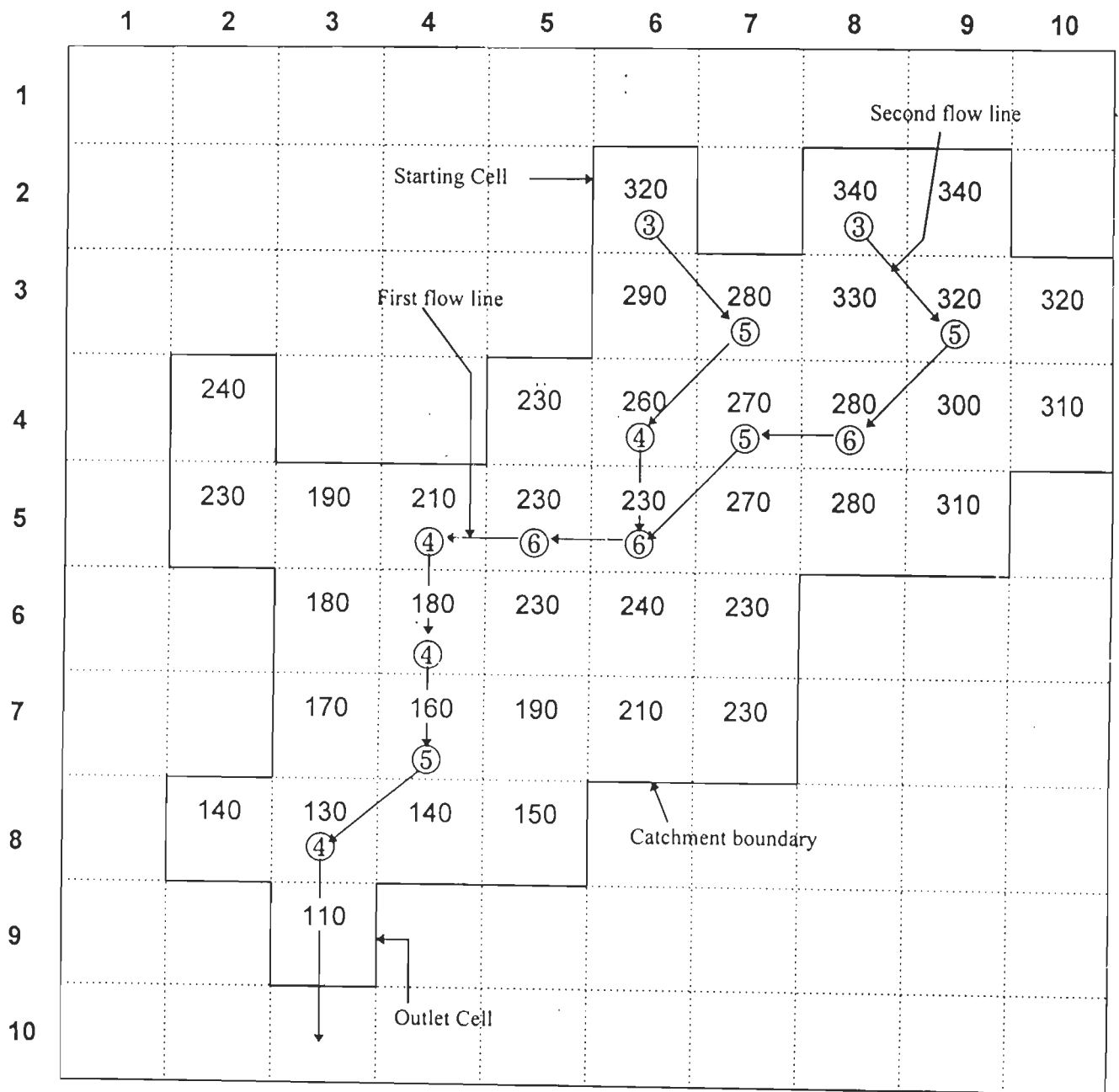
4.4.5.1 Flow Line Approach

Conventionally, the computation of flow directions for a DEM is carried out rowwise, i.e. cell by cell in a row. Computation of flow direction by the proposed method is independent of their code (1 to 8), and therefore leads necessity to check the closed paths within the network. The closed paths can be defined as the path of flow which starts and ends to the same cell and these are 1-5, 5-1, 8-4, 4-8, 7-3, 3-7, 6-2, 2-6 (Fig. 4.8).

In the present study, a flow line approach has been developed where flow direction code of previous cell identifies the next cell to be processed. In other words, after computing the flow direction of first cell, the next cell to be processed is one towards which the flow from first cell is received, and this need not necessarily be the next cell of the same row. This process continues till the first flow line reaches the outermost cell of the catchment. The next flow line starts from the cell adjoining the one from which the previous flow line had started. This flow line gets terminated at the point where either it joins an already processed flow line or reaches to the outlet cell of the catchment. In this manner, the flow directions of all the grid cells are computed and assigned flow direction codes.

Fig. 4.9 illustrates the details of Flow Line Approach. In this example, the processing starts from cell (2,6). The steepest slope of this cell is towards direction '3', therefore water flows to cell (3,7). The processing now starts from cell (3,7) which consists of steepest slope towards flow direction '5'. This way the processing continues till the first flow line terminates at the outlet cell (9,3). Next time, the processing starts from cell (2,8) and terminates at cell (5,6). This approach is repeated till flow direction of all cells within the catchment are assigned.

Sometimes, a grid cell may have multi flow directions thereby indicating that there is some confusion even though the DEM is depressionless. In practice, the general approach to resolve such situation is to select that flow direction which has been encountered first. This flow direction may not be the realistic flow direction and that it is possible that the flow may loop back to this point or it may get terminated in between.



Numbers encircled are Flow Direction values.
 Number in grids are elevation values.

Fig 4.9 : Flow Direction Computations Using Flow Line Approach in a 10 x 10 Sample Elevation Data

Fig. 4.10 illustrates the method of resolving such conflicting flow directions. For example, in Fig. 4.10 (a) the flow line at cell (2,2) consists of equal slopes in '2' and '4' directions of flow. Since, direction '2' is computed first the flow is routed towards cell (2,3). On examination of cell (2,3), the steepest slope has a flow direction of '2', thus the next cell to be processed is (2,4) with elevation value of 280m. Since, this cell is surrounded by higher or equal elevation cells in a 3x3 window, therefore the flow can not be routed back to cell (2,3) which has equal elevation. Under such circumstances, flow line stops at cell (2,4), and assigns a code '9'. To solve this problem, the flow direction of cell (2,2) is visually assigned as '4' so that the flow line can now be processed further. Fig. 4.10 (b) shows the modified flow directions on the basis of visual inspection of DEM.

Fig. 4.11 shows the flow chart of flow line approach, while Figs. 4.12 and 4.13 show the flow charts of the flow direction and identifying the location of cell to be processed respectively.

4.4.6 DETERMINATION OF FLOW ACCUMULATION VALUES AND CHANNEL NETWORK

Flow accumulation value of each cell indicates the number of cells that would route the flow to it (O'Callaghan and Mark, 1984). These values are derived from flow direction data obtained as above. A drainage channel represents the points at which runoff is sufficiently concentrated. If the spatial concentration of surface runoff is simulated at those points where this runoff exceeds a given threshold value, it is considered to be a part of the drainage network (O'Callaghan and Mark, 1988). The threshold method of channel network extraction is based on minimum contributing area, an area required to drain, to a point such that a channel is formed (Jenson and Domingue, 1988).

In this study, channel network of the catchment is derived from the flow accumulation values and flow direction data. All cells with area greater than a specified value (area threshold value) are classified as part of the drainage network. Thus, several drainage network can be derived from a DEM using different threshold values i.e. minimum contributing area to form a channel. Amongst the various channel networks the one

	1	2	3	4	5
1	340	330	310	310	300
2	320	300 ②	280 ②	280 ⑨	300
3	310	280	300	300	290
4	270	300	290	300	290
5	260	280	300	310	280

(a) 5 x 5 Sample Elevation Data of Flow Direction Termination

	1	2	3	4	5
1	340	330	310	310	300
2	320	300 ④	280 ⑤	280 ⑥	300
3	310	280	300	300	290
4	270	300	290	300	290
5	260	280	300	310	280

(b) Flow Direction Solved by Visual Inspection

Fig. 4.10 : Illustration of Method to Resolve Conflicting Flow Directions

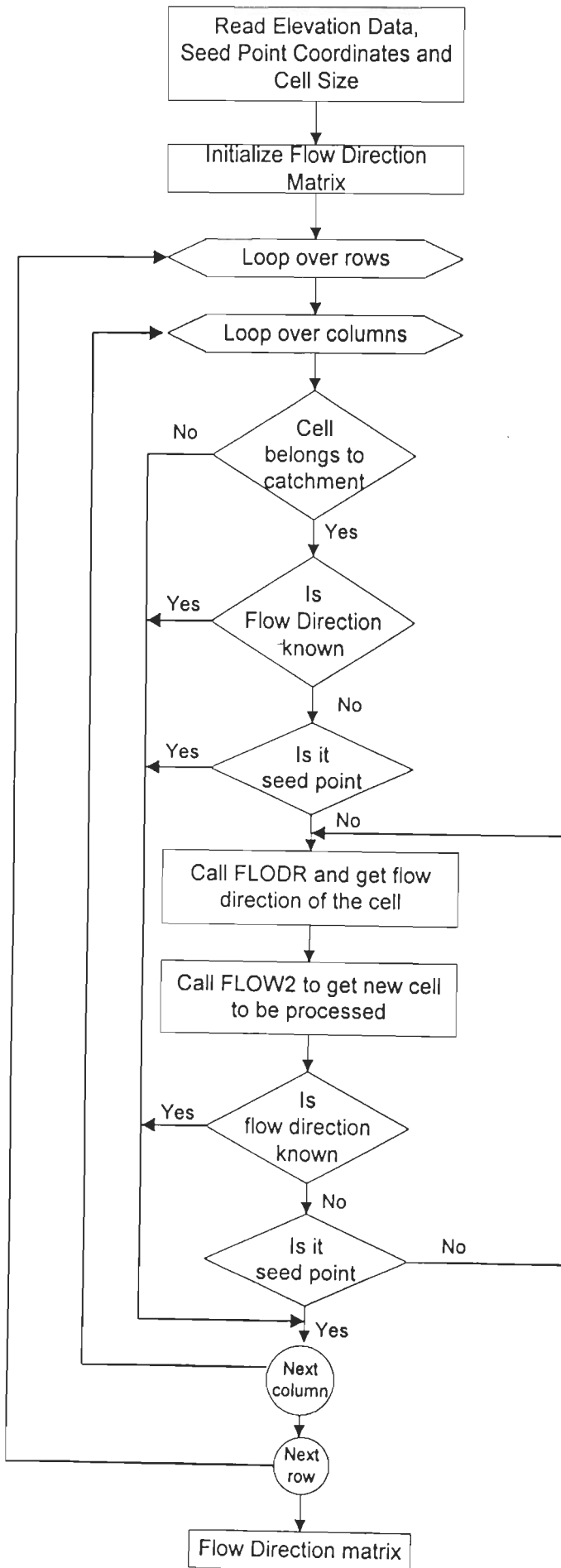
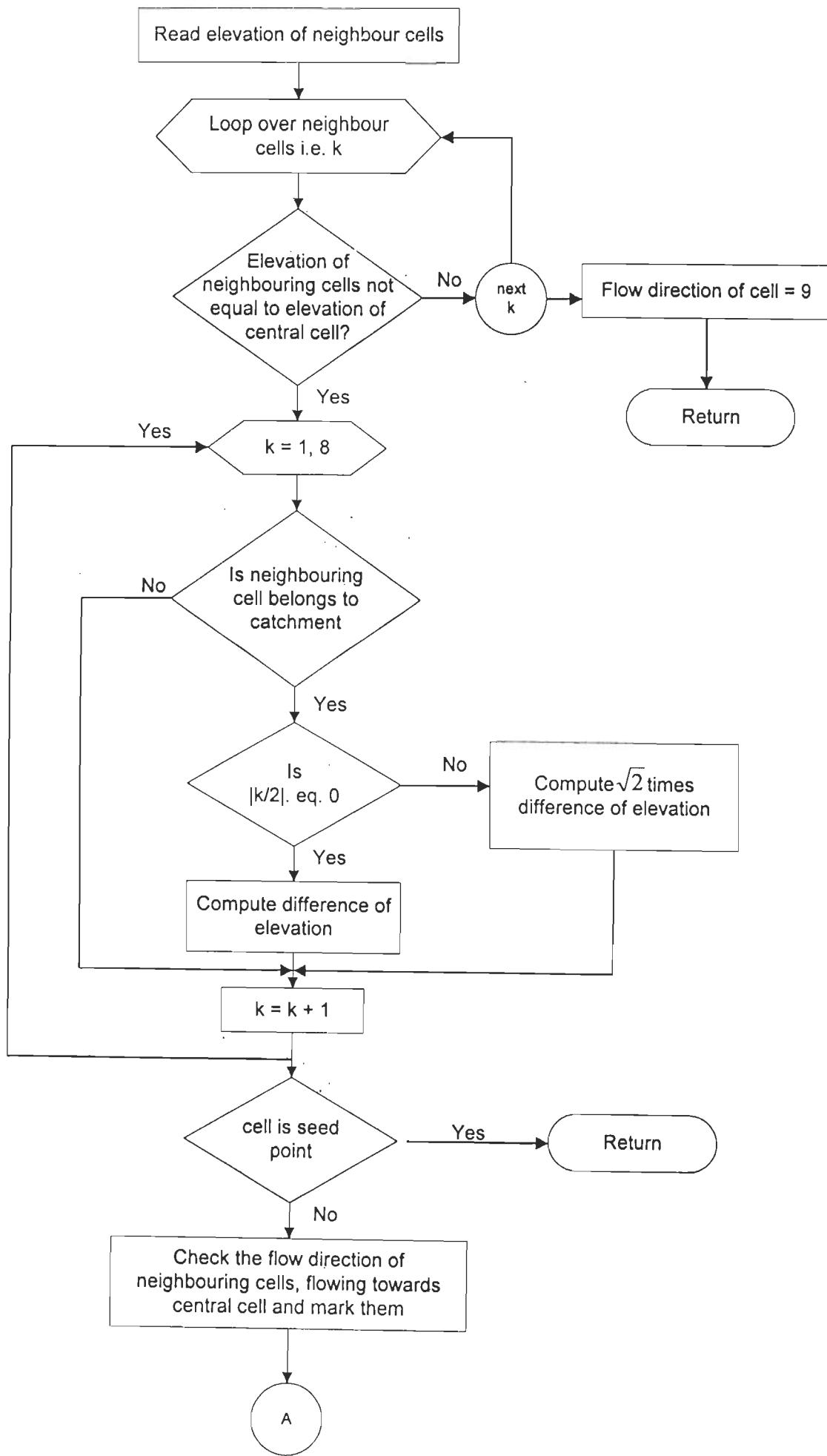


Fig. 4.11 : Flow Chart to get Flow Direction



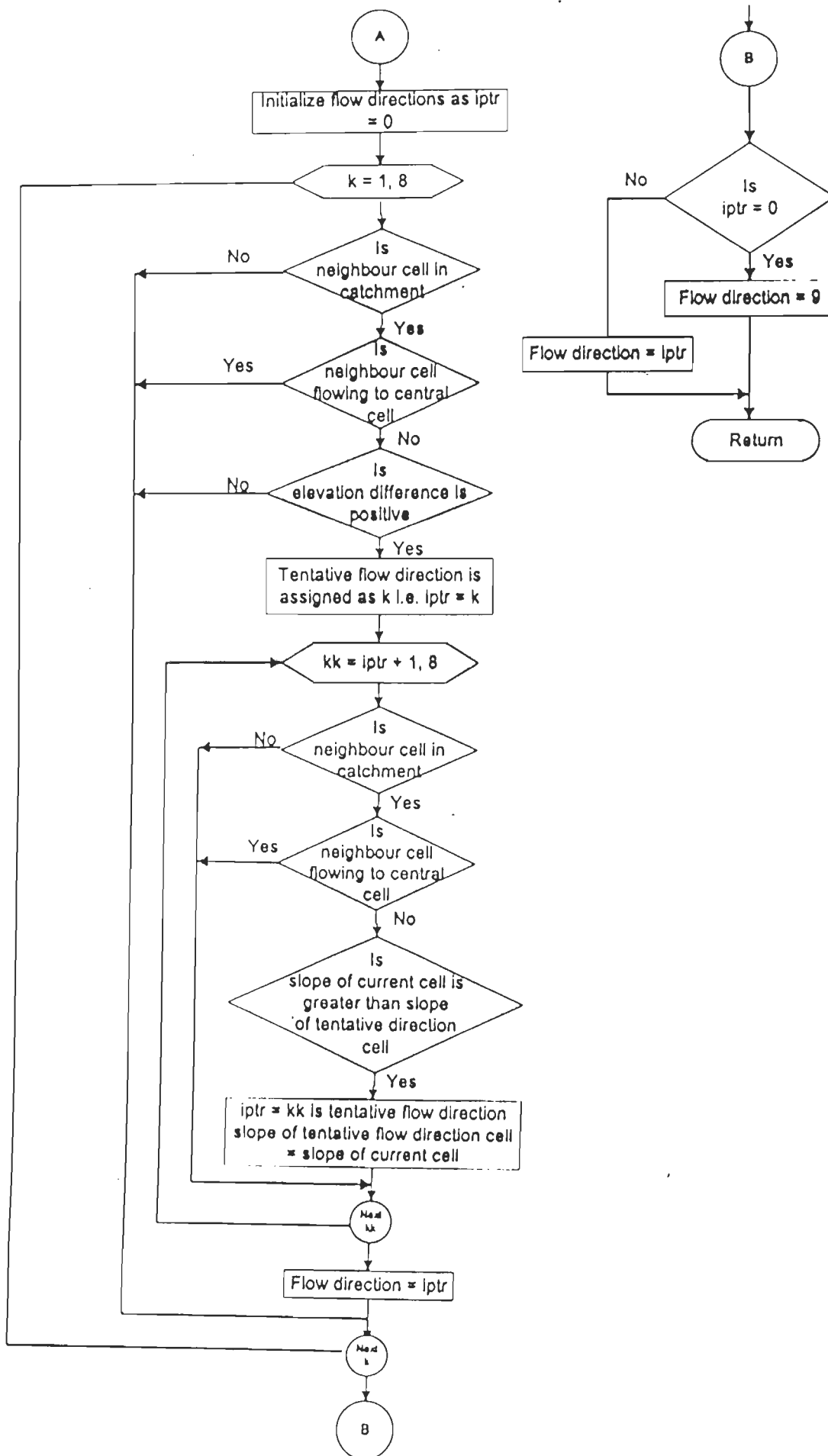


Fig. 4.12 Flow Chart of Subroutine FLODR

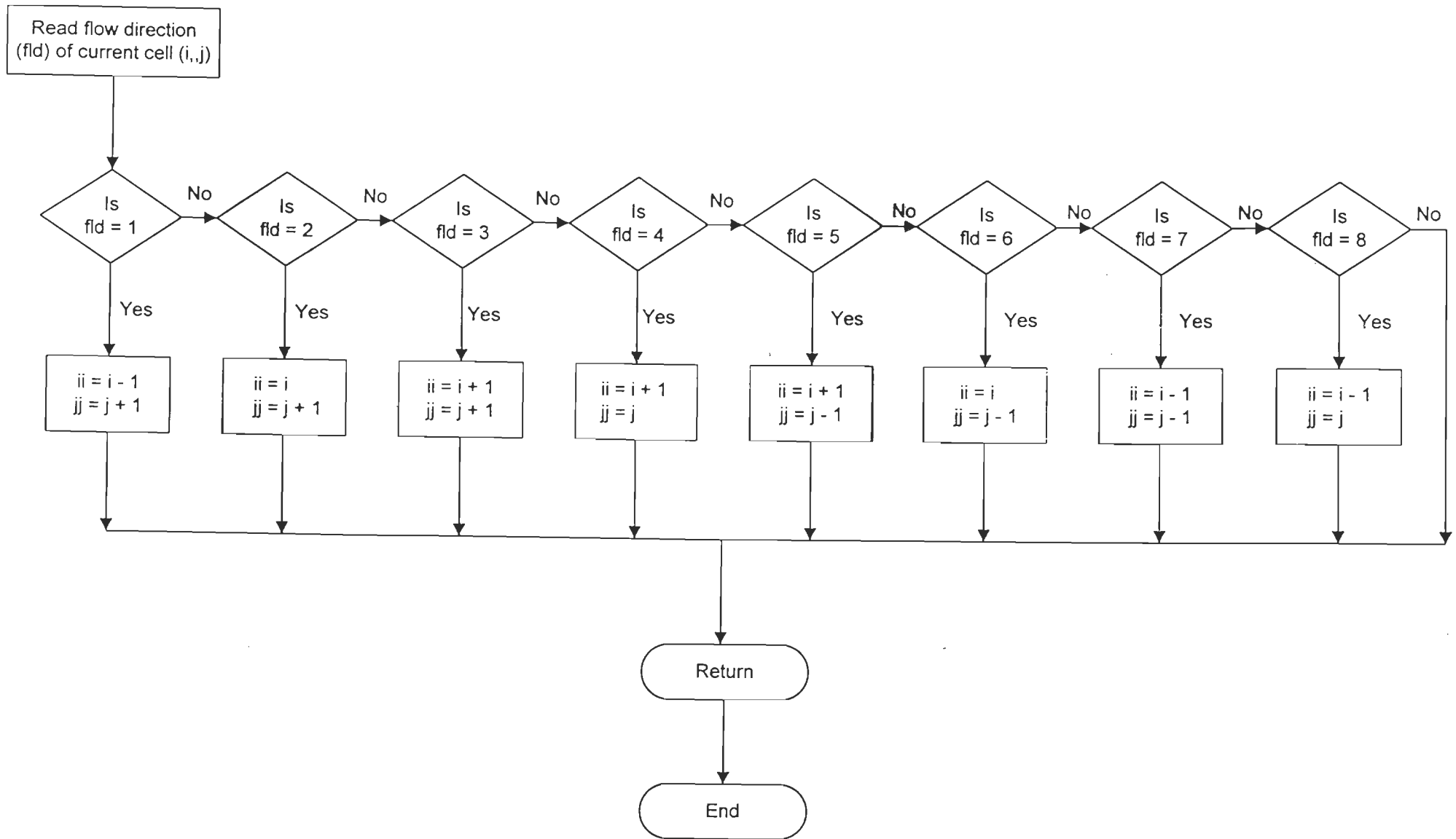


Fig. 4.13 Flow Chart for Subroutine FLOW2

which corresponds close to ground network is selected. A flow chart for computing flow accumulation values and channel network matrix has been shown in Fig. 4.14.

4.4.7 COMPUTATION OF OVERLAND FLOW PATH AND SLOPE

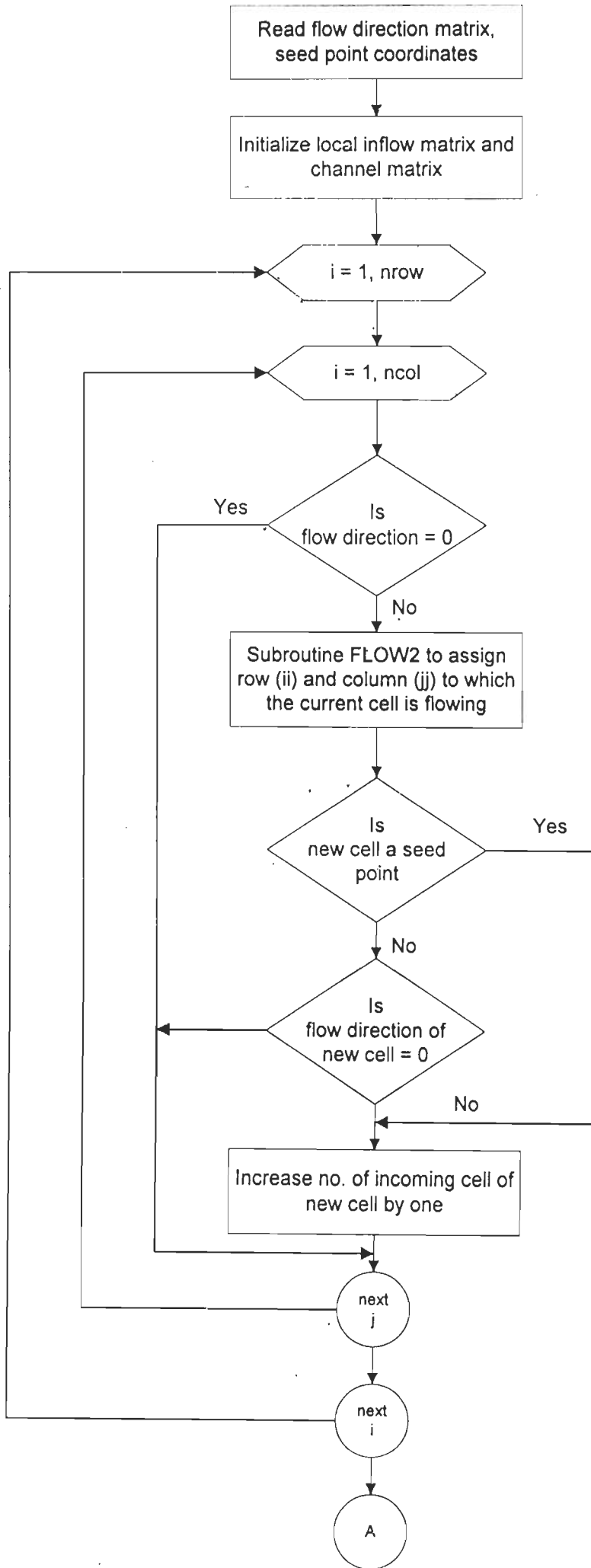
From channel network, overland flow length is required to be used in runoff modelling. The channel cells with odd number value of flow directions (i.e. 1,3,5,7) have flow length as ($\sqrt{2} \times$ cell size), whereas the even number of flow directions (i.e. 2,4,6,8) have flow length equal to cell size.

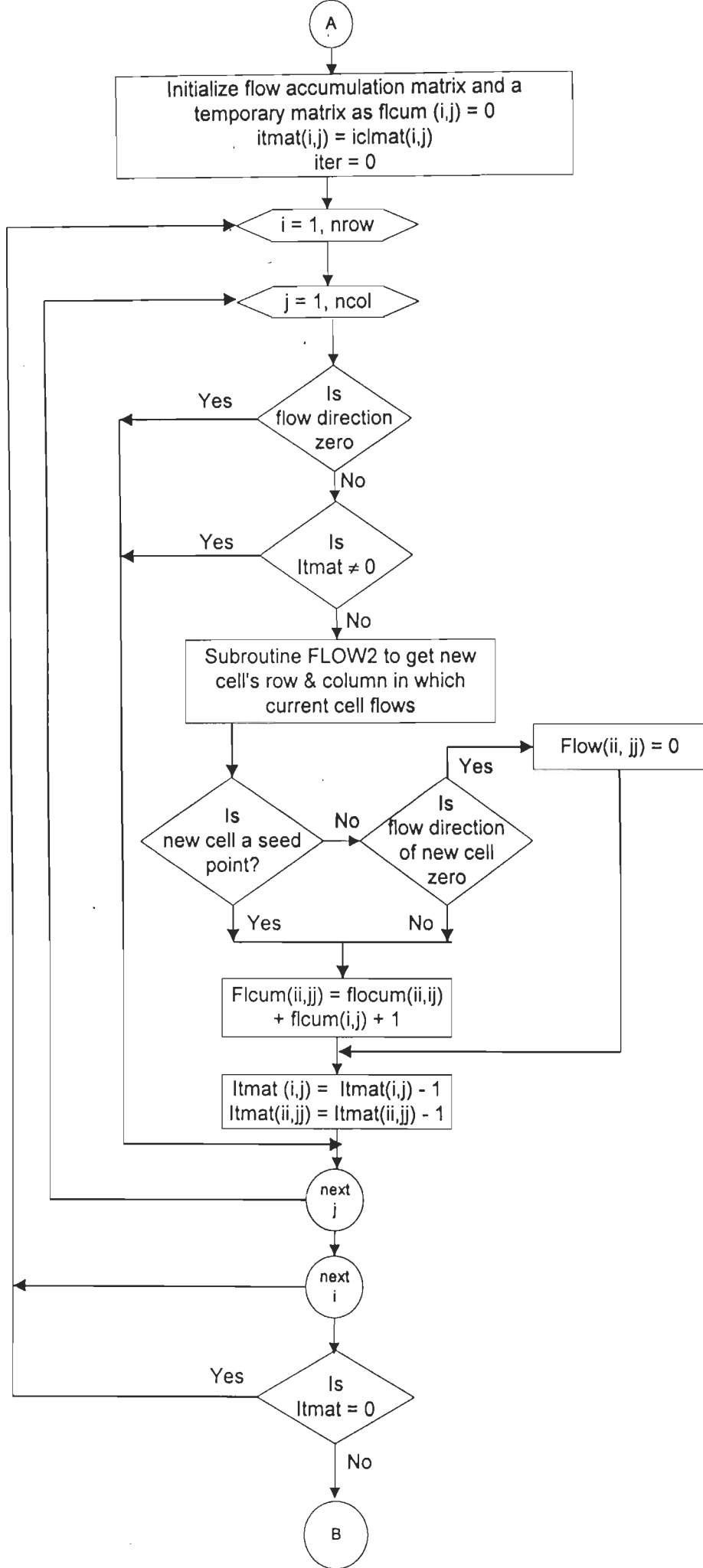
The slope computation requires a depressionless DEM. Ritter's approach (1987) to compute slope considers only four neighbouring pixels in a 3x3 window of elevation values. According to this approach, the slope for a central cell is computed from its normal vector. The relationship for the computation of slope of central cell P_0 (Fig.4.15) considers the four neighbouring cells P_1, P_2, P_3 and P_4 , with elevations Z_1, Z_2, Z_3 and Z_4 respectively. The vectors n_e and n_s may be defined as $(2L, 0, Z_3-Z_1)$ from cell P_3 to cell P_1 and $(0, 2L, Z_2-Z_4)$ from cell P_2 to cell P_4 respectively. If P_0 happens to be on the edge of the database, its elevation is used in place of the missing cell. The cross product ($n_s \times n_e$) of these vectors give a normal vector pointing out towards space. The angle of this normal vector with horizontal plane is the slope of any cell. The slope in terms of rise over run can be calculated using equation 4.1 as given below:

$$\text{Slope} = [(Z_1 - Z_3) + (Z_4 - Z_2)]^{1/2} / 2L \quad (4.1)$$

where L is the size of square cell.

In this study, a computer program has been developed to compute the overland flow length and channel slope, segmentwise as well as for the entire catchment. The flow charts for computing slope by above algorithm and segmentwise information of slope overland flow path etc. are shown in Figs. 4.16 and 4.17 respectively.





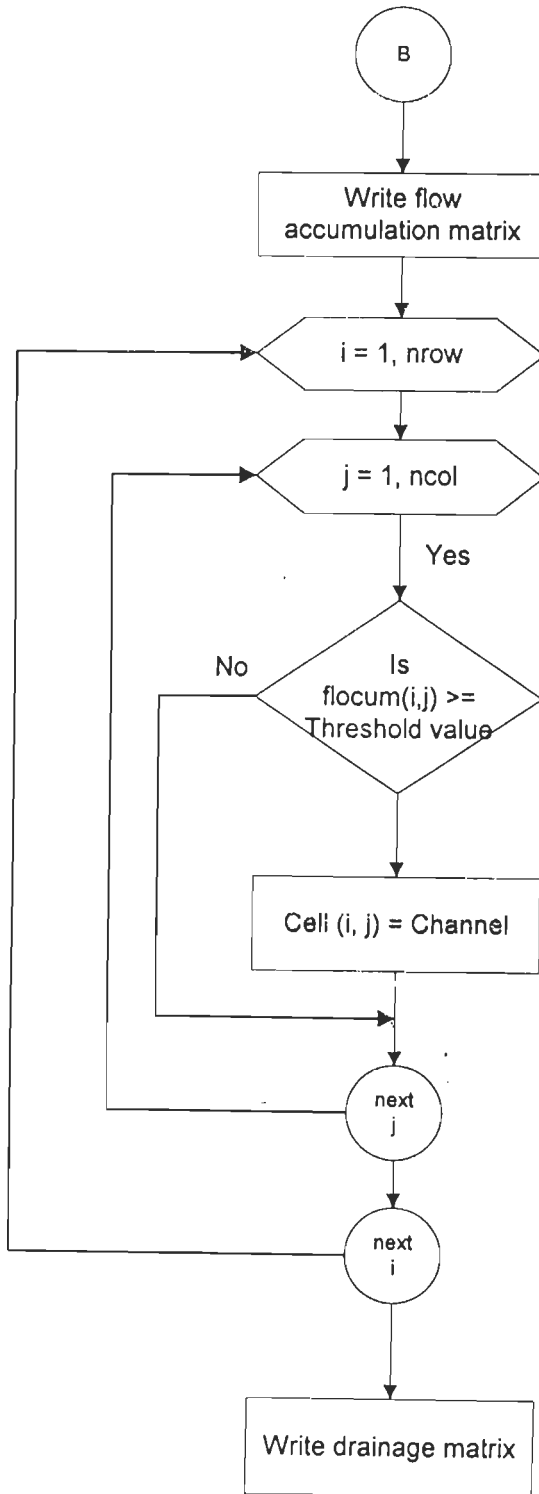


Fig. 4.14 Flow Chart to get Flow Accumulation and Channel Matrix

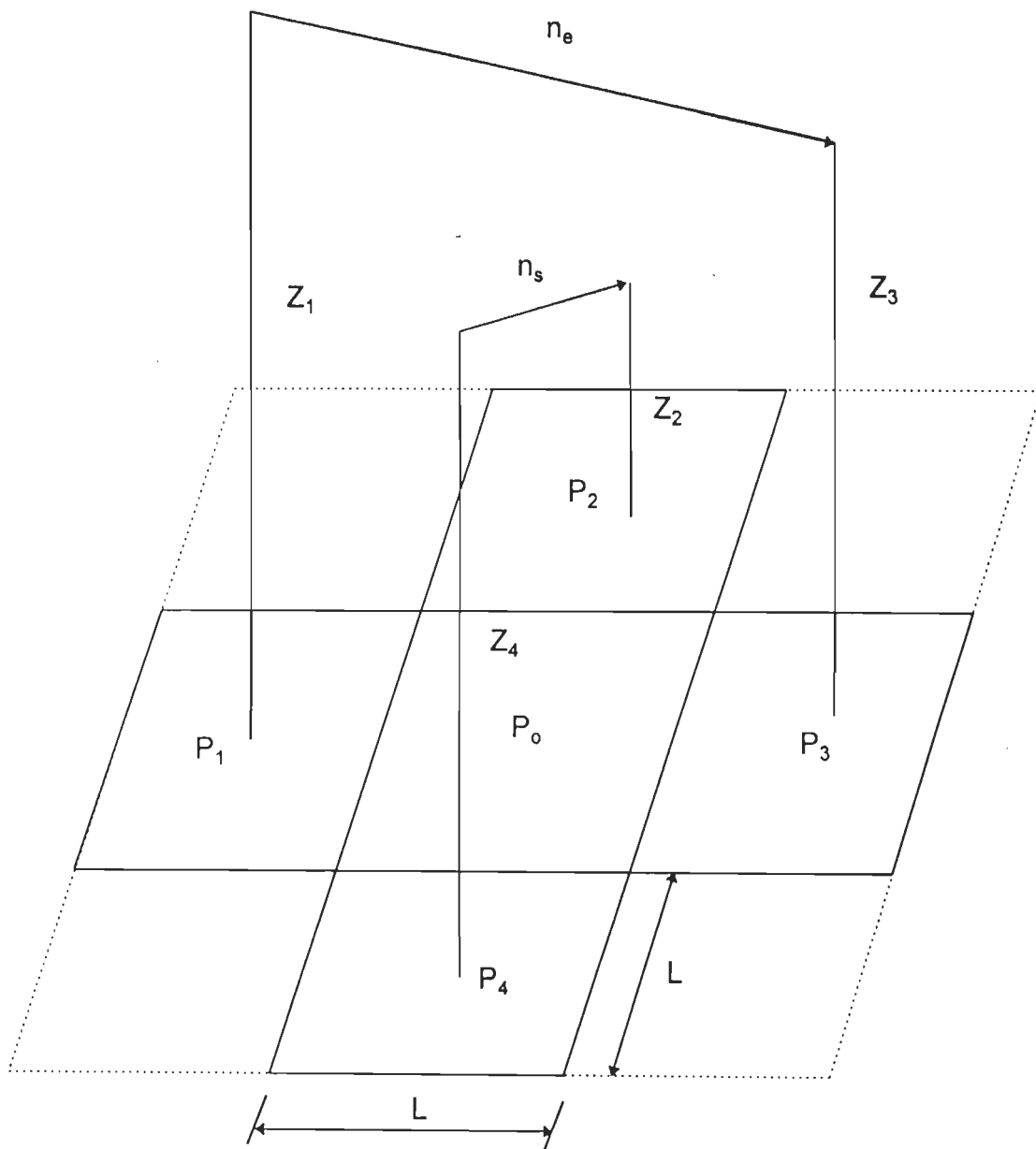


Fig 4.15 : Slope Computation for Central Cell P_0 with Relation to its Four Neighbours P_1, P_2, P_3 & P_4

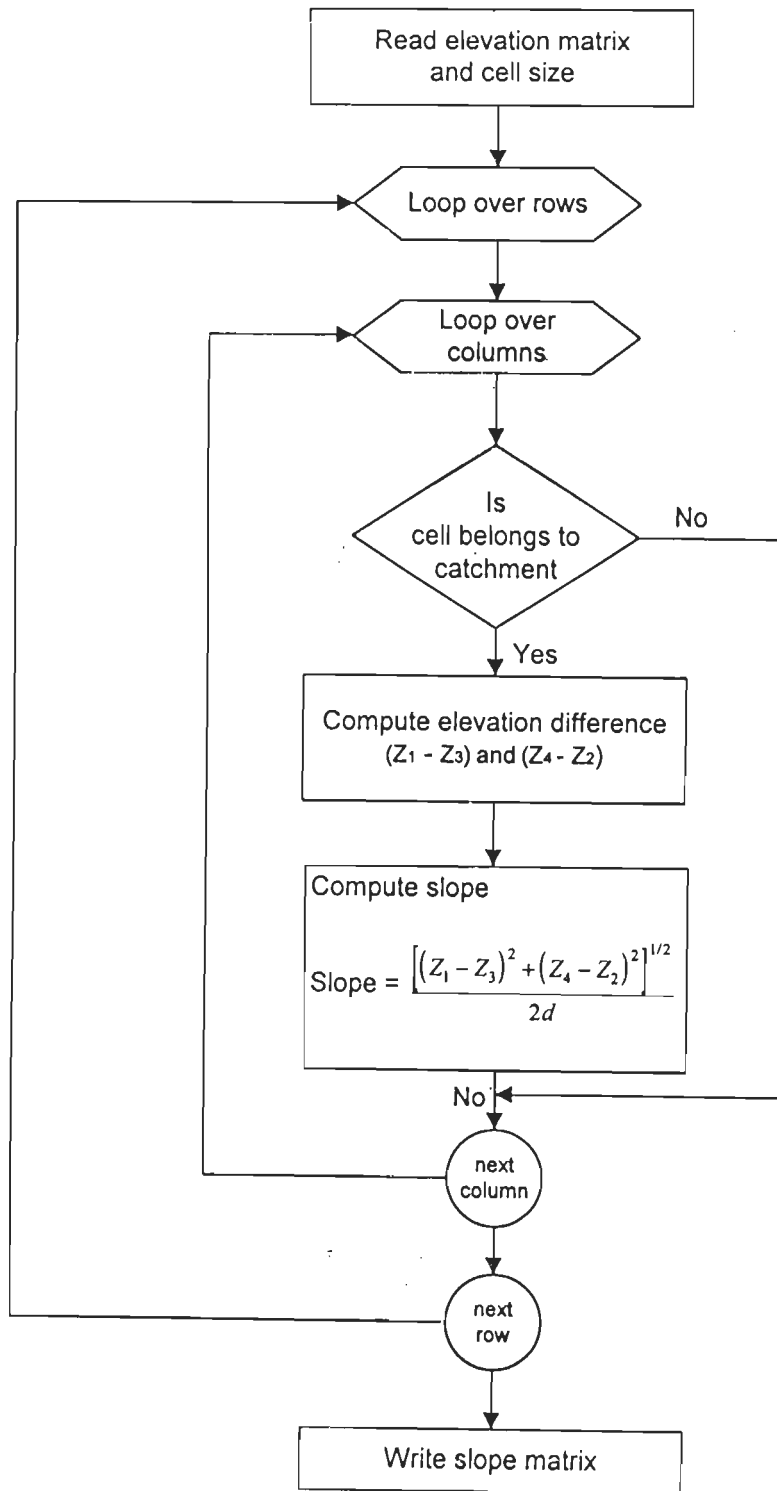
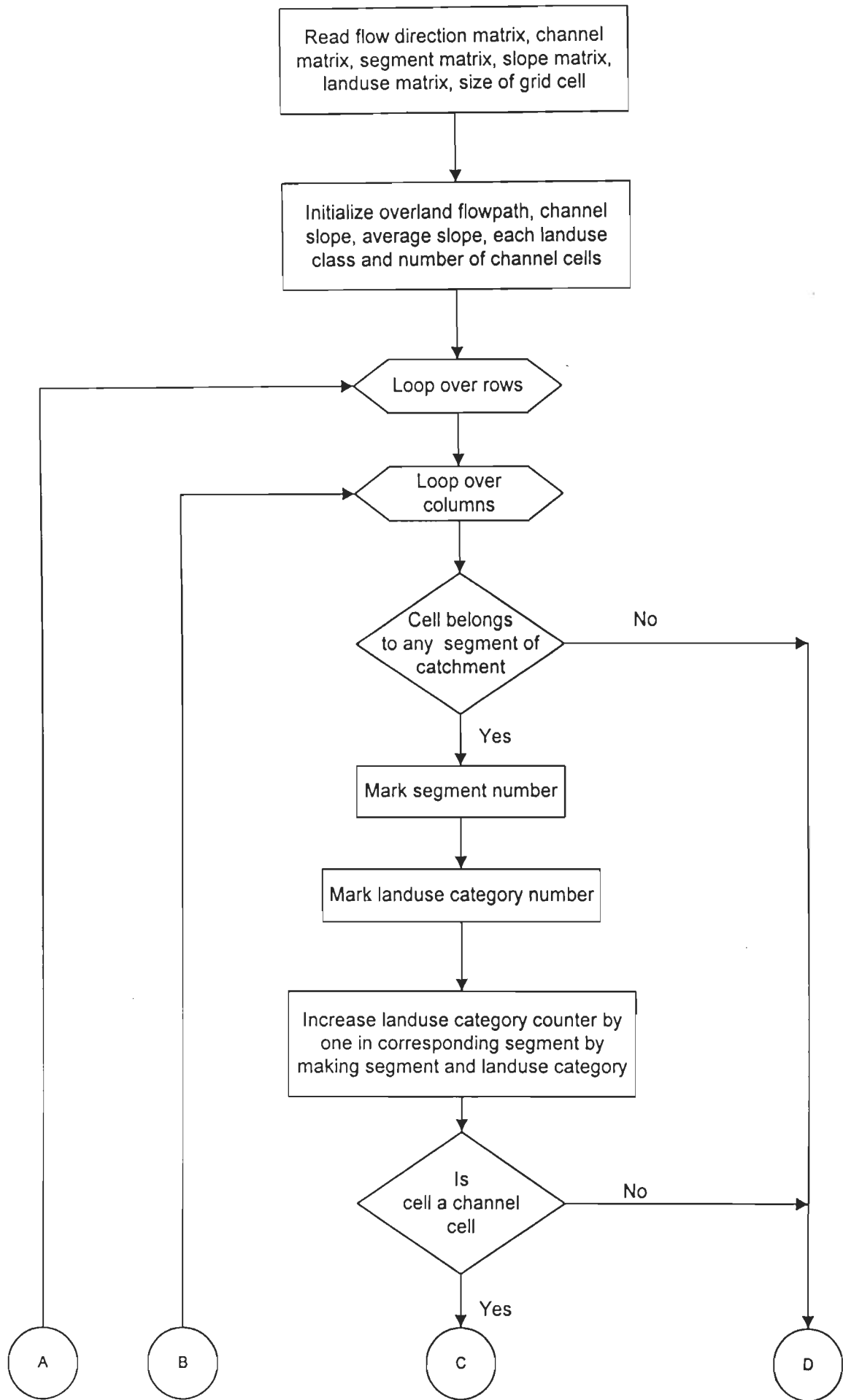


Fig. 4.16 Flow Chart of Ritter's Algorithm for Computing Slope



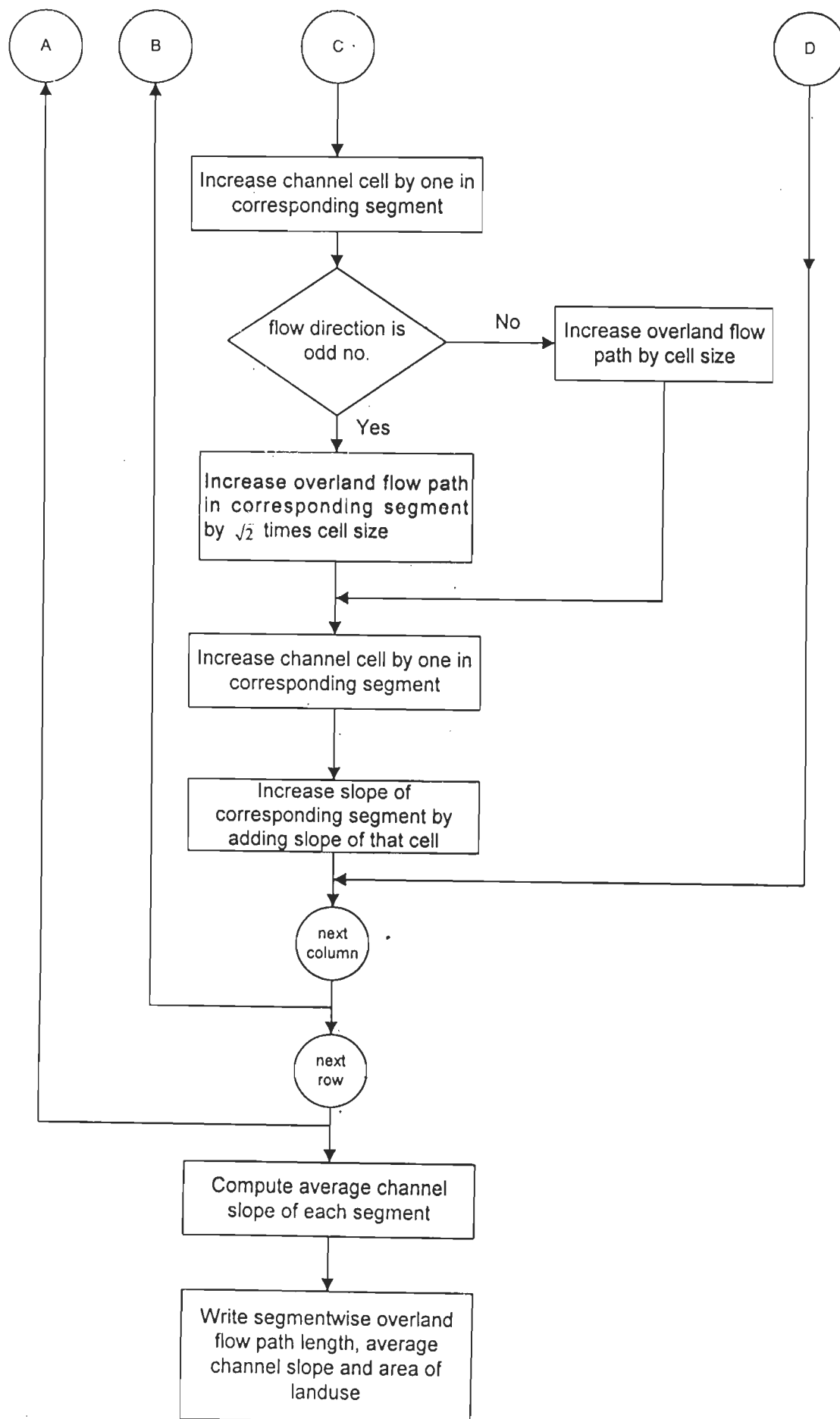


Fig. 4.17 Flow Chart to obtain Segmentwise Information of Overland flow path, Average Channel Slope and Landuse Area

4.5 PROCESSING OF REMOTELY SENSED DATA

In Watershed Module of SRBM model, the interception (EPXM), potential evaporation from lower zone (K3) and proportion of impervious area (IMPV) parameters can be derived using remote sensing data. The quantitative assessment of these parameters is based on landuse information to be extracted from latest remote sensing data. The remote sensing data product is not geometrically stable thus any area or length measurements on it may not be correct. To correct these measurements the image has to be geometrically rectified with the ground or existing map as explained in next section.

4.5.1 GEOMETRIC REGISTRATION OF REMOTE SENSING DATA

Registration is the process by which the geometry of an image area is made planimetric. It is a process of translation and rotation of an image so that the same set of objects are positioned coincident with respect to reference map. This process involves relating the ground control point (GCP) pixel coordinates to their respective map coordinates. This is the most precise geometric correction since each pixel can be referenced not only by its row and column but also by any standard measurement unit. For accurate delineation of area, direction and distance measurements, geometric registration is required to be performed.

The common technique of registration of satellite data involves the use of mathematical relationships with the help of coordinates of GCPs, located on the map and as well as image. The GCPs are usually well defined points such as road intersections, airport runway intersections, bend in rivers and prominent coastline features. First, second or third degree polynomials can be used to register the satellite data, depending on the number of control points and accuracy desired. The values of the coefficients in a polynomial are derived by solving the polynomial, which are then substituted in the original equation. The root mean square (r.m.s.) error between the computed coordinates and the measured coordinates from the registered image is assessed. This value should be less than the spatial resolution of satellite data, otherwise the registration process is repeated by detecting sequentially all GCPs having r.m.s. values greater than the threshold limit, till the desired accuracy is achieved.

4.5.2 CLASSIFICATION OF REMOTE SENSING DATA FOR LANDUSE

Landuse inventories are needed for optimal utilization and management of land and water resources. It is now well established that remote sensing data have a great potential for the collection of update land use information (Rango et al., 1983; Engman and Gurney, 1991,a; Rao et al., 1991; Cruise and Miller, 1993). Two methods are usually employed in mapping landuse categories; (i) visual interpretation technique and (ii) digital classification technique.

Visual interpretation technique uses tone, texture, pattern, shape, size, shadow and location to derive landuse information. Digital classification technique uses either of the two methods viz., (i) supervised classification method or (ii) unsupervised classification method. The supervised classification method attempts to relate pixel groups with actual land cover types. These pixel groups are known as information classes or training samples. The unsupervised classification method simply determines the characteristics of non-overlapping groups of pixels, in terms of their spectral band values. These groups are known as spectral classes, and their relationships with information classes have to be worked out through field work, map or aerial photographic interpretation (Mather, 1987).

In this study, Clustering Unsupervised Classification technique has been used for the classification of remote sensing data to derive landuse information. This technique is generally a two stage process (Jenson, 1986). In the first stage, the cluster centers are established by building cluster groups, and statistics generated. In the second stage, the classification is carried out using a minimum distance to mean classifier. The technique generally requires four types of information, as given below;

- (i) Radius in spectral space
- (ii) Spectral space distance parameter used for merging the clusters (usually double of radius)
- (iii) Number of pixels to be processed before merging
- (iv) Maximum number of clusters to be identified

In this approach, the analyst can merge or group a number of clusters as per the values obtained after examination. The landuse information obtained from remotely sensed data have been used to compute interception (EPXM) and lower zone evaporation parameter (K3).

4.6 RUNOFF SIMULATION USING WATERSHED MODULE OF SRBM MODEL

This study has been carried out for the two scenarios. In first scenario, three segments of the catchment as explained earlier (section 4.4.4) have been considered, while in other scenario the entire catchment has been considered to be homogeneous and treated as one segment.

Uniformly distributed rainfall in each segment has been one of the major input parameters required by the model, which may be obtained by Thiessen Polygon method. A computer program has been written to compute values of daily rainfall in each segment using area of Thiessen Polygon. Similarly, the average daily rainfall values for entire catchment has been computed. A flow chart for computing segmentwise rainfall using Thiessen polygon has been given in Fig. 4.18. Thus, raingauge adjustment factor (K1) in the SRBM model may now be considered redundant. The other input parameter for the model is evaporation. Due to non-availability of field data, the evaporation in the study area is assumed to be uniform all over the catchment.

In the catchment, runoff contribution from impervious area is assumed to be negligible, since there is no impervious area within the catchment which is draining directly to the channel. The other impervious areas include buildings and roads. The study area being a hilly terrain, buildings are usually small in size and metal roads are also very few to be detected at 72.5m resolution of remotely sensed data., therefore, areal extent of impervious area and its effect is considered to be negligible. Hence, the proportion of impervious area (IMPV) in the model has been taken zero.

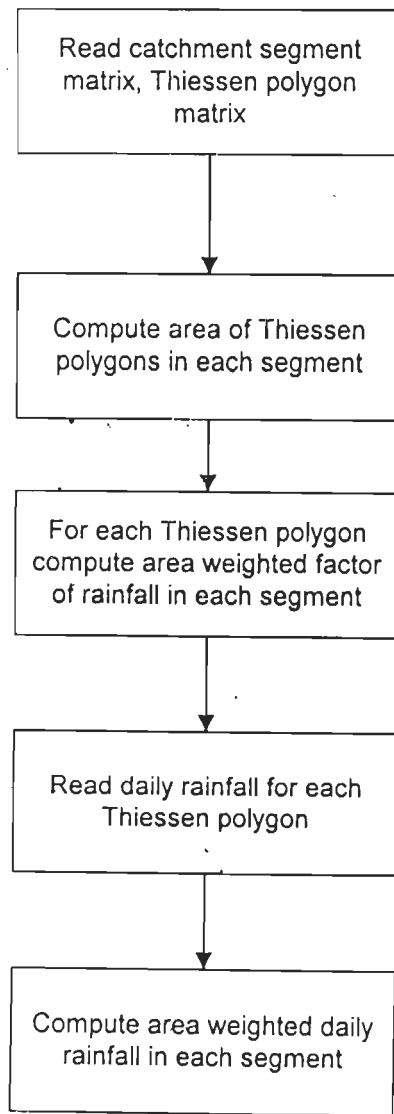


Fig. 4.18 Flow Chart for Computation of Segmentwise Rainfall using Thiessen Polygon

The values of other parameters of the model such as UZSN, LZSN, CB, CC, K24L, K24EL, IRC, KK24 and KV (refer to Table 4.1) have been calibrated for runoff volumes for a year. These parameters have been adjusted, based on the accuracy criteria described by Fleming (1975) i.e. correlation coefficient, variance of residual and explained variance as well as visual comparison between the observed and simulated results. After having achieved the satisfactory calibration, the calibrated values of these parameters have been used to compute runoff for two more years, and compared with the measured values to validate the model. The model computes correlation coefficient, variance of residual and explained variance between the monthly observed and simulated runoff values for assessing the accuracy of calibration.

4.7 SENSITIVITY ANALYSIS

Sensitivity analysis is a technique used to understand the relative importance of each parameter of the model (Fleming, 1975). The sensitiveness of the important calibration parameters is examined by two approaches; (i) quantitative approach, and (ii) qualitative approach (Bathurst, 1986). In the first approach, the value of single parameter is varied at a time from its calibrated value and the effect on the simulated hydrograph is assessed quantitatively by the root mean square value of the differences between the measured and simulated discharges. The sensitivity of a parameter is also depicted by the percent error in predicted peak discharge. In qualitative approach, the assessment of sensitivity of each parameter is made by comparing the graphical plots of the simulated hydrographs and accounting for the differences by physical reasoning.

In this study, sensitivity analysis of the model parameters has been carried out segmentwise using both the approaches for nominal lower zone soil moisture (LZSN), infiltration parameter (CB), interflow parameter (CC), interflow recession parameter (IRC) and ground water recession parameter (KK24). The other parameters such as subsurface flow parameters (K24L) evaporation from ground water (K24EL) and variable ground water recession (KV) have been calibrated for final adjustment. Initially, the values of these calibration parameters have been taken as zero and then increased, if necessary, to

improve the accuracy. These parameters have not been found sensitive as they did not change the total runoff volume but adjust the volume with time. In sensitivity analysis, only one parameter is varied at a time, upto $\pm 30\%$ in each segment and its effect on total runoff has been observed.

The methodology adopted to study the rainfall-runoff relationship using SRBM model has been applied on River Giri catchment in H.P. (India). Next chapter describes the details of the study area and data used.

CHAPTER 5

STUDY AREA AND DATA USED

5.1 THE UPPER YAMUNA CATCHMENT

The catchment area of river Yamuna upto Tajewala headworks is known as upper Yamuna Catchment in H.P., (India) (Fig. 5.1). The Yamuna river rises in the Uttarkashi District of Uttar Pradesh from Yamnotri glacier near Bandarpunch at an elevation of about 6320m. The Rishiganga, the Uma, the Hanuman Ganga and several other tributaries from the lesser Himalayan ranges and ridges join river Yamuna.

The river Tons is the largest Himalayan tributary of the Yamuna. It rises from the north-eastern slope of Bandarpunch at an elevation of 3900m. At Tiuni, Tons is met by Pebbar river and flows down upto its confluence with Yamuna below Kalsi. At this site, the Tons carries twice the water that is carried in the Yamuna, and considered as the principle source of that river.

The river Giri is another important tributary of the Yamuna. It rises near Shimla and joins Yamuna near Paonta Sahib. The drainage pattern is such that most of the tributaries join the next higher order streams at approximately the same acute angle with hardly any abrupt bends.

5.2 THE RIVER GIRI CATCHMENT

A part of river Giri catchment upto Yashwant Nagar has been selected for the present study (Fig. 5.2). The river Giri is a major tributary of Yamuna catchment of the Indo-Gangatic plains which originates from Kupar Tibba in Shimla District, at an elevation of 3358m above msl, and joins river Yamuna upstream of Paonta Sahib. A barrage is built across river Giri almost at the end of the river before joining Yamuna at Jatoon, downstream of Dadahu. The study catchment, covering an areal extent of 1378.25 km². up to Yashwant Nagar gauging site, is situated between 30° 45' North to 31° 30' North latitudes and 77° 00' East to 77° 45' East longitudes.

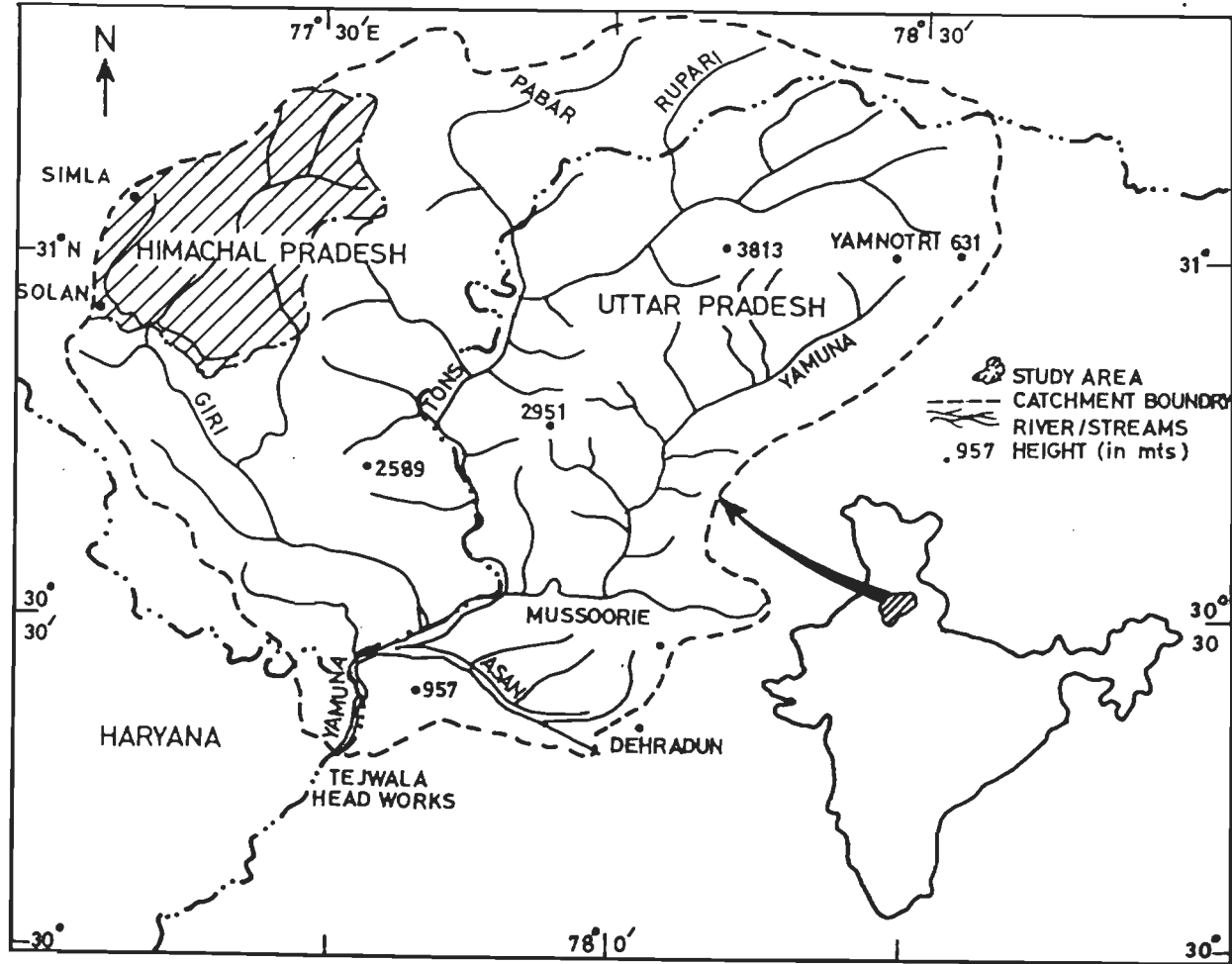


FIG. 5-1: THE UPPER YAMUNA CATCHMENT

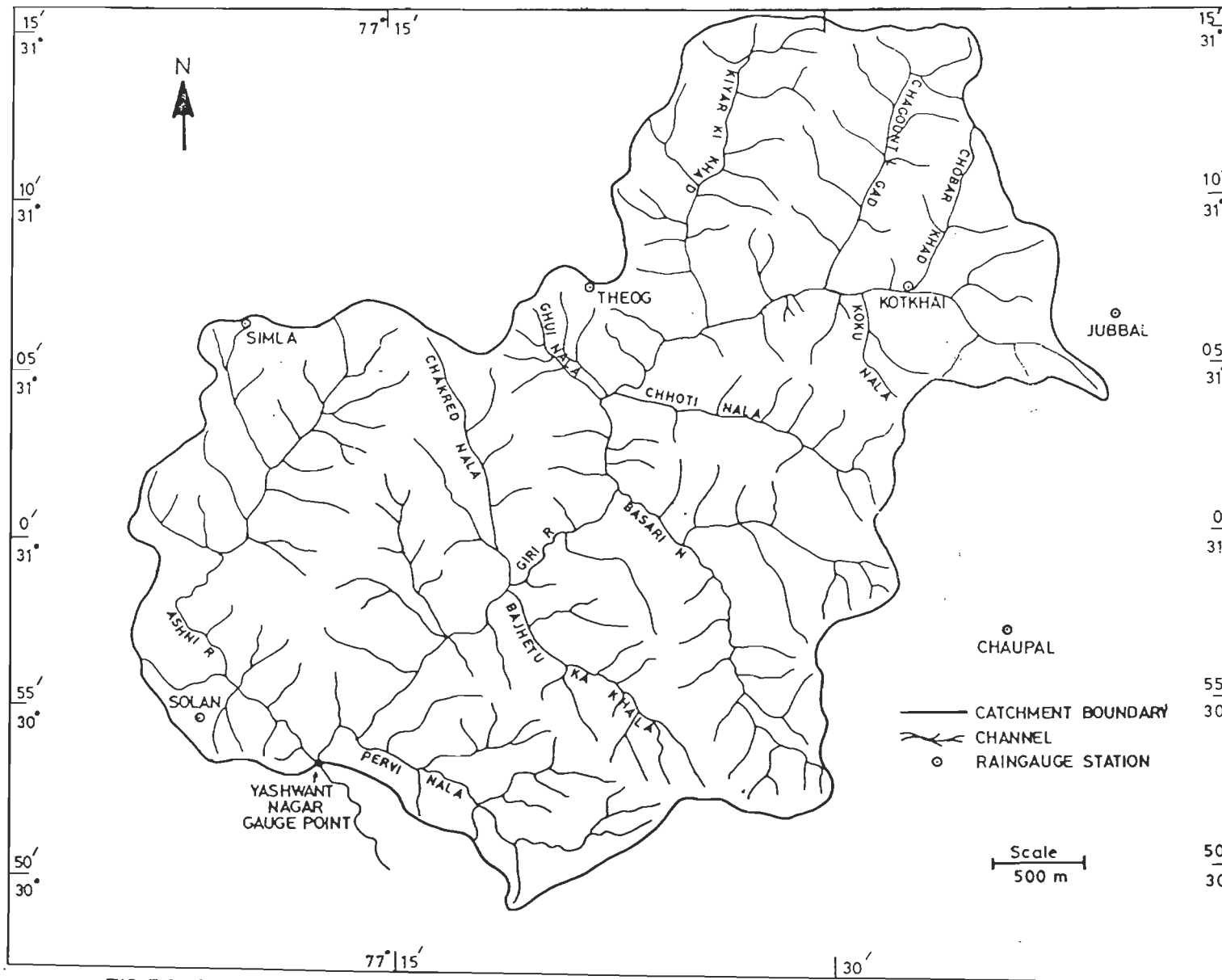


FIG.5.2 : GIRI CATCHMENT UPTO YASHWANT NAGAR GAUGING SITE

5.2.1 RIVER NETWORK

The catchment is heavily dissected by the stream network, as shown in Fig. 5.2. The total length of river Giri up to Yashwant Nagar gauging site is around 55 km. The upper half of the river is flowing towards West and the remaining towards South-West direction. The major tributaries joining left bank of the river are Koku Nala, Chooti Nala, Basari river, Bajhetu Ka Khala and Pervi Nala, while the right bank tributaries are Chobar Khad, Chagountl Gad, Kiyar Ki Khad, Ghui Nala, Chakred Nala and river Ashni. Among these, the longest tributary is river Ashni which flows towards South-West and takes turn of about 90 near Kandaghat and then flows towards South-East to finally meet river Giri at Yashwant Nagar. The overall drainage pattern in the catchment is like a tree with branches well spread out, and may be called as dendritic pattern (Rao et al., 1991).

5.2.2 TOPOGRAPHY

The physiography of the area is essentially dictated by the hills and valley slopes, and are characterised by terrace formation on either sides of slopes for cultivation (Rao et al., 1991). The elevation of the catchment ranges from 900m to 3300m above msl. The area consists of massive mountainous tract with series of ridges and spurs divided by river valleys.

5.2.3 CLIMATE

The climate during the summer months viz., March to May is generally cool, healthy and agreeable. Rainy season extends from June to October, and is characterised by heavy to very heavy rainfall. Winter season experienced by severe cold, extends from November to February. Normal annual temperature in the catchment is 15⁰ C, with 20⁰ C as maximum monthly temperature in June and 5⁰ C as minimum monthly temperature in January. The normal annual rainfall in the catchment is about 1400mm, and normal rainfall in monsoon period is about 900mm. The climatic conditions in the catchment vary from place to place as a direct result of varying altitude.

5.2.4 GEOLOGY

The catchment lies in the vast mountainous tract of the Middle Himalaya. The geological formation of the area consists of stratified rocks, which is divided into Himalayan and sub-Himalayan systems. The Himalayan part through which the Giri river passes consists of rough slates, phyllites, micaceous schists, sandstone, limestone and quartzites. The Sub-Himalayan zone or the Shiwaliks consists of mainly sandstone, red shales and red clay (Rao et al., 1991). A geological map is shown in Fig. 5.3.

5.2.5 SOILS

The major soil classes in the catchment are given in the Atlas of Agriculture Resources of India (Das Gupta, 1980). The catchment area is covered with sub-montane soil and brown hill soil. The sub-montane soils are siliceous from dark brown to dark sandy loam rich in humus. The brown hill soils are loam to silty clay, texturally. These are derived from Tertiary sedimentaries of sandstone, shale and micaceous gray sandstones (Kowasa, 1988). A soil map of the area is shown in Fig. 5.4.

5.2.6 VEGETATION

The lower area of the catchment is covered by shrubs while the middle area corresponding to sub-tropical climate has Chir as the most prominent species of forest. The higher temperate zone consists of Conifers, like Kail and Deodar along with Fir and Spruce in the extreme north. The landuse pattern in the catchment indicates that about three-fourth area is non-agricultural land which consists of forests, waste land, pastures and grass land. Fig. 5.5 shows the landuse map of the area, prepared by H. P. Remote Sensing Cell.

5.3 DATA AVAILABILITY

The hydrologic model (already explained in chapter 4) which simulates the land phase of hydrological cycle requires the evaluation of a large number of parameters and their spatial distribution, along with the necessary time series of data for calibration, validation and operation of the model. Data collection was carried out through a number of visits to

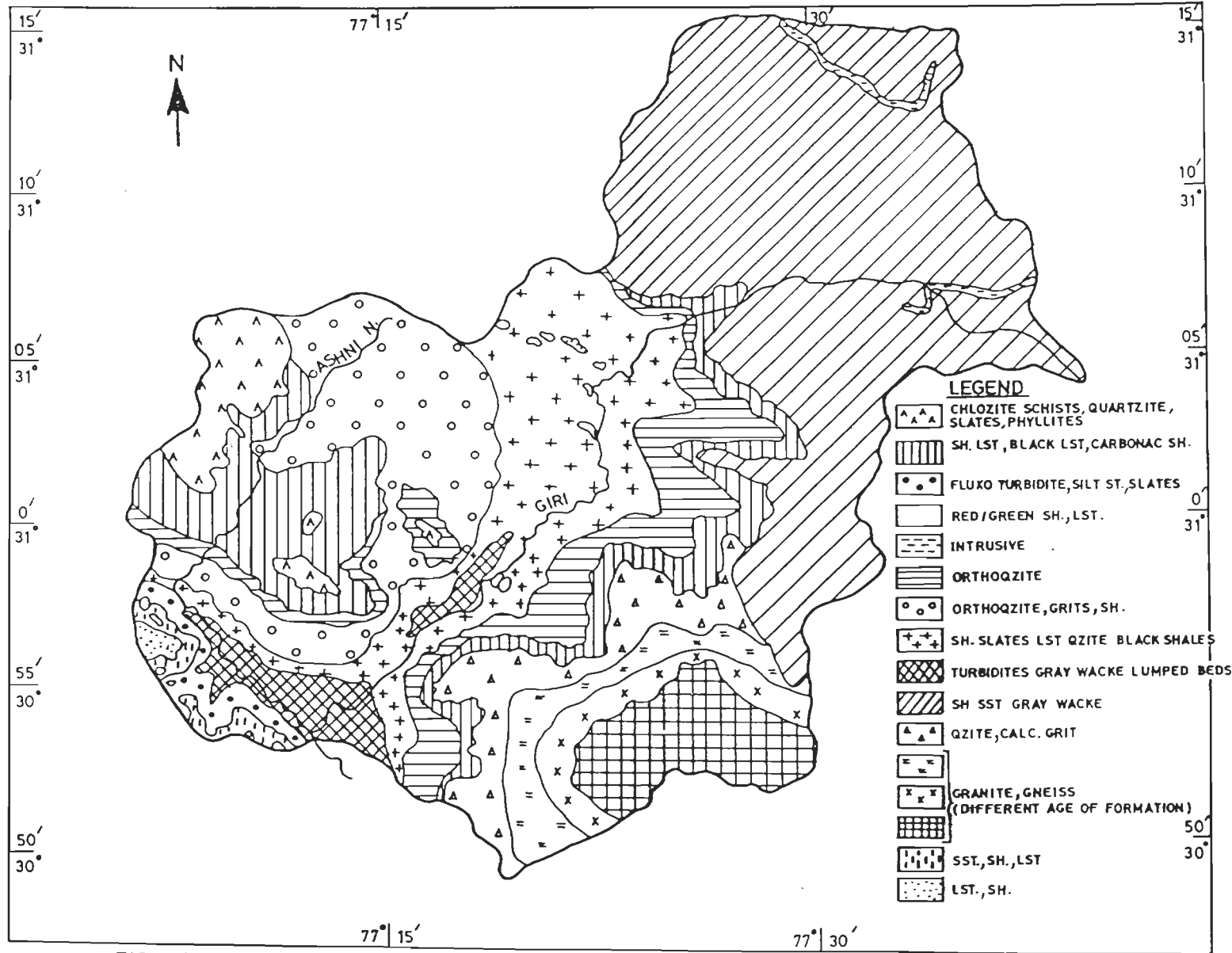


FIG. 5-3: GEOLOGICAL MAP OF RIVER GIRI CATCHMENT
(SOURCE: THAKUR AND RAWAT, 1992)

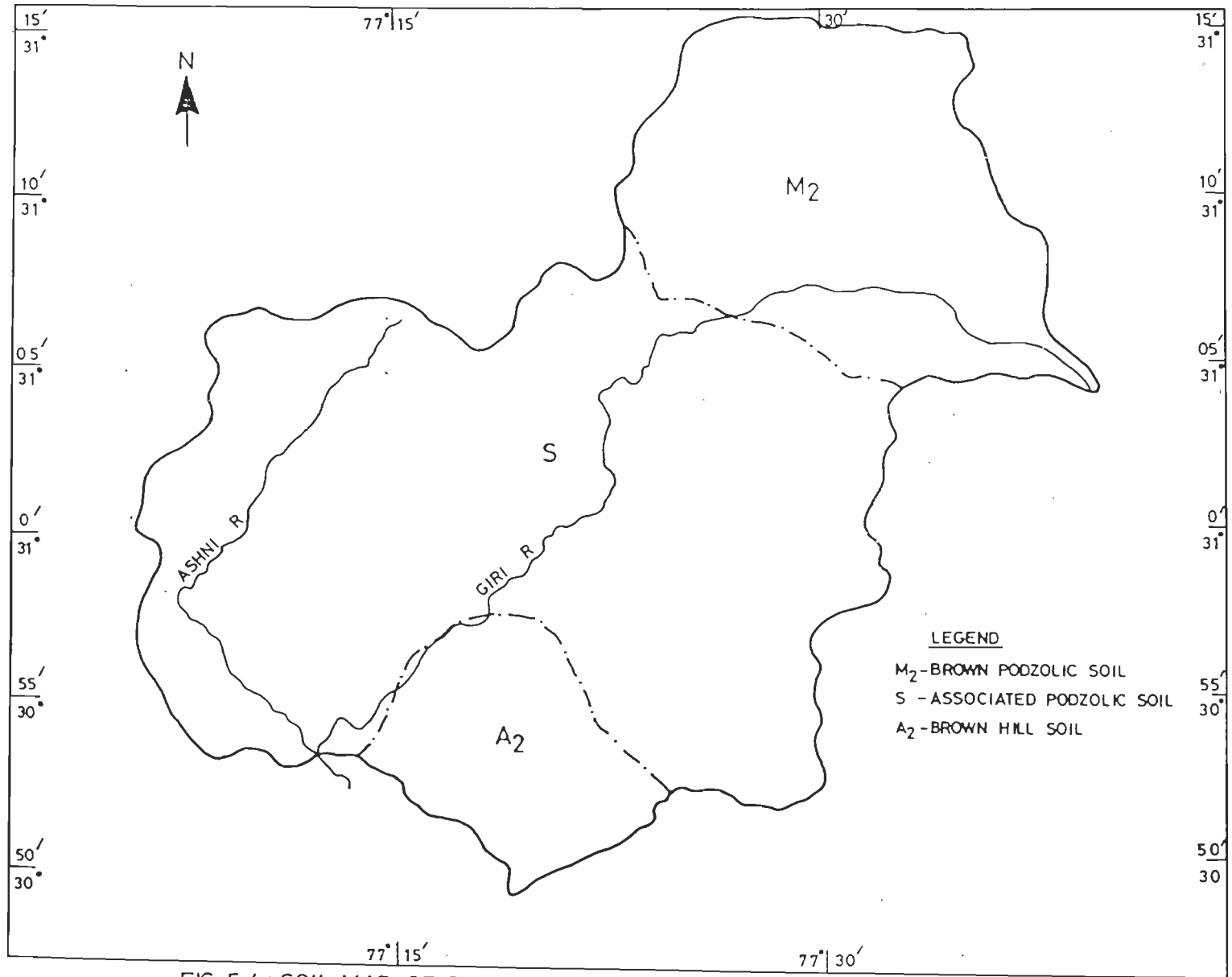


FIG. 5-4 : SOIL MAP OF RIVER GIRI CATCHMENT
(SOURCE : DAS GUPTA, 1980)

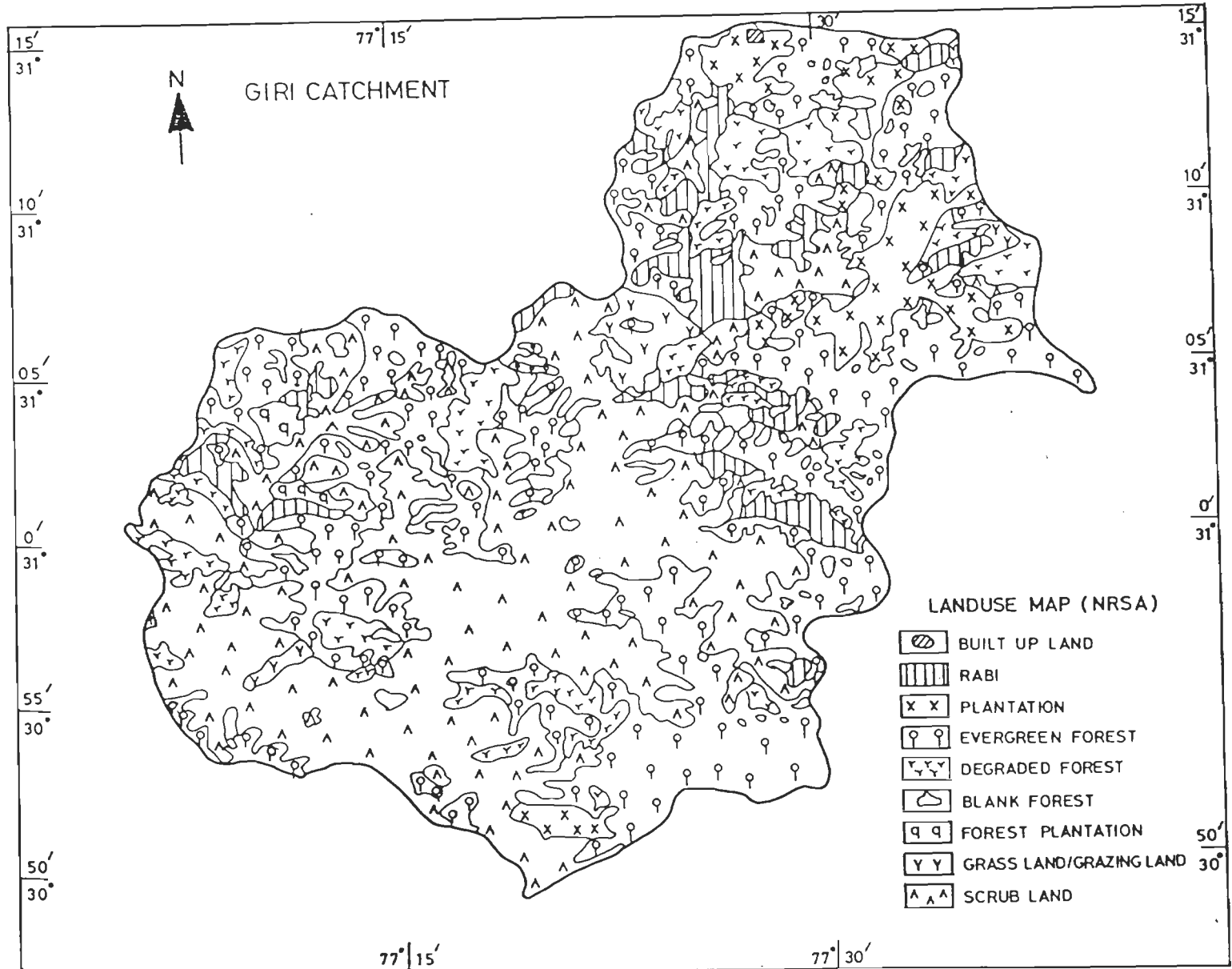


FIG. 5-5: LAND USE MAP PREPARED FROM IRS IMAGERIES OF NOV 88 & MARCH 89 AND S.O.I. MAPS
 (SOURCE : H. P. REMOTE SENSING CELL, 1991)

different Offices in Himachal Pradesh and various sites in the catchment. Available hydrometeorological data were compiled for the years 1989, 1991 and 1992. Basically, three types of data were required;

- (i) Topographical and other maps
- (ii) Hydrometeorological data such as rainfall, evaporation data and streamflow data, and
- (iii) Satellite data

5.3.1 TOPOGRAPHICAL AND OTHER MAPS

The study area is covered in two topographical map Nos. 53E and 53F at 1:250000 scale, and seven topographical map Nos. 53E/4, 53E/7, 53E/8, 53E/12, 53F/1, 53F/5 and 53F/9 at 1:50000 scale. Soil map and Geological map have also been used to study the soil types and Geological characteristics of the catchment.

5.3.2 HYDROMETEOROLOGICAL DATA

The various hydrometeorological data, available in the study area, are rainfall at six stations, evaporation at one station and discharge at the outlet of the catchment. The details of these data are given in Table 5.1.

Table 5.1 Details of Hydrometeorological data used in the study

<i>S.No.</i>	<i>Data Type</i>	<i>Frequency</i>	<i>Gauging Station</i>	<i>Years</i>
1	Rainfall	Daily	Solan Shimla Theog Kotkhai Jubbal Chopal	1989, 1991, 1992
2	Evaporation	Daily	Solan	1989*, 1991; 1992
3	Discharge	Daily	Yashwant Nagar	1989, 1991, 1992

* Only Monthly Data

5.3.2.1 Rainfall Data

For the present study, rainfall data were collected for six raingauge stations whose locations are shown in Fig.5.2. The four raingauge stations at Solan, Shimla, Theog and Kotkhai are situated inside the catchment, whereas the remaining two stations situated at Jubbal and Chopal are outside but close to the catchment. The daily rainfall data were available for these stations for the monsoon period (June to October) of years 1989, 1991 and 1992. These raingauge stations provided the representative coverage of spatial variability in rainfall throughout the catchment.

5.3.2.2 Evaporation Data

The evaporation data in the catchment is available at only one station, located at Solan. The daily pan evaporation data available at this station were collected for two years i.e. 1991 and 1992 and monthly evaporation data for the year 1989.

5.3.2.3 Discharge Data

Discharge data were available only at the outlet gauging station at Yashwant Nagar, which is about 1km. downstream after confluence of river Ashni and Giri. The daily discharge data from June to October for years 1989, 1991 and 1992 were available.

5.3.3 SATELLITE DATA

Satellite data are required to obtain latest drainage pattern and land cover information of the study area. The study area is covered by one scene of LANDSAT as well as IRS image. The details of satellite data used in this study are given in Table 5.2.

Table 5.2 Details of Satellite Data Used

<i>S.No.</i>	<i>Path/Row no.</i>	<i>Date</i>	<i>Satellite & Sensor</i>	<i>Data Type</i>
1	158/038	27 Mar.1977	LANDSAT MSS	FCC
2	158/038	4 Oct.1980	LANDSAT MSS	Band 5
3	29/46	3 Mar.1989	IRS LISS I	Digital Data in bands 1,2,3&4

The data products described in this chapter were used to obtain various parameters for the rainfall-runoff model. ILWIS (Integrated Land and Water Information System), which is basically a Geographic Information System, also comprises of image processing modules. This package was used for the digitization of maps as well as image processing of satellite data.

Next chapter describes the analysis procedure to extract input parameters from various data, required for rainfall-runoff modelling approach used in this study.

CHAPTER - 6

ANALYSIS OF DATA

6.1 INTRODUCTION

The data collected for this study has been used for the generation of DEM and extraction of catchment parameters, analysis of remote sensing data and integration of these data within the hydrological model to assess runoff. This chapter comprises of results obtained by detailed analysis of DEM, satellite data and hydrometeorological data.

6.2 DEVELOPMENT OF DEM OF GIRI CATCHMENT

Initially, the contours from topographical maps have been digitized at 200m interval, using A₀ digitizing table hooked to ILWIS. Interpolation is performed after rasterization of contour file, using module named Interpolation module provided within the system. Bilinear interpolation has been used for generating a DEM of grid size of 500m by 500m. The generated DEM for Giri catchment, thus comprises of 103 rows and 112 columns for an area of 1378.25 km² with a total of 5513 grid cells fall within the catchment. The accuracy of DEM generated above has been checked by comparing the elevations of more than 200 well distributed points within the catchment from topographical map. The correlation coefficient has been found to be 0.996 with a standard error of 44m. This error is acceptable since contours have been digitized at 200m interval and interpolated at 500m grid size.

6.3 ANALYSIS OF DEM

DEM, thus developed of the study area has been analysed for segmentation of catchment, computation of flow direction and flow accumulation and finally for extraction of drainage network. The DEM is initially examined for the depressions, and 76 single cell depressions have been identified. These depressions have been removed according to the algorithm defined in chapter 4 (section 4.4.2). Segmentation, flow direction and flow accumulation values have been obtained from the depressionless DEM, and have been described below:

6.3.1 SEGMENTATION OF CATCHMENT

As mentioned in section 4.4.4, the Giri catchment has been divided into three segments with the help of area-elevation curve (Fig. 6.1). The straight line portion of this curve i.e. between 1600m to 2300m elevation range has been defined as Segment 2 or Midland, while the region above 2300m elevation has been defined as Segment 1 or Upland, whereas below 1600m elevation it has been defined as Segment 3 or Low land. As outlet is the lowermost point in any catchment, hence whole catchment lies above the elevation of outlet i.e. 900m. The area of Segment 1, 2 and 3 are 337.00, 693.00 and 348.25 km² respectively (see Plate 6.1).

6.3.2 COMPUTATION OF FLOW DIRECTION AND FLOW ACCUMULATION VALUES

Flow direction data have been computed by two approaches i.e. conventional approach and Flow Line approach. On comparing the flow direction obtained using Flow Line and conventional approaches it has been found that 23 grid cells have undefined flow directions using conventional approach, whereas by Flow Line approach there are only 8 such cells. On reallocation of unassigned flow directions to these 23 cells as obtained by conventional approach, a total of 79 cells are affected, while only 42 cells are affected when using Flow Line approach. Table 6.1 lists the location of such undefined cells, as identified by both the above approaches. For better visualization, flow direction codes computed by conventional and Flow Line methods are shown in Fig. 6.2 and 6.3 respectively.

Flow accumulation values have been determined using flow direction values as obtained by Flow Line Approach. The starting cells of each flow lines are assigned zero flow accumulation values. At the outlet, which drains the whole area has a flow accumulation value of 5513 i.e. total number of grid cells in the catchment.

Segment	Elevation (M)	Area (sq.km.)
1	>2500	337.00
2	<2500 and >1600	693.00
3	<1600	348.25

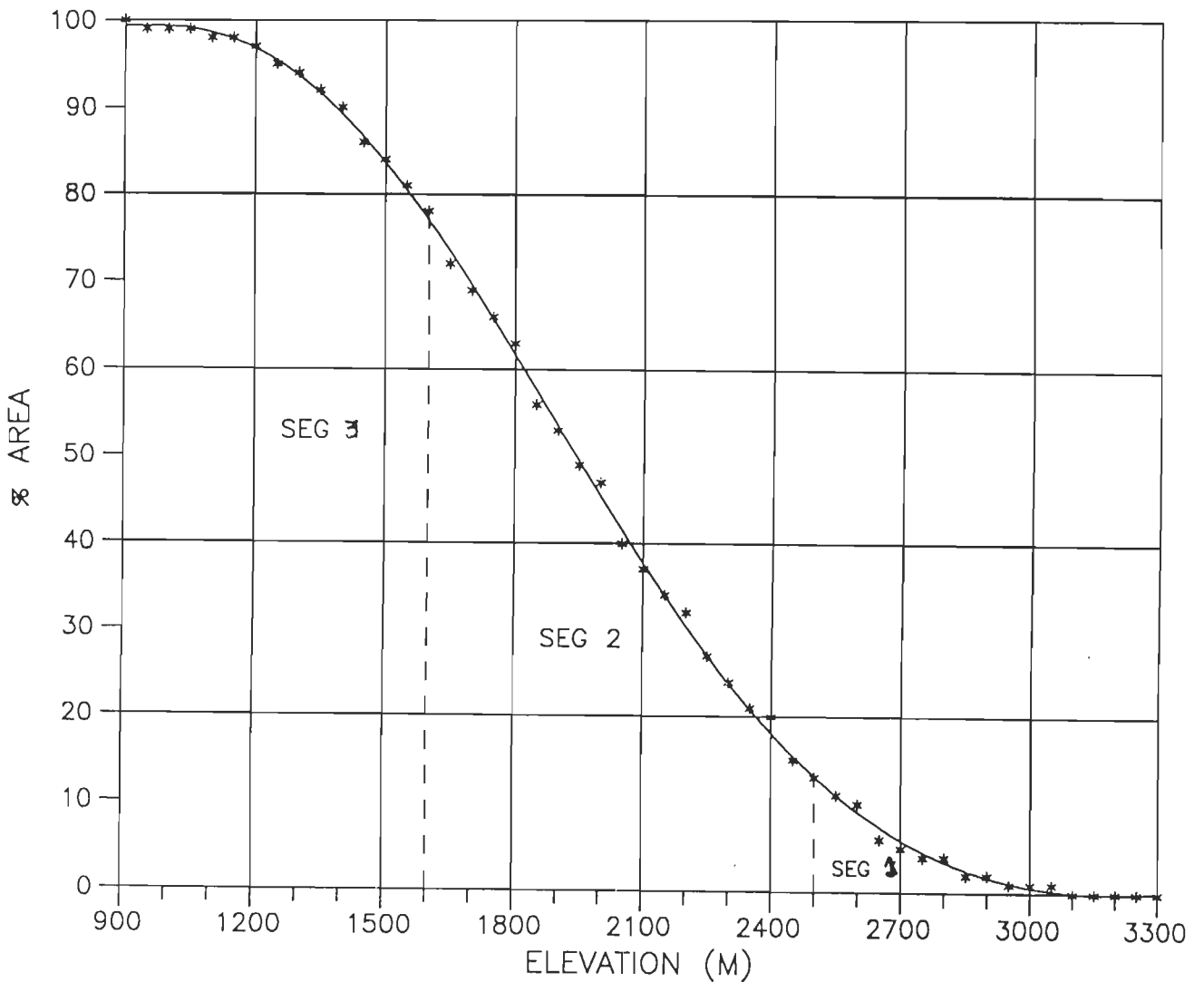


Fig.6.1 Area Elevation Curve of Giri Catchment

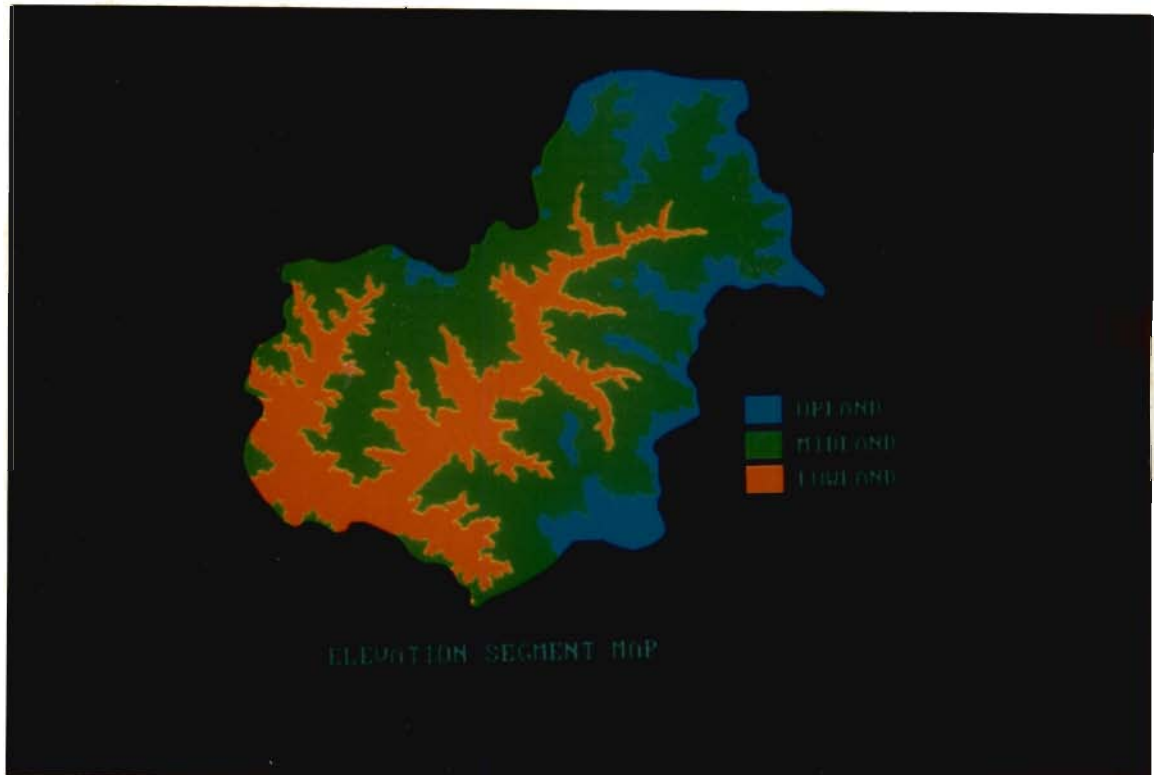


Plate 6.1 Elevation Segment Map of Giri Catchment

Table 6.1 Location of Cells with Undefined Flow Direction

S.No.	DEM		Conventional Approach		Flow Line Approach	
	Row no.	Col. no.	Undefined Flow Direction	No. of affected cells	Undefined Flow Direction	No. of affected cells
1	3	76	yes	1	yes	1
2	4	83	yes	1	yes	1
3	29	58	yes	1	yes	1
4	32	55	yes	2	no	--
5	33	84	yes	6	yes	6
6	33	88	yes	3	no	---
7	34	98	yes	3	no	---
8	36	71	yes	2	no	---
9	37	68	yes	5	no	---
10	44	57	yes	2	no	---
11	47	72	yes	2	no	---
12	56	22	yes	3	no	---
13	57	26	yes	2	no	---
14	59	53	yes	14	yes	14
15	64	75	yes	2	no	---
16	67	76	yes	2	yes	2
17	68	47	yes	3	yes	3
18	70	42	yes	7	yes	7
19	74	55	yes	2	no	---
20	83	32	yes	3	no	---
21	83	42	yes	2	no	---
22	85	38	yes	2	no	---
23	88	42	yes	2	no	---
Total			23	72	8	35

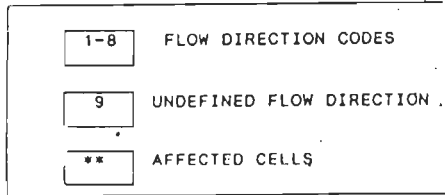


Fig. 6.3 Flow Direction map using Flow Line Approach

6.3.3 EXTRACTION OF CHANNEL NETWORK

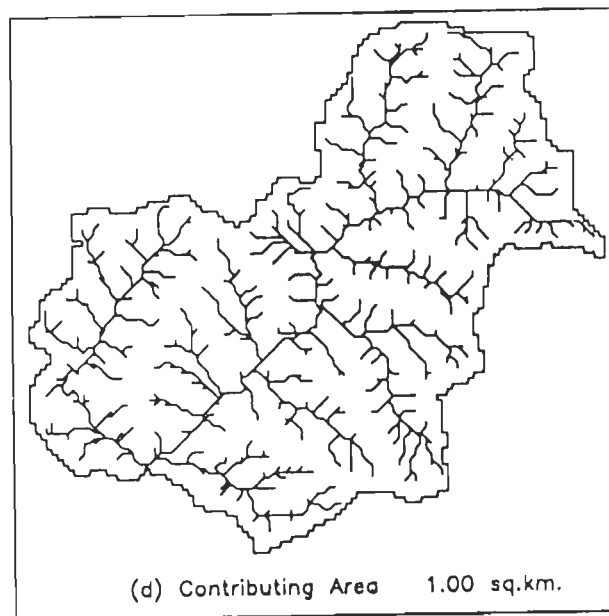
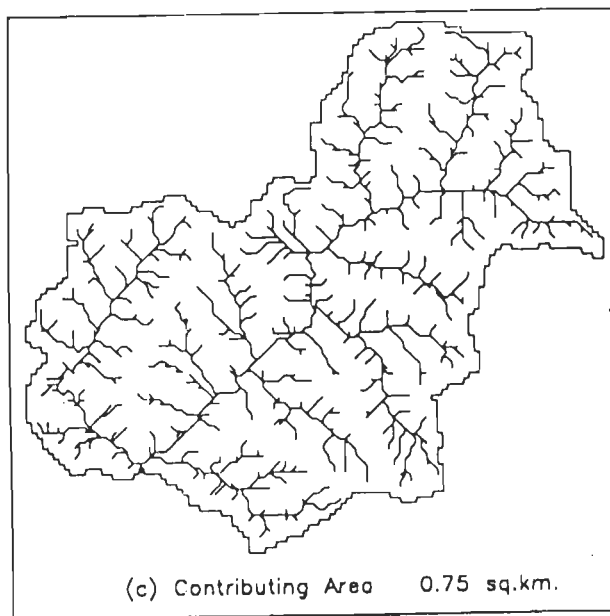
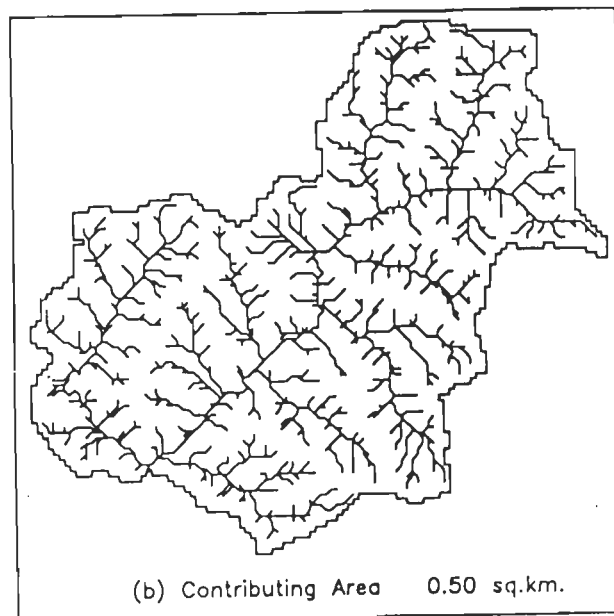
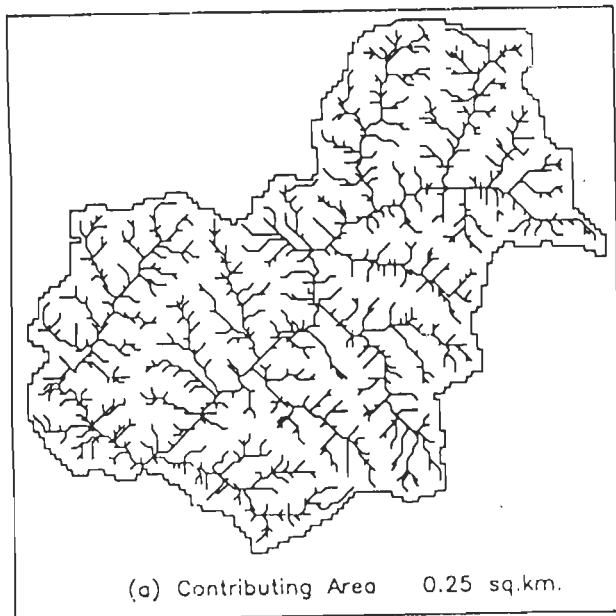
The drainage network of the catchment has been delineated using flow direction and flow accumulation data. Eight drainage networks (Fig. 6.4) have been obtained for different threshold values of area varying from 0.25 km² to 2.00 km². The drainage networks generated using area threshold approach are compared with the drainage network of toposheets at 1:250,000 scale. It has been observed that drainage network generated from DEM with area threshold value as 0.75 km² matches closely to the drainage network depicted on toposheets.

6.3.4 COMPUTATION OF MODEL PARAMETERS FROM DEM

Area of segments, parameter RIVER, overland flow length and channel slope which are model parameters of SRBM have been derived from DEM. Segmentwise area is determined on the basis of grid cells for each elevation zone. Parameter RIVER is computed for each segment as the ratio of area contributing directly to channel to the total catchment area.

For each set of drainage network, overland flow length has been computed and compared to the overland flow length obtained from topographical map and is given in Table 6.2. The overland flow path for drainage network as obtained from topographical map has been computed as 764.52 km. The overland flow length of drainage network with threshold value of 0.75 km² is 789.105 km, and matches closely to overland flow length as obtained from topographical map. It is observed from Table 6.2 that the overland flow length decrease at a lesser rate with a constant increment of area threshold value. A total of 331 links have been counted from the topographical map. For different sets of area threshold values, the number of links are shown in Table 6.2. It is found that the total number of links as obtained from different sets of drainage network are more when compared to the total number of links as obtained from topographical maps. The reason being that as the area threshold value decreases the number of links increases.

The average flow path slope is computed by taking average of the slope of channel cells in each segment. A concise information of these parameters for each segment as well as for the entire catchment has been given in Table 6.3.



Contd.

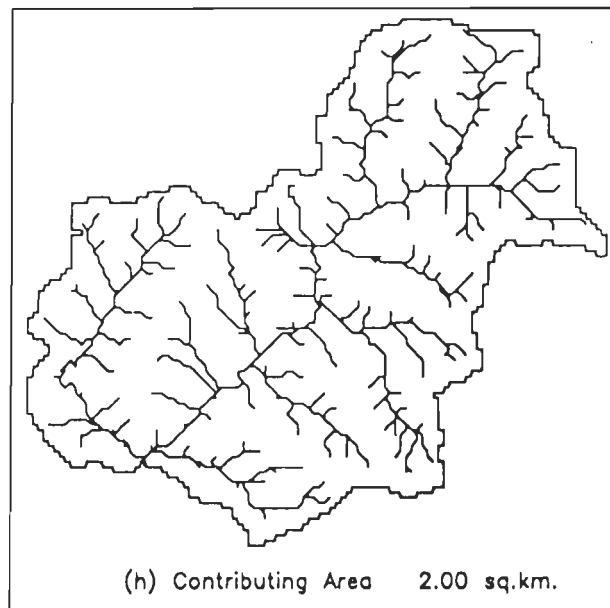
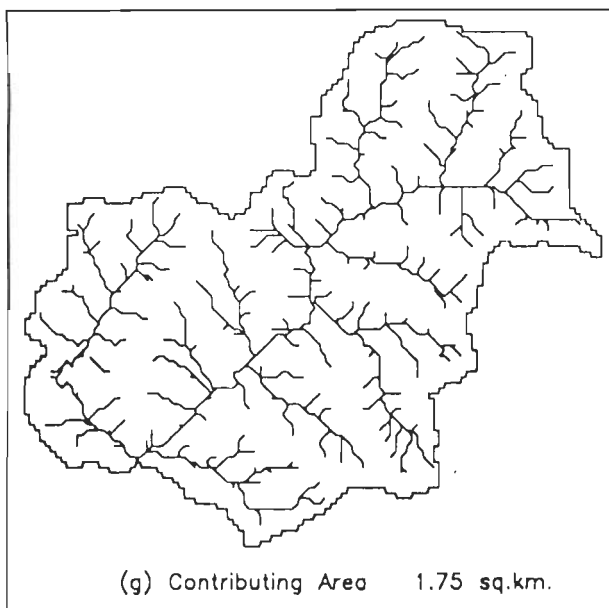
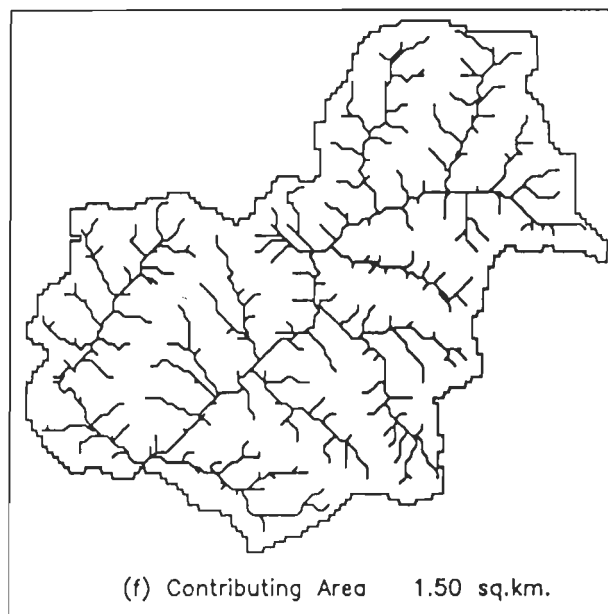
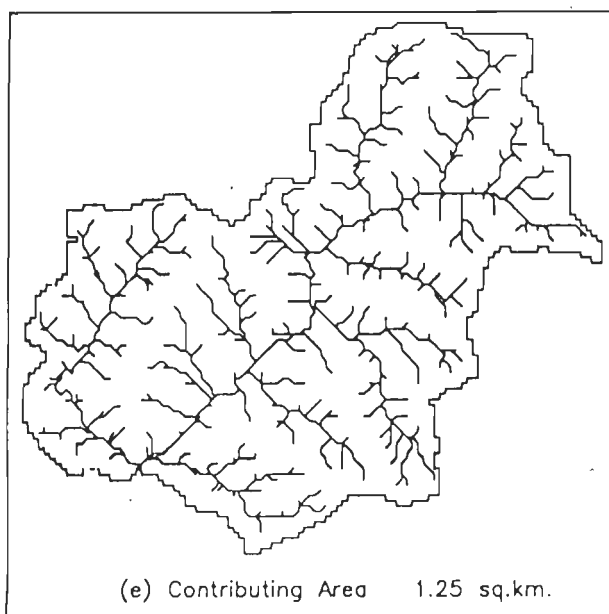


Fig. 6.4 Channel Network for Various Threshold Contributing Area

Table 6.2 Overland Flow Length for Different Sets of Drainage Networks

<i>S.No.</i>	<i>Area Threshold in km²</i>	<i>Overland Flow Length in km</i>	<i>% Variation with Topographical Map</i>	<i>No. of Links</i>
1	0.25	1108.180	44.95	1056
2	0.50	902.669	18.07	741
3	0.75	789.105	3.22	568
4	1.00	718.676	-5.99	481
5	1.25	661.685	-13.45	414
6	1.50	618.179	-19.07	353
7	1.75	587.038	-23.21	304
8	2.00	552.360	-27.75	270

Table 6.3 Catchment Characteristics Computed by DEM.

<i>Parameter</i>	<i>Segment 1</i>	<i>Segment 2</i>	<i>Segment 3</i>	<i>Entire Catchment</i>
Area (km ²)	337.00	693.00	348.25	1378.25
Overland flow length (km)	77184	349382	362539	789105
Channel slope	0.26	0.23	0.18	0.21
RIVER	0.245	0.747	1.00	1.00

6.4 ANALYSIS OF REMOTE SENSING DATA

For this study, IRS LISS I digital data of March 3, 1989 has been used for deriving landuse information in the catchment. The analysis has been performed on ILWIS using its image processing module. IRS images have been coregistered with topographical map and the catchment has been extracted. Best bands are selected for landuse classification, on the basis of image statistics of all four bands. The details of the analysis are given below:

6.4.1 GEOMETRIC REGISTRATION OF IRS DATA

Geometric registration of bands 1, 2, 3 and 4 with base map of the catchment is performed, using second order transformation function. ILWIS calculates the transformation coefficients based on the assumption that the relation between real world coordinates and coordinates of image to be registered, is a second order function. A minimum of 6 control tie points are required for this purpose (ILWIS Manual vol. 2, 1990).

Six intersection points are selected as ground control points for registration. Table 6.4 gives the location of control points in the base map i.e. topographic map and slave map (map to be registered), square of residuals (D_{row} and D_{col}), and standard deviation of residuals (σ) for accepted registration.

With the same set of control points, the registration was performed using the affine transformation which resulted standard deviation of 2.81 pixels while second order transformation resulted 0.83 pixel. Therefore, second order transformation has been adopted for the geometric registration of satellite image. Nearest neighbour method has been used for resampling the original image to generate the geo-coded image.

Table 6.4 Statistics of Registration Points

<i>S. N.</i>	<i>Base Map</i>		<i>Slave Map</i>		<i>Square of Residuals</i>	
	<i>X</i>	<i>Y</i>	<i>Row</i>	<i>Col.</i>	<i>Drow</i>	<i>Dcol</i>
1	39400	35400	251	602	0.03	0.50
2	33200	33500	294	517	-0.06	-0.89
3	11700	10000	675	284	-0.02	-0.03
4	4000	18400	582	157	0.07	0.55
5	22400	19200	519	401	-0.17	-0.72
6	31600	21800	458	521	0.15	0.86

Sigma (σ)= 0.83 pixel

6.4.2 IMAGE STATISTICS OF IRS DATA

The satellite data has been analysed to find minimum and maximum brightness value mean, median, standard deviation and predominant value in each band using univariate statistics. The image statistics has been summarised in Table 6.5.

Table 6.5 Univariate Statistics of IRS LISS I, 1989 Data

<i>Band</i>	<i>1</i>	<i>2</i>	<i>3</i>	<i>4</i>
1 Mean	36.6	21.54	27.55	36.97
2 Median	35	21	26	37
3 Std. dev.	8.95	6.29	10.59	9.21
4 Predominant	29 (6772)*	16 (8265)*	15 (5484)*	43 (5257)*
5 Minimum	13	9	8	10
6 Maximum	127	127	127	120

*' Number in bracket shows the frequency.

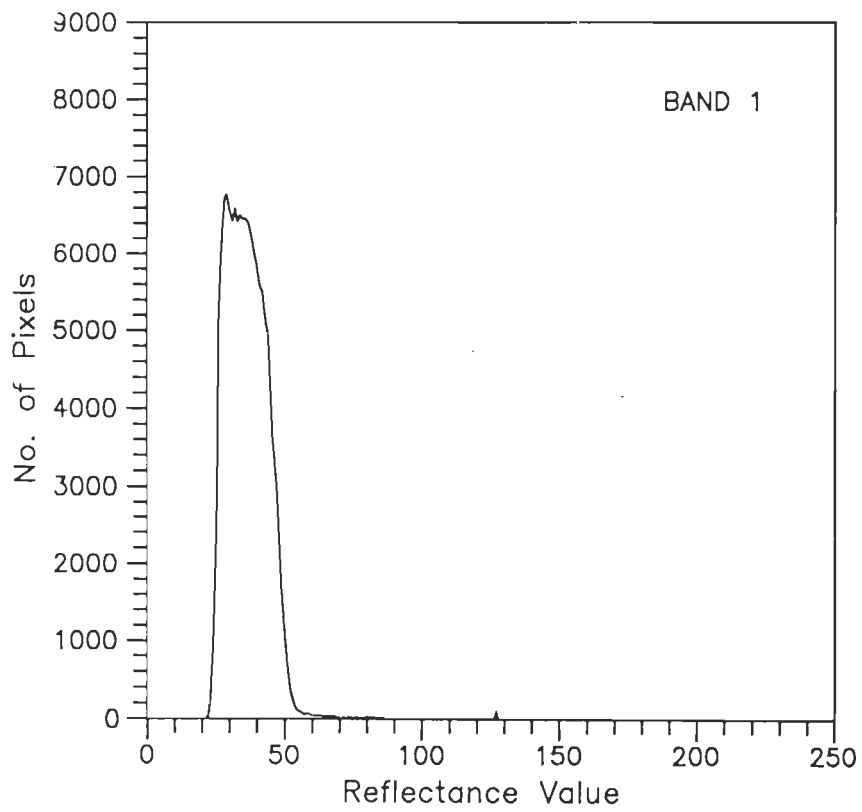
It has been observed from the univariate statistics that the range of brightness value in each band is nearly same but dominating brightness value is different for each band. Histogram of LISS I bands 1, 2, 3 and 4 have been shown in Figs. 6.5 (a), (b), (c) and (d). The visual appearance of these images have been enhanced by linear stretching, and are shown in Plates 6.2 (a), (b), (c) and (d). From histograms and univariate statistics it seems that band 1 is similar to band 4 and band 2 is similar to band 3. As univariate statistics provide completely independent information, therefore multivariate statistics has been performed to study the inter-relationship of bands. The mutual interaction of bands can be measured by variance-covariance matrix (Table 6.6) and correlation matrix (Table 6.7).

Table 6.6 Variance-Covariance Matrix of IRS LISS I, 1989 Data

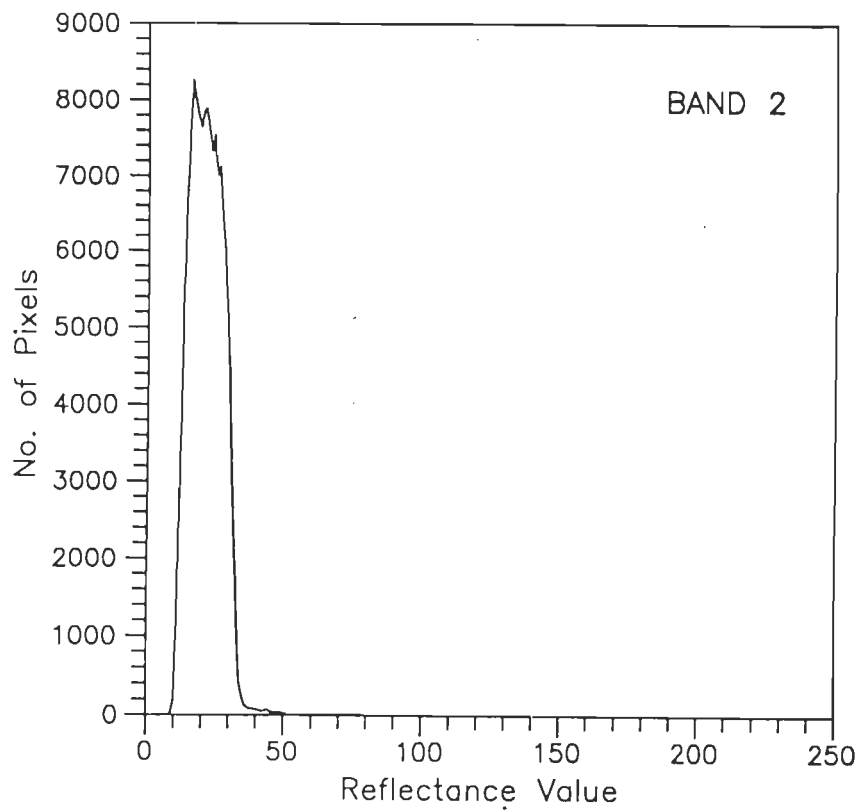
	Band 1	Band 2	Band 3	Band 4
Band 1	80.1			
Band 2	26.6	39.5		
Band 3	45.2	62.4	112.1	
Band 4	61.8	26.3	47.4	84.9

Table 6.7 Correlation Matrix of IRS LISS I, 1989 Data

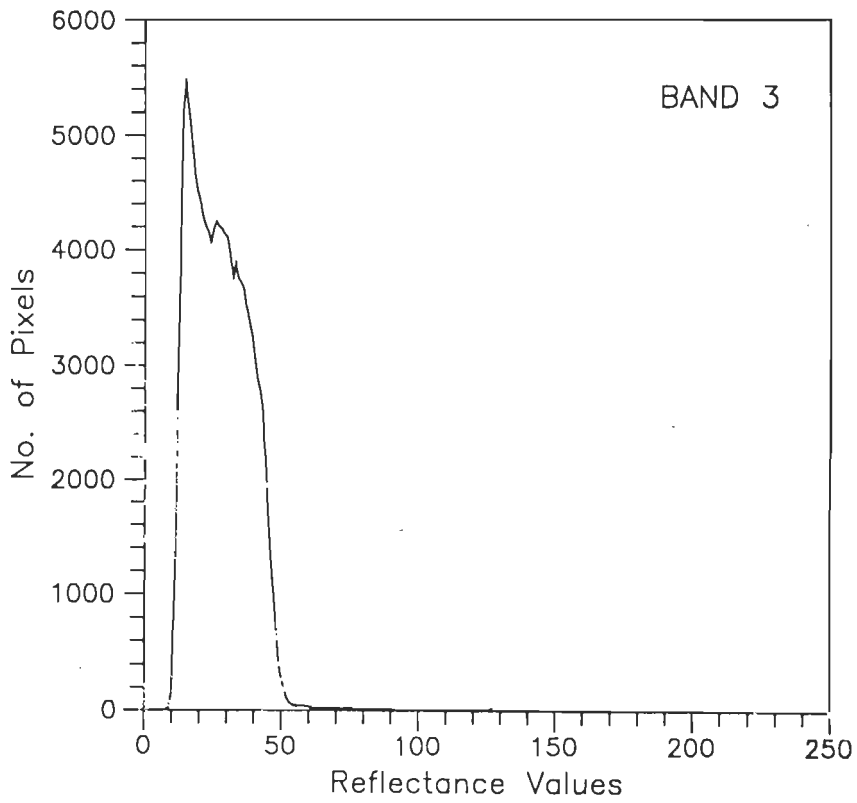
	Band 1	Band 2	Band 3	Band 4
Band 1	1.000			
Band 2	0.472	1.000		
Band 3	0.477	0.937	1.000	
Band 4	0.750	0.454	0.486	1.000



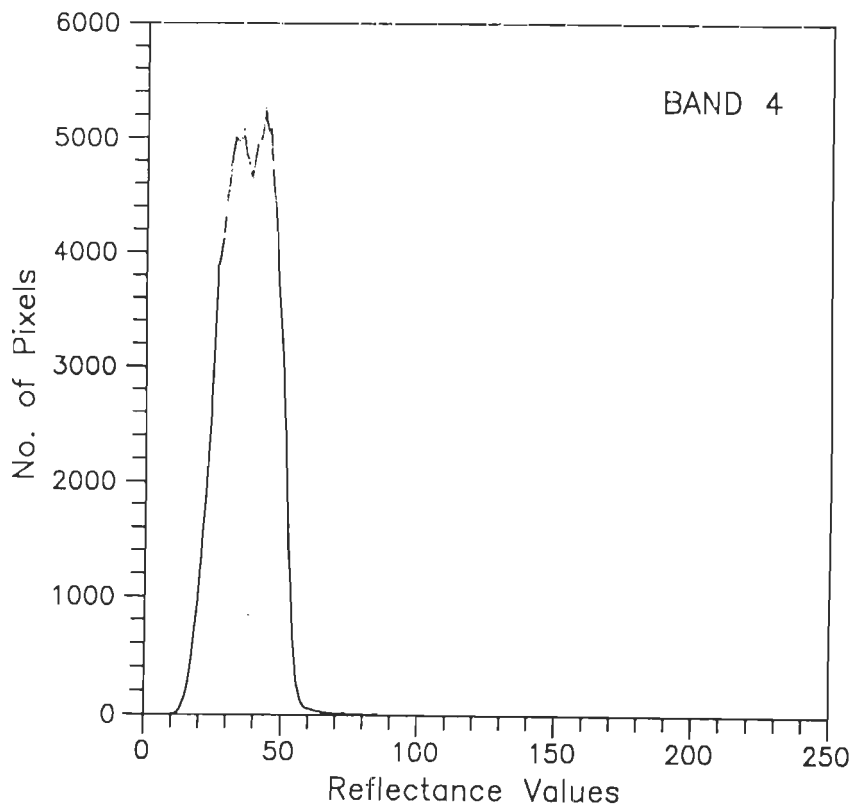
(a)



(b)



(c)



(d)

Fig.6.5 (a), (b), (c), (d) Histogram of IRS LISS I Bands 1, 2, 3 & 4

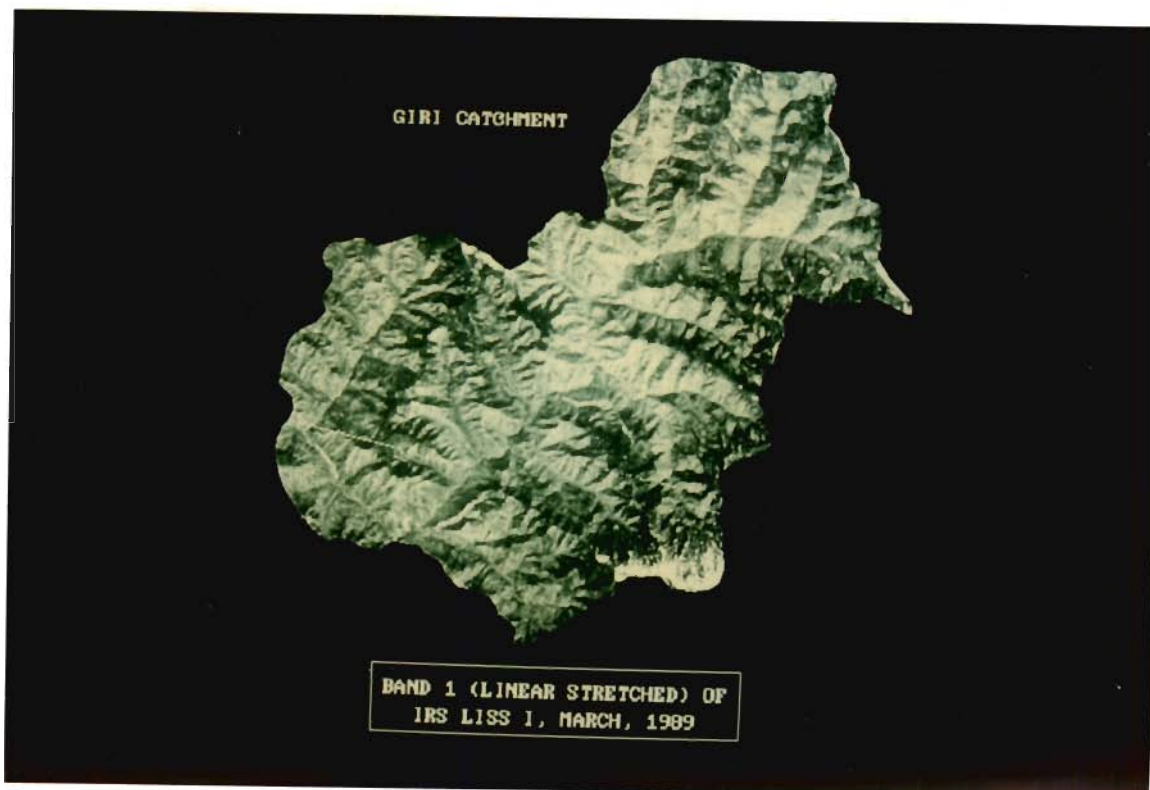


Plate 6.2 (a) Linearly Stretched Image of Band 1

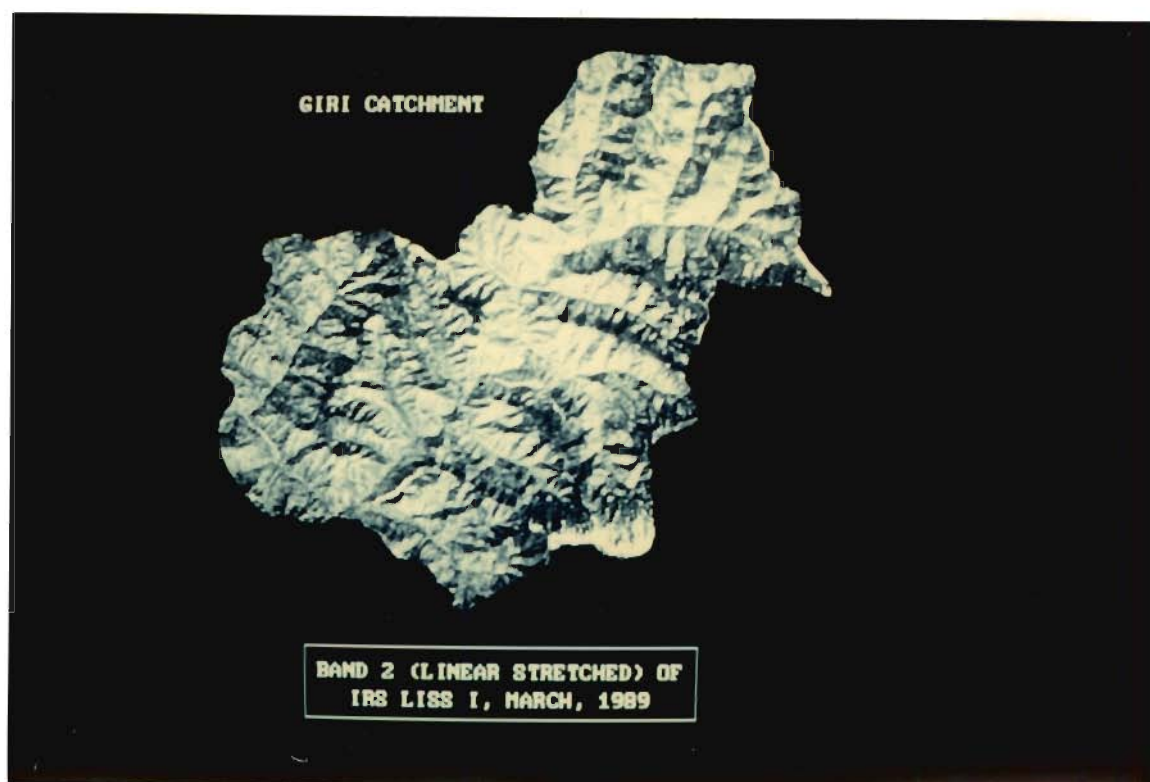


Plate 6.2 (b) Linearly Stretched Image of Band 2

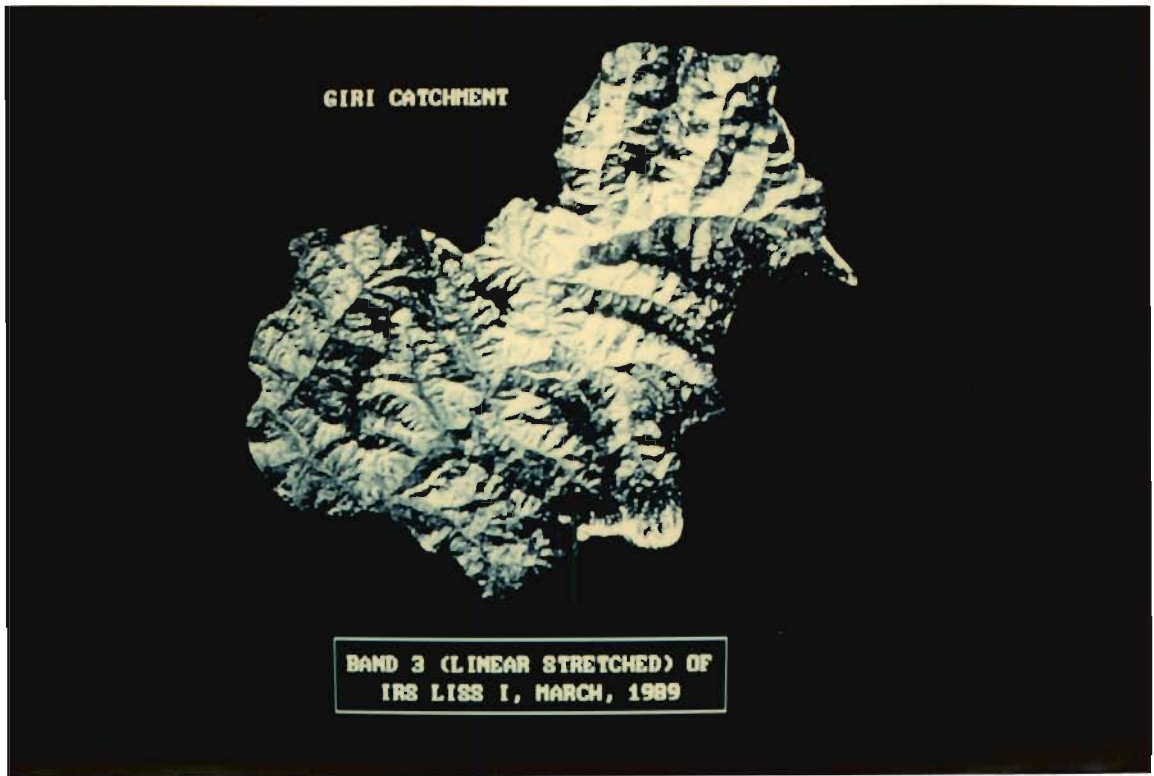


Plate 6.2 (c) Linearly Stretched Image of Band 3

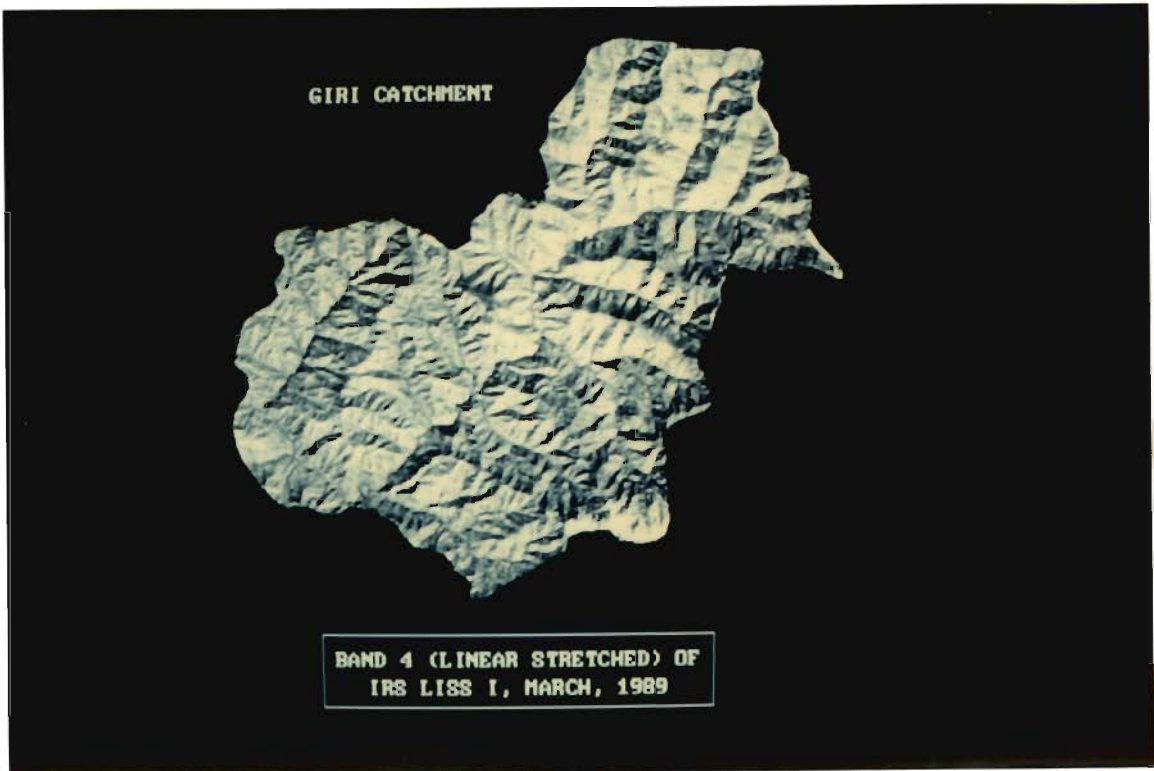


Plate 6.2 (d) Linearly Stretched Image of Band 4

Correlation matrix exhibits the inter-relation of bands. Table 6.6 shows that band 3 has largest variance (112.1) and band 2 the smallest (39.5). It is also seen that bands 2 and 3 are highly correlated with correlation coefficient of 0.937. Thus bands 1, 3 & 4 has been used for further analysis.

6.4.3 DETERMINATION OF LANDUSE INFORMATION

Landuse information within the catchment have been obtained by digital analysis of IRS LISS I data. For better visualization of different landuse classes, a false colour composite has been generated using bands 4, 3 and 1 (Plate 6.3).

The landuse classification has been performed using an unsupervised clustering technique. The maximum number of clusters and minimum distance between clusters as desired for classification are 15 and 8 respectively. After merging, other cluster interactively, four classes could be easily separated out spectrally viz thick forest, thin forest, cultivation and grass land. Water features, due to their small areal coverage, have been merged with cultivation mainly. Plate 6.4 shows the landuse classification of the study area. The areal coverage of various landuse classes in each segment as well as in entire catchment for year 1989 has been shown in Table 6.8.

Table 6.8 Landuse Classes within the Catchment for 1989.

<i>S.No</i>	<i>Land use Class</i>	<i>Segment 1 (in km²)</i>	<i>Segment 2 (in km²)</i>	<i>Segment 3 (in km²)</i>	<i>Entire Catchment (in Km²)</i>
1.	Thick forest	183.75	264.00	104.00	551.75
2.	Thin forest	52.75	160.25	73.00	286.00
3.	Cultivation	86.25	197.75	147.50	431.50
4.	Grass land	14.25	71.00	23.75	109.00
	Total	337.00	693.00	348.25	1378.25



Plate 6.3 False Colour Composite of Giri Catchment



Plate 6.4 Segmentwise Landuse Map of Giri Catchment

The landuse classification has been verified on ground during two field visits carried out in October 1994 and October 1995. Plates 6.5, 6.6, 6.7, and 6.8 show runoff gauging site, thick forest, thin forest, cultivated and grass land respectively on the ground. The landuse classification accuracy has been assessed by comparing classified digital map with the landuse information collected during field visits as well as landuse map prepared by Himachal Pradesh Remote Sensing Cell, Shimla. Table 6.9 shows a contingency table to represent classification accuracy.

Table 6.9 Contingency Table Depicting Classification Accuracy

<i>Actual Landuse Classes</i>	<i>Interpreted Landuse Classes (in Pixels)</i>					<i>Percent Accuracy</i>
	<i>Thick Forest</i>	<i>Thin Forest</i>	<i>Cultivation</i>	<i>Grass Land</i>	<i>Total</i>	
1. Thick Forest	126	14	0	1	141	89.4
2. Thin Forest	7	142	2	1	163	87.1
3. Cultivation	4	3	241	13	26	92.3
4. Grass Land	0	11	6	59	76	77.6
Total	137	170	249	85	641	

$$\text{Overall accuracy} = (568/641) * 100 = 88.6\%$$

The overall accuracy of classification has been found as 88.6%. The accuracy of grass land is 77.6% found to be low as compared to accuracy of other classes.

For years 1991 and 1992, the remote sensing data was not available, thus, the change in landuse pattern has been observed by analysing LANDSAT FCC of 1977 and band 5 imagery of 1980 using visual interpretation method (Fig. 6.6 and 6.7). The area of the catchment computed from 1977 and 1980 images was found to be 1352.40 km² and 1359.04 km² respectively. These areas are 1.9% and 1.4% less as compared to area obtained from DEM. This difference may be due to standard FCC LANDSAT images used for analysis. A comparative landuse information for entire catchment has been given in Table 6.10.



Plate 6.5 Runoff Gauging Site at Yashwant Nagar



Plate 6.6 Thick Forest in Giri Catchment



Plate 6.7 Thin Forest in Giri Catchment



Plate 6.8 Cultivated and Grassland in Giri Catchment

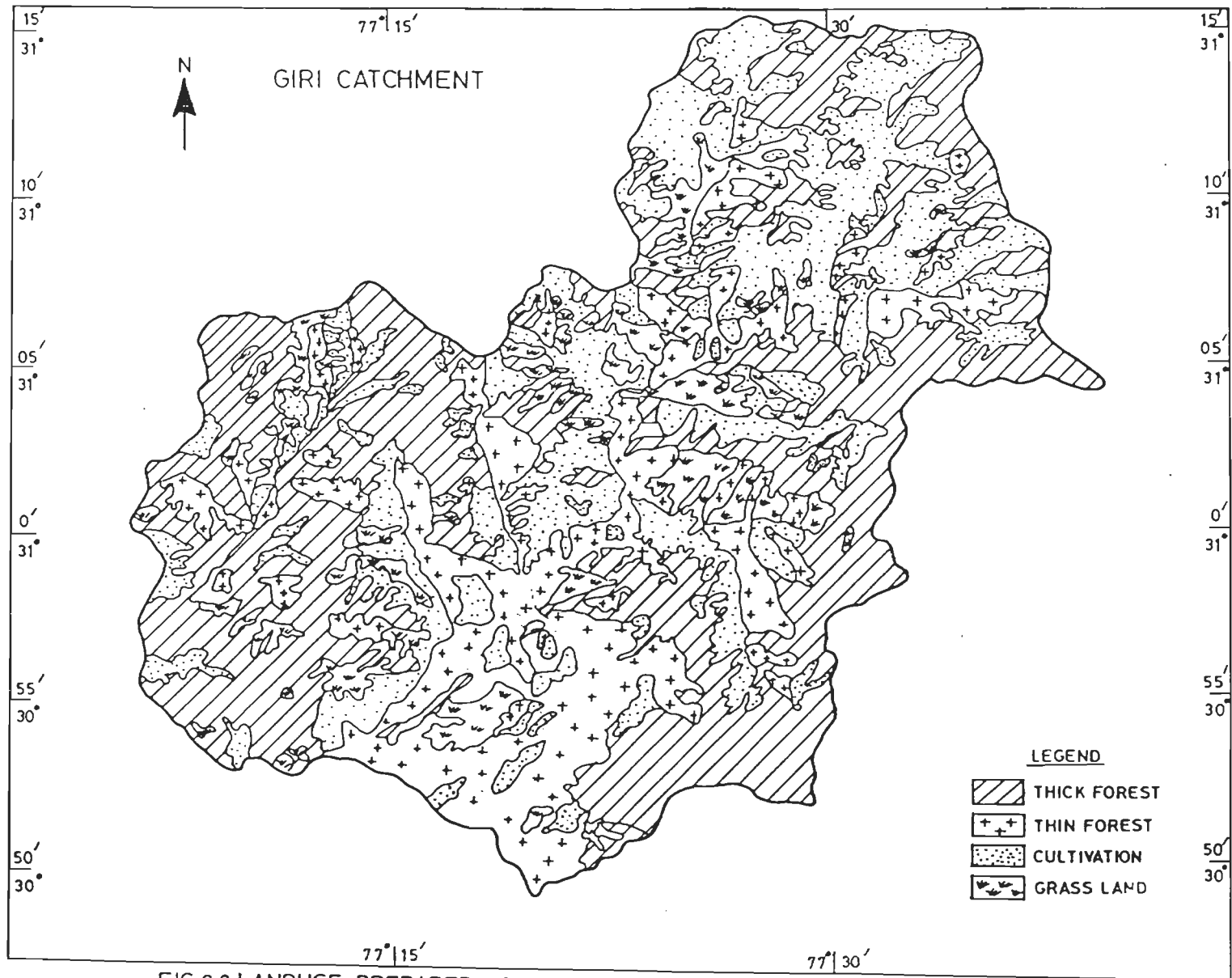


FIG.6.6:LANDUSE PREPARED FOR LANDSAT FCC OF MARCH 1977

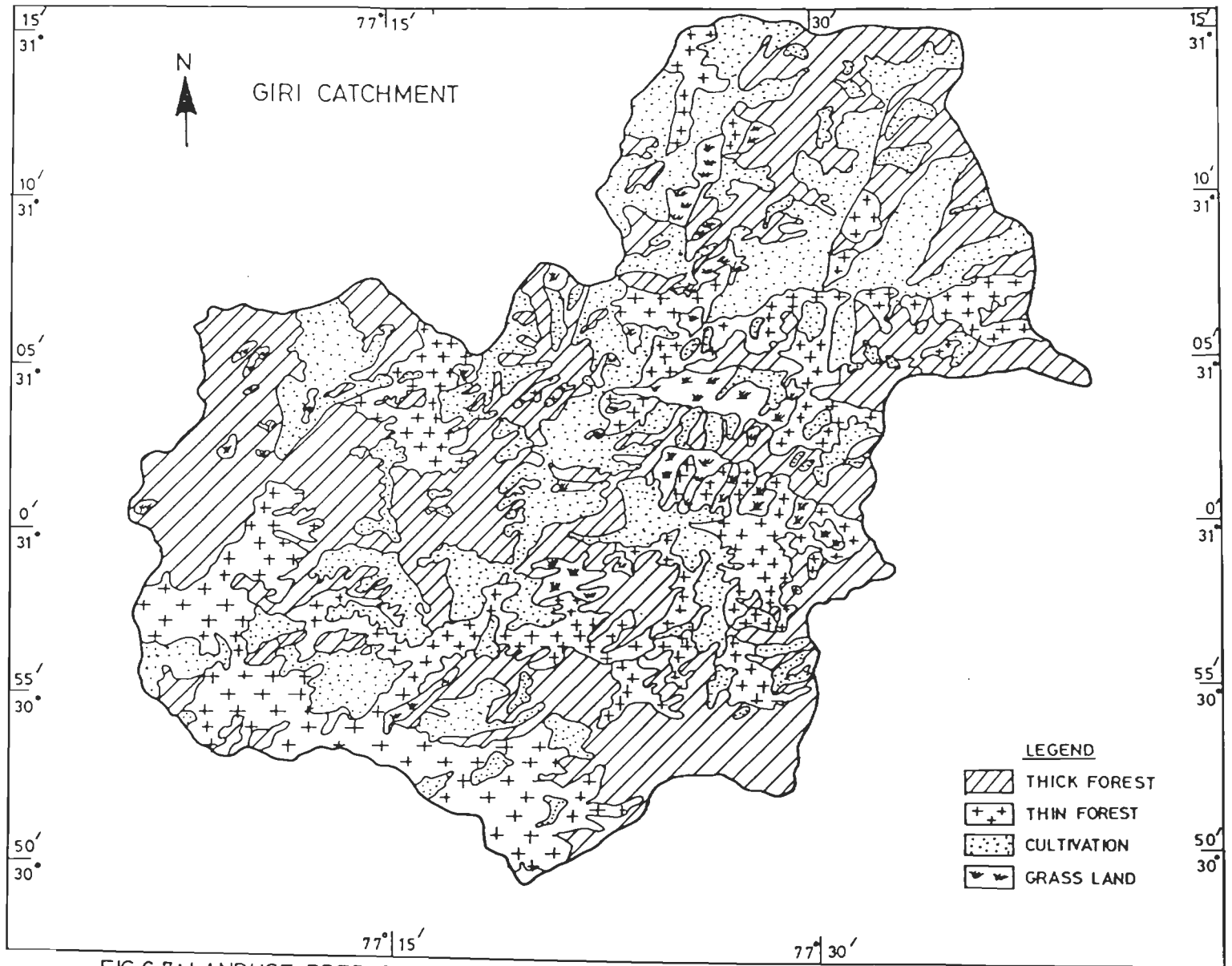


FIG.6.7: LANDUSE PREPARED FROM LANDSAT MSS BAND 5 IMAGERY OF OCTOBER 1980

Table 6.10 Comparison of Landuse Information for Years 1977, 1980 and 1989

S. No.	Landuse	<i>Visual analysis of LANDSAT imagery of</i>				<i>Digital analysis of IRS LISS I data of</i>	
		<i>March 1977</i>		<i>October 1980</i>		<i>March 1989</i>	
		<i>km²</i>	<i>%</i>	<i>km²</i>	<i>%</i>	<i>km²</i>	<i>%</i>
1.	Thick Forest	611.831	45.24	553.156	40.70	551.75	40.00
2.	Thin Forest	267.787	19.80	342.675	25.21	286.00	20.75
3.	Cultivation	353.574	26.14	385.700	28.38	431.50	31.31
4.	Grass Land	119.206	8.82	77.512	5.71	109.00	7.91
	Total	1352.40	100.00	1359.04	100.00	1378.25	100.00

By comparing the landuse information of 1977, 1980 and 1989 years of the catchment it is found that there is a small change in areal extent of landuse classes. Therefore, the landuse pattern for years 1991 and 1992 has assumed to be nearly the same as that of year 1989.

6.4.4 COMPUTATION OF MODEL PARAMETERS FROM REMOTE SENSING DATA

Three model parameters, namely IMPV, EPXM and K3 are associated with landuse. In the Giri catchment, the impervious area contributing directly to channel is almost negligible because this class could not be identified neither during field visits or with the help of remote sensing data. Therefore, the value of this factor has been assigned zero in the model. Interception (EPXM) mainly depends on the precipitation and landuse information of the area. Typical values of interception rates, given by Fleming and Mckenzie (1983) are given in Table 6.11. The evaporation from lower zone also depends on the landuse of the area. This is determined using a parameter K3 which is an index to actual evaporation. The

suggested values of this parameter for various landuse classes are given by Fleming and Mckenzie (1983), as shown in Table 6.11.

Table 6.11 Typical Values of Maximum Interception Rates (EPXM) and Lower Zone Evaporation Parameter (K3)

(Source: Fleming and Mckenzie, 1983)

<i>S.No.</i>	<i>Landuse class</i>	<i>EPXM (in mm/hr)</i>	<i>K3</i>
1	Grass land	2.5	0.23
2	Moderate Forest Cover	3.8	0.28
3	Heavy Forest Cover	5.1	0.30

In the present study, the values of EPXM and K3 have been obtained from landuse data and typical values given in Table 6.11 using area weighted technique for each segment as well as for the entire catchment, as given in Table 6.12.

Table 6.12 Values of Parameters EPXM and K3 for the Model.

<i>Parameter</i>	<i>Segment 1</i>	<i>Segment 2</i>	<i>Segment 3</i>	<i>Entire catchment</i>
EPXM	4.1	3.8	3.5	3.9
K3	0.28	0.27	0.26	0.27

The values of EPXM and K3 for each segment and entire catchment as obtained above has been used for the calibration and validation of model.

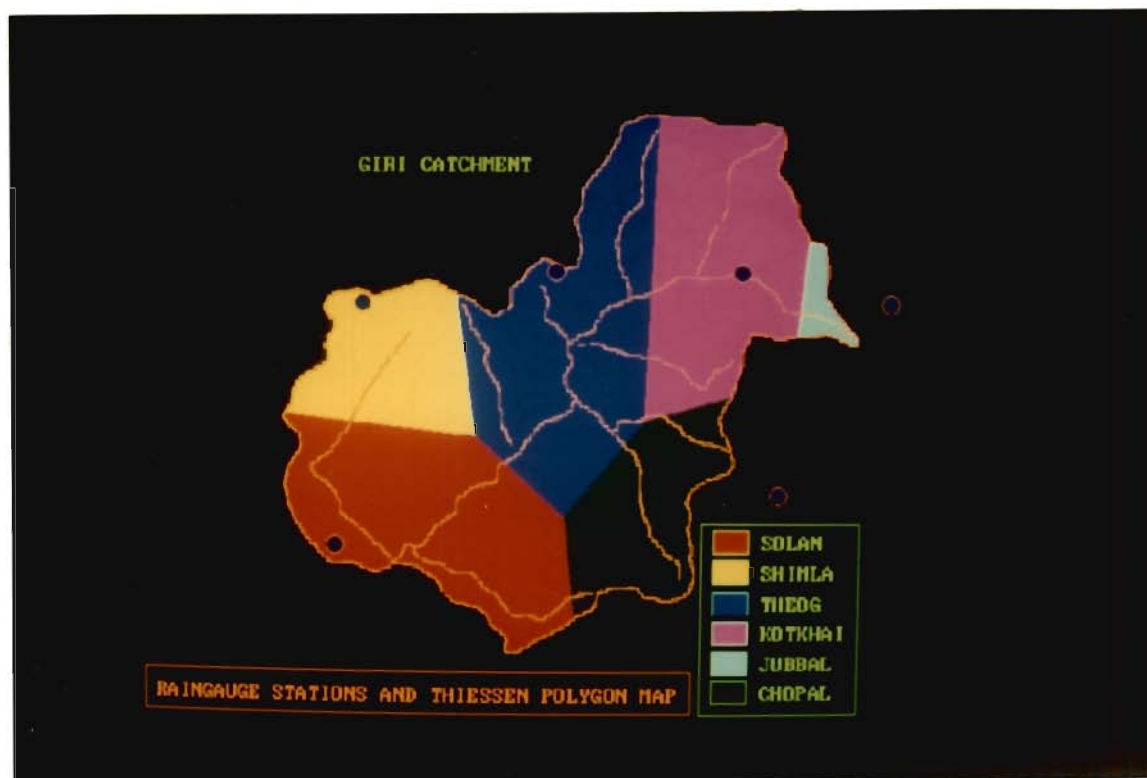


Plate 6.9 Thiessen Polygon Map of Giri Catchment

6.5 ANALYSIS OF RAINFALL DATA

Rainfall, a primary input data to the model, is a point measurement within a catchment. The uniformly distributed average rainfall for each segment has been computed using Thiessen Polygon method. A Thiessen Polygon has been prepared with the help of six available raingauge stations (Plate 6.9), and has been digitized in raster form using ILWIS. A computer program has been written to compute area of each Thiessen Polygon for each segment, which needs input as segment map and Thiessen polygon map. The area of various polygons in each segment has been shown in Table 6.13.

Table 6.13 Segmentwise Area Coverage of Thiessen Polygons

<i>Thiessen Polygon</i>	<i>Segment 1 (km²)</i>	<i>Segment 2 (km²)</i>	<i>Segment 3 (km²)</i>	<i>Entire Catchment (km²)</i>
Solan	0.50	144.00	195.00	339.00
Simla	9.75	114.25	38.75	162.75
Theog	48.25	217.00	97.50	362.75
Kotkhai	162.50	141.75	8.75	313.00
Jubbal	22.00	1.00	0.00	23.00
Chaupal	94.00	75.00	8.00	177.00
Total	337.00	693.00	348.25	1378.25

The daily average segmentwise rainfall as well as daily average rainfall in entire catchment for years 1989, 1991 and 1992 have been computed, and used as input to the model. The results obtained after analysis of DEM, remote sensing data and meteorological data as tabulated in Tables 6.3 and 6.12 are used for calibration and validation of the model, and described in next chapter.

CHAPTER 7

MODEL CALIBRATION, VALIDATION AND SENSITIVITY ANALYSIS

7.1 INTRODUCTION

The various parameters extracted from DEM and remote sensing as well as ancillary data have been presented in previous chapter. In this chapter, the parameters that have been derived in chapter 6 are used as input to the SRBM model for obtaining runoff from the catchment. The results of runoff simulation, model performance and sensitivity analysis have been explained in this chapter.

7.2 SIMULATION OF RUNOFF FROM SRBM MODEL

The runoff estimation has been carried out for two different scenarios; segmentwise as well as for the entire catchment. The concept of simulation has been illustrated as in Fig. 2.1, where the physical system of a catchment is shown on the left, and the mathematical model is shown on the right. The time and space variability of the input and output parameters have been quantified by measurements. The measurements may have some errors, which may be due to an inability to measure completely the areal variations in magnitude and timing of the mass and energy exchange as well as due to measurement errors.

When the model is used to simulate the behaviour of the catchment system, it produces output containing the effects of the input deficiencies. The simulation output is then compared with the recorded output containing the output deficiencies, in order to test and verify the accuracy of the model. To achieve the required model accuracy, the parameter values are adjusted until the agreement between simulated and recorded output is satisfactory. This parameter adjustment process is called the calibration of model parameters (Fleming, 1975).

The model calibration in general involves the manipulation of a specific model to reproduce the response of the catchment within some range of accuracy. In a calibration procedure, an estimation of the parameters is made which can't be measured directly in the field or the measurement procedure itself is time consuming.

If the model contains a large number of parameters, it is always possible to provide a combination of parameter values which permit a good agreement between the measured and simulated output values. However, this does not guarantee an optimal parameter value. The calibration might be achieved purely by numerical curve fitting without considering whether the parameter values so obtained are physically reasonable or not. Further, it might be possible to achieve multiple calibrations which are equally satisfactory based on different combinations of parameter values. In order to find out whether a calibration is satisfactory, or which combination is most correct, the calibration is validated against data different from those actually used for calibration (Stephenson and Freeze, 1974).

Klemes (1986) also supported the above by stating that the performance characteristics derived from the calibration data set do not give enough evidence as satisfactory model operation. Thus, the validation data must be different from those used for calibration.

The use of statistical criteria such as correlation coefficient, variance, standard deviation, absolute error, standard error etc., are another basis for assessing the accuracy of the calibration. These are used as guides for parameter adjustment alongwith the use of technique in pattern recognition. This is the method where continuous hydrographs of the recorded and simulated flow are plotted for observation and difference between the two hydrographs is examined. Fleming (1975) suggested that the parameters are adjusted to improve the hydrograph fit based on the combination of the statistical criteria and overall shape of the hydrograph.

For both the scenarios, analysis of DEM and remote sensing data has been carried out to assess several model input parameters; overland flow path length (L), slope (SS), ratio

of segment area contributing directly to channel to total catchment area (RIVER), proportion of impervious area to segment area (IMPV), canopy interception (EPXM), evaporation from lower zone (K3) as presented in Tables 6.3 & 6.12.

Before starting the calibration process for runoff, some of the model parameters have been assigned their values as given in Table 7.1 (refer to appendix A-1). To convert daily value of precipitation into hourly values the parameters gradient, standard deviation and cut-off points (GR, SD & CP) are also assigned. Fleming and Mckenzie (1983) have given the values of these parameters for two different rainfall conditions i.e. (i) low rainfall and (ii) high rainfall conditions. For the present study, the value of GR, SD and CP parameters have been selected for high precipitation, as presented in Table 7.2. The initial storages were assumed depending upon the field conditions and hydrograph shape.

Table 7.1 Assumed Values of Some Model Parameters

(Source : Fleming and Mckenzie, 1983)

<i>S.No.</i>	<i>Parameters</i>	<i>Description</i>	<i>Values</i>
1	POWER	Exponent in infiltration function	2
2	POINT	Run indicator without snow case	0
3	UZSNWF	Weight factor for antecedent pot. ET	0
4	PEADJ	Monthly evaporation adjustment factor	1
5	GAGEPE	Pot. ET adjustment factor for segment	1
6	NN	Manning's coefficient for overland flow	0.04
7	K1	Raingauge adjustment factor	1

Table 7.2 Typical Values for Gradient (GR), Standard Deviation (SD) and Cut-off point (CP)

(Source: Fleming and Mckenzie, 1983)

<i>Description of Rainfall</i>	<i>No. of Points</i>	<i>GR</i>	<i>SD</i>	<i>CP</i>
	1	3	3	0
Total annual precipitation of around 2000mm. Rainfall is usually of short to medium duration	2	0.4	0	1
	3	0	0	4
	4	3	3	0
	5	0	0	1
	6	0	0	4

The values of remaining parameters such as UZSN, LZSN, CB, CC, K24L, K24EL, IRC, KK24, KV have been obtained through calibration process as described above. The initial values of these parameters were assumed on the basis of ranges (refer to appendix A-1) suggested by Fleming and McKenzie, (1983).

The calibration of runoff is done for year 1989. To assess the accuracy of calibration results, model computes three standard statistical values i.e. correlation coefficient (cr), variance of residual (vr) and explained variance (ev). The parameter values were changed one at a time to study its effect on the simulated hydrograph. The set of parameter values for which simulated runoff gives highest correlation coefficient and explained variance, lowest variance of residual value as well as reasonable agreement with recorded runoff hydrograph (including peaks) has been selected as final calibrated values.

The calibrated parameter values for each segment of the catchment has been given in Table 7.3. Fig. 7.1 shows pattern of simulated and recorded hydrographs (discharge time series of monsoon season of year 1989) for the best fit run. Daily simulated runoff values for years 1989, 1991 and 1992 for both the cases alongwith recorded runoff valued have been given in appendix A-2. Principal peaks for monsoon season are well simulated. Two major simulated peak discharge values are 140.89 and 162.16 cumecs as compared to recorded peak discharges of 144.00 and 195.10 cumecs on 31st July, 1989 and 29th August 1989

**Table 7.3 Calibrated Values of the Parameters Adapted for the Study
Catchment Segmentwise**

S.No.	Parameters		Segment		
	Name	Description	1	2	3
1	UZSN	Nominal Upper Zone Soil Moisture	35	35	35
2	LZSN	Nominal Lower Zone Soil Moisture	390	425	450
3	CB	Infiltration Index	8	10	14
4	CC	Interflow Index	1.00	1.20	1.40
5	K24L	Fraction of ground water lost to inactive ground water	0.02	0.04	0.05
6	K24EI	Evaporation from Groundwater	0.00	0	0
7	IRC	Interflow Recession parameter	0.75	0.55	0.35
8	KK24	Groundwater Recession parameter	0.99	0.96	0.94
9	KV	Variable Groundwater Recession	0.05	0.10	0.20

Table 7.4 Summary of Simulated Runoff for Catchment Considering Segmentation

S.No	Month	Calibration		Validation			
		Year 1989		Year 1991		Year 1992	
		recorded volume (m ³)	simulated volume (m ³)	recorded volume (m ³)	simulated volume (m ³)	recorded volume (m ³)	simulated volume (m ³)
1	JUN	174.70	140.03	149.40	79.16	93.30	120.55
2	JUL	413.90	439.78	217.50	151.88	427.10	396.51
3	AUG	1627.50	1752.09	558.90	636.47	1840.60	1783.05
4	SEP	1136.40	1161.50	652.30	648.22	1598.80	1564.61
5	OCT	304.40	300.59	204.90	133.30	351.60	291.14
6	Total	3656.90	3793.99	1783.00	1649.03	4311.40	4155.87
7	cr		0.9993		0.9915		0.9993
8	vr ^{**}		14.0264		16.5121		4.8879
9	ev ^{***}		99.08%		92.13%		99.80%

^{*} correlation coefficient
^{**} variance of residuals
^{***} explained variance

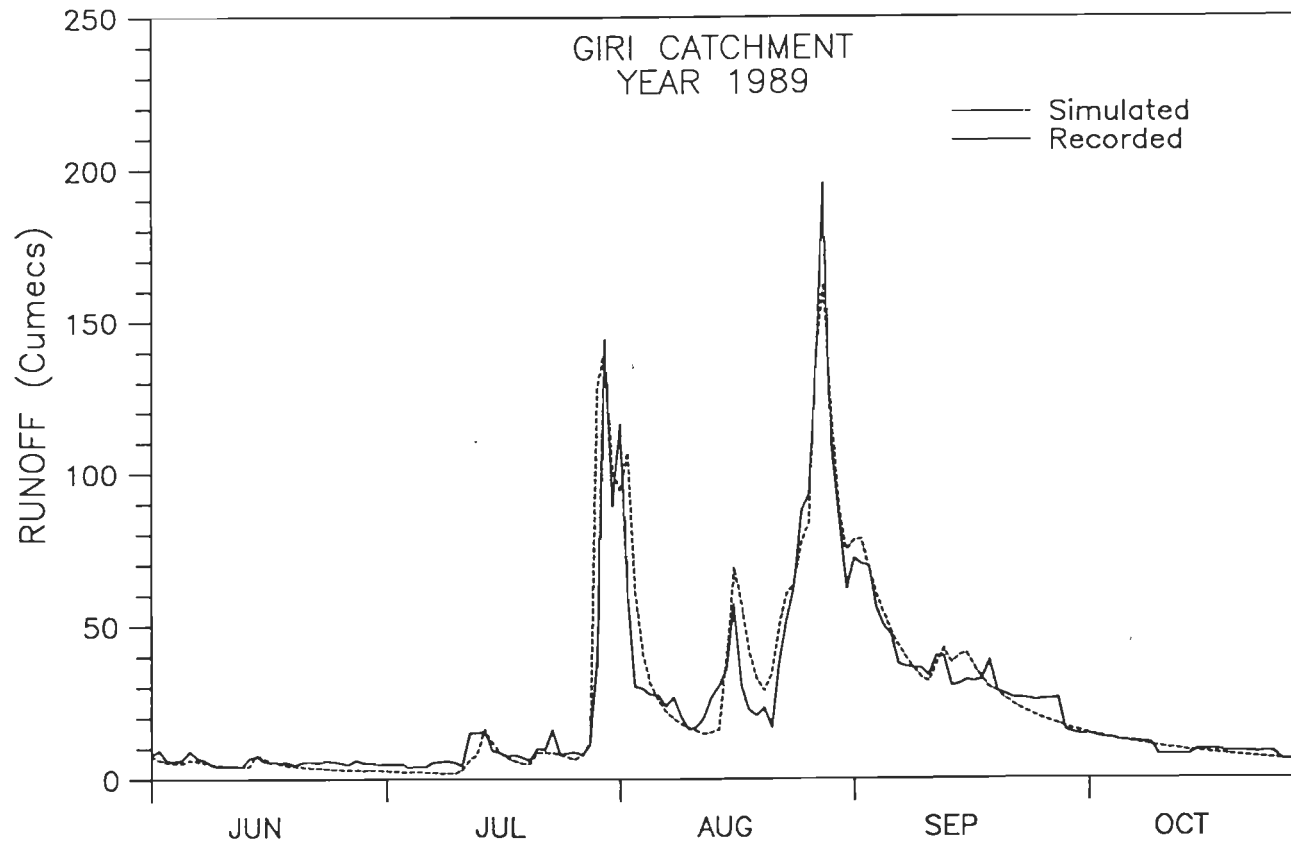


Fig.7.1 Calibration of Watershed Module of SRBM Considering all the Three Segments for Year 1989

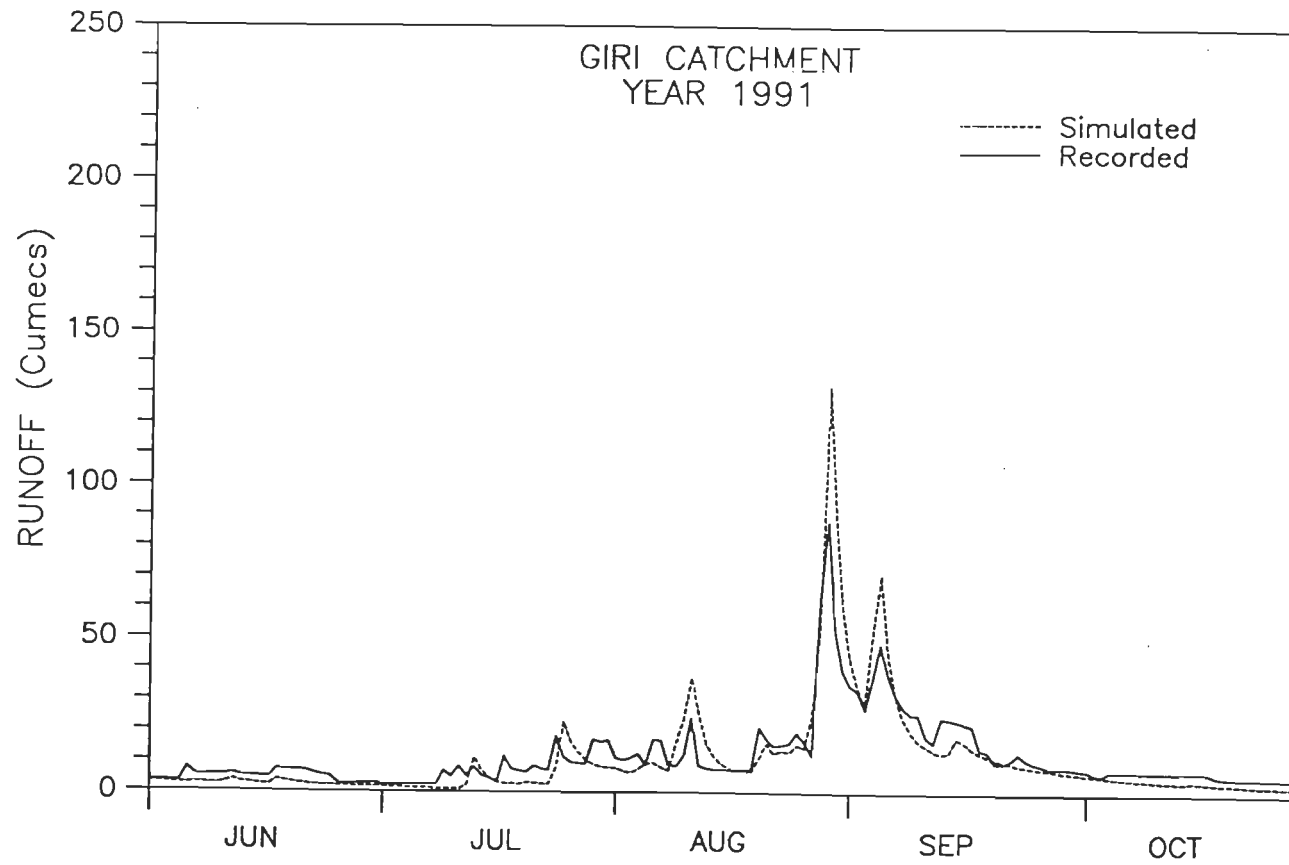


Fig.7.2 Validation of Watershed Module of SRBM Considering all the Three Segments for Year 1991

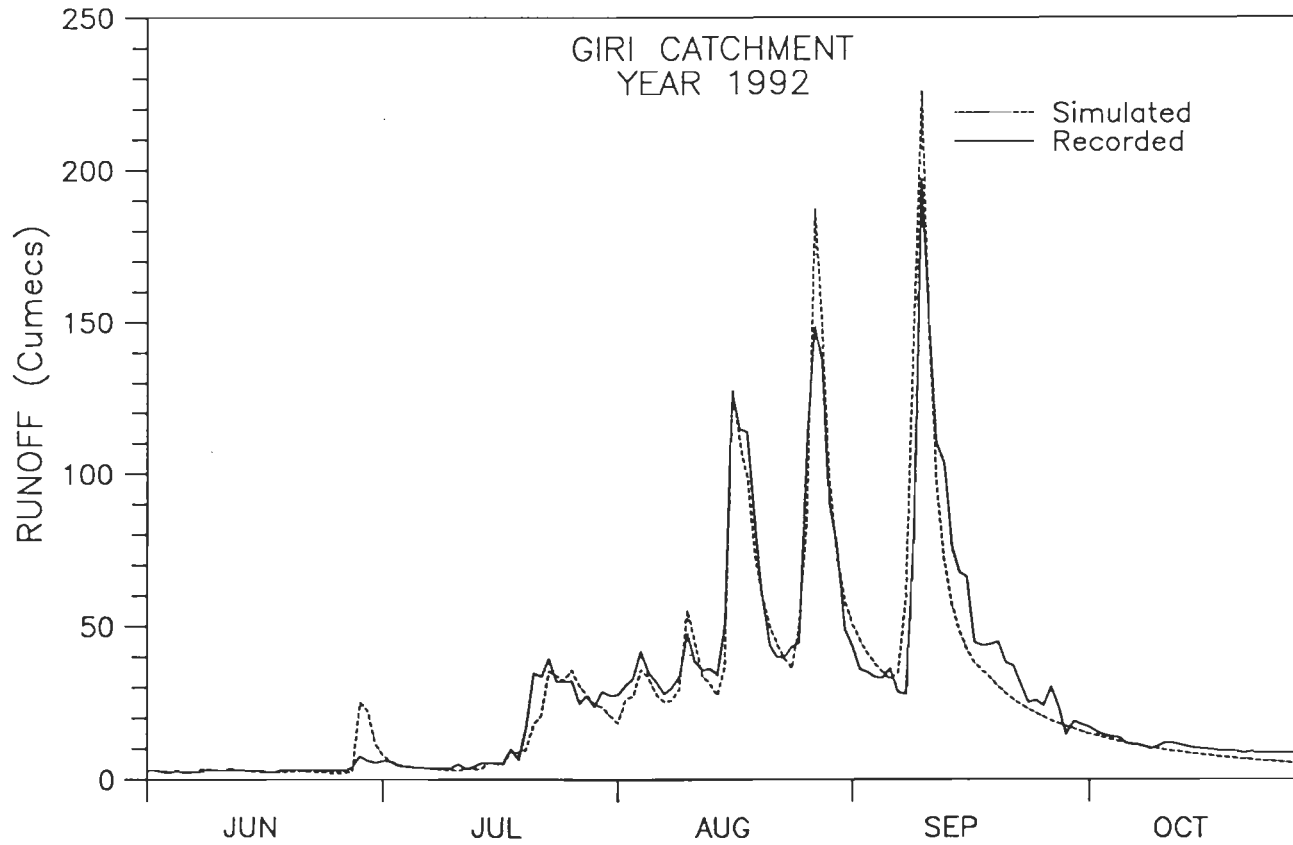


Fig.7.3 Validation of Watershed Module of SRBM Considering all the Three Segments for Year 1992

respectively (refer to appendix A-2). Comparison of the monthly mass balance between the recorded and simulated hydrographs for year 1989 are shown in Table 7.4. The total simulated runoff is found to be about 3.7% in excess of recorded runoff.

The validation of model has been carried out for years 1991 and 1992. The hydrographs of recorded and simulated runoff values for these years are shown in Figs. 7.2 & 7.3. In both graphs, the timing of peaks are well matched. In year 1991, the maximum simulated peak runoff occurred on August 30 followed by another peak on September 6 with runoff as 132.31 and 71.38 cumecs respectively. The recorded runoff for these dates were observed to be 88.30 and 48.30 cumecs respectively (refer to appendix A-2). The simulated peak discharges are slightly higher than recorded one. Monthly mass balance between recorded and simulated hydrograph for 1991 is shown in Table 7.4. The total simulated runoff is found to 7.5% less that of recorded.

In year 1992, three major peaks are found i.e. on August 17, August 28 and September 11 (Fig. 7.3). The simulated runoff values for these dates are 127.53, 187.04 and 225.89 cumecs respectively while the recorded runoff are 127.20, 148.30 and 196.80 cumecs (refer to appendix A-2). These data show that there is a good resemblance between the two discharge values. Monthly runoff values of recorded and simulated flow for 1992 year are given in Table 7.4. The total simulated runoff is found to be 3.6% less than the recorded runoff.

In second case, the catchment has been considered as a single homogeneous unit, and calibration performed for year 1989. The calibrated parameter values for best fit run are given in Table 7.5. The monthly runoff volumes for 1989 (Table 7.6) are found to be matching while total simulated runoff volume is about 6% more than the recorded volume. The peaks are also well matched as shown in Fig. 7.4. The first major peak occurred on July 31 following the another peak on August 2 and the highest peak of season on August 29. The simulated runoff volumes on these dates are 140.96, 119.09 and 189.76 cumecs respectively and recorded volumes are 144.00, 116.20 and 195.10 cumecs respectively (refer to

Table 7.5 Calibrated Values of the Model Parameters for Catchment Considering as a Single Unit

S.N.	Parameter		Entire Catchment
	Name	Description	
1	UZSN	Nominal upper zone soil moisture	35
2	LZSN	Nominal lower zone soil moisture	425
3	CB	Infiltration index	10
4	CC	Interflow index	0.95
5	K24L	Fraction of ground water lost to inactive ground water	0.03
6	K24EL	Evaporation from groundwater	0
7	IRC	Interflow recession parameter	0.55
8	KK24	Groundwater recession parameter	0.96
9	KV	Variable groundwater recession parameter	0.05

Table 7.6 Summary of Simulated Runoff for Catchment Considering as a Single Unit

S.No	Month	Calibration		Validation			
		Year 1989		Year 1991		Year 1992	
		recorded volume (m ³)	simulated volume (m ³)	recorded volume (m ³)	simulated volume (m ³)	recorded volume (m ³)	simulated volume (m ³)
1	JUN	174.70	161.68	149.40	84.98	93.30	110.80
2	JUL	413.90	358.90	217.50	124.54	427.10	369.48
3	AUG	1627.50	1807.52	558.90	600.55	1840.60	2047.20
4	SEP	1136.40	1233.20	652.30	618.49	1598.80	1612.70
5	OCT	304.40	315.58	204.90	153.02	351.60	330.05
6	Total	3656.90	3876.89	1783.00	1581.58	4311.40	4470.23
7	cr		0.9990		0.9908		0.9967
8	vr ^{**}		34.7904		10.0645		41.1769
9	ev ^{***}		97.73%		95.20%		98.35%

^{*} correlation coefficient
^{**} variance of residuals
^{***} explained variance

appendix A-2). These peak flows (simulated and recorded) are close to each other which defines the reliability of results produced by the model.

The year 1991 data has been used for validation of results and the hydrographs are shown in Fig. 7.5. The simulated peak with runoff value 132.52 cumecs has been found to be higher than the recorded peak of runoff value 88.30 cumecs (refer to appendix A-2). The total simulated runoff volume is less by 11% than the recorded runoff. The hydrograph of another validation year i.e. 1992 is shown in Fig. 7.6. All the simulated peaks are found to be slightly higher than the recorded peaks. The simulated peaks occurring on August 17, August 28 and September 11 have runoff volumes as 169.72, 164.26 and 225.03 cumecs against the recorded peaks of 127.20, 148.30 and 196.80 cumecs respectively (refer to appendix A-2). The total simulated runoff is found to be 3.7% more than the recorded runoff,

With the above discussions, the following observations are made;

- (i) The hydrograph volumes are in good agreement for both the calibration year and validation year.
- (ii) The principal peaks are well simulated in time and runoff volumes except for the year 1991 peaks which are generally high.
- (iii) The monthly runoff volumes are also reasonably well simulated.

Keeping in view the validation results, the calibration obtained for three segments as well as entire catchment may be considered as satisfactory. While comparing the calibration and validation results for three segments of the catchment and catchment as a single unit, it is inferred that;

- (i) The total hydrograph volumes are best simulated in case of catchment with three segments.
- (ii) The major hydrograph peaks are also in general well simulated for segmented catchment as compared to catchment as a single unit.

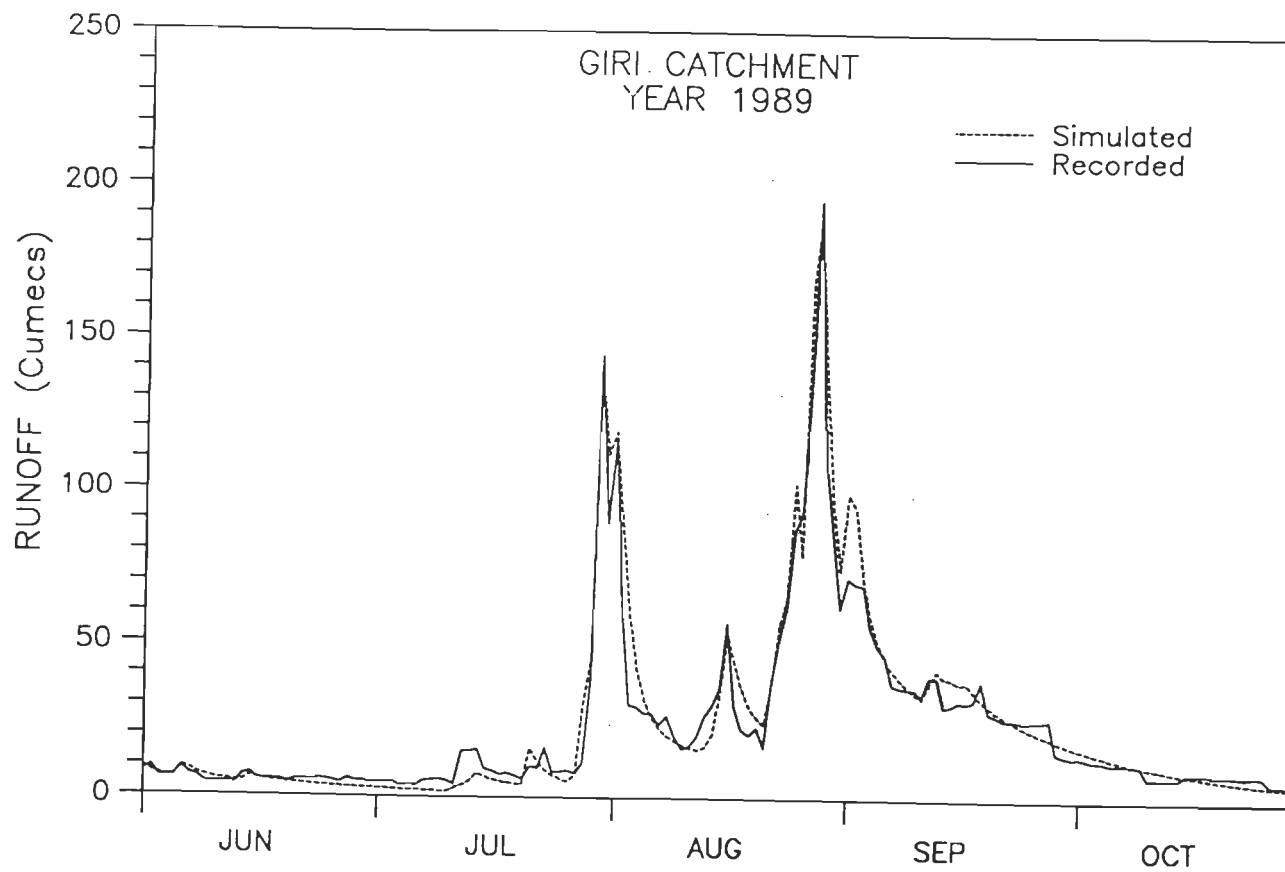


Fig.7.4 Calibration of Watershed Module of SRBM Considering Entire Catchment as a Single Unit for Year 1989

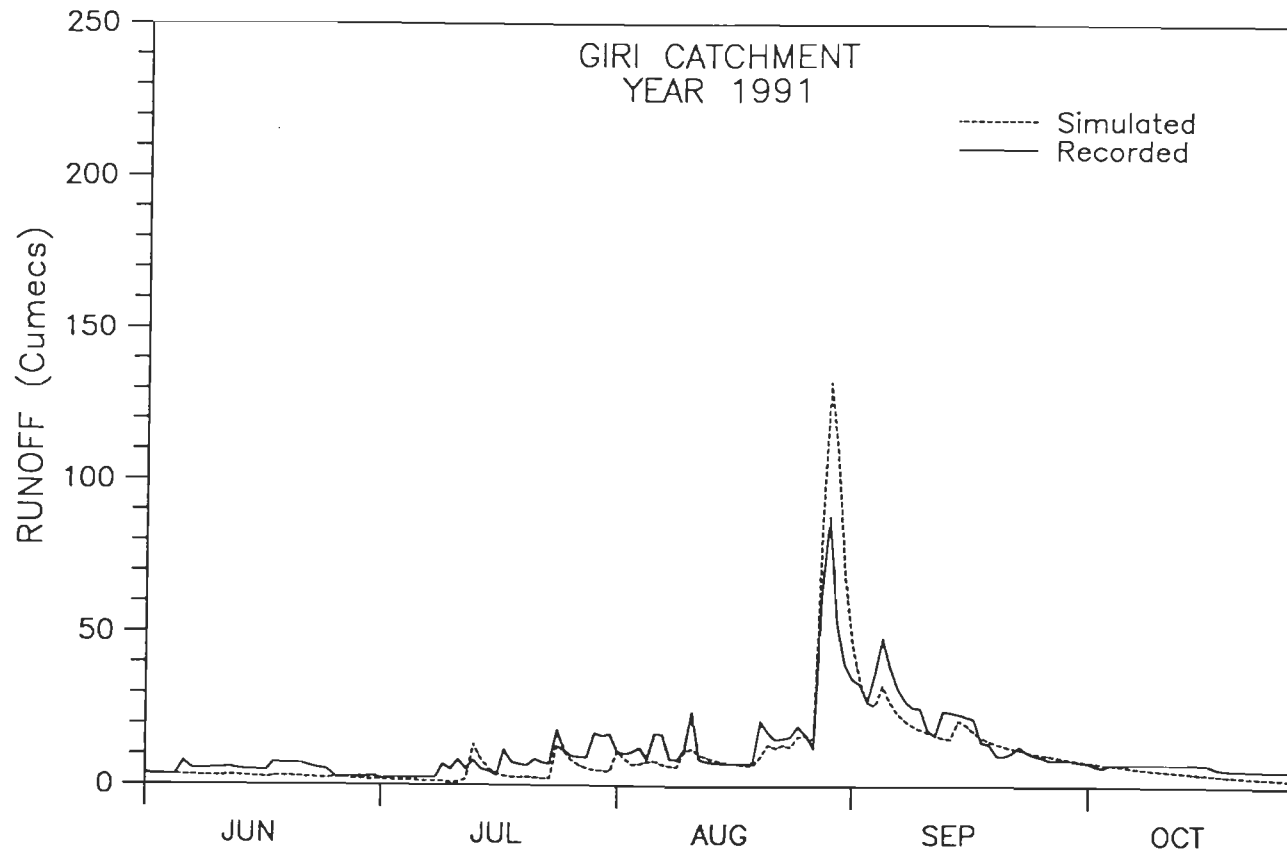


Fig.7.5 Validation of Watershed Module of SRBM Considering Entire Catchment as a Single Unit for Year 1991

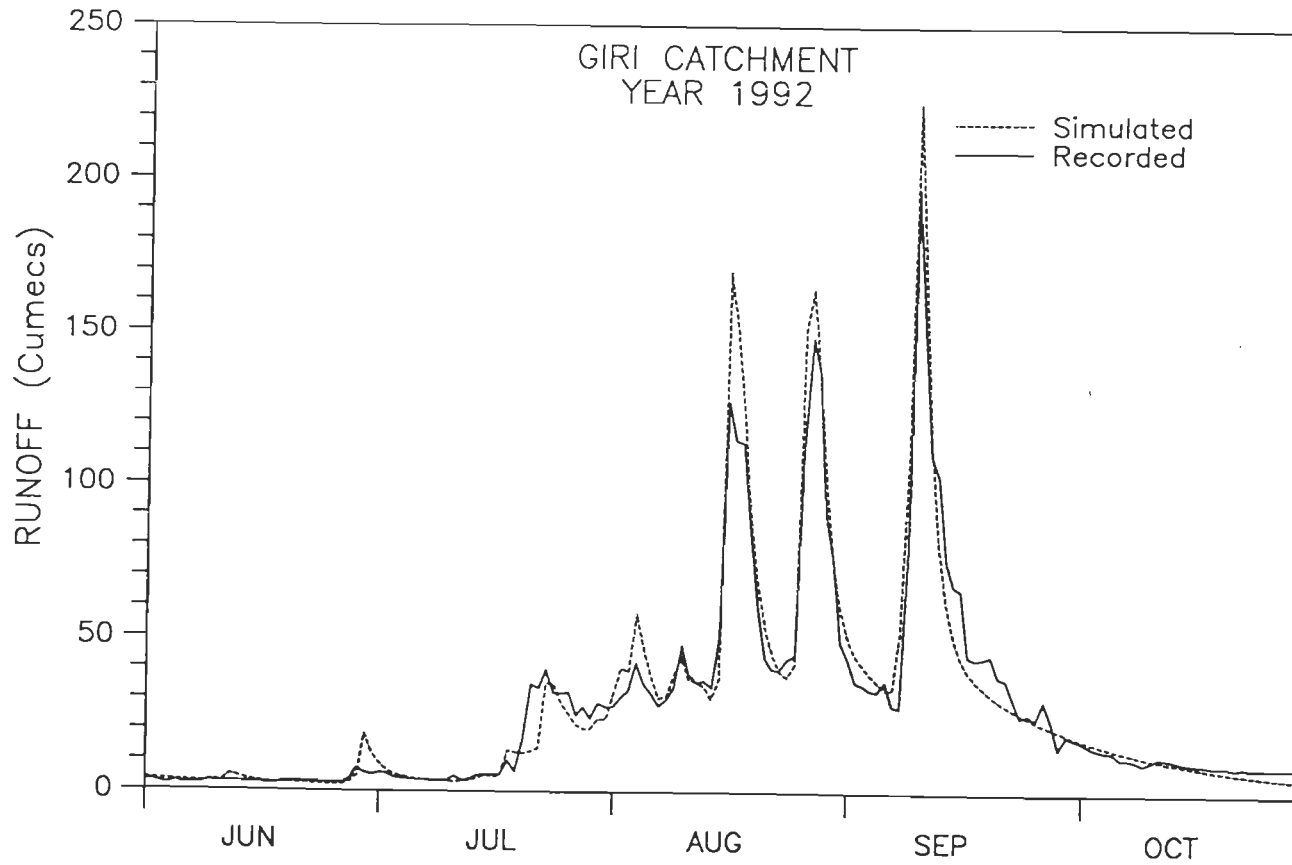


Fig.7.6 Validation of Watershed Module of SRBM Considering Entire Catchment as a Single Unit for Year 1992

(iii) The statistical parameters i.e. correlation coefficient, variance of residual and explained variance are also found to be better for the catchment when it is divided into three segments.

The above observations indicate that better simulation can be obtained by dividing the catchment into segments depending upon topography soils, landuse or other hydrological units.

The sensitivity analysis of the model is also performed and described below.

7.3 SENSITIVITY ANALYSIS

The aim of the sensitivity analysis is to examine the sensitiveness of important calibration parameters for runoff. Sensitivity analysis of the model parameters such as nominal lower zone soil moisture (LZSN), infiltration (CB), interflow index (CC), interflow recession (IRC) and groundwater recession (KK24) have been carried out segmentwise on 1989 data.

In this analysis, the simulated hydrograph based on the set of calibrated parameters for all segments has been referred to as the 'reference' simulation. The range over which the value of each parameter was altered is based on the limits within which each parameter can reasonably be evaluated.

In sensitivity analysis, the value of a parameter is changed slowly upto $\pm 30\%$ and its effect on the total runoff has been observed. The percent change in the runoff volume with corresponding change in parameter values has been given in Table 7.7. The sensitivity of various parameters can also be visualized by the runoff hydrographs which have been drawn for parameter values changed upto $\pm 20\%$. Figs. 7.7, 7.8, 7.9, 7.10 and 7.11 present the sensitivity of lower zone soil moisture (LZSN), infiltration (CB), interflow index (CC), interflow recession (IRC) and groundwater recession (KK24) parameters respectively. Fig. 7.12 shows the percent variation in runoff with percent change in parameter value.

Table 7.7 Sensitivity Analysis of Calibration Parameters

<i>% Variation in Calibrated Parameters</i>	<i>% variation in simulated runoff volume by parameter</i>				
	<i>LZSN (Lower Zone Soil moisture)</i>	<i>CB (Infiltration)</i>	<i>CC (Interflow index)</i>	<i>IRC (Interflow recession)</i>	<i>KK24 (Groundwater recession)</i>
-30	37.23	5.56	-4.73	0	-
-20	23.65	3.48	-2.49	0	-
-15	17.45	2.51	-1.66	0	-
-10	11.39	1.59	-1.07	0	-
-5	5.56	0.77	-0.49	0	9.70
-3	-	-	-	-	8.56
-2	-	-	-	-	7.20
-1	-	-	-	-	4.74
1	-	-	-	-	-8.18
5	-5.29	-0.70	0.45	0	-
10	-10.34	-1.39	0.83	0	-
15	-15.25	-2.02	1.18	0	-
20	-19.74	-2.60	1.50	-0.01	-
30	-28.28	-3.70	1.98	-2.25	-

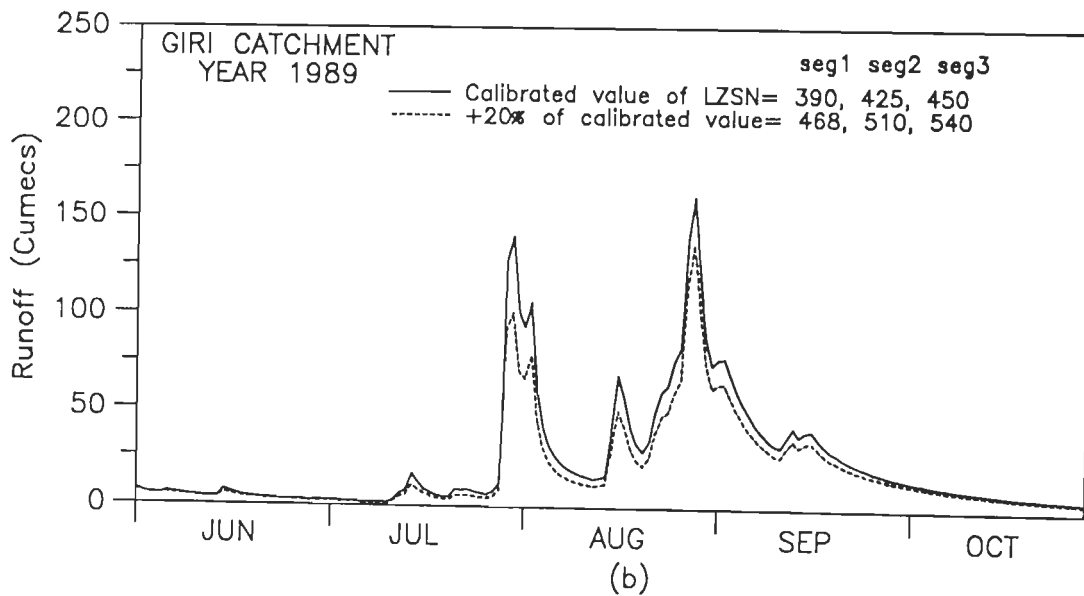
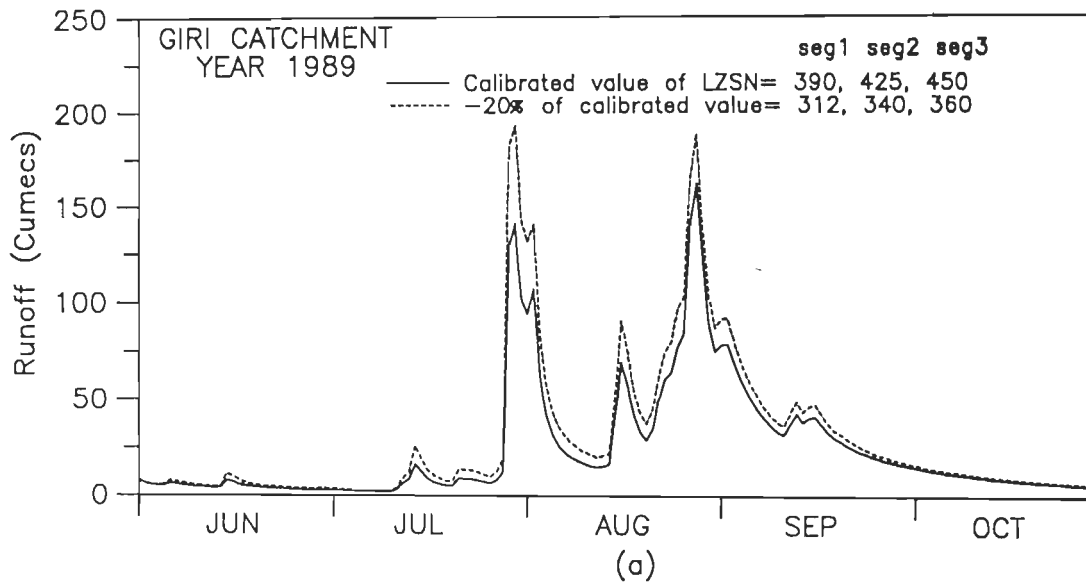


Fig.7.7 (a) & (b) Sensitivity of Nominal Lower Zone Soil Moisture Parameter (LZSN)

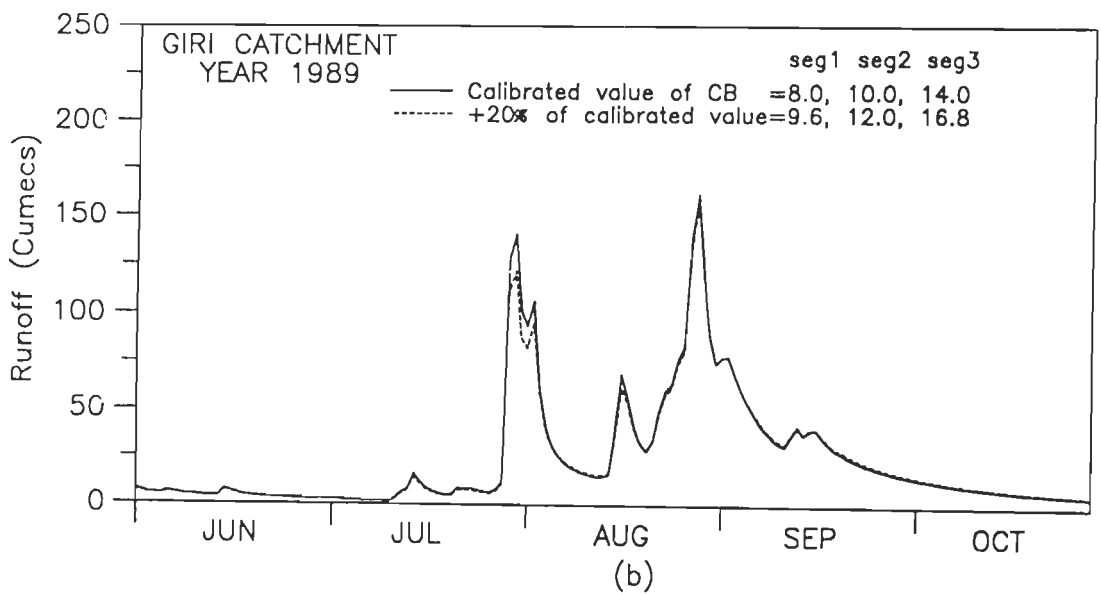
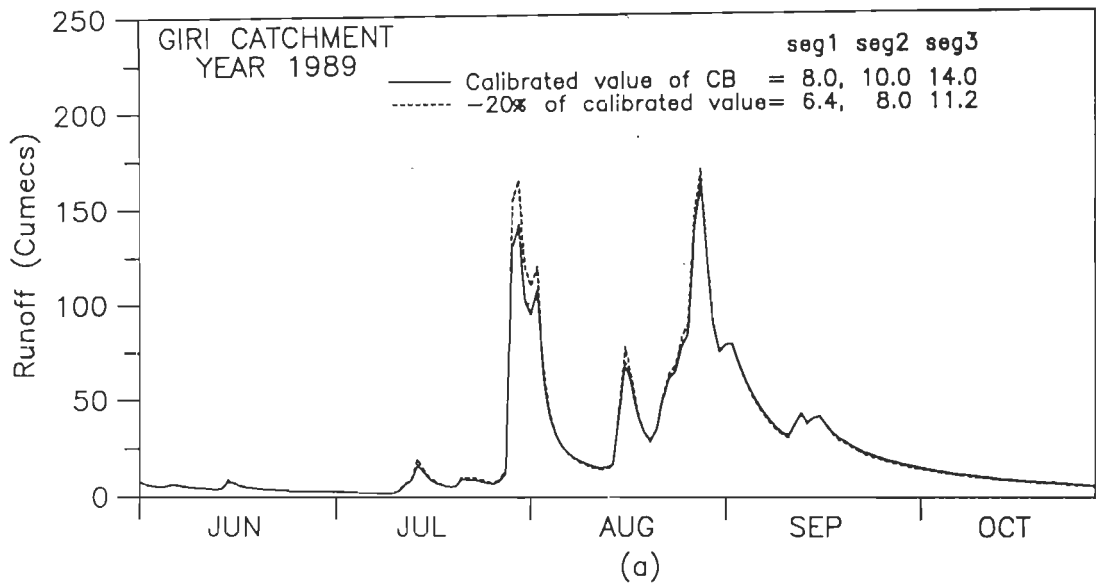


Fig.7.8 (a) & (b) Sensitivity of Infiltration Parameter (CB)

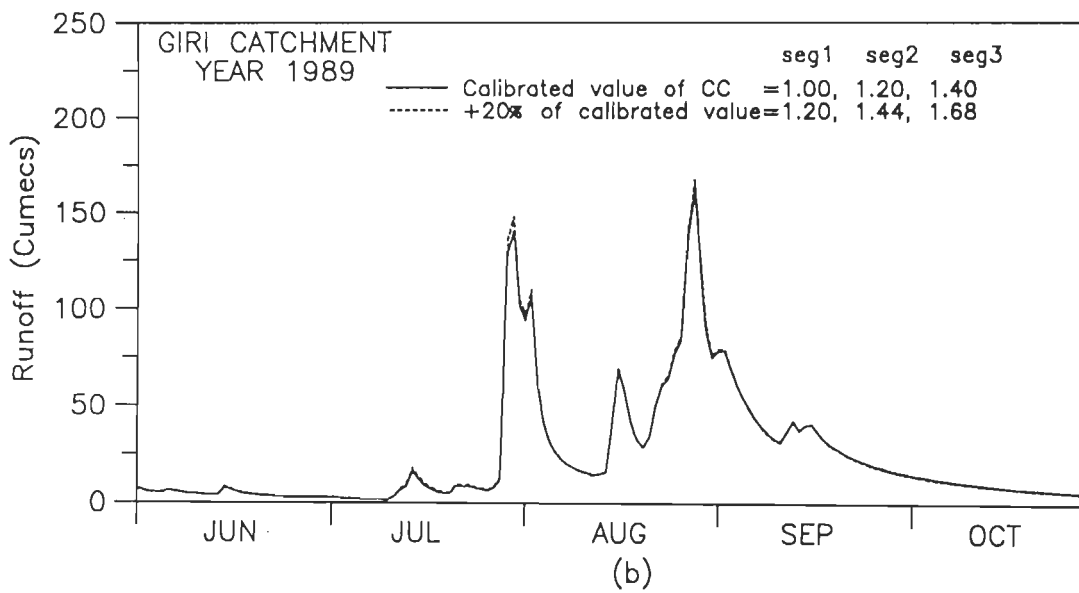
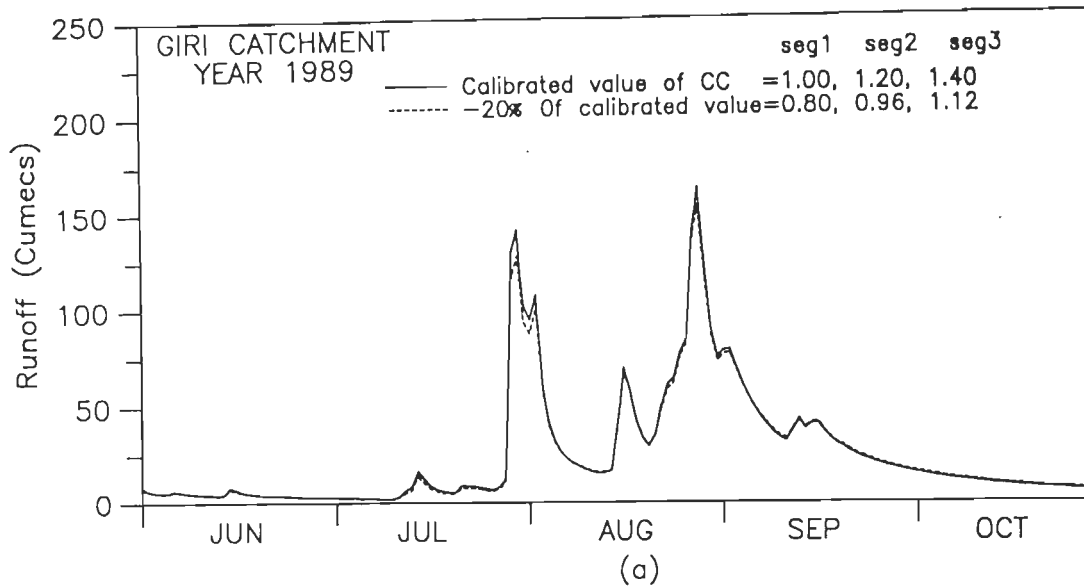


Fig.7.9 (a) & (b) Sensitivity of Interflow Parameter (CC)

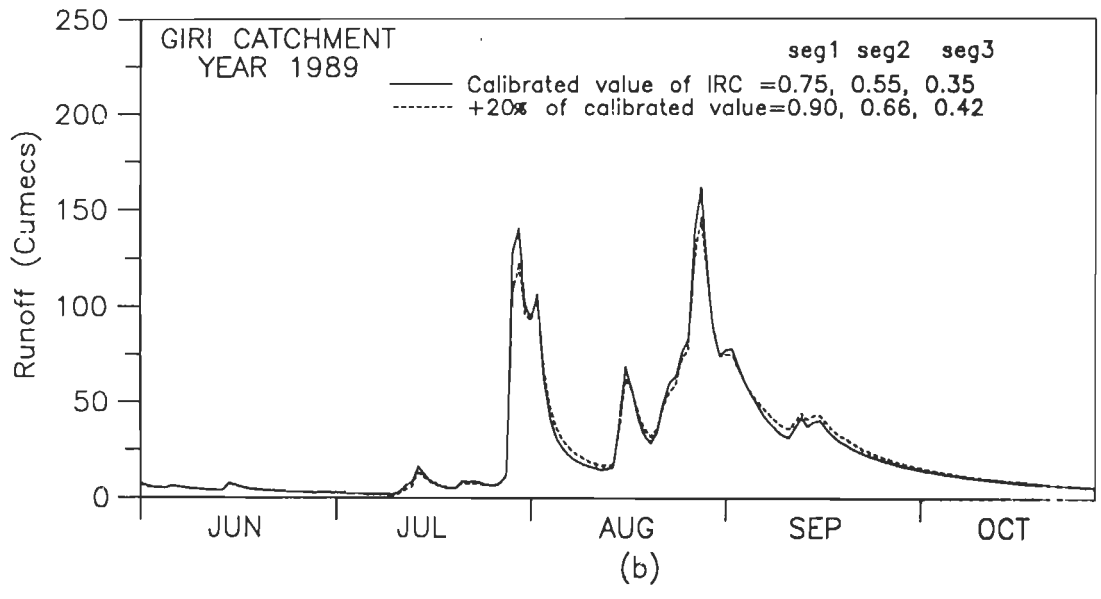
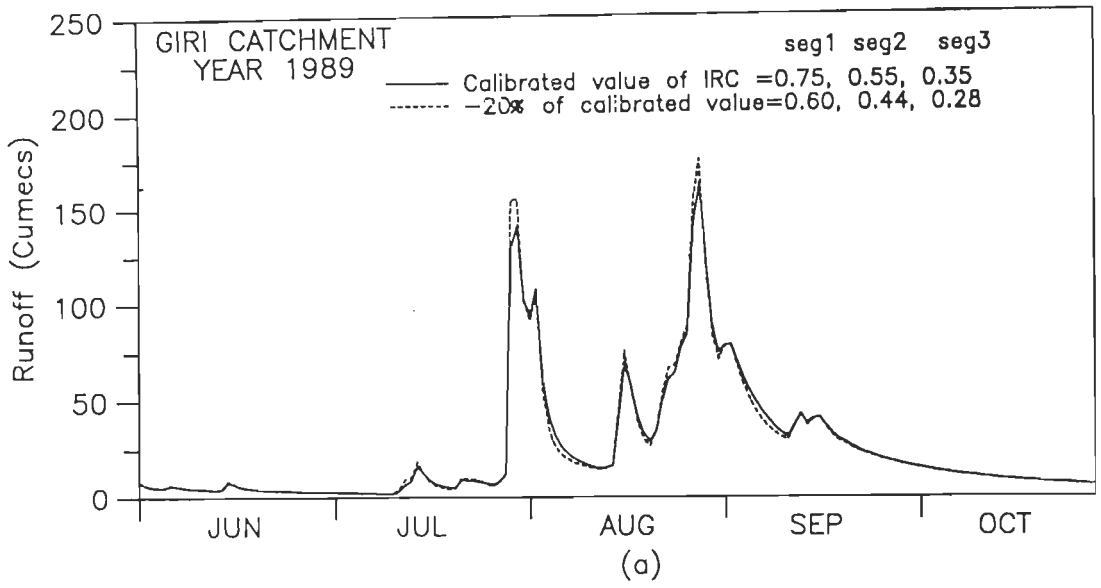


Fig.7.10 (a) & (b) Sensitivity of Interflow Recession Parameter (IRC)

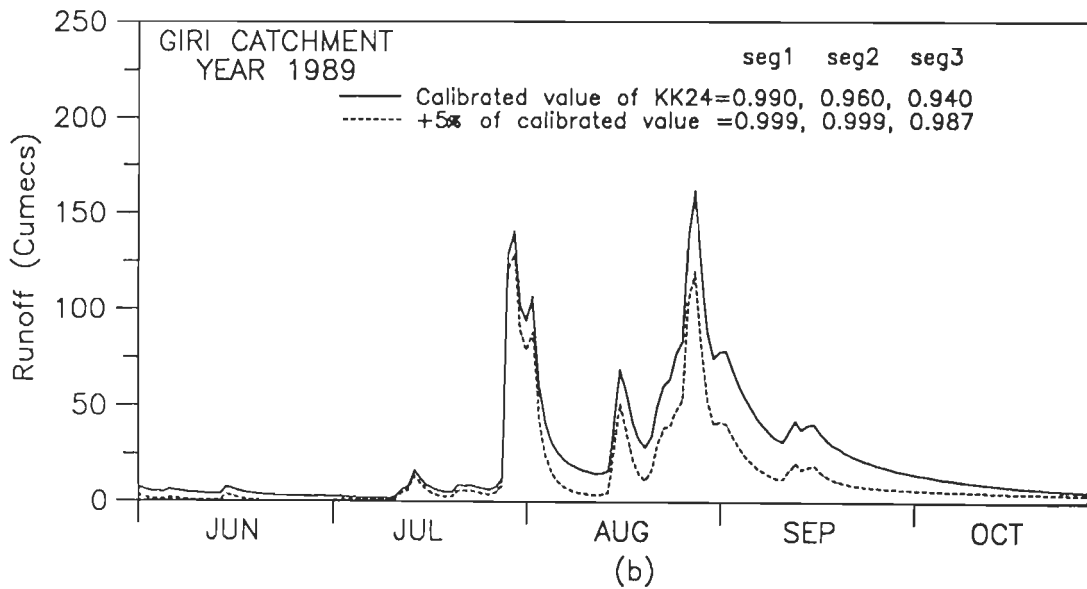
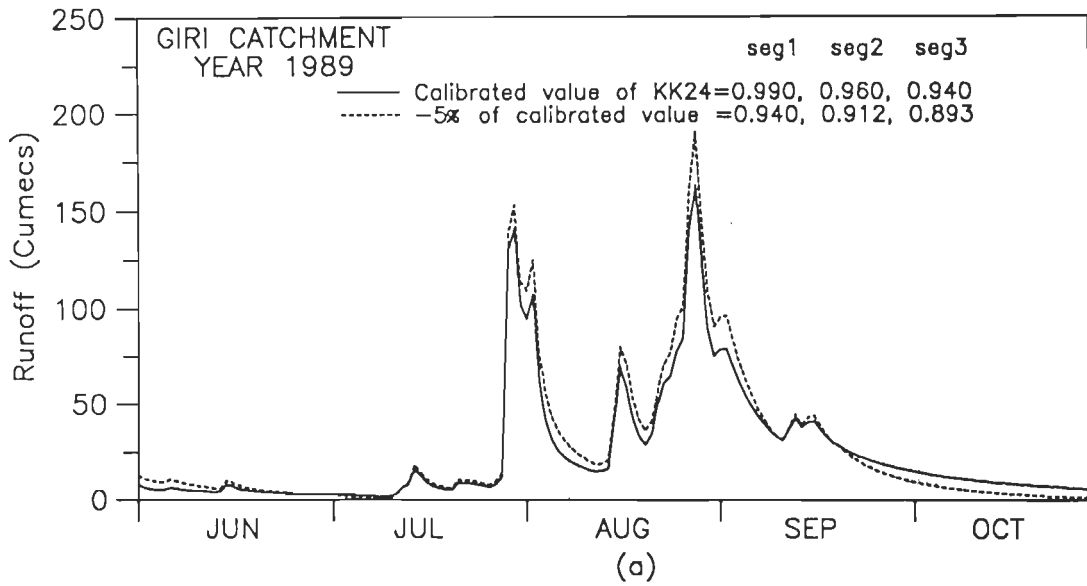


Fig. 7.11 (a) & (b) Sensitivity of Groundwater Recession Parameter (KK24)

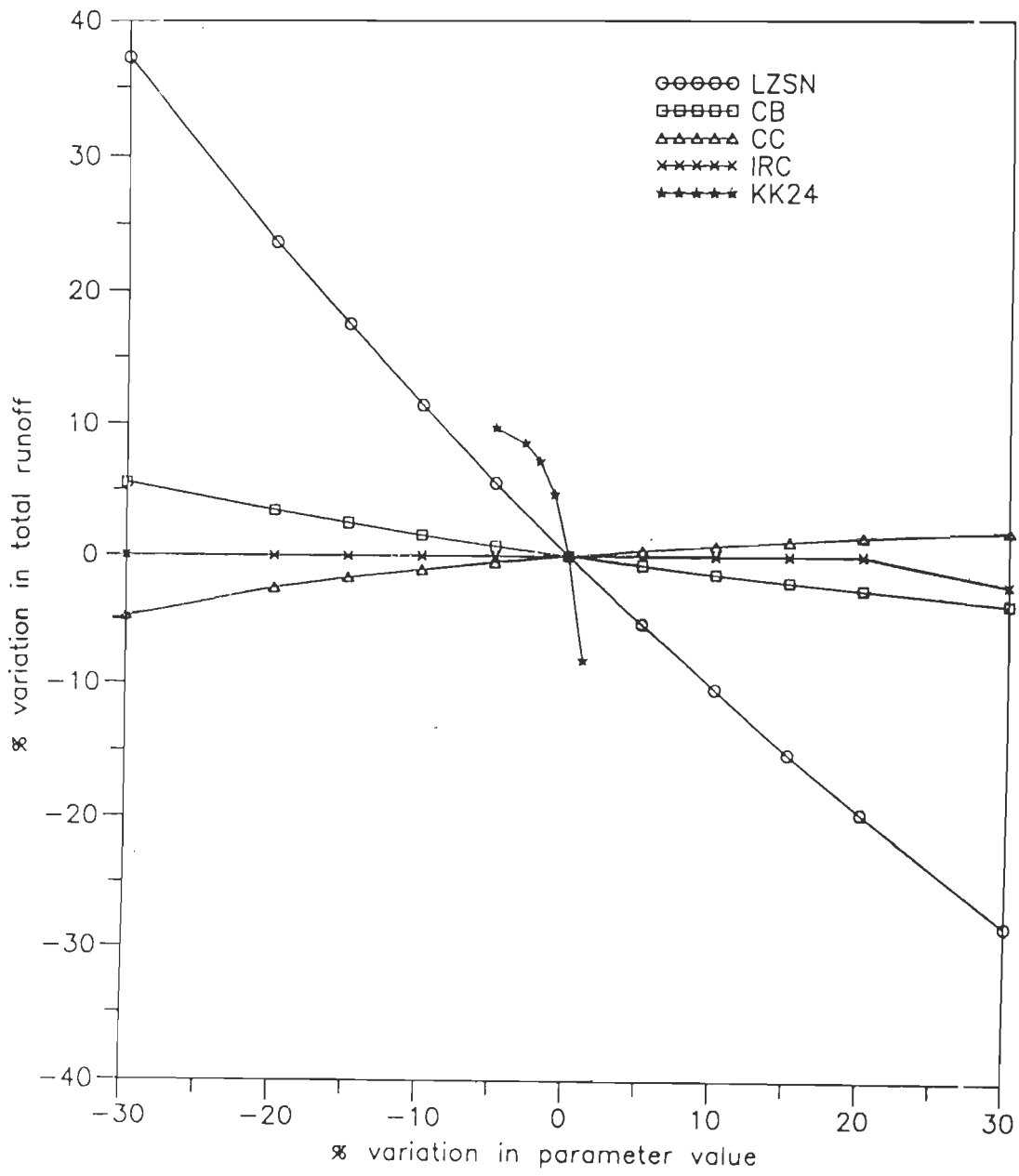


Fig.7.12 Sensitivity of Various Parameters

7.3.1 SENSITIVITY OF LOWER ZONE SOIL MOISTURE (LZSN)

For the reference simulation, the values of LZSN have been found to be 390, 425 and 450 mm for segments 1, 2 & 3 respectively. Fig. 7.7 shows that the decrease in lower zone soil moisture resulted in higher peaks and increased runoff volume. It is due to less storage space available in the unsaturated zone, resulting in early saturation and thus increasing the overland flow. The reverse effect is observed while LZSN is increased.

7.3.2 SENSITIVITY OF INFILTRATION PARAMETER (CB)

Sensitivity of infiltration parameter (CB) has been shown in Fig. 7.8. The calibrated value of CB in segments 1, 2 and 3 are 8, 10 and 14 respectively. Fig. 7.12 shows that as the value of CB increases, the runoff volume decreases in first three months (i.e. June to August) and increases in later months making marginal net impact. It is due to increased infiltration and less overland flow in the early months, but increased ground water contribution in the later months. From Table 7.7, it is observed that 30% change in CB value causes only 5% change in net runoff volume.

7.3.3 SENSITIVITY OF INTERFLOW INDEX (CC)

The interflow index initially is decreased by 30%, the runoff volume decreased only by 0.73%, however if it is increased by 30%, the runoff volume increased only by 1.98% (as clear from Table 7.7 and Fig 7.12). For 20% variation in interflow index, the hydrographs in Fig. 7.9 depict that both the runoff volume and peak increase with increase in CC. It is due to increase in interflow volume.

7.3.4 SENSITIVITY OF INTERFLOW RECESSON PARAMETER (IRC)

Fig. 7.12 and Table 7.7 show that the interflow recession parameter (IRC) does not affect significantly the total runoff volume. However, as indicated in Fig. 7.10, 20% increase in IRC value reduces the runoff in first two months after onset of monsoon (i.e. June and July) and increases subsequently. During June and July when soil is unsaturated, water get stored and runoff volume reduces. Whereas in September and October when soil become saturated and recession is high, the stored water is recessed at faster rate and

joins the channel, producing increased runoff in later months i.e. September and October. The value of IRC affects the monthly distribution of runoff only marginally keeping the total runoff volume unchanged.

7.3.5 SENSITIVITY OF GROUNDWATER RECESSON PARAMETER (KK24)

The ground water recession rate varies from 0.9 to 0.999, and is sensitive in a very small range. If the value of KK24 is decreased by more than 5%, its effect on runoff volume becomes almost nil (Fig. 7.12). Since reference values have been set near to upper limit i.e 0.999, increase in KK24 value is considered only upto 1%. The runoff volume decreases as the value of KK24 increases. It is due to increase in groundwater flow. The surface runoff volume has been observed to increase by 9.7% with a decrease in KK24 by 5%, whereas runoff is decreased by 8.18% with 1% increase in KK24 value. This parameter is very sensitive as can be seen in Fig. 7.11.

On the basis of results discussed above some conclusions have been drawn which are presented in the next chapter.

CHAPTER 8

CONCLUSIONS AND RECOMMENDATIONS

8.1 SUMMARY

In the present study, an attempt has been made to estimate some of the parameters of watershed module of SRBM model using DEM and IRS LISS I remote sensing and ancillary data to compute the runoff in Giri river catchment of H.P., India. The catchment has been divided into three segments on the basis of area elevation curve. A DEM at 500m grid size has been generated from the topographic maps and used to compute the flow directions using Flow Line approach to route the flow at the outlet of the catchment. Channel network within the catchment area has been obtained from the DEM using the criteria of Minimum Contributing Area. This channel network has been used to compute overland flow length and its slope for each segment as well as for the entire catchment. Computer programs have been developed to derive the flow directions, channel network, slope and overland flow length.

Unsupervised clustering technique has been used for landuse classification from IRS LISS I digital data of year 1989. The various landuse classes identified are thick forest, thin forest, cultivated land and grass land. Interception storage (EPXM) and potential evapotranspiration from lower zone (K3) parameters have been derived from landuse data, using an area weighted technique for each segment as well as for the entire catchment.

In the SRBM model, average rainfall for each segment has been computed using Thiessen Polygon Method, taking raingauge adjustment factor (a calibration parameter) for each segment as 1. Other parameters required for the model such as Nominal Lower Zone Soil moisture (LZSN), Nominal Upper Zone Soil moisture (UZSN), Infiltration parameter (CB), Interflow index (CC), Interflow Recession (IRC), Groundwater Recession (KK24), Fraction of groundwater lost to inactive groundwater (K24L), Evaporation from groundwater (K24EL) and Variable Recession rate of groundwater (KV) have been adjusted during the calibration process.

The daily data of rainfall, runoff and evaporation of Giri catchment for the year 1989, 1991 and 1992 were used. Calibration has been carried out for 1989 data. The value of the parameters which produced a reasonably matched hydrograph (shape, volume and peaks) with the recorded hydrograph as well as satisfactory correlation coefficient, variance of residuals and explained variance has been adopted. The runoff results from the calibrated model has been verified for the years 1991 and 1992. Sensitivity analysis has also been carried out for year 1989 for all the three segments of the catchment.

8.2 CONCLUSIONS

On the basis of results it can be concluded that;

- (1) Landuse based model parameters such as interception storage (EPXM) Lower Zone evaporation (K3) and Impervious area (IMPV), which are generally difficult to collect from the field, can be conveniently obtained with the help of remote sensing data.
- (2) DEM can be effectively used for extracting the channel network and other catchment parameters such as Overland Flow Length and Slope.
- (3) A Flow Line Approach has been developed for determination of the flow directions, useful for deriving the channel network. The unique aspect of this approach is the determination of a large number of parameters such as slope, flow direction, length of the channel, overland flow length in a single scan of the DEM data, thereby obliterating the multi scan of DEM data as have been adopted by Jenson and Domingue (1988) and O'Callaghan and Mark (1984). This approach results in significant saving of computer time (approximately 80%) (Kumar, 1997).
- (4) Model can be effectively utilized to estimate runoff by integrating it with DEM and remote sensing data.

- (5) The segmentation of the catchment improves the simulation of runoff when compared to results considering the entire catchment as a single homogeneous unit.
- (6) The sensitivity analysis shows that the model is extremely sensitive for Lower Zone Soil Moisture (LZSN) and Groundwater Recession (KK24) parameters. Hence, the value of these parameters should be estimated with great care. Furthermore, it is observed that infiltration (CB) and interflow (CC) indices are found to be less sensitive.
- (7) The proposed model can be applied to ungauged catchment with similar environmental and land conditions.

8.3 RECOMMENDATIONS AND FUTURE SCOPE

Based on the present work the following recommendations are made for future studies:

1. A grid size of 500m has been used in this study in view of availability of limited computer memory and speed of processing. It is suggested that a finer grid size may be adopted, preferably in correspondence to pixel size of remote sensing data .
2. Since the Flow Line approach defines the movement of water over land surface on the basis of slope this information may be helpful for defining route of soil movement within the catchment. This may lead to a better definition of sources of soil erosion and may provide better estimates to soil erosion yields within the catchment.
3. Even though single year remote sensing data have been used in the modelling approach, it is suggested that at least two to three years of satellite data at a minimum interval of five years should be taken so that any changes in landuse types which may have occurred during this period are easily discernible. This will help in studying the effect of changing pattern of landuse on runoff.

4. In the absence of detailed hydrometeorological information such as maximum and minimum temperature, humidity, wind speed and sun shine hours, daily evaporation data has been used in the SRBM model. Ghosh (1991) has made an attempt in this direction to show the effect of evapotranspiration on runoff simulation. Further, this information has been utilized for a large number of hypothetical scenarios on landuse change and its effect on runoff. It is suggested that instead of evaporation data if evapotranspiration data is used along with remote sensing and DEM, better estimates of runoff may be obtained.

5. IRS 1C PAN data has stereoscopic capabilities, which may be used for the generation of DEM with some inputs of spot elevations acquired through Global Positioning System (GPS) observations in the field. This will remove the ambiguity of using the approximate contour information as available in topographical maps. The GPS observations, may further be used in remote sensing analysis for better geometrical registration of satellite data.

APPENDIX A1

The details of the parameters of Watershed Module of Strathclyde River Basin Model (SRBM) as described by Fleming and McKenzie (1983) are given below:

(1) POWER This is the exponent (b) used in the infiltration function shown in equation (a1.1).

$$FS = \frac{INF}{(LZS - 1 / LZSN)^b} \quad (a1.1)$$

where

- FS = segment mean infiltration capacity (inches) at time = t.
- INF = a parameter representing an index infiltration level, physically related to the characteristics of the catchment (inches).
- LZS = Actual value of solid moisture storage at time = t-1 in the lower zone, inches per unit area.
- LZSN = Nominal value of soil moisture storage in the lower zone. Equivalent to the field capacity in inches per units area.
- b = Exponent - a value of 2 is usually adopted.

(2) POINT This parameter is thought to have been incorporated for a particular study and is thus now unnecessary. It should be assigned the value of zero.

(3) UZSNWF This is the weight factor in equation (a 1.2)

$$UZSNT = UZSN + UZSNWF * AEPI \quad (a 1.2)$$

where

- UNZSNT = Nominal upper zone storage total
- UZSN = Nominal upper zone storage
- UZSNWF = Weight factor
- AEPI = Antecedent potential evapotranspiration storage.

The effect of the UZSNWF is to vary UZSN in a seasonal manner since AEPI will vary seasonally. It is however usually assigned as zero and can be increased to improve the simulation over the annual cycle.

- (4) PEADJ This parameter consists of 12 monthly adjustments to adjust the evaporation data input so that it is representative of the whole catchment. If no data is available to calculate this parameter, all values should initially be assigned as 1.0.
- (5) GAGEPE This parameter is used to adjust the average catchment potential evaporation to an average potential evaporation for each segment. An initial value of 1.0 should be used.
- (6) K1 This parameter is the proportion of the long-term average segment precipitation to the long-term average gauge precipitation. The long-term average segment precipitation is usually found from an isohyetal map.
- (7) IMPV This is the proportion of the impervious area to the total segment area. In country areas this is usually very small (e.g. 0.01).
- (8) EPXM This is the canopy interception storage in millimeters.
- (9) UZSN This is the nominal upper zone storage. It is dependent to a certain degree upon LZSN and CB. An initial estimate of UZSN can be found from Table A.1.1 as a proportion of LZSN.

Table A1.1 Estimating UZSN from LZSN

WATERSHED	UZSN
Steep slopes, Limited vegetation, Low depression storage	0.06 LZSN
Moderate slopes, Moderate vegetation, Moderate depression storage	0.08 LZSN
Mild slopes, Heavy forest cover, High depression storage	0.16 LZSN

- (10) LZSN This parameter is the nominal lower zone storage in millimetres and as can be seen from eqn. a. 11. plays an important part in calculating the infiltration. It is usually found from calibration in conjunction with the parameter CB.
- (11) CB This parameter governs the infiltration rate into the lower zone. It is in units of mm/hr and is usually found from calibration. It ranges from .5 mm/hr to about 30 mm/hr.
- (12) CC This parameter is an index to the ratio of the increment added to interflow detention to the increment added to surface runoff detention. It is found from calibration and is usually between 0.5 and 3.0.
- (13) K3 This parameter is an index to the actual evaporation which takes place. It can be estimated as a fraction of the segment area covered by forest and deep rooted vegetation.
- (14 & 15) K24L & K24 EL These parameters control the loss of water from active groundwater. K24L is the fraction of groundwater which is lost to deep inactive groundwater. K24EL is the fraction of the segment where groundwater can be reached by deep rooted vegetation Both these parameters are usually assigned as zero.
- (16 & 17) L & SS L is the average flow path length in metres and SS is the average flow path slope. They are usually found by taking a grid of points from a map of the catchment and simply scaling from the map. The more points used, the more representative the average values will be.
- (18) NN This is Manning N value for the overland flow.
- (19 & 20) IRC & KK24 These parameters are the interflow and groundwater recession rates. They can be estimated graphically. or found from trail simulation runs.

They are expressed by the following.

$$\text{IRC} = \frac{\text{Interflow discharge on any day}}{\text{Interflow discharge 24 hours earlier}}$$

$$\text{KK24} = \frac{\text{Groundwater discharge on any day}}{\text{Groundwater discharge 24 hours earlier}}$$

Typical values are 0.5 - 0.9 for IRC and 0.9 - 0.99 for KK24.

- (21) KV This is used to allow a variable recession rate for groundwater . It is usually set at zero and increased if necessary to improve groundwater recession.
- (22) RIVER This parameter is the ratio of the segment area contributing directly to the river, to the total segment area. The last segment (furthest downstream) must always have RIVER = 1.0
- (23 - 29) UZSI, LZSI, SGWI
GWSI, RESI, SRGXI
SCEPI, AEPI These parameter represent the initial storages with the watershed. These parameters can usually be estimated after trial run. If the previous year has already been calibrated then the initial storages are simply the final values from the previous year. All values are in millimetres.
- (30 - 32) GR, SD, CP These parameters are only used if hourly precipitation data is not available. They are used to produce synthetic hourly precipitation from authentic daily data. There are 6 possible values for each parameter. The first 3 values of each parameters relate to the number of rain events in a day while the remaining 3 values relate to the duration. The various parameters are calculated by analysing some authentic hourly data from the catchment and constructing scatter diagrams. Once the scatter diagrams have been formed, then various gradients (GR), standard deviations (SD) and cut-off points (CP) are tried out until most of the points are enclosed in the envelope.

APPENDIX A2

The measured and simulated daily runoff values for years 1989, 1991 and 1992 for both the cases, i.e., considering segments and entire catchment as a single homogeneous unit has been given below :

Date	Year 1989			Year 1991			Year 1992		
	Simulated runoff considering		Recorded runoff	Simulated runoff considering		Recorded runoff	Simulated runoff considering		Recorded runoff
	segment	entire catchth		segment	entire catchth		segment	entire catchth	
1	2	3	4	5	6	7	8	9	10
JUN									
1	7.68	9.30	8.00	2.96	3.83	3.50	2.96	3.83	3.20
2	6.26	7.74	9.40	2.85	3.68	3.40	2.85	3.68	3.20
3	5.51	6.78	6.00	2.74	3.53	3.40	2.74	3.53	2.30
4	5.28	6.42	6.10	2.64	3.39	3.10	2.64	3.39	2.20
5	5.19	6.13	6.60	2.55	3.25	3.30	2.54	3.25	3.00
6	6.30	9.54	9.10	2.53	3.15	7.80	2.45	3.12	2.10
7	5.88	8.68	6.90	2.94	3.19	5.40	2.36	3.00	2.30
8	5.32	7.31	6.30	2.75	3.03	5.20	3.22	2.89	2.40
9	4.93	6.45	4.40	2.50	2.89	5.30	3.46	3.23	2.90
10	4.64	5.88	4.10	2.57	2.88	5.50	2.94	3.33	3.00
11	4.40	5.47	4.20	2.86	2.97	5.40	2.65	3.10	2.70
12	4.20	5.16	4.40	3.83	3.29	5.80	3.69	5.25	3.00
13	4.01	4.90	4.00	3.28	3.20	5.20	3.22	4.75	2.90
14	4.15	4.89	6.90	2.90	2.99	5.10	2.88	3.97	2.80
15	7.78	6.44	7.60	2.64	2.83	5.00	2.65	3.48	2.80
16	6.74	5.77	5.70	2.45	2.70	4.90	2.49	3.16	2.70
17	5.62	5.29	5.40	2.37	2.58	4.90	2.36	2.94	2.30
18	4.90	4.94	5.40	4.06	2.96	7.60	2.26	2.77	2.30
19	4.46	4.67	5.40	3.43	2.95	7.20	2.39	2.63	3.10
20	4.14	4.44	4.60	3.23	2.95	7.20	2.23	2.51	3.10
21	3.91	4.24	5.50	2.75	2.79	7.10	2.59	2.61	3.20
22	3.71	4.06	5.60	2.49	2.64	7.00	2.42	2.55	3.20
23	3.54	3.89	5.20	2.32	2.51	6.00	2.25	2.40	3.30
24	3.39	3.73	5.90	2.20	2.40	5.50	2.13	2.27	2.90
25	3.25	3.57	5.60	2.10	2.29	5.30	2.03	2.17	2.90
26	3.12	3.43	5.30	2.00	2.20	3.00	1.94	2.07	2.90
27	3.00	3.29	4.70	1.92	2.11	2.80	2.04	2.18	2.90
28	2.89	3.16	6.10	1.84	2.02	2.90	2.60	2.99	4.00
29	2.81	3.09	5.30	1.77	1.94	2.80	25.12	5.12	7.50
30	3.00	3.03	5.30	1.70	1.86	2.80	22.46	8.65	6.20

1	2	3	4	5	6	7	8	9	10
JUL									
1	2.85	2.91	4.80	1.63	1.79	2.90	11.84	12.47	5.40
2	2.70	2.79	4.80	1.57	1.71	2.40	7.98	9.10	6.10
3	2.58	2.67	4.80	1.51	1.65	2.60	6.02	6.97	5.80
4	2.47	2.56	4.80	1.45	1.58	2.60	5.00	5.70	4.50
5	2.37	2.46	3.90	1.39	1.52	2.50	4.42	4.92	4.20
6	2.28	2.36	4.10	1.34	1.46	2.50	4.03	4.42	4.00
7	2.20	2.27	3.90	1.29	1.40	2.50	3.74	4.08	3.90
8	2.11	2.17	5.40	1.24	1.34	2.50	3.51	3.82	3.80
9	2.03	2.09	5.60	1.20	1.29	2.50	3.32	3.61	3.70
10	1.96	2.00	5.90	1.15	1.24	6.90	3.15	3.44	3.90
11	1.89	1.92	5.40	1.11	1.19	5.10	2.99	3.29	3.90
12	3.02	2.91	4.10	1.07	1.14	8.40	2.98	3.15	5.00
13	6.29	3.92	15.00	2.11	2.09	5.30	3.34	3.53	3.60
14	8.11	5.28	15.00	11.20	13.44	8.10	3.34	3.65	4.20
15	16.29	7.90	15.70	7.09	8.53	5.20	3.44	4.43	5.50
16	12.11	6.90	9.10	4.59	5.56	4.70	5.63	5.40	5.60
17	8.80	5.87	8.50	3.29	3.89	3.20	5.19	4.93	5.60
18	7.00	5.22	7.50	2.83	3.08	11.70	5.08	5.08	5.40
19	5.88	4.78	7.90	2.76	2.77	7.60	9.34	13.40	10.00
20	5.10	4.46	7.20	2.54	2.61	7.00	9.00	12.83	6.50
21	5.11	4.21	6.20	3.15	2.81	6.50	9.58	12.53	16.90
22	8.66	16.09	10.10	3.01	2.62	8.60	18.00	12.99	34.80
23	8.49	11.80	9.70	2.71	2.41	7.50	21.02	14.15	33.60
24	8.62	9.06	16.10	2.49	2.31	7.20	35.44	35.17	39.60
25	7.91	7.24	8.40	7.96	13.25	18.10	33.96	35.25	32.20
26	7.16	6.06	8.70	22.90	11.01	11.50	32.39	28.88	32.00
27	6.45	5.34	8.80	16.29	8.27	9.60	35.88	25.55	32.40
28	7.82	7.70	7.90	12.89	6.68	9.40	30.87	21.90	24.80
29	11.89	30.98	11.33	10.69	5.72	9.30	27.54	20.53	37.50
30	128.73	46.00	39.30	9.08	5.18	17.20	24.71	20.54	33.90
31	140.89	140.96	144.00	8.35	5.05	16.40	23.80	23.78	38.80

1	2	3	4	5	6	7	8	9	10
AUG									
1	101.35	111.67	89.50	7.97	4.71	17.00	20.88	23.44	27.50
2	94.19	119.09	116.20	7.96	11.35	11.10	18.66	31.68	27.70
3	106.89	89.02	59.40	7.00	8.79	10.50	26.37	40.40	31.00
4	61.42	59.64	30.20	6.28	6.95	11.10	27.32	39.04	33.00
5	41.06	42.24	29.70	7.57	7.20	12.50	35.99	58.03	42.00
6	31.08	32.23	27.60	9.22	7.96	8.80	33.13	46.30	35.00
7	25.57	26.33	27.50	9.57	8.16	17.10	27.95	37.21	32.00
8	22.16	22.70	23.80	8.10	7.20	16.90	25.44	30.52	38.00
9	19.83	20.35	26.70	7.11	6.56	8.90	25.95	31.07	30.00
10	18.10	18.71	20.30	16.03	6.30	8.70	29.59	37.74	33.90
11	16.74	17.48	16.10	24.01	11.40	12.10	55.35	43.94	47.70
12	15.62	16.49	17.00	37.39	12.12	24.30	44.77	36.77	38.30
13	14.75	15.76	20.00	25.68	10.42	8.90	33.79	35.78	35.60
14	15.17	16.64	26.70	16.10	9.32	7.90	31.44	34.41	36.40
15	16.20	20.55	30.20	11.74	8.57	7.60	27.40	30.43	34.00
16	40.10	32.93	36.20	9.49	8.01	7.50	36.89	37.21	51.00
17	69.13	53.55	57.00	8.16	7.57	7.40	127.53	169.72	127.20
18	57.36	44.84	30.30	7.28	7.19	7.40	110.25	152.36	114.60
19	41.81	35.82	22.50	6.99	6.86	7.50	98.55	125.86	113.90
20	32.85	29.71	20.60	6.74	6.57	7.70	73.62	91.23	85.40
21	28.78	26.59	23.20	11.22	9.55	21.30	59.92	68.77	60.00
22	34.40	24.17	16.70	15.95	13.68	17.50	50.55	53.89	43.80
23	49.82	36.51	37.10	12.88	12.48	15.30	44.16	44.94	40.00
24	60.43	56.71	51.30	13.69	13.55	15.70	31.53	39.30	39.80
25	63.94	65.70	62.30	13.23	12.87	16.20	36.29	37.49	43.40
26	77.22	102.66	87.50	15.60	16.28	19.60	51.10	41.80	44.70
27	83.88	78.86	93.30	14.60	16.65	16.70	83.74	150.07	112.50
28	139.30	168.26	137.30	24.73	15.36	12.40	187.04	164.26	148.30
29	162.16	189.76	195.10	52.19	86.43	62.00	149.03	136.92	137.60
30	121.54	136.34	110.30	132.31	132.52	88.30	98.29	101.63	90.00
31	89.24	96.28	85.90	89.68	107.96	53.00	72.51	74.99	76.30

1	2	3	4	5	6	7	8	9	10
SEP									
1	74.67	74.31	62.10	60.21	68.96	40.00	58.52	59.40	49.00
2	78.09	99.64	71.90	43.51	47.15	35.00	50.76	49.94	43.30
3	78.41	94.76	70.00	34.79	35.20	33.30	45.63	44.62	36.00
4	69.05	72.73	69.60	28.29	27.64	27.40	41.20	41.22	35.00
5	60.89	59.98	56.10	51.70	26.29	36.30	37.87	38.47	33.30
6	54.03	51.39	49.90	71.38	33.00	48.30	34.97	35.93	33.00
7	48.28	45.97	46.90	45.25	27.41	38.90	32.64	33.83	36.40
8	43.46	42.13	37.40	31.75	23.87	32.00	34.67	33.43	28.50
9	39.40	39.20	36.60	24.32	21.53	28.00	58.76	51.83	27.80
10	35.97	36.81	36.20	19.96	19.88	25.70	149.35	109.65	18.00
11	33.05	34.77	36.10	17.21	18.61	25.60	225.89	225.03	196.80
12	31.63	33.06	33.60	15.36	17.58	18.50	144.64	168.97	150.00
13	37.18	37.92	40.00	14.02	16.69	16.50	96.17	113.408	110.00
14	42.48	42.05	39.90	13.05	15.89	24.60	71.13	1.05	103.30
15	37.76	39.81	30.40	13.45	15.58	24.30	57.03	62.34	75.70
16	40.19	39.35	30.80	18.03	21.50	23.70	48.23	51.17	67.40
17	40.92	37.88	32.10	16.72	20.17	22.70	42.20	44.20	66.20
18	36.55	38.40	31.80	14.71	17.69	22.20	37.76	39.59	44.7-
19	32.73	35.57	32.30	13.22	16.03	14.50	35.46	36.61	43.60
20	29.72	32.84	38.60	12.10	14.85	13.90	33.12	34.38	44.00
21	28.37	30.71	28.70	11.24	13.94	10.10	30.33	32.24	44.80
22	26.24	28.94	27.50	10.53	13.18	10.00	28.04	30.42	38.00
23	24.49	27.40	26.40	9.94	12.53	11.10	26.10	28.82	37.20
24	23.01	26.01	26.30	9.42	11.94	13.20	24.42	27.37	31.40
25	21.72	24.74	26.10	8.96	11.40	11.10	22.92	26.03	25.00
26	20.56	23.56	25.50	8.54	10.90	10.10	21.58	24.78	26.00
27	19.52	22.44	25.80	8.15	10.42	9.40	20.37	23.60	24.00
28	18.56	21.40	25.90	7.80	9.97	8.70	19.27	22.49	30.30
29	17.68	20.40	26.30	7.46	9.54	8.60	18.26	21.44	23.40
30	16.87	19.46	15.60	7.15	9.13	8.60	17.32	20.44	14.70

1	2	3	4	5	6	7	8	9	10
OCT									
1	16.12	18.57	14.80	6.86	8.74	8.30	16.49	19.49	19.00
2	15.41	17.72	14.20	6.58	8.37	8.00	15.67	18.60	18.00
3	14.76	16.91	14.40	6.32	8.01	7.70	14.92	17.74	17.10
4	14.14	16.15	13.50	6.07	7.67	6.50	14.23	16.93	15.50
5	13.57	15.42	13.10	5.83	7.35	6.40	13.59	16.16	14.70
6	13.03	14.72	13.20	5.61	7.04	7.60	12.99	15.43	14.00
7	12.52	14.06	12.40	5.40	6.74	7.60	12.42	14.73	13.80
8	12.04	13.44	12.30	5.20	6.46	7.60	11.89	14.07	11.80
9	11.59	12.84	12.20	5.01	6.18	7.50	11.40	13.44	11.60
10	11.16	12.27	12.00	4.83	5.92	7.30	10.93	12.83	11.20
11	10.76	11.72	11.70	4.65	5.68	7.30	10.49	12.26	10.00
12	10.37	11.20	7.80	4.49	5.44	7.20	10.07	11.72	10.90
13	10.01	10.71	7.80	4.33	5.21	7.20	9.68	11.20	12.10
14	9.67	10.24	7.80	4.18	4.99	7.20	9.31	10.70	11.90
15	9.34	9.79	7.70	4.04	4.78	7.20	8.96	10.23	11.40
16	9.04	9.36	7.70	3.91	4.58	7.60	8.63	9.78	10.60
17	8.74	8.95	9.40	4.36	4.39	7.40	8.32	9.35	10.30
18	8.46	8.56	9.40	4.15	4.21	7.40	8.02	8.94	10.00
19	8.20	8.19	9.40	3.93	4.04	7.20	7.74	8.55	9.90
20	7.95	7.84	9.30	3.77	3.87	6.00	7.47	8.18	9.50
21	7.71	7.50	8.80	3.63	3.71	5.60	7.22	7.82	9.40
22	7.48	7.18	8.80	3.50	3.55	5.55	6.98	7.48	9.20
23	7.26	6.87	8.80	3.37	3.41	5.40	6.75	7.16	8.80
24	7.05	6.57	8.50	3.26	3.27	5.40	6.53	6.85	9.30
25	6.85	6.29	8.30	3.15	3.13	5.30	6.33	6.56	8.80
26	6.66	6.02	8.90	3.05	3.00	5.40	6.13	6.27	8.80
27	6.48	5.76	8.50	2.95	2.88	5.40	5.94	6.01	8.80
28	6.30	5.52	6.20	2.85	2.76	5.30	5.76	5.75	8.80
29	6.14	5.28	6.00	2.76	2.65	5.30	5.59	5.50	8.80
30	5.98	5.06	5.90	2.68	2.54	5.30	5.43	5.27	8.80
31	5.82	4.85	5.60	2.60	2.43	4.80	5.27	5.04	8.80

REFERENCES

- Abbott, M.B., J.C. Bathurst, J.A. Cunge, P.E.O'Connell and J.Rasmussen (1986, a), "An Introduction to the European Hydrological System - System Hydrologique European SHE, 1 : History and Philosophy of a Physically Based Distributed Modelling System" *Jr. of Hydrology*, vol. 87, pp 45-59.
- Abbott, M.B., J.C. Bathurst, J.A. Cunge, P.E.O'Connell and J.Rasmussen (1986, b), "An Introduction to the European Hydrological System - System Hydrologique European SHE, 2 : Structure of a Physically Based Distributed Modelling System" *Jr. of Hydrology*, vol. 87, pp 61-77.
- Agyei, Y.G., G. Willgoose and F.P.D. Troch, (1995) "Effects of Vertical Resolution and Map Scale of Digital Elevation Models on Geomorphological Parameters used in Hydrology", *Hydrological processes*, vol. 9, pp 363-382.
- Allord, G.J. and F.L. Scarpace (1979), "Improving Streamflow Estimates Through the Use of LANDSAT", In: *Satellite Hydrology*, (M. Deutsch, D.R. Wiesnet and A. Rango eds.), pp 284-291.
- Amorocho, J. (1975), "An Application of Satellite Imagery to Hydrologic Modeling - The Upper Sinu River Basin, Colombia", Presented to the Symposium on the Application of Mathematical Models in Hydrology, Bratislava, 9 pp.
- Anderson, D.G. (1979), "Satellite Versus Conventional Methods in Hydrology", In: *Satellite Hydrology*, (M. Deutsch, D.R. Wiesnet and A. Rango eds.), pp 33-35.
- Anderson, M.G. and T.P. Burt (1985), "Modelling Strategies" In: *Hydrological Forecasting*, (M.G. Anderson and T.P. Burt eds.), Wiley, Chichester, U.K., pp 1-13.
- Bagchi, A.K. (1981), "Snowmelt Runoff in Beas Basin Using Satellite Imageries", Unpublished Ph.D. Thesis, Department of Civil Engineering., University of Roorkee, Roorkee.

Band, L.E., (1986), "Topographic Partition of Watershed Using Digital Elevation Model", *Water Resources Research*, vol. 22, no. 1, pp 15-24.

Barrett, E.C. and D.W. Martin (1981), "The Use of Satellite Data in Rainfall Monitoring", Academic Press, London.

Bathurst, J.C. (1986), "Sensitivity Analysis of the System Hydrologique Europeen For An Upland Catchment" *Jr. of Hydrology*, vol. 87, pp 103-123.

Barrett, E.C. and R.W. Herschy (1986), "A European Perspective on Satellite Remote Sensing for Hydrology and Water Management", In: *Hydrologic Application of Space Technology*, (A.I. Johnson ed.), IAHS publ. no. 160, pp 3-12.

Beven, K. (1985), "Distributed Models" In: *Hydrological Forecasting*, (M.G. Anderson and T.P. Burt eds.), Wiley, Chichester U.K., pp 405-435.

Black, R.E. (1973), "Simulation of Flow Records for an Ephemeral Stream", Unpublished M.Sc. Thesis, University of Strathclyde, Glasgow, U.K.

Blackie, J.R. and C.W.O. Eeles (1985), "Lumped Catchment Models" In: *Hydrological Forecasting*, (M.G. Anderson and T.P. Burt eds.), Wiley, Chichester U.K., pp 311-345.

Bondelid, T.R., T.J. Jackson and R.M. McGwen (1980), "Comparison of Conventional and Remotely Sensed Estimates of Runoff Curve Numbers in Southeastern Pennsylvania", *ALSM-ASP Convention*, St. Louis, pp 80-96.

Briggs, I. (1981), "Integration of Elevation Data with Remotely Sensed Data", *Proceedings of LANDSAT 81*, Canberra, pp 4.1.1-4.1.4.

Burrough, P.A. (1986), "Principles of Geographical Information Systems for Land Resources Assessment", Oxford, Clarendon Press.

Caselles, V. and J. Delegido, (1987), "A Simple Model to Estimate the Daily Value of the Maximum Evapotranspiration as from Satellite Temperature and Albedo Images", *Int. Jr. of Remote Sensing*, vol. 8, pp 1151-1162.

- Chakraborti, A.K., (1992), "Remote Sensing Applications in Water Resources Development in India", In: Hydrological Development in India Since Independence, Publisher National Institute of Hydrology, Roorkee, India, pp73-97.
- Chaw, V.T. (1964), "Handbook of Applied Hydrology: A Compendium of Water Resources Technology", McGraw Hill, New York.
- Chidley, T.R.E., and R.S. Drayton, (1986), "Visual Interpretation of Standard Satellite Images for the Design of Water Resources Schemes", In: Hydrological Applications of Space Technology, (A.I. Johnson ed.), IAHS publ.no. 160, pp 249-256.
- Clarke, R.T. (1973) "Mathematical Models in Hydrology", FAO Irrigation and Drainage Paper no. 19.
- Connors, K.F., T.W. Gardner and G.W. Petersen (1986), "Digital Analysis of the Hydrologic Components of Watersheds Using Simulated SPOT Imagery", In: Hydrologic Applications of Space Tecnology, (A.I. Johnson ed.), IAHS Publ. no. 160, pp 355-365.
- Cragwall, J.S. (1979), "Remote Sensing in Hydrology - A Challenge to Scientists", In: Satellite Hydrology, (M. Deutsch, D.R. Wiesnet and A. Rango eds.), pp 3-7.
- Crawford, N.H. and R.K. Linsley (1966), "Digital Simulation in Hydrology, Stanford Watershed model IV", Dept. of Civil Engg., Stanford University, Tech. Report 39.
- Cruise, J.F. and R.L. Miller (1993), "Hydrologic Modeling with Remotely Sensed Databases", Water Resources Bulltin, vol. 29, no. 6, pp 997-1002.
- Danish Hydraulic Institute, Lecture Notes and Exercises, Training Course (1989), "Hydrological Computerised Modelling System (SHE)", Danish Hydraulic Institute, Denmark.
- Das Gupta, S.P. (1980), "Atlas of Agricultural Resources of India", publ. National Atlas and Thematic Mapping Organisation.

Das, S.N., K.K. Narula and R. Laurin (1992), "Runoff Potential Indices of Watersheds in Tilaiya Catchment, Bihar (India) Through Use of Remote Sensing and Interpretation of GIS", *Photonirvachak, Jr. of the Indian Society of Remote Sensing*, vol. 20, no. 4, pp 207-221.

DeVantier, A. and A.D. Feldman, (1993), "Review of GIS Applications in Hydrologic Modeling", *Jr. of Water Resources planning and Management, ASCE*, vol. 119, no. 2, pp 246-261.

Dhanju, M.S. (1983), "Studies of Himalayan Snow Cover Area from Satellite", In: *Hydrological Applications of Remote Sensing and Remote Data Transmission*, (B.E. Goodison ed.), IAHS publ. no. 145, pp 401-409.

Dickson, A. (1984), "Interactive River Flow Forecasting", Unpublished M.Sc. Thesis, University of Strathclyde, Glasgow, U.K.

Eagleson, P.S. (1978), "Climate, Soil and Vegetation", *Water Resources Research*, vol. 14, pp 705-776.

Eash, D.A. (1994), "A Geographic Information System Procedure to Quantify Drainage Basin Characteristics", *Water Resources Bulletin*, vol. 30, no. 1, pp 1-8.

Eckhardt, J.R. and C.F. Leaf (1986), "Satellite Data Input to Windy Gap Computerized Streamflow Forecasting Model", In: *Hydrologic Application of space Technology*, (A.I. Johnson ed.), IAHS publ. no. 160, pp 349-354.

Engman, E.T. and R.J. Gurney (1991, a), "Remote Sensing in Hydrology", Chapman and Hall, London.

Engman, E.T. and R.J. Gurney (1991, b), "Recent Advances and Future Implications of Remote Sensing for Hydrologic Modeling", In: *Recent Advances in the Modelling of Hydrologic System*, (D.S. Bowles and P.E. O'Connell eds.), Kluwer Academic publisher, Netherland, pp 471-495.

- Engman, E.T. (1993), "Remote Sensing", In: Handbook of Hydrology, (D.R. Maidment, ed.), McGraw Hill, pp 24.1-24.23.
- Fellows, J.D. and R.M. Ragan, (1986), "The Role of Cell Size in Hydrology Oriented Geographic Information System", In: Hydrologic Application of Space Technology, (A.I. Johnson ed.), IAHS publ. no. 160, pp 453-460.
- Fleming, G. (1975), "Computer Simulation Techniques in Hydrology", Elsevier, New York.
- Fleming G. and R.S. McKenzie (1983), "River Basin Model for Water and Sediment Resources Assessment User Guide Volume : 1, The Watershed Model", Internal Publ. no. HY-82-7, Department of Civil Engg., University of Strathclyde, Glasgow, U.K.
- Fleming, G. and C. Hynes (1985), "Mid-Sutherland River System Flooding Study", Department of Civil Engineering, University of Strathclyde, Glasgow, U.K.
- Fleming, G. and R.E. Black (1974), "Simulation of Flow records for an Australian Catchment using the Stanford Watershed Model IV", Civil Engg. Transactions, CE vol. 16, no. 2, pp 103-107.
- Fleming, G. and S. Dowling (1987), "Catchment Modelling at Loch Fleet", Intrim Report, Department of Civil Engineering, University of Strathclyde, Glasgow, U.K.
- Follansbee, W.A. (1973), "Estimation of Average Daily Rainfall From Satellite Cloud Photograph", NOAA Technical Memorandum NESS 44, Washigton, D.C., 39 pp.
- Fortin, J.P., P. Villeneuve, A. Guilbot and B. Seguin (1986), "Development of a Modular Hydrological Forecasting Model Based on Remotely Sensed data for Interactive Utilization on a Microcomputer", In: Hydrologic Application of space Technology, (A.I. Johnson ed.), IAHS publ. no. 160, pp 307-319.

France, M.J. and P.D. Hedges, (1989), "The Appropriate Use of Remotely Sensed Satellite Data for Water Resources Assessment and Modelling", In: Remote Sensing for Operational Applications, (E.C. Barrett and K.A. Brown, eds.), pp 147-153.

Garbrecht, J. and L.W. Martz (1993), "Network and Sub Watershed Parameters Extracted from Digital Elevation Model, The Bill Creek Experience", Water Resources Bulletin, vol. 29, no. 6, pp 909-916.

Garg, P.K. (1991), "Development of a catchment Scale Erosion Model for Semi Arid Region and Its Implementation Through Remote Sensing" Unpublished Ph.D. Thesis, University of Bristol, U.K.

Ghosh, S.K., (1991), "River Basin Management Using Remote Sensing and Assessment of Data Input to Hydrological Model as Derived from Satellite Data", Unpublished PH.D. Thesis, University of Strathclyde, Glasgow U.K.

Ghosh, S.K. and G. Fleming, (1993), "Use of LANDSAT 5 TM Data for Estimation of Evapotranspiration for a Scottish Basin", IAMAP-IAHS 93, J3 Symposium, Yokohima, Japan.

Groves, J.R. and R.M. Ragan (1983), "Development of a Remote Sensing Based Continuous Streamflow Model", 17th Int. Sym. on Remote Sensing of Environment, Ann Arbor, Michigan, pp 447-456.

Groves J.R., R.M. Ragan and R.B. Clapp, (1983), "Development and Testing of a Remote Sensing Based Hydrological Model", In: Hydrological Applications of Remote Sensing and Remote Data Transmission, (B.E. Goodison ed.), IAHS publ. no. 145, pp 601-612.

H.P. Remote Sensing Cell , Shimla (1991), "Land use/ Land Cover Map of Shimla, Solan and Sirmaur Districts"

Hardy, J.R. (1981), "Chapter 2 In: Terrain Analysis and Remote Sensing", (J.R.G. Townshend ed.), London George Allen & Unwin, Sydney.

Helmlinger, K.R., P.Kumar and E.E. Georgliou (1993), "On the Use of Digital Elevation Model Data for Hortonian and Fractal Analysis of Channel Networks", *Water Resources Research*, vol. 29, no. 8, pp 2599-2613.

Hogg, J., J.E. McCormack, S.A. Roberts, M.N. Gahegan and B.S. Hoyle, (1993), "Automated Derivation of Stream - Channel Networks and Selected Catchment Characteristics from Digital Elevation Models", In: *Geographical Information Handling - Research and Application*, (P.M. Mather ed.), John Wiley & Sons Ltd., pp 207-235.

Holmgren, P. (1994), "Multiple Flow Direction Algorithms for Runoff Modelling in Grid Based Elevation Models: An Empirical Evaluation", *Hydrological Processes*, vol. 8, pp 327-334.

Holtan, H. N., G. J. Stilther, W. H. Henson and N. C. Lopze, (1975), "USDAHL - 74 revised model of watershed hydrology", *Agricultural Research Service, U.S. Department of Agriculture, Technical Bulletin no. 1578.*

Hynes, C. (1985), "The Impact of Landuse and River Channel Geometry on Flooding in the River Oykel, Scotland", Unpublished M.Sc. Thesis, University of Strathclyde, Glasgow, U.K.

ILWIS (1992), *User's Manual Volume 1 & 2*, ITC, Netherlands.

Jackson, T.J. (1993), "Measuring Surface Soil Moisture Using Passive Microwave Remote Sensing", *Hydrological Processes*, vol. 7, pp 139-152.

Jackson, T.J. and R.M. Ragan (1977, a), "Value of LANDSAT in Urban Water Resources Planning", *Jr. of Water Resources Planning & Management Division*, vol. 103, no. WR1, pp 33-46.

Jackson, T.J. and R.M. Ragan (1977, b), "Test of LANDSAT Based Urban Hydrologic modelling", *Jr. of Water Resources Planning & Management Division*, vol. 103, no. WR1, pp 141-157.

Jackson, T.J. and T.R. Bondelid (1984), "Runoff Curve Numbers From LANDSAT Data, Renewable Resources Management - Application in Remote Sensing", ASP, Falls Church, pp 543-573.

Jensen J.R. (1986), "Introductory Digital Image Processing A Remote sensing Perspective", Prentice - Hall, Englewood cliffs, New Jersey.

Jenson S.K., (1985), "Automated Derivation of Hydrologic Basin Characteristics from Digital Elevation Model Data", Proceedings of Auto Carto - 7, Washington D.C., pp 301-310.

Jenson S.K., (1991), "Applications of Hydrologic Information Automatically Extracted from Digital Elevation Models", Hydrological Processes, vol. 5, pp 31-44.

Jenson S.K. and C.M. Trautwein, (1987), "Methods and Applications in Surface Depression Analysis.", Proceedings of Auto Carto - 8, Baltimore, Maryland, pp 137-144.

Jenson S.K. and J.O. Domingue, (1988), "Extracting Topographic Structure from digital elevation Data for Geographic Information System Analysis", Photogrammetric Engg. and Remote Sensing, vol. 54, no. 11, pp 1593-1600.

Johnson, L.E. (1989), "MAPHYD - A Digital Map Based Hydrologic Modelling System", Photogrammetric Engg. and Remote Sensing, vol. 55, no. 6, pp 911-917.

Jupp, D.L.B. and J.D. Kalma (1989), "Distributing Evapotranspiration in a Catchment Using Airborne Remote Sensing", Asian - Pacific Remote Sensing Jr., vol. 2, no. 1, pp 13-25.

Kemp, K.K. (1992), "Spatial Models for Environmental Modelling with GIS" Proceedings of 5th Int. Symp. Spatial Data Handling, Charleston, South Carolina, pp 524-533.

- Killpack, D.P. and R.M. McCoy (1981), "An Application of LANDSAT Derived Data to a Regional Hydrologic Model", *Remote Sensing Quarterly*, vol.3,no. 2, pp 27-33.
- Kite, G.W. (1978), "Development of a Hydrologic Model for a Canadian Watershed", *Canadian Jr. of Civil Engineering*, vol. 5, no. 1, pp 126-134.
- Kite, G.W. (1991), "A Watershed Model Using Satellite Data to a Mountain Basin in Canada", *Jr. of Hydrology*, vol. 128, pp 157-169.
- Klatt, P. and G.A. Schultz (1983), "Flood Forecasting on the Basis of Radar Rainfall Measurement and Rainfall Forecasting", In: *Hydrological Application of Remote Sensing and Remote Data Transmission*, (B.E.Goodison ed.), IAHS publ. no. 145, pp 307-315.
- Klemes, V. (1986), "Operational Testing of Hydrlogical Simulation Models", *Hydrological Science Jr.*, vol. 31, no. 1, pp 13-24.
- Kotoda, K. (1986), "Estimation of River Basin Evapotranspiration", *Environmental Research Center Paper*, no. 8, Environmental Research Center, The University of Tsukuba, Ibaraki, 305, Japan.
- Kouwen, N. (1988), "WATFLOOD : A Micro Computer Based Flood Forecasting System Based on Real Time Weather Radar", *Canadian Water Resources Jr.*, vol. 13, no. 1, pp 62-77.
- Kouwen, N., E.D. Soulis, A. Pietroniro, J. Donald and R.A. Harrington (1993), "Grouped Response Units for Distributed Hydrologic Modeling", *Jr. of Water Resources Planning and Management*, American Society of Civil Engg., vol. 119, no. 3, pp 289-305.
- Kawosa, M.A., (1988), "Remote Sensing of the Himalaya", Natraj Publisher, Dehradun.

Kumar, C.P. (1991), "Application of SHE Model to Hemavati (upto Sakleshpur) Basin", Report no. CS-46, National Institute of Hydrology, Roorkee.

Kumar, M.S. (1997), "Delineation of Stream Network using DEM", Unpublished M.E. Dissertation, Civil Engg. Deptt., University of Roorkee, Roorkee.

Link, L.E. (1983), "Compatibility of Present Hydrologic Models with Remotely Sensed Data", Proceedings of 17th Int. Symp. on Remote Sensing Environment, pp 133-153.

Linsley, R.K. and N.H. Crawford (1960), "Computation of Synthetic Streamflow Record on a Digital Computer", Int. Association of Scientific Hydrology, publ. no. 51, pp 526-538.

Llamas, J., A.P. Planamdon and S.M.U. Ahmed (1980), "Adoption of the Standard Watershed Model to Canadian Conditions", Proceedings Int. Conference on Water Development, Taipei, Taiwan, pp 419-437.

Mark, D.M. (1983), "Automated Detection of Drainage Networks from Digital Elevation Model", Proceedings of 6th Int. Symp. on Automated Cartography, Auto Carto 6, pp 288-295.

Martz, L.W. and J. Garbrecht (1993), "Automated Extraction of Drainage Network and Watershed Data from Digital Elevation Models", Water Resources Bulletin, vol. 29, no. 6, pp 901-908.

Mather, P.M. (1987), "Computer Processing of Remotely Sensed Images", John Wiley & Sons.

Mauser, W. (1984), "Calculation of Flood Hydrographs Using LANDSAT Derived Landuse Information in the Dreisam Watershed, South West Germany", Advanced Space Research, vol. 4, no. 11, pp 211-216.

Mckenzie, R.S. (1983), "The Effect of Snow Processes and Landuse Changes On Hydrological Response", Unpublished Ph.D. Thesis, University of Strathclyde, Glasgow, U.K.

Moore, I.D., R.B. Grayson and A.R. Ladson (1991), "Digital Terrain Modelling : A review of Hydrological, Geomorphological and Biological Applications", Hydrological Processes, vol. 5, pp 3-30.

Morris, E.M. (1980), "Forecasting Flood Flows in Grassy and Forested Basins Using a Deterministic Distributed Model", Int. Association of Scientific Hydrology, Publ. no. 129, pp 247-255.

Morris, W.V. (1968), "Water", Department of Energy, Mines and Resources, Ottawa.

Neumann, P. and G.A. Schultz (1989), "Hydrological Effects of Catchment Characteristics and Landuse Changes Determined by Satellite Imageries and GIS", In : Remote Sensing and Large Scale Global Processes, IAHS Publ. no. 186, pp 169-176.

Nielsen, S.A. and E. Hansen (1973), "Numerical Simulation of The Rainfall-Runoff on a Daily Basis", Nordic Hydrology, vol. 4, pp 171-190.

Nigam, A.K., P.K. Garg and S.K. Ghosh (1995), "Utility of IRS LISS-II Data for the Extraction of Basin Characteristics", Indian Surveyer, pp 1-11.

O'Callaghan, J.F. and D.M. Mark (1984), "The Extraction of Drainage Networks From Digital Elevation Data", Computer Vision, Graphics and Image Processing, vol. 28, pp 328-344.

Oke, V.V.O. (1991), "The Changing River Basin: A Process Approach to Reservoir Management", Unpublished Ph.D. Thesis, University of Strathclyde, Glasgow, U.K.

O'Loughlin, E.M. (1986), "Prediction of Surface Saturation Zones in Natural Catchments by Topographic Analysis", Water Resources Research, vol. 22, pp 794-804.

- Overton, D.E. and M.E. Meadows (1976), "Storm Water Modeling", Academic Press, New York.
- Papo, H.B. and E. Gelbman (1984), "Digital Terrain Models for Slopes and Curvature", Photogrammetric Engg. and Remote Sensing Jr., vol. 50, no. 6, pp 695-701.
- Peck, E.L., R.S. McQuiney, T.N. Keefer, E.R. Johnson and J.L. Erekson (1981, a), "Review of Hydrologic Models for Evaluating Use of Remote Sensing Capabilities", NASA-CR-166674.
- Peck, E.L., T.N. Keefer, and E.R. Johnson (1981, b), "Strategies for Using Remotely Sensed Data in Hydrologic Models", NASA-CR-66729.
- Petrie, G. (1990), "Photogrammetric Methods of Data Acquisition for Terrain Modelling", In: Terrain Modelling in Surveying and Civil Engineering, (G. Petrie and T.J.M. Kennie, eds.), Whittles Publishing, pp 27-48.
- Peucker, T.K. and D.H. Douglas (1975), "Detection of Surface Specific Points by Local Parallel Processing of Discrete Terrain Elevation Data", Computer Graphic and Image Processing, vol.4, pp 375-387.
- Quinn, P.F. and K.J. Beven (1993), "Spatial and Temporal Prediction of Soil Moisture Dynamics, Runoff Variable Source Area and Evapotranspiration for Plynlim on Mid-Wales", Hydrological Processes, vol. 7, pp 425-448.
- Quinn, P., K. Beven, P. Chevallier and O. Planchan (1991), "The Prediction of Hill Slope Flow Paths for Distribution Hydrologic Modelling Using Digital Terrain Models", Hydrological Processes, vol. 5, pp 59-80.
- Ragan, R.M. and T.J. Jackson (1975), "Use of Satellite Data in Urban Hydrologic Models", Jr. of Hydraulics Division, ASCE, vol. 101, no. HY-12, pp 1469-1475.

- Ragan, R.M. and T.J. Jackson (1980), "Runoff Synthesis Using LANDSAT and the SCS Model", Jr. of the Hydraulic Division, American Society of Civil Engineers, vol. 106, no HY5, pp 667-678. .
- Ramamoorthi, A.S., S. Thiruvengadachari and A.V. Kulkarni (1991), "IRS-1A Applications in Hydrology and Water Resources", Current Science, vol. 61, no. 3 & 4, pp 180-188.
- Rango, A. (1980), "Operational Applications of Satellite Snow Cover Observation", Water Resources Bulletin, vol. 16, no. 6, pp 1066-1073.
- Rango, A. (1985), "Assessment of Remote Sensing Input to Hydrologic Models", Water Resources Bulletin, vol. 21, no. 3, pp 423-432.
- Rango, A. (1988), "Resources in developing an operational snowmelt runoff forecast model with remote sensing input", Nordic Hydrology, vol. 19, no. 2, pp 65-76.
- Rango, A., A. Feldman, T.George and R.M. Ragan (1983), "Effective Use of LANDSAT Data in Hydrologic Models", Water Resources Bulletin, vol. 19, no. 2, pp 165-174.
- Rao, C.S., C.V. Shyemala and T.V.S. Rao (1991), "Evaluation of Integrated Watershed Management Programme, Flood Prone River - Upper Yammuna - U.P. and H.P.", Utility Publications Ltd., Secunderabad, India.
- Ritter, p. (1987), "A Vector Based Slope and Aspect Generation Algorithms", Jr. of Photogrammetric Engineering and Remote Sensing, vol. 53, no. 8, pp 1109-1111.
- Rott, H. (1986), "Estimation of Daily Runoff Based on METEOSAT Data" In: Hydrologic Applications of Space Technology, (A.I. Johnson ed.), IAHS Publ. no. 160, pp 321-330.

Salmonson, V.V., R. Ambaruch, A.Rango and J.P. Ormsby (1975), "Remote Sensing Requirements as Suggested by Watershed Model Sensitivity Analysis", Proceedings of 10th Int. Symp. on Remote Sensing of Environment, Ann Arbor, pp 1273-1284.

Schultz, G.A. (1986), "Satellite Data as Input for Long-term and Short-term Hydrological Models", In: Hydrologic Applications of Space Technology, (A.I.Johnson ed.), IAHS Publ. no. 160, pp 297-306.

Seethapati, P.V., V.K. Chaubey and S.K. Jain (1989), "Geo-morphology and Drainage Pattern in North Eastern Gujrat (Sabarmati Basin)", CS-23, National Institute of Hydrology, Roorkee.

Sharpnack, D.A. and G. Akin (1969), "An Algorithm for Computing Slope and Aspect from Elevations", Jr. of Photogrammetric Engineering and Remote sensing, vol. 35, no. 3, pp 247-248.

Sherman, L.K. (1932), "Streamflow Rainfall by the Unit Graph Method", English News Record, no. 108, pp 501-505.

Singh, V.P. (1989), "Hydrologic System Volume II, Watershed Modelling", Prentice Hall, New Jercey.

Singh, V.P. (1994), "Elementary Hydrology", Prentice Hall of India Pvt. Ltd., New Delhi.

Skidmore, A.K. (1989), "A Comparison of Techniques for Calculating Gradient and Aspect from a Gridded Digital Elevation Model", Int. Jr. of Geographical Information System, vol. 3, no. 4, pp 323-334.

Slack, R.B. and R. Welch (1980), "Soil Conservation Service Runoff Curve Number Estimated from LANDSAT Data", Water Resources Bulletin, vol. 16, pp 887-893.

Smith, M.B. and M. Brilly (1992), "Automated Grig Element Ordering for GIS Based Overland Flow Modelling", Jr. of Photogrammetric Engineering and Remote Sensing, vol. 58, no. 5, pp 579-585.

- Soer, G.J.R. (1980), "Estimation of Regional Evapotranspiration and Soil Moisture Condition Using Remotely Sensed Crop Surface Temperature", *Remote Sensing of Environment*, vol. 9, no. 1, pp 27-45.
- Stephenson, G.R. and R.A. Freeze (1974), "Mathematical Simulation of Subsurface Flow Contributions to Snowmelt Runoff, Reynolds Creek Watershed, Idaho", *Water Resources Research*, vol. 10, pp 284-294.
- Still, D.A. and S.F. Shih (1985), "Using LANDSAT to Classify Landuse for Assessing the Basinwide Runoff Index", *Water Resources Bulletin*, vol. 21, no. 6, pp 931-940.
- Strubing, G. and G.A. Schultz (1983), "Estimation of Monthly River Runoff Data as the Basis of Satellite Imagery", *Hydrological Application of Remote Sensing and Remote Data Transmission*, (B.E. Goodison ed.), IAHS Publ. no. 145, pp 491-498.
- Subramanaya, K. (1987), "Engineering Hydrology", Tata McGraw Hill, New Delhi.
- Sugawara, M. (1961), "On the Analysis of Runoff Structure About Several Japanese Rivers", *Japanese Jr. of Geophysics*, vol. 2, no. 4, pp 1-76.
- Thakur, V.C. and B.S. Rawat (1992), "Geological Map of The Western Himalaya", Published under the Authority of the Surveyour General of India.
- Uchida, S. and T. Hoshi (1988), "On the Regional Characteristics of Actual Evapotranspiration Derived from LANDSAT MSS and Elevation Data", *Geocarto International*, vol. 2, pp 57-66.
- U.S. Department of Agriculture (1972), "Soil Conservation Service, National Engineering Handbook", Section-4, Hydrology U.S. Govt. Printing Office, Washington, D.C.
- U.S. Army Corps of engineers (1981), "HEC-1 Flood Hydrograph Package, User Manual", Hydrologic Engineering Center, Davis, California.

Viessman, W., J.W. Knapp, G.L. Lewis and T.E. Harbaugh (1977), "Introduction to Hydrology", IEPA Dun-Donnelley Publisher, New York.

Walker, R.A. (1979), "Regional Soil Erosion by Mathematical Modelling", Unpublished Ph.D. Thesis, University of Strathclyde, Glasgow, U.K.

Woolhiser, D.A. (1973), "Hydrologic and Watershed Modeling - State of the Art", Transactions of the ASCE, vol. 16, pp 533-559.

Zevenbergen, L.W. and C.R. Thorne (1987), "Quantitative Analysis of Land Surface Topography", Earth Surface Processes and Landforms, vol. 12, pp 47-56.